# Cultural transmission of reproductive success: Causal mechanisms, genetic consequences, and machine-learning-based inference

Jérémy Guez

MUSÉUM NATIONAL D'HISTOIRE NATURELLE
Ecole Doctorale Sciences de la Nature et de l'Homme – ED 227

Année 2022/2023

N°attribué par la bibliothèque

# THÈSE

Pour obtenir le grade de

DOCTEUR DU MUSÉUM NATIONAL D'HISTOIRE NATURELLE
Spécialité: Génétique des populations

Présentée et soutenue publiquement par

Jérémy Guez

Le 23 mars 2023

---

# Transmission culturelle du succès reproducteur :
## Mécanismes causaux, conséquences génétiques et inférence par apprentissage automatique

---

Sous la direction de :

Évelyne Heyer (Pr MNHN), de Frédéric Austerlitz (DR CNRS) et de Flora Jay (CR CNRS)

Devant un jury composé de :

Violaine Llaurens, Directrice de recherche, CNRS, MNHN, Présidente du jury
Évelyne Heyer, Professeure des universités, MNHN, Directrice de thèse
Frédéric Austerlitz, Directeur de recherche, CNRS, Co-directeur de thèse
Flora Jay, Chargée de recherche, CNRS, Co-directrice de thèse
Sylvain Billiard, Maître de conférences, Université de Lille, Rapporteur
Arnaud Estoup, Directeur de recherche, INRAE, Rapporteur
Céline Scornavacca, Directrice de recherche, CNRS, Examinatrice
Anna-Sapfo Malaspinas, Maîtresse de conférences, Université de Lausanne, Examinatrice

# Thesis summary

## Résumé en français

La transmission culturelle du succès reproducteur (TCSR) est un processus lors duquel les individus ont un nombre d'enfants positivement corrélé à celui de leurs parents. Ce phénomène a des effets sur la diversité génétique des populations, allant même jusqu'à accroître dans certains cas la fréquence de certaines maladies génétiques dans les populations concernées (Austerlitz and Heyer, 1998). Dans un premier temps, cette thèse examine en détails, à partir de la littérature, les causes et conséquences de ce phénomène. Les différents contextes dans lesquels peut apparaître la TCSR sont explorés, chez l'humain ainsi que dans d'autres espèces. Ces réflexions aboutissent à des arguments invitant à considérer comme une force évolutive à part entière la transmission du succès reproducteur d'origine non-génétique, une forme générale de la TCSR. Dans un second temps, la thèse présente un article de recherche (Guez *et al.*, 2022), utilisant une modélisation de la TCSR fondée sur une extension du modèle de Wright-Fisher (Sibert *et al.*, 2002), pour simuler l'évolution de populations d'individus diploïdes avec recombinaison. Ces simulations ont permis de disséquer le phénomène, séparant les effets dus à l'accroissement de la variance du succès reproducteur de ceux produits par la transmission du succès reproducteur elle-même. Différents effets sont explorés en détails, notamment les impacts sur des statistiques classiques de génétique des populations, comme le $D$ de Tajima et les fréquences alléliques, ainsi que sur des mesures moins communes telles que les indices de déséquilibre des arbres de coalescence. Enfin, les effets de la TCSR sur l'inférence d'une expansion démographique sont analysés, révélant une sous-estimation du facteur de croissance d'une population lorsque la TCSR n'est pas prise en compte. Ce dernier résultat suggère une potentielle sous-estimation de l'expansion néolithique, si les populations concernées ont été sujettes à la TCSR. Dans une troisième partie, des méthodes fondées sur l'apprentissage

automatique sont construites dans le but d'inférer correctement la TCSR conjointement à la démographie de la population. Ces méthodes reposent sur deux approches entrainées et testées sur des données génomiques simulées : l'inférence bayésienne par approximation (ABC) utilisant des statistiques résumées, et les réseaux de neurones convolutifs (CNN) entrainés directement à partir des données génomiques brutes. Les inférences réalisées par différentes versions de ces deux méthodes sont comparées, montrant que la méthode la plus performante combine les deux approches. Ceci révèle la possibilité de distinguer la TCSR de certains processus démographiques dans des données génomiques et d'inférer assez précisément les deux. Des recherches futures pourront explorer la distinction de la TCSR d'autres processus, comme la sélection naturelle et la structure génétique, afin d'appliquer efficacement ces méthodes à des données génomiques réelles humaines ou d'autres espèces.

# English summary

Cultural Transmission of Reproductive Success (CTRS) is a process in which individuals' progeny size is positively correlated with their parents' progeny size. This phenomenon impacts genetics, sometimes even increasing genetic disease risks in the populations where it occurs (Austerlitz and Heyer, 1998). First, this thesis examines the literature in detail, to reveal the potential causes and consequences of this phenomenon. The different contexts in which CTRS can appear are explored, in humans and other species. These aspects lead us to consider nongenetic TRS, a general form of CTRS, as a full-fledged evolutionary force. In a second chapter, the thesis presents a research paper (Guez *et al.*, 2022), using a modeling of CTRS based on an extension of the Wright-Fisher model (Sibert *et al.*, 2002), to simulate the evolution of diploid populations with recombination. These simulations allowed us to dissect the phenomenon, disentangling the effects due to the increased variance of reproductive success from those produced by the transmission of the reproductive success itself. Various effects are explored in detail, including impacts on classical population genetics statistics, such as Tajima's $D$ and allelic frequencies, as well as on less common statistics such as coalescent tree imbalance indices. Finally, the effects of CTRS on demographic expansion inference are analyzed, revealing an underestimation of the growth factor when CTRS is not considered. This last result suggests a potential underestimation of the Neolithic expansion, if the populations concerned were subject to CTRS. In a third chapter, machine learning methods are designed to correctly infer CTRS jointly with population demography. These methods are based on two approaches trained and tested on simulated genomic data: approximate Bayesian inference (ABC) using summary statistics, and convolutional neural networks (CNN) trained directly on raw genomic data. The inferences made by different versions of these two methods are compared, showing that the best-performing method combines both approaches. This reveals the possibility of distinguishing CTRS from demographic processes using genomic data and inferring both accurately. Future research should explore the distinction of CTRS from other processes, such as natural selection and genetic structure, in order to effectively apply these inference methods to human or other species real genomic data.

# Contents

# Introduction

## 0.1 Population genetics

### 0.1.1 Introduction

Population genetics studies the evolution of genetic diversity within populations over generations. Its central object is the gene, an entity carried by the individuals of the population and inherited from their parents. Several versions of a gene may exist, called **alleles**. From one generation to the next, the proportions of the different alleles fluctuate in the population, under the effect of major **evolutionary forces** that we will describe here.

The first evolutionary force impacting allele frequencies in a population is **mutations** (1d). It corresponds to the random change from one allele to another, making heredity less faithful. Thus, in a population where all individuals carry the same allele, a new child may carry a novel allele due to a mutation. This allele can then increase in frequency or disappear, depending on the number of descendants that this first carrier will have. In population genetics, the frequency of mutations apparition in a population is called **mutation rate**. Mutations increase genetic diversity by creating new alleles in the population.

A second evolutionary force is **genetic drift** (1a). It corresponds to the stochastic effects on the fluctuation of alleles. More precisely, from one generation to the next, some individuals reproduce more than others due to random events. As a result, the alleles carried by these individuals increase in frequency in the next generation, while the alleles carried by individuals reproducing less than average decrease in frequency. From one generation to the next, random fluctuations in allele frequencies are observed due to drift. At a certain point, an allele can reach a state called **fixation**: it has invaded the population and is present in all individuals,

and all other alleles have disappeared. Genetic drift depends on two main parameters: the duration of evolution and the size of the population. The longer the time considered, the more prominent the effects of drift. The larger the population, the smaller the drift. For a theoretical population of infinite size, drift does not exist. Drift tends to reduce genetic diversity by leading to the random fixation of alleles.

A third significant force in evolution is **natural selection** (1b). It occurs when individuals have different probabilities of reproducing, depending on the alleles they carry. This probability is called **fitness**. Alleles raising individual fitness are likely to increase in frequency over generations. However, genetic drift makes this process non-deterministic: in a case of two alleles with equal frequency when selection starts, the beneficial allele may disappear rapidly by chance, but this is more likely to happen to the less beneficial allele. Due to this interaction with drift, natural selection will have less effect on a small population since it is under strong drift. The effects of selection also depend on its strength, which is modeled in population genetics by the **selection coefficient**, often noted $s$. This strength of selection corresponds to the size of the advantage in fitness brought by the beneficial allele. Individuals carrying this allele will be $1 + s$ times more likely to reproduce than individuals carrying the unfavorable allele. For example, for $s$ being 0.1, individuals carrying the beneficial allele will have a probability to reproduce 10% higher than individuals carrying the other allele. Natural selection tends to reduce genetic diversity by fixing the most favorable alleles.

A fourth evolutionary force is **recombination** (1c). It concerns the evolution of combinations of alleles within the population. Let us consider two genes in the population, each with two alleles: A and a, B and b. When individuals carry either AB or ab, new combinations can appear only with recombination, allowing the birth of Ab and aB individuals. The frequency at which this happens is called the **recombination rate**. Recombination increases genetic diversity in a way because it allows novel combinations of alleles to appear. However, it does not change allelic frequencies.

A fifth evolutionary force is **migration** (1e). To take it into account, we must consider at least two populations. Migration occurs if alleles pass from one population to the other, through reproduction between members of the two populations. Thus, a new allele may appear in a population, not by mutation, but because it comes from another population. We can define a **migration rate** from a population to another, corresponding to the proportion of alleles migrating from population 1 to population 2. Migration rates can be asymmetrical: for example, more alleles

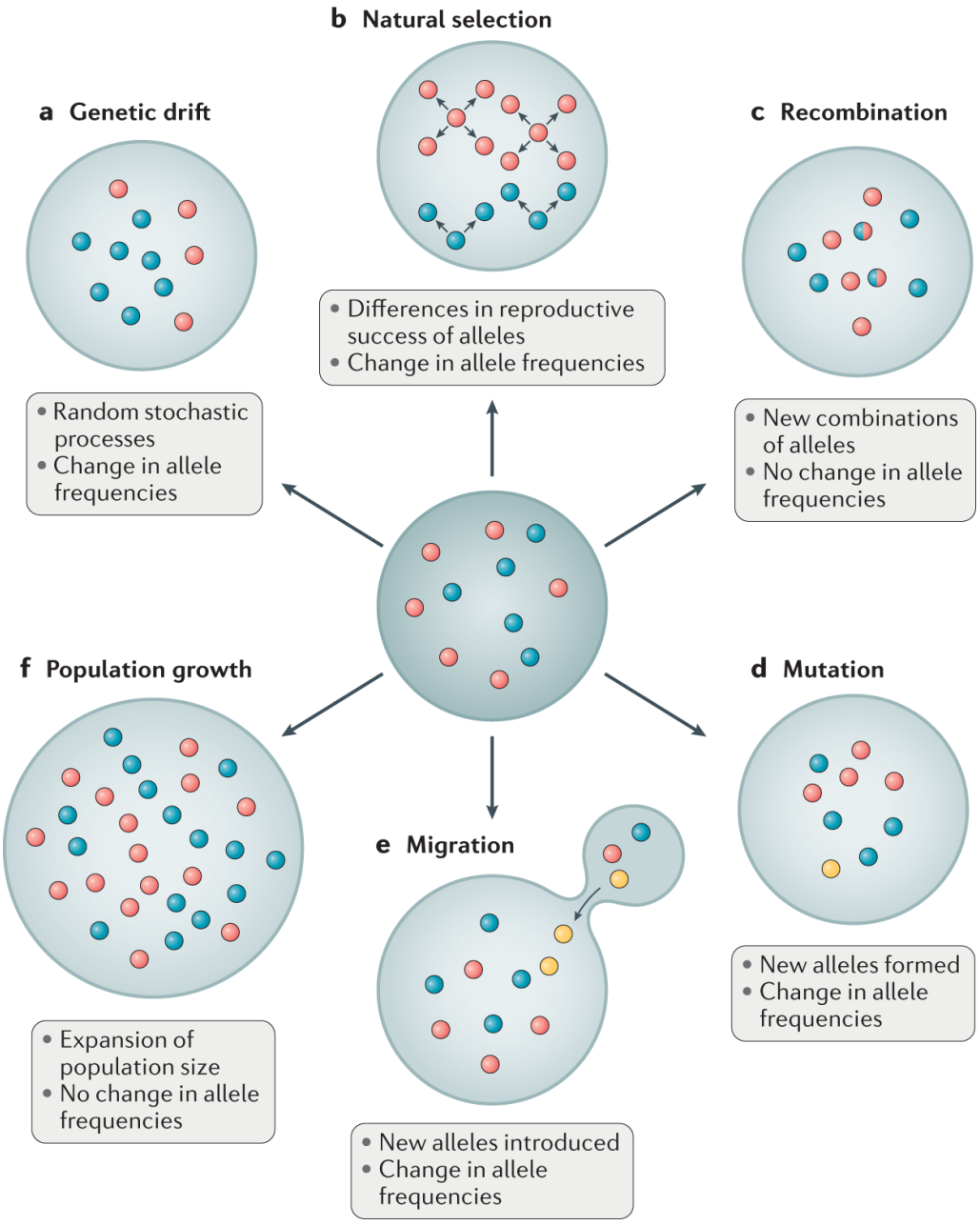


Figure 1: **Schematic view of the impacts of the major evolutionary forces on genetic diversity.** Figure from Adeyemo *et al.* (2021)

can migrate from 1 to 2 than the opposite. For a given population, migration tends to increase diversity, since it can bring in foreign alleles not previously present in the population.

This two-populations, two-alleles, two-genes model is deliberately simplistic. It allows us to analyze theoretically the main statistical principles underlying population genetics. For example, 10% of the population may have an adenine (A) at a given position, while the rest of the population has a cytosine (C). Within this population, these positions in the genome where multiple alleles exist concomitantly are called **Single Nucleotide Polymorphisms**, or **SNPs**. In theory, mutations can affect any base pair in an individual's genome, making it different at that position from its parent. The frequencies and combinations of SNPs change in the population over generations due to the five evolutionary forces described above.

### 0.1.2 Modeling population genetics

To model the history of a population of constant size, we can create a first generation $g$ of $N$ individuals ($N$ being the population size). We then produce the $N$ individuals of the next generation, $g+1$. The parents of each individual in $g+1$ can be chosen randomly among the individuals of $g$. The individuals of $g$ are then erased (i.e., non-overlapping generations). We can repeat this process for $5N$ generations, at which point we have 95% chance of having reached a common ancestor for the whole population. This modeling can work but has a major disadvantage. Only one of the individuals of generation $g$ is the ancestor of all the individuals of the last generation. This means that all calculations made to build the descendants of the other individuals of $g$ are useless, since they have no descendants in the last generation. In other words, since these individuals have no impact on the genetics of the present population, modeling them implies useless calculations.

**Coalescent theory** allows overcoming this problem (Kingman, 1982). This theory models the genetic history of a population not from the past to the present like the previous model (**forward-in-time model**, Fig. 2a), but starting from the present and going back to the common ancestor (**backward-in-time model**, Fig. 2c). From a computational point of view, the advantage of this method lies in the fact that we only compute the ancestors of the individuals present in the last generation (i.e., ancestors that had an impact on present-day population genetics). Moreover, we can focus on reconstructing the history of a sample of individuals taken from the population. By focusing only on the sampled individuals, we do not

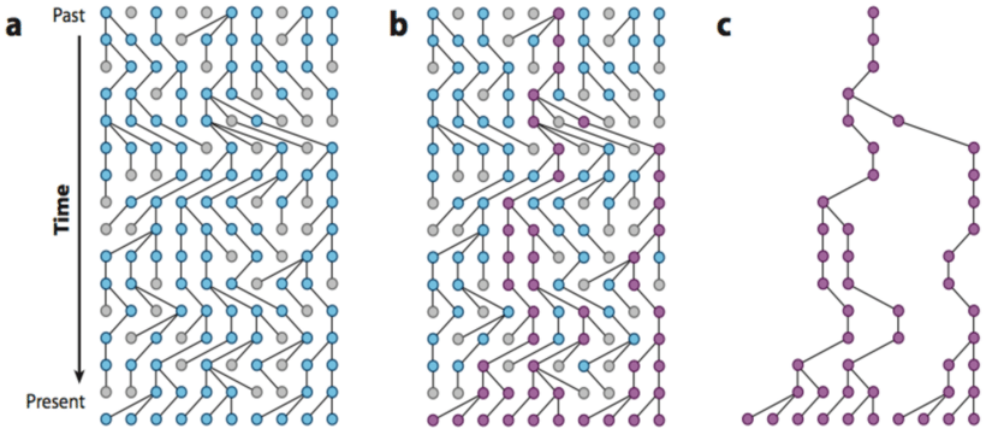


Figure 2: **Ineffectiveness of forward-in-time modeling.** Figure from Grünwald and Goss (2011). (a) Forward-in-time modeling of a population of $N = 10$ haploid individuals. Individuals that died without children are in grey, others are in blue. (b-c) Individuals present or having descendants in the last generation are in red. All other individuals are not useful to explain the genetic diversity in the last generation.

needlessly calculate the past of many present individuals we would not sample, nor past individuals that do not have alive descendants.

Backward-in-time modeling relies on the hypotheses of a panmictic population (i.e., individuals mate randomly) and non-overlapping generations. We start with the $n$ individuals sampled in the present-day generation. We are then interested in the probability that two of these $n$ individuals have the same parent in the previous generation. If this happens, both individuals' lineages will be merged in the previous generation: this is called a coalescent event. Statistically, there is a $1/N$ chance that a coalescent event will happen in the previous generation, and a $1 - (1/N)$ chance that it will not. In order to have at most one coalescent event in each generation, we assume that $n$ is very small compared to $N$. We then want to evaluate the coalescence time, i.e., the number of generations until $n$ lineages become $n - 1$ lineages. We will note this coalescence time $T_n$. It is a random variable that follows a geometric distribution since it corresponds to the number of attempts (i.e., the number of generations) before reaching the first success (i.e., a coalescence event). Assuming the generation time is very small compared to $T_n$ - this stems from the assumptions $n << N$ and $N$ is very big - we can switch to an exponential distribution (i.e., a continuous version of the geometric distribution). We know the expectation of this law: $2N/n(n-1)$, as well as its variance: $4N^2/(n^2(n-1)^2)$.

We use this method to go back from $n$ individuals to their common ancestor, by computing the expectation of $T_n, T_{n-1}, ..., T_2$ successively. The smaller $k$ is, the

larger $E[T_k]$ will be, with $E[T_2] = N$. Therefore, in the case of a constant-size population, coalescence events happen mostly near the present and become rarer as we go back in time. The total time of $n$ lineages until the coalescence of the last two lineages (Time to Most Recent Common Ancestor, **TMRCA**) is $\sum_{i=2}^{n} Ti$, which is $2N(1 - 1/n)$. We can schematize these coalescent events with a binary tree, called **coalescence tree**. In this tree, the leaves correspond to present-day individuals and each internal node to a past individual. The root will be the ancestor of all present individuals (the Most Recent Common Ancestor, **MRCA**). The branch lengths correspond to the coalescence times. In a population of constant size, the branches are thus increasingly long as one goes up in the tree.

We can simulate the mutation process by randomly placing them on the tree branches. A long branch will have more mutations than a short branch. Therefore, there is a link between coalescence time, branch length, and number of mutations: a long coalescence time corresponds to long branches and the accumulation of many mutations. We will use in this thesis the **infinite sites model** (Kimura, 1968), commonly used in population genetics: by assuming an infinite number of sites, we can remove the possibility that multiple mutations fall on the same site, which would complicate the mathematical derivations and rarely happens in humans.

It is also possible to model changes in population size by changing $N$ over time. There is a population expansion if $N$ is small in the older past and increases in the more recent past. In the opposite case, it is a demographic contraction. After an expansion, the coalescence times will get longer due to the increase of $N$. This is quite intuitive: the population being larger, it takes much longer to trace back the ancestor of two individuals, which therefore are particularly distant genetically from each other (i.e., a large number of mutations separate them). On the contrary, in the case of a contraction, the coalescence rate will increase, the individuals being more related. Therefore, knowing the coalescent tree of a sample with its branch lengths (i.e., coalescence times) makes it possible to have insight on the population's demography over time.

This initial coalescent model is the simplest. It only considers genetic drift, and only changes in population size are possible. Several extensions were subsequently developed, including natural selection, recombination, and migrations. As for natural selection, the difficulty lies in that an individual probability of reproducing depends on his parents. This dependence on past history makes backward models more challenging to develop. However, mathematical work has been done to allow the inclusion of natural selection in coalescent models (Kaplan *et al.*, 1988, 1989;

Hudson and Kaplan, 1995; Nordborg *et al.*, 1996; Nordborg, 1997).

It is also possible to include recombination in the coalescent model. In this case, there will be more than one tree, but rather a sequence of trees. Each tree will represent the history of a genomic region between two recombination points. Two adjacent trees differ only by one recombination event in the past, so they have only one difference. This difference can concern the trees' topology (the branching structure) or the branch lengths. By taking advantage of the similarities between nearby trees, it is possible to store the trees without repeating redundant information. An example of this format is the Ancestral Recombination Graph (ARG, Rasmussen *et al.*, 2014) or the tree sequence (ts, Kelleher *et al.*, 2016).

### 0.1.3 Inferring the past from the genome

Several processes can impact the genetic diversity of a population. For example, population size changes affect coalescent trees' branch lengths (see above). Conversely, we can investigate past demographic changes by sampling genomes from the population. Other processes can be detected, such as natural selection (Booker *et al.*, 2017) or migration (Palamara and Pe'er, 2013). Classically, we attempt to reconstruct past events by computing specific measures on a sample of genomes. These measures are called summary statistics. Some of them are particularly well-known and used often, and here we explain the principles behind the ones used in this thesis.

Genetic diversity in the most simple case of neutral evolution depends on population size ($N$) and the mutation rate ($\mu$). These two parameters are included within the $\theta$ parameter, which represent the total genetic diversity in a population, with $\theta = 2N\mu$. Several methods for estimating $\theta$ from genomic data were designed. Watterson's estimator of $\theta$ is defined as: $\hat{\theta_k} = \frac{k}{\sum_{i=1}^{n-1} 1/i}$, with $k$ the number of SNPs in a sample $n$ of genomes (Watterson, 1975). With $\hat{\theta_k}$, the more SNPs there are, the higher the genetic diversity. Another estimator of $\theta$ is based on the computation of the mean number of pairwise differences within the sample ($\pi$) (Tajima, 1983). The following formula can be used: $\hat{\theta_\pi} = \frac{n}{n-1} \sum_{i=1}^{k} 2p_i(1-p_i)$, with $p_i$ the allele frequency of mutation $i$. In the case of neutral evolution (only drift is at work, and the population size is constant), these two estimators of $\theta$ are equivalent. However, when the model deviates from the neutral model, they will differ. The measure called Tajima's $D$ relies on this difference (Tajima, 1989). This summary statistic evaluates the distance from neutrality by calculating the difference between the av-

erage pairwise differences in the sample ($\hat{\theta_\pi}$) and the scaled number of SNPs ($\hat{\theta_k}$), divided by the standard deviation of this difference. When Tajima's $D$ is negative, $\hat{\theta_k}$ is lower than $\hat{\theta_\pi}$, which happens when there is an excess of rare mutations. This excess appears in the case of positive natural selection or when the population has expanded. When Tajima's $D$ is positive, there is a deficit of rare alleles, as in the case of a contraction of the population size or of balancing selection.

A more exhaustive measure of allelic frequencies is also commonly used: the site frequency spectrum (SFS) (Fig. 3). Mutations are grouped into rarity classes, and the frequencies of each class are computed. The first class counts the mutations present only in one haploid individual in the sample (also called singletons). This class strongly impacts Tajima's $D$. The next class counts the mutations present in two haploid individuals in the sample (doubletons). The last class, of the most common mutations, counts those present in all but one individual in the sample. The difference between this class and the singletons can be noticed only if we know which is the ancestral allele and which is the derived one, generally by using an outgroup (i.e., the allele present in the outgroup can be considered as ancestral). In that case, the SFS is "unfolded" and has $n-1$ classes, with $n$ the sample size. When the ancestral allele is not known, we use the folded SFS, which has $n/2$ classes. The SFS allows a subtler analysis than Tajima's $D$, and its relation with the shape of the coalescent tree is often straightforward. For example, a tree with very long terminal branches, as in the case of expansion, will have an excess of rare mutations (and a negative Tajima's $D$).

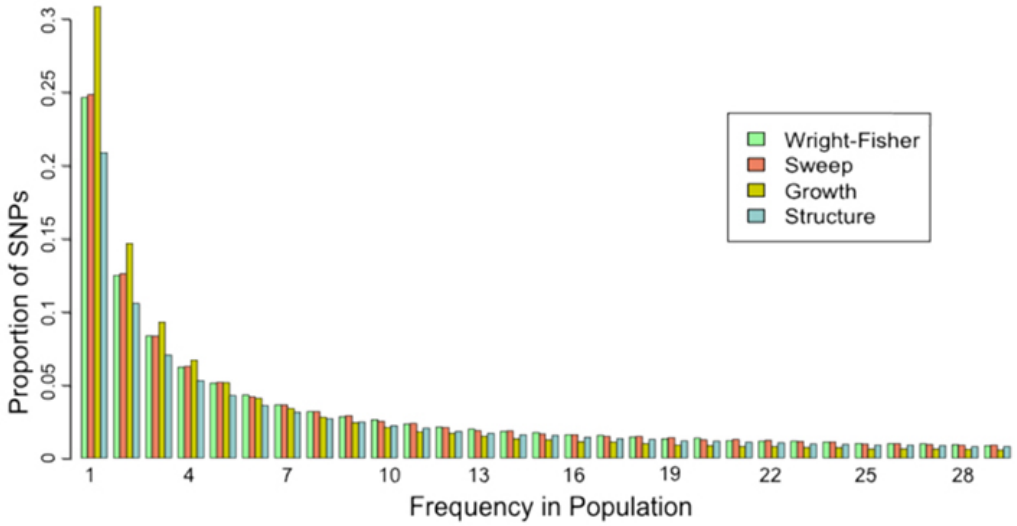


Figure 3: **Site Frequency Spectrum under several models.** Wright-Fisher is a model where individuals mate randomly and generations are not overlapping. Sweep is the process where a mutation becomes fixed due to selection. Growth is a population size expansion. Structure is when several subpopulations, with differences in allelic frequencies, coexist within a population. Figure from momi2 tutorial (https://radcamp.github.io/AF-Biota/07_momi2_API.html).

Some summary statistics are computed directly on coalescent trees' topology. In that case, we need to reconstruct the tree from the sampled genomic data, and several algorithms exist for this reconstruction (cf Methods section in Chapter 3). Imbalance indices measure the asymmetry of the tree, while balance indices measure its symmetry (Fig. 4). The more symmetrical the tree, the lower its imbalance indices and the higher its balance indices. There is a large variety of (im)balance indices, such as Sackin (Sackin, 1972), Colless (Colless, 1982), $B_1$ (Shao and Sokal, 1990), $B_2$ (Shao and Sokal, 1990), and Fusco (Fusco and Cronk, 1995). We will detail these indices in Chapters 2 and 3. Another summary statistic computed on trees' topology is the number of polytomies (Fig. 4). It corresponds to the number of non-binary nodes in the tree (e.g., tree 7 has a non-binary node located at the root in Fig. 4). It is equal to 0 in the classical coalescent, which assumes that the sample size is very small compared to the population size, and hence impossible that more than two lineages coalesce at the exact same time. In other types of models, such as in a forward model, it is possible to have non-binary nodes, and counting them can provide some information on the population history. However, it is essential to differentiate between two types of non-binary nodes. The first contains the real non-binary nodes, which come from multiple simultaneous coalescence events in an ancestor (due, for example, to a very high fitness of the ancestor). The second one

contains multiple coalescence events due to the process of tree reconstruction from the genomic data. Indeed, if there are no mutations on a branch of the real historical tree, the inferred tree might merge the nodes at both ends of the branch, resulting in a triple coalescence.

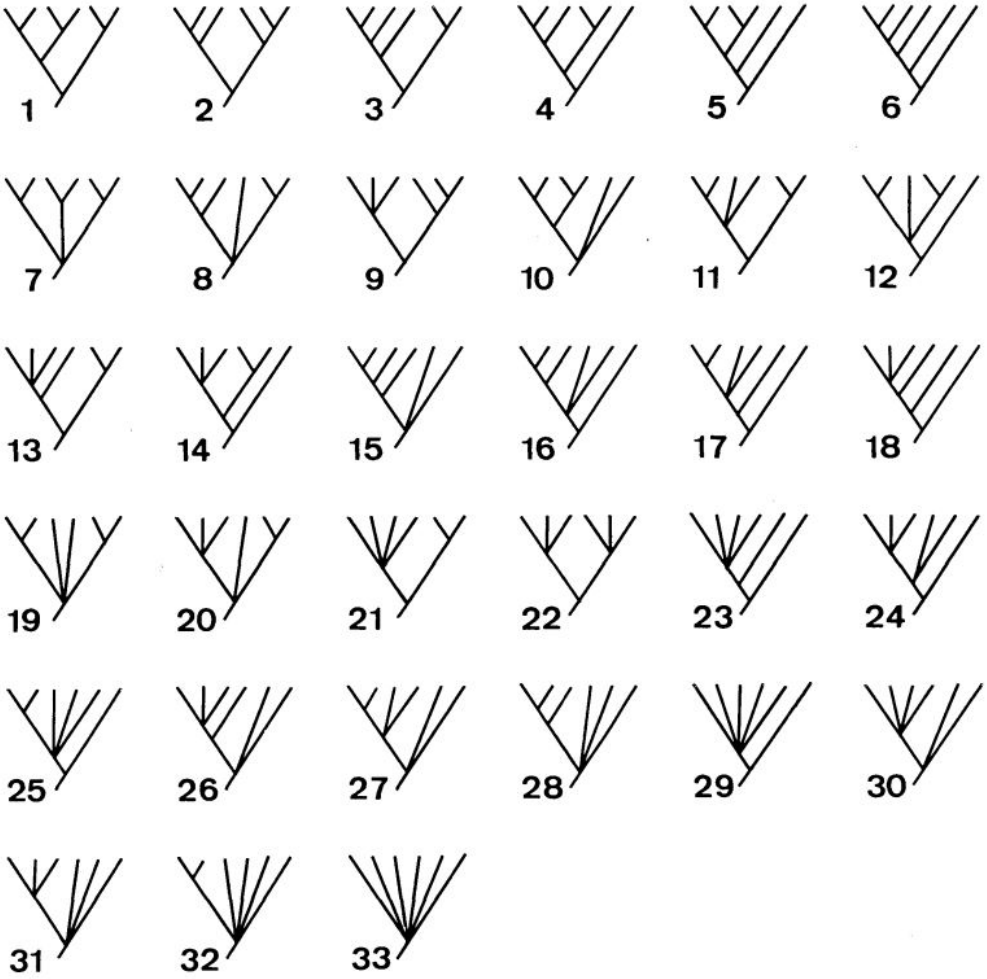


Figure 4: **All 33 possible coalescent trees of 6 samples.** First row (1-6) shows all possible *binary* coalescent trees of 6 samples, from the less imbalanced (1) to the most imbalanced (6). (The ranking is true for some imbalance indices but not for all of them. Some adjacent trees are considered equally imbalanced according to some indices.) Unlike binary trees 1-6, the trees 7-33 contain polytomies. The numbers of interior nodes (including the root) for trees 1-6, 7-18, 19-28, 29-32, and 33 are 5, 4, 3, 2, and 1, respectively. Number of polytomies is computed by counting the non-binary nodes. Figure and description from Shao and Sokal (1990).

### 0.1.4 Cultural Transmission of Reproductive Success

This thesis concerns a process that is little studied in population genetics, compared to the five evolutionary forces discussed above: the **Cultural Transmission**

**of Reproductive Success** (CTRS). This process occurs when the number of children of an individual correlates with the number of siblings for nongenetic reasons (Austerlitz and Heyer, 1998). Thus, individuals from large families will themselves tend to have more children than average (Fig. 5). In the case of natural selection, the fitness transmission from parents to children is conveyed through the vertical transmission of fitness-increasing alleles. In contrast, with CTRS, this transmission occurs through other means.

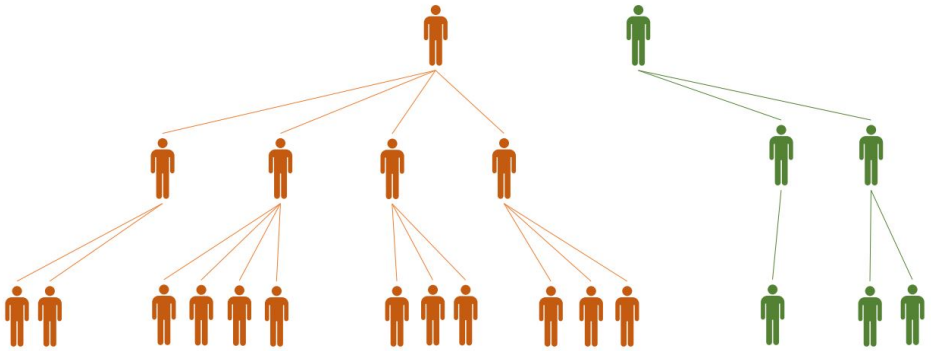

Figure 5: **Cultural Transmission of Reproductive Success (CTRS).** Individuals from the red (resp. green) lineage inherit culturally a propensity to have more (resp. less) children than average.

In human populations, CTRS can occur for three different reasons: (i) the cultural influence of parents on children on reproductive behavior, (ii) cooperation between siblings that increases their fitness, and (iii) the vertical transmission of resources correlated with fitness. These resources can be material, social (e.g., the transmission of social rank), or cultural (such as hunting techniques). The cultural transmission of the propensity to leave one's birthplace can also lead to a form of CTRS. Indeed, lineages whose descendants tend to leave the population will appear less fertile, as they will contribute less to the genetics of their population (Gagnon and Heyer, 2001; Gagnon *et al.*, 2006).

Parent-child correlations in the number of siblings were measured in several human populations. In particular, these correlations exceed 0.2 among Mormons (Wise and Condie, 1975), Hutterites (Pluzhnikov *et al.*, 2007), in the United States (Murphy, 1999) and in several European countries (Pearson *et al.*, 1899; Bresard, 1950; Murphy and Wang, 2001).

However, although the existence of correlations has been established, it is still to be determined to which extent they are genetic (and therefore indicative of a process of natural selection) and/or cultural (and therefore a process of CTRS). In

the case of a genetic transmission, we face the so-called **Fisher's paradox** (Hughes and Burleson, 2000): since selection reduces the genetic variance in the population until none is left, why do we still find parent-children correlations in progeny size nowadays? An inheritance as faithful as genetic inheritance, combined with such strong correlations, should reduce diversity rather quickly and leave only the fitness-enhancing allele in the population. Once the favorable allele has invaded the population, correlations would be null. In the case of a cultural transmission, this erosion of variance is less likely to occur, since this transmission is not very faithful from one generation to the next. The absence of Fisher's paradox in a cultural transmission is thus an argument for its proponents (Heyer *et al.*, 2012). However, different explanations have been given to explain the persistence of correlations in the case of genetic transmission of reproductive success. For example, the correlations can be caused by the transmission of very multigenic traits, for which the mutation rate is high because mutations can appear in a large part of the genome. The fidelity of inheritance is therefore reduced, and the erosion of variance is absent or less rapid. We will discuss other answers to Fisher's paradox in Chapter 1.

The transmission of reproductive success has several effects on the genome, including a decrease in genetic diversity. This is true regardless of the transmission origin, genetic (natural selection) or cultural (CTRS). However, depending on the origin of TRS, some effects will be different. The first difference appears in the presence of recombination. In this case, the effects of natural selection will be restricted to the region of the locus under selection. The CTRS, on the other hand, will affect the whole genome, since CTRS is not carried by a particular gene but by a cultural trait. In the case of multigenic selection, however, many genomic regions may also be affected. Yet, multigenic selection differs in its effects from CTRS. One of the differences is the neutral regions of the genome concerning multigenic selection, whereas CTRS impacts the entire genome. We will discuss other differences between CTRS and multigenic selection in Chapter 1.

The effects of CTRS on the genome are multiple. Genetic diversity is reduced, which might increase the propensity of genetic diseases in the population. This has been shown in the Saguenay-Lac-Saint-Jean region of Quebec, where a fairly strong CTRS has occurred for 12 generations. Several genetic diseases occur in high frequency in this population, such as some forms of Cytochrome C oxidase deficiency and Spastic ataxia that are non-existent or sporadic in other human populations (Austerlitz and Heyer, 1998). The topology of coalescent trees is also impacted by CTRS, with a stronger imbalance than the neutral case. The imbalance is a measure

of tree skewness for which several indices exist (see section 0.1.3). Moreover, branch lengths are also impacted, with a non-homogeneous reduction of the branches: the oldest branches are more reduced than the recent branches. We will discuss the effects of CTRS on population genetics in more detail in Chapters 1 and 2.

CTRS is not solely occurring in humans. It has been detected in several animal species, such as hyenas (Engh *et al.*, 2000; Ilany *et al.*, 2021), cetaceans (Frere *et al.*, 2010; Whitehead *et al.*, 2017), and monkeys (Kawai, 1958; Whiten *et al.*, 1999; Leca *et al.*, 2007; Hobaiter *et al.*, 2014; Robbins *et al.*, 2016). Furthermore, although we use the term cultural TRS here, it would be more accurate to speak of nongenetic TRS, to explicitly include any vertical transmission of fitness that is not carried by genes. This generalization allows the inclusion of processes such as TRS produced by any parental effect (e.g., a parent who is more robust than average for nongenetic reasons may have more children than average, who will also be more robust than average, due the good parental care the parent can provide, and so on.) Similarly, ecological inheritance can lead to nongenetic TRS: a parent born in a favorable environment will have more children than average and may transmit this fitness-correlated environment to his descendants. In sum, nongenetic TRS is a broad phenomenon that encompasses different mechanisms and affects many species. Whatever the mechanism of fitness transmission, as long as it is not genetic, we are dealing with nongenetic TRS with all the effects on the genome mentioned above. This diversity of nongenetic TRS encourages further investigation of this process's effects and the development of methods to detect it from the genome. We will discuss the generalization of CTRS in Chapter 1.

## 0.2 Inference methods

To infer past events within a population, we can compute different summary statistics (see section 0.1.3, and others not mentioned there, such as F statistics or linkage disequilibrium). However, several events may have the same effect on a given summary statistic. For example, the number of SNPs decreases in the case of a bottleneck, as well as in the case of natural selection. Similarly, Tajima's $D$ becomes negative in the case of an expansion as well as in the case of natural selection. The difficulty often lies in distinguishing between several processes with similar effects. In this thesis, one of the objectives will be to distinguish between CTRS and demographic events. Chapter 2 will show how they can be confused, by measuring the bias in demographic inference when CTRS occurred in the population. Chapter 3 will develop methods to remove this bias and achieve a correct joint inference of CTRS and demography. The main principles of the inference methods that we will use in Chapter 3 are introduced in this section. The more technical details will be detailed in the Methods section of Chapter 3.

An inference method can address two type of tasks: **classification** or **regression**. The first task aims at dividing data into two or more classes. For example, it would classify images in the cat or dog category. In population genetics, we may want to distinguish populations that have undergone a recent period of natural selection on a given gene from those that have not. The second task, regression, seeks to find from the data the value of a parameter or several parameters whose prior is continuous. For example, we could infer the age of a tree by knowing its diameter and height. In population genetics, we may want to infer from genomic data the intensity of natural selection and the type and the intensity of a demographic event. We will therefore have two parameters to infer: the selection coefficient $s$, and the growth factor $g$. If we infer $s = 0$ and $g = 10$, there was no selection and a demographic growth where the population size was multiplied by 10. If we infer $s = 0.1$ and $g = 0.1$, there is a selection coefficient of 0.1 and the population size was divided by 10 (a contraction).

In this thesis, we will use two main categories of inference methods to solve regression tasks. The first approach relies on the combination of several summary statistics, and the second is based on machine learning directly applied to raw genomic data. This section will describe both approaches, using the above $s$ and $g$ parameters inference as an example.

### 0.2.1 Combining several summary statistics

We have seen that several processes can affect the same summary statistic similarly. In order to tell these processes apart, we can combine several summary statistics. For example, we can observe a low genetic diversity, due to contraction, natural selection, or a combination of both. By observing a negative Tajima's $D$, we can rule out the hypothesis of a decrease in diversity due to contraction alone. Of course, the reality is generally more complex, and combining more than two summary statistics is often necessary. In order to make this inference by combination, several methods are possible, such as **Approximate Bayesian Computation** (ABC), **neural networks** applied to summary statistics. In this thesis, we will use ABC and detail this method here.

Approximate Bayesian Computation (Beaumont *et al.*, 2002; Csilléry *et al.*, 2010, 2012), as its name indicates, is a **Bayesian inference** method. To perform a Bayesian inference (Fig. 6), we need two elements. The first is a **likelihood function**: it defines the probability of observing data knowing the parameters of a model. For example, the likelihood function would say: *"there is a 1% chance of observing this genomic data, given that the parameters are* $s = 0.1$ *and* $g = 2$*"*. The full likelihood function will state the probability of each possible SNPs combination in the sample, given each possible parameter's combination of values. The second necessary element for Bayesian inference is the **prior**: it is the distribution of the belief we have about the parameters to be inferred, before any inference. For example, let us say we know that the demographic event was an expansion, and we know it was not more than tenfold. We also know that the selection coefficient is not above 0.2. In that case, the prior of $g$ could be a uniform distribution with parameters $]1, 10]$, and the prior of $s$ could be a uniform distribution with parameters $[0, 0.2]$. It will then suffice to apply Bayes' formula: $posterior = (prior \times likelihood)/evidence$ (the evidence is used here to normalize the posterior to 1, and corresponds to the marginal likelihood, i.e., the probability that the data are observable). The **posterior** would be the parameters joint probability distribution after inference, and the most probable values can be used as point estimates of the parameters.

In practice, it is possible, although not always easy, to have a sensible prior. However, the likelihood function is often far too complex to be computed entirely. Therefore, applying this exact Bayesian framework to our population genetics questions is impossible. To overcome this problem, we will use ABC, which allows us to perform Bayesian inference without knowing the exact likelihood function. The

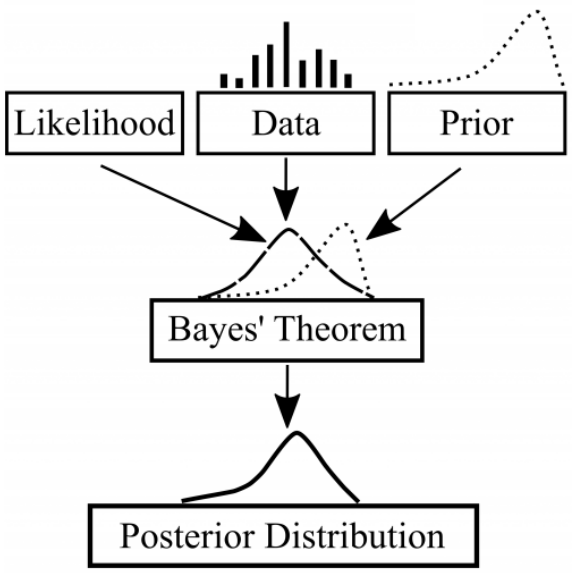


Figure 6: **Schematic view of Bayesian inference.** Figure from Ankit Rathi's website.

idea is to approximate the likelihood function with computer simulations (Fig. 7). To do this, we will randomly draw the parameters in the prior distribution, in order to simulate the genetic data. Many simulations are performed, until the set of parameters-data pairs obtained gives us an approximation of the likelihood function. The distribution of the observed data in simulations for a given pair of parameters will correspond to the probability of these data given the parameters. Using our prior and this approximation of the likelihood function, we can then compute the probability of the parameters knowing the data, which will be our posterior.

Different algorithms exist for ABC (one of them is described in Fig. 7), but all rely on an approximation of the likelihood function through simulations. However, the problem lies in correctly approximating the likelihood function when a large number of possible genetic data exist for a sample of $n$ individuals. A good approximation of the likelihood function requires estimating the probability of observing each possible data set, for each given parameter combination. This would require many simulations to cover all combinations of data and parameters. Therefore, we use **summary statistics** to reduce the **dimensionality** of the data and approximate the likelihood function with fewer simulations. Once the data are summarized, we can look for the likelihood function of observing a given combination of summary statistics, knowing the model parameters.

In Chapter 3, we will use a version of ABC called **ABC random forest** (Pudlo *et al.*, 2016; Raynal *et al.*, 2019). This method approximates the likelihood function

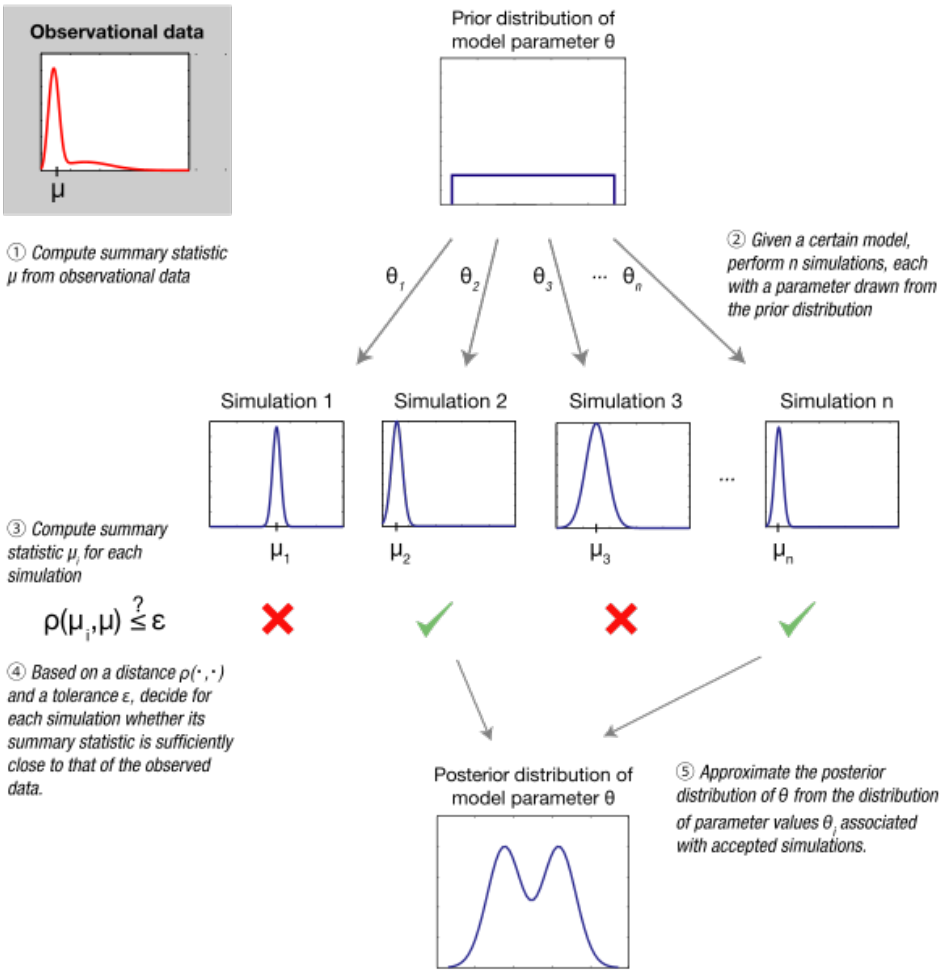


Figure 7: **Approximate Bayesian Computation.** This basic example uses the rejection algorithm. Figure from Sunnåker *et al.* (2013)

by using **decision trees**. The details will be presented in the Methods section of Chapter 3. It is only necessary to remember that, as for any ABC method, we will simulate a large number of genetic data by randomly drawing the parameters in a prior. Then, we will compute summary statistics and train the algorithm to find the probability of observing the summary statistics knowing the parameters (the approximate likelihood function). This algorithm will build the likelihood approximation by observing the parameters and the associated summary statistics of a training dataset. It will then be possible to find the posterior from another set, called the test set. For each genetic data of the test set, we can compute the summary statistics and infer the parameters, by choosing for example the most probable parameters given the observed summary statistics as our inference (i.e., the mode of the probability distribution). Finally, the inferred parameters can be compared

to the true parameters used for the simulations, in order to evaluate the inference accuracy.

### 0.2.2 Deep learning on raw genomic data

This second method will infer directly from raw genomic data without using summary statistics. Deep learning is particularly adapted to this task because it can find information by itself within complex data. We will use a complex convolutional neural network, called SPIDNA and designed by Sanchez *et al.* (2021). We will detail its architecture in the Methods section of Chapter 3, and more details can be found in the original paper. Here we will introduce the basic principles of neural networks, and address the general issue of their applications in population genetics.

#### What are neural networks?

**Neural networks** (McCulloch and Pitts, 1943) are a class of data analysis methods often used for inference. We will use them to infer the parameters of a population genetics model from genomic data. A neural network can address the two inference tasks described above: **classification** or **regression**. Neural networks are, in fact, mere functions applied one after the other, sometimes in complex sequences, in order to analyze data. These sequences of functions are constructed through a learning process. This means these functions contain variable parts that will be modified during a training phase until they are optimal. When these function sequences are correctly optimized, they can extract the desired information from the input data. A neural network always has one or more input values, which correspond to the data to be analyzed, and one or more output values, which correspond to the information extracted from these input data. Between the input and the output is this sequence of functions to optimize. The type and organization of these internal functions are what we call the neural network **architecture**.

The variable parts of the internal functions network are optimized during a **training phase**. During this phase, the network will "observe" input data with their associated output. The variable parts of the functions will be modified little by little during this phase. The objective is that at the end of this phase, when the network is given the input data, it responds with output values as close as possible to the true values (i.e., we want to minimize the difference between the network outputs values and the true values). We evaluate the quality of the network optimization by

presenting it with new input data, which it will never have seen during the training and for which we know the true output values. The difference between the output values of the network and the true output values will be the basis for evaluating the quality of the network optimization. Sometimes, the network may give excellent results on the data it has already seen (**training set**) and wrong results on the data not used for training (**test set**). In this case, we say that there is **overfitting**. This means that the variable parts of the network have been over-optimized, to the point that the correct input-output relationship is only achieved on the data already seen. One of the major challenges is reaching good results on the test set, thus achieving a form of **generalization**. We will now explore different types of neural network architectures, from the simplest to more complex forms.

### The perceptron

The **perceptron** (Fig. 8) is the simplest type of neural network: it corresponds to a single neuron. It is composed of five parts.

1. The input vector $\vec{x}$, containing the data we want to analyze. This vector can be of any length between 1 and $\infty$. It is the object to analyse, for example an encoded image or genomic data from a sample of individuals.

2. The weights $\vec{w}$. Each value of the input vector $\vec{x}$ is associated with a weight in $\vec{w}$. The weights are real numbers that can evolve during the training phase. These weights correspond to the variable part of the functions introduced in the previous section. An optimizable value with no association to any input can be added. This bias $b$ allows a greater learning capacity.

3. A weighted sum function, which adds the input values weighted by their associated weights: $\sum_{i=0}^{n} w_i \times x_i + b$, with $n$ being the length of the vectors $\vec{w}$ and $\vec{x}$.

4. The **activation function**. Several types of activation functions exist. One of the simplest is the Heaviside step function: it is defined on $\mathbb{R}$ and has only two output values, 0 or 1. The Heaviside function outputs 0 for any value lower than 0, and 1 for any value higher than 0. Therefore, it is only used in the case of a classification task. In this case, we will need this step to transform the continuous value of the weighted sum (part 3) into a binary value. By associating 0 to the cat category and 1 to the dog category, it is possible to

use the activation function to transform the weighted sum of part three into a cat or dog classification. In the case of a regression, the Heaviside function is absent. We can take the result of the weighted sum (part 3) directly as the output value of the network: the perceptron will then be equivalent to a **linear regression**. Otherwise, we can replace the Heaviside function by a non-binary and non-linear output function, like the sigmoid ($\mathbb{R} \rightarrow ]0,1[$). In the latter case, we will have a **sigmoid neuron**, a slightly modified version of the classical perceptron.

5. The final part is the output vector $\vec{y}$. In a classification task, this is the output of the activation function. In a linear regression, it is the output of the weighted sum function.

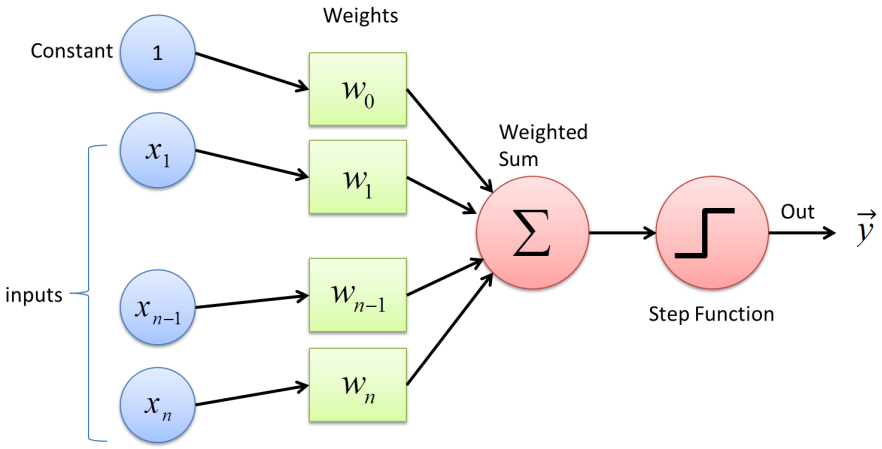


Figure 8: **Diagram of a perceptron.** The weight $w_0$ corresponds to the bias $b$ in the text. Figure modified from the deepai website.

It remains now to optimize the weights, so that the expected output values correspond as closely as possible to the observed output values. For this, several algorithms exist. Their role is to define how to modify the weights little by little to reach optimization. We will briefly describe one of these algorithms, called **gradient descent** (Fig. 9). It is an iterative method that minimizes the distance between the expected and observed outputs on the training set. This distance is represented by the **loss function**, $L(w)$ (also called the **cost function**). Several loss functions exist, the most common being the **Mean Squared Error** (MSE) of the differences between the observed (i.e., the true) and predicted outputs (also called $L^2$ norm), according to this formula: $\frac{1}{n}\sum_{i=1}^{n}(y_i - \hat{y}_i)^2$, with $y_i$ the observed outputs and $\hat{y}_i$ the predicted outputs. We will have reached optimization by finding the values of the weights for which $L(w)$ is the lowest for the training dataset. In other words,

we look for the minimum of the loss function $L(w)$. To find it, we need to know the gradient of $L(w)$ and move in the opposite direction, in order to move toward its lowest point. In practice, we initialize $\vec{w}$ randomly; then we modify it at each iteration $j$ according to the following formula:

$$w_{j+1} = w_j - \gamma \times \nabla(L(w_j))$$

Two parameters impact the magnitude of the change in $\vec{w}$ at each iteration: (1) $\gamma$, the learning rate, which can be fixed or evolve in a predetermined way during the iterations, and (2) the loss function gradient, which varies during the optimization process, depending on the values of $\vec{w}$. We repeat the operation until we reach a gradient of 0 (or until a predefined number of iterations has been done). It is possible that the minimum found is only a local minimum and that a lower global minimum exists, meaning the optimization of $\vec{w}$ could be better. Finding the global minimum is one of the challenges of gradient descent and of neural networks that use this optimization method to modify their weights.

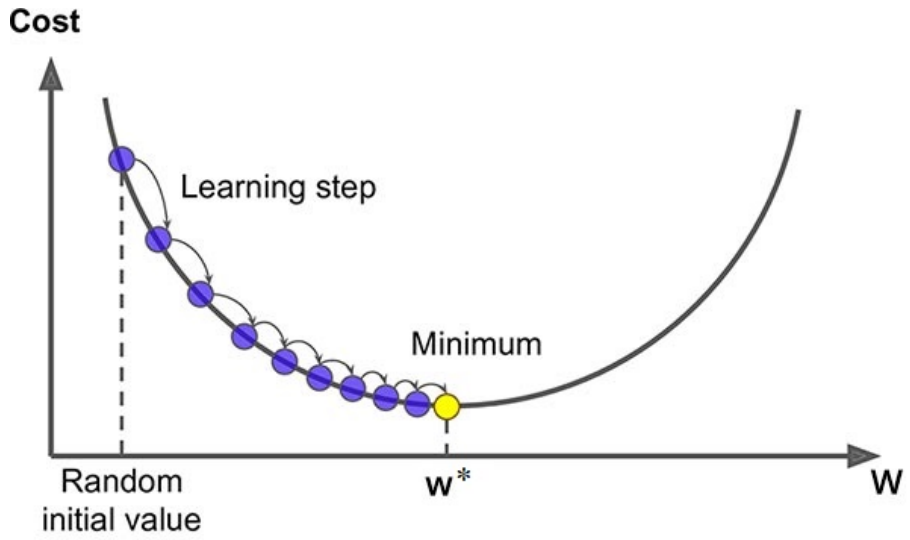


Figure 9: **Diagram of gradient descent.** $w^*$ is the optimal value that the gradient descent algorithm tries to find. Figure modified from Saugat Bhattarai's website.

### Multilayer perceptron

The limitation of the perceptron is its inability to analyze non-linearly separable data (Minsky and Papert, 1969). The **multilayer perceptron** (MLP), also called

**fully connected network**, allows to tackle nonlinear problems, which is the case of most problems in practice. Simply put, the MLP links several perceptrons together.

More precisely, the MLP architecture includes at least three layers of neurons (Fig. 10): the input layer, the hidden layer and the output layer. There can be more than one hidden layer, but we will keep a simple example with only one hidden layer. One of the particularities of the MLP is that it is fully connected. This means that all input layer neurons connect to all hidden layer neurons, and all hidden layer neurons connect to all output layer neurons. Each of these connections corresponds to a weight $w$, which can evolve during the training phase, as for the perceptron. There will be more weights than for the perceptron, and they will be organized in more layers.

Each neuron of a hidden layer will have for value the result of a weighted sum function of the previous layer, followed by a nonlinear activation function. For the first hidden layer, the formula would be: $\vec{a}^1 = \sigma(W^1\vec{x} + \vec{b}^1)$, with $\vec{a}^1$, the output values of the neurons of the first hidden layer; $\sigma$, an activation function such as the sigmoid; $W^1$, the matrix of weights linking the neurons of the input layer to the first hidden layer; $\vec{x}$, the input values; $\vec{b}^1$, the bias vector. The other $L$ layers use this formula: $\vec{a}^l = \sigma(W^l\vec{z}^{l-1} + \vec{b}^l)$, with $l$ the current layer, and $\vec{z}$ the output vector of a layer. The optimized values are all the weights $W = \{W^1, W^2, ..., W^L\}$ and all the biases $\vec{b} = \{b^1, b^2, ..., b^L\}$. More recently, it has become common to use the ReLU (Rectified Linear Unit) function instead of the sigmoid as an activation function. This function allows to train more easily deep networks (i.e., with many hidden layers) and is defined as follows: $ReLU(x) = max(0, x)$.

The MLP training is performed using the gradient descent method presented for the perceptron. First, the weights of the network are randomly initialized. Then, as for the perceptron, the gradient of the loss function is computed with respect to the weights to understand how a slight modification of the weights affects the loss. In the case of a complex network like the MLP, the loss gradient is computed for each input data for all weights using a method called **backpropagation** (Rumelhart *et al.*, 1986). This method computes recursively the gradient in each layer with respect to the previous layers using the chain rule. More than the loss gradient for a single data point is required: the total gradient is computed for all the data. This gradient will allow a modification of the weights in the right direction with the formula: $W_{j+1} = W_j - \gamma \times \nabla(L(W_j))$. At each iteration $j$, the weights are modified, hence reducing the loss and approaching the optimal values.

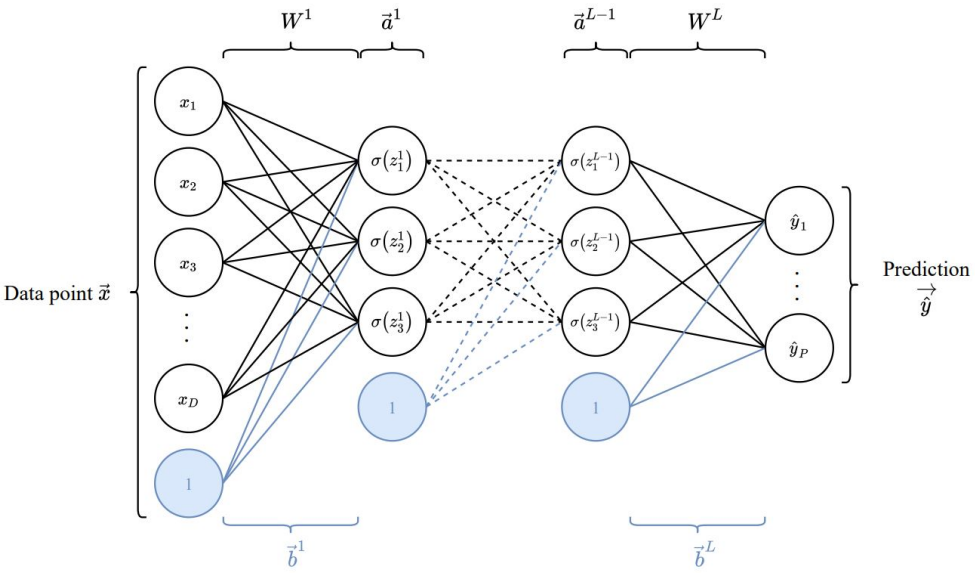


Figure 10: **Diagram representing a multilayer perceptron (MLP).** A data point $\vec{x}$ passes through a series of hidden layers defined by their weights $W^l$ and bias $b^l$. Each output $z^l$ of an hidden layer passes through an activation function $\sigma$. Last layer outputs the prediction of the network $\vec{\hat{y}}$. Figure and description from Sanchez (2022).

In practice, we often use a version of the gradient descent called **stochastic gradient descent**. This choice is motivated by a limitation of gradient descent: the gradient must be computed for the whole data set at each iteration. For a relatively long gradient to compute in a complex network, the total computation time for each iteration will be too long to handle. Stochastic gradient descent tackles this issue by dividing the training dataset into parts called **mini-batches**. At each iteration, the gradient is computed on one mini-batch only, and the weights are modified accordingly. At the next iteration, we use another mini-batch, until the network has seen at least once all the data.

In theory, any function can be approximated with a sufficiently complex MLP. However, the larger and deeper the MLP, the more difficult and time-consuming it is to optimize the weights. In some cases, computers will not have the necessary computational capacity. For this purpose, other types of networks have been developed later, such as **Convolutional Neural Networks** (CNN), which we will briefly describe in the next section.

### Convolutional Neural Networks

Unlike an MLP, the hidden layers of a CNN (Lecun *et al.*, 1998) can be of several types. The **convolution** is the major type of layer, and gives its name to the CNN. As input, each convolution layer takes a matrix C, the previous layer's output. The convolution layer applies a **filter** A on **sub-matrices** B of this input matrix C (Fig. 11). A filter, also called mask or kernel, is a weight matrix of the same dimension as the sub-matrices B. Applying a filter consists in computing the weighted average of the product of the weights with the values of the same index in the sub-matrix B (in other words the weighted average of the Hadamard product of the matrices A and B). This filter slides on matrix C, outputting one result per sub-matrix B. The matrix of the results will be the layer's output. We define the filter's moving steps over matrix C by two **stride** parameters, one that defines the displacement of the filter in the direction of the rows and the other in the direction of the columns. The weights to be optimized are those carried by the different cells of the filter. Therefore, there will be much fewer weights to optimize than in an MLP, which is fully connected, and the computation time will be faster. In practice, each layer comprises several filters, each independently optimized. Each filter can capture different information in the data.

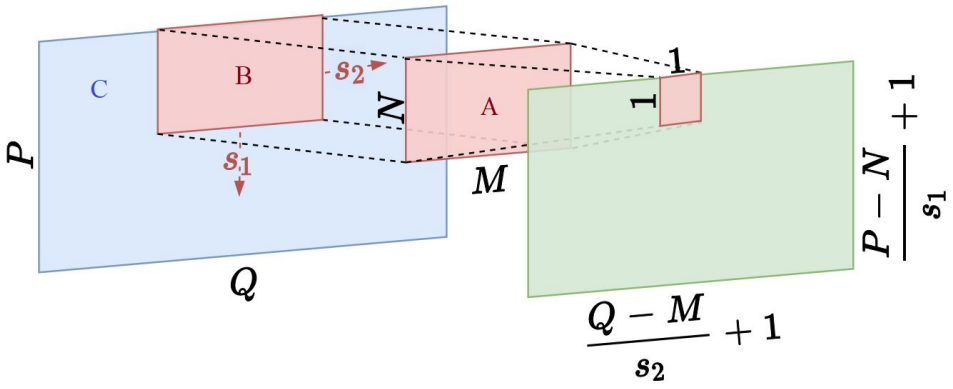


Figure 11: **Diagram of a convolution filter in two dimensions.** The filter A (in red) is applied over a matrix C (in blue), resulting in the green matrix. Each element of the green matrix is computed by performing the weighted average of the Hadamard product between the mask and the corresponding window over the blue input matrix C. $s_1$ and $s_2$ denote the strides of the filter in the two dimensions. Figure and description adapted from Sanchez (2022).

### Deep learning in population genetics

There are two ways to use deep learning (DL) for inference in population genetics: applying the neural network to summary statistics or applying it directly to raw genomic data. In this thesis, we have opted for the second strategy for DL, and will compare its learning capacity to that of ABC random forest (ABCrf) on summary statistics. As for ABCrf, we will perform the training and testing phases on separate sets of simulated data. We will use the same data for ABC and DL to make the comparison as fair as possible.

The genomic input data are formatted as SNP matrices. These matrices have in rows the different individuals and in columns the loci. The cells of the matrix can contain a 0 or a 1, with each cell representing the allele state for the given individual at the given locus (0 representing the ancestral allele). The matrix is associated with a position vector containing the absolute or relative positions in the genome of each SNP (Fig. 12).

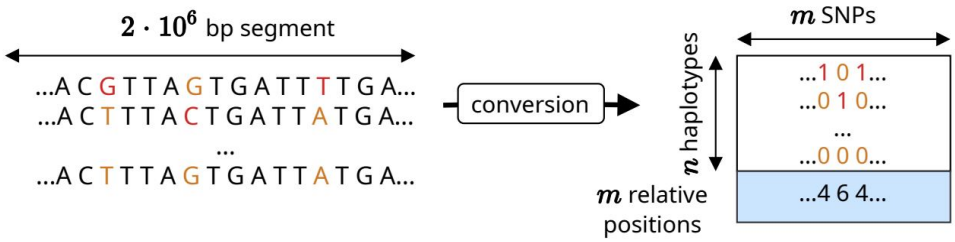


Figure 12: **Converting genomic data to a SNP matrix.** Here, recent alleles (in orange) are encoded by ones and ancestral alleles (in red) by zeros. The SNP matrix has a relative position vector that encodes the distance of each SNP to its right neighbour. An absolute position vector can also be used. Figure and description adapted from Sanchez (2022).

Since the rows of the SNP matrix correspond to the individuals, one should be able to swap rows without changing the matrix information. However, a CNN is naturally sensitive to spatial information, and might want to look for patterns in the order of the rows. Several solutions exist to inform the network of the rows' exchangeability. The first solution would be to train the network to understand the absence of information in the order of the rows, which can be helped with data augmentation (e.g., deliberately permuting the rows). However, this induces a loss of computational resources because the network must learn the exchangeability of the rows in addition to its task. Several studies have explored an alternative solution: ordering individuals according to a specific criterion (Flagel *et al.*, 2019; Torada *et al.*, 2019). However, Chan *et al.* (2018) chose to make the neural network

exchangeable by design by adding invariant operations (Zaheer *et al.*, 2017). Sanchez *et al.* (2021) used a similar technique, based on Lucas *et al.* (2018)'s work. They applied it to SPIDNA, the network architecture we will use here. The Methods section in Chapter 3 will describe SPIDNA's architecture in more details.

## 0.3 Thesis objectives

This thesis investigates the topic of nongenetic TRS on several axes, all interconnected.

### 0.3.1 Chapter 1: A review of TRS

TRS is a complex phenomenon in its causes and consequences. It belongs to different bodies of literature: sociology, anthropology, demography, medical genetics, population genetics, and evolutionary biology. The first chapter reviews the topic of TRS from the perspectives of different disciplines in order to answer several major questions. The first part of this chapter deals with the evidences of TRS in human populations and analyzes the modalities of this process. The second part addresses the different mechanisms leading to TRS in humans and touches on the problematic question of the origins of TRS: are they genetic or cultural? The third part will explore the different effects of TRS on population genetics and review the literature on the inference of nongenetic TRS. The fourth part generalizes nongenetic TRS beyond humans. It was indeed described in other animals and it might even affect all living organisms, raising the question of its importance as an independent force in evolutionary theory. This first chapter thus provides an understanding of the importance of nongenetic TRS by considering its presence not only in humans but in other species as well, while addressing the complexity of its origins and consequences. This chapter will be the starting point for a review paper manuscript.

### 0.3.2 Chapter 2: CTRS effects on population genetics

The second chapter is an article accepted in the journal Genetics. Its objective is to study the different impacts of CTRS on genetics using simulations and coalescent tree analyses. It shows that the impact of CTRS on population genetics is complex and composed of different subparts. We study the temporal dimension of CTRS to reveal its effects over time, as well as its interactions with demographic processes. Furthermore, we show that allelic frequencies are impacted by CTRS yielding a bias in demographic inference. This chapter thus raises the question of the accuracy of demographic inference in species that have undergone a CTRS process.

### 0.3.3 Chapter 3: Joint inference of CTRS and demography

The third chapter aims at correcting this bias in demographic inference under CTRS. To do so, we develop and compare several inference methods based on ABC random forest and deep learning. By training the algorithms on simulated data from populations with both demographic and CTRS histories, we can learn to distinguish the two. The goal is to infer demographic history and CTRS intensity successfully. Furthermore, by comparing ABC random forest algorithms using different summary statistics, we can gain insight into which ones matter most in distinguishing the two processes, thus providing a better understanding of their interactions. This chapter is a research paper manuscript that we aim to submit ultimately.

### 0.3.4 Chapter 4: CTRS and other processes

This chapter analyses preliminary results concerning the comparison of CTRS with other processes (monogenic positive selection and migration). Several coalescent tree topology statistics that are impacted under CTRS are examined under selection, CTRS, or a combination of both, using computer simulations. The results are presented across time to compare the dynamics of their evolution under such processes, as well as across the genome to reveal differences in genomic patterns. Imbalance is also measured on inferred coalescent trees (using relate, Speidel *et al.*, 2019) across chromosome 22 in two real populations genomic data (Sardinians and Yakut, HGDP, Bergström *et al.*, 2020), in order to compare them. Effects of migration on CTRS detection are also explored, using a realistic multipopulation model (Gravel *et al.*, 2011) to which we added CTRS.

# Chapter 1

# A review of TRS

## Introduction

In 1899, Pearson *et al.* published a paper entitled "On the Inheritance of Fertility in Mankin", where they formally proved the existence of a progeny size inheritance using the British Peerage genealogical data. Fisher (1930) extended this analysis a few decades later and computed from the same dataset a heritability of progeny size of around 40%. Scientific interest dwelled on this question for the next century, with a number of studies evaluating the extent of this inheritance in several human populations around the World. They showed that most populations display a positive although relatively weak correlation in progeny size between parents and children (up to 0.2), with rare cases of null or negative correlations (Murphy, 1999). These positive correlations will be called here "transmission of reproductive success" (TRS). The first part of this review will gather evidence of TRS in human populations from various studies, and examine the processes affecting it.

One of the main questions regarding TRS has been the so-called Fisher's Paradox (Kirk *et al.*, 2001; Rodgers and Doughty, 2000): according to Fisher's fundamental theorem of natural selection, such an inheritance should rapidly yield an erosion of the variability in fertility in the population, to the point where selection stops and the correlation between parents and children fitness disappears. The positive correlations in progeny size between parents and children measured in many human populations have thus puzzled scientists for decades, with various hypotheses proposed as an answer. Another point of debate concerns the causes of TRS (Rodgers and Doughty, 2000; Beaujouan and Solaz, 2019; Bernardi, 2016) in those popula-

tions: are they due to cultural or genetic factors? This question is related to Fisher's Paradox. In fact, in the case of cultural TRS, the paradox is less of an issue due to the substantial variance in cultural practices appearing at each generation. On the other hand, in a genetic TRS, the genetic mutation rate in Humans seems too low to bring enough variability to counteract the erosion of variance. This review will thus discuss in detail both possible causes of TRS in light of studies from various fields.

Geneticists' interest in this question has long been related to this matter of genetic causes of TRS. However, Nei and Murata (1966) approached this topic's relation to genetics from another angle and demonstrated theoretically the effects of TRS on genetic diversity, showing its decrease due to a smaller effective size. It is worth noting that its impact on genetics will have distinct properties depending on its cause: when the transmission from parents to children is conveyed by genetics, the process can be assimilated to natural selection, with recombination constraining the effects to the locus under selection and its genomic region. On the other hand, when TRS is nongenetic (e.g., cultural) and thus unrelated to any locus in particular, the effects will span the entire genome, yielding low diversity in all loci and increasing risks of genetic diseases in the population (Austerlitz and Heyer, 1998). This specific impact of cultural TRS has thus been used to detect such a process from numerous human populations genomic data (Blum *et al.*, 2006; Heyer *et al.*, 2015). This impact on the whole genome has another consequence: it can be a confounding factor for demography inference based on genetic data. We will in the second part review the literature about the impact of TRS on population genetics and compare it to other processes.

It is possible to generalize the notion of nongenetic transmission of reproductive success to other species than humans. Indeed, since several animal species have a culture, they can transmit fertility by this means, for example, by social rank transmission. Other pathways of nongenetic inheritance, such as ecological inheritance, could also lead to nongenetic TRS. The third part of this review focuses on a generalization of nongenetic TRS by exploring different mechanisms and species involved.

This topic is of utmost importance for three main reasons. First, fertility transmission is a central part of the evolutionary process in any species. Second, understanding better this process will help detecting it in genomic data, which matters not only for understanding populations' cultural aspects, but also to improve the inference of other processes (e.g., selection or demographic history). Last, nongenetic

TRS challenges the modern synthesis (Huxley, 1942) which only includes natural selection, and calls for an extended synthesis.

## 1.1 Evidence of TRS in humans

Several studies have evaluated the impact of sibship size on progeny size. In many populations, positive correlations were found between the two values (Murphy, 1999; Duncan *et al.*, 1965; Jennings and Leslie, 2013). These correlations exceed 0.1 in several populations: in the United Kingdom (Berent, 1953; Murphy, 1999), in the United States (Ben-Porath, 1975; Johnson and Stokes, 1976), and several continental European countries (Murphy and Wang, 2001; Reher *et al.*, 2008; Kolk, 2014; Rotering, 2017; Beaujouan and Solaz, 2019). Correlations exceeding 0.2 have sometimes been estimated, such as among Mormons (Wise and Condie, 1975), Hutterites (Pluzhnikov *et al.*, 2007), in the USA (Murphy, 1999), and several European countries (Pearson *et al.*, 1899; Bresard, 1950; Murphy and Wang, 2001). Other studies showed that childbearing timing is also transmitted, with, for example, a parent-child correlation in age at first birth or age at marriage, these traits being often correlated with total reproductive success (Manlove, 1997; Barber, 2001; Steenhof and Liefbroer, 2008; van Poppel *et al.*, 2008; Monden and Smits, 2009; Jennings *et al.*, 2012; Stanfors and Scott, 2013). However, there are sometimes correlations in the total number of children, without correlations in age at first birth (Reher *et al.*, 2008). In some cases, correlations with the reproductive success of other family members have been shown, such as with grandparents (Kolk, 2014; Danziger and Neuman, 1989) or mothers-in-law (Rotering, 2017).

On the other hand, some studies have found null or very weak correlations (Langford and Wilson, 1985; Bocquet-Appel and Jakobi, 1993; Gagnon and Heyer, 2001; Cazes, 2009; Dahlberg, 2013), sometimes even negative ones (Wise and Condie, 1975; Cools and Kaldager Hart, 2017). However, null correlations in reproductive success are not contradictory with positive correlations in the number of effective offspring (i.e., the number of offspring that remain in the population and have at least one child in it). The Quebec founder population is a good example of this, with very low correlations in progeny size (males: 0.01, females: 0.05), but stronger correlations in effective progeny size (males: 0.11, females: 0.12) (Gagnon and Heyer, 2001). This discrepancy occurs because of differential migration, with a transmission of the propensity to remain in the original population. Fairly strong correlations in effective progeny size (0.34) were measured in the $18^{\text{th}}$ century in the population of

Saguenay Lac Saint Jean in Quebec (Austerlitz and Heyer, 1998). However, studies focus generally on the correlation in complete progeny size (Murphy, 2012), whereas concerning the impact of TRS on the genetic diversity of the population of interest, it is the correlation in effective progeny size that matters (Gagnon *et al.*, 2006). It would be interesting to estimate more often the correlation in effective progeny size, as it can be stronger than the correlation in complete progeny size.

Several factors impact parent-child correlations in progeny size. The period studied has an effect, with low correlations in pre-transitional populations (Desjardins *et al.*, 1991; Gagnon and Heyer, 2001) and stronger correlations after the demographic transition (Murphy, 1999; Murphy and Wang, 2001; Reher *et al.*, 2008; Bras *et al.*, 2013). This increase is thought to be caused by the increased control of fertility, allowing individuals to reach their ideal number of children (Bongaarts, 2001) and mimic parental progeny size all the more (Murphy, 2013; Beaujouan and Solaz, 2019). Results in developing countries support this hypothesis, showing lower correlations than in developed countries' populations, which could be explained by their weaker birth control (Murphy, 2012). However, other studies find a decrease in correlations within a population over time (Rotering, 2017; Beaujouan and Solaz, 2019). This decrease can result from a reduction in parental influence on children and an increased emphasis on individual achievement at the expense of traditional observance (Buhr *et al.*, 2018; Beaujouan and Solaz, 2019). Increased social mobility (Glass *et al.*, 1986; Goody, 1973), mass education (Breen, 2010), and declining adherence to religious traditions (Lehrer and Chiswick, 1993) participate in the weakening of the link between parental and child progeny size (Beaujouan and Solaz, 2019). The disappearance of large progeny sizes in modern times can also explain the decrease in correlations over time (Rotering, 2017; Beaujouan and Solaz, 2019). Finally, the growth or decay of intergenerational correlations after the demographic transition may depend on the populations considered and the causes of TRS.

Parental and offspring gender may also have an impact, with a tendency for stronger transmission through mothers than fathers (Wise and Condie, 1975; Murphy, 1999; Murphy and Knudsen, 2002; Beaujouan and Solaz, 2019). This difference could be due to the greater proximity of the woman to the parental family sphere (Goldscheider *et al.*, 2015), as well as to the prevalence of the woman over the couple's fertility decisions. This prevalence would fade in the modern period (Bauer and Kneip, 2013). When TRS is produced by a patrilineal transmission of resources, we can expect a stronger correlation with father's progeny size than mother's progeny size (such as in Darlu, 2019). Social class may also play a role: in the Caribbean,

stronger correlations have been measured for socially privileged individuals with more opportunities to achieve their ideal number of children (Jennings and Leslie, 2013). This pattern may be reversed, with high social classes in France showing less pronounced TRS (Desplanques, 1985; Deville, 1979). The strength of TRS can also depend on progeny size, with a more substantial effect of parental progeny size on children's progeny size when it is far from the mean, suggesting a TRS driven by extreme progeny sizes (Breton *et al.*, 2005; Breton and Prioux, 2009; Boehnke *et al.*, 2007; Booth and Kee, 2009; Beaujouan and Solaz, 2019). Family rank may also have an effect, with correlations twice as high between the progeny sizes of elders and their parents compared to other siblings (Johnson and Stokes, 1976; Reher *et al.*, 2008). However, other studies do not find this effect (Murphy and Knudsen, 2002). Individuals' satisfaction with their childhood can also increase the correlations (0.175 vs. 0.022, Johnson and Stokes, 1976), as can proximity to the parents' lifestyle (assessed by the number of years of education, 0.218 vs. 0.118, Johnson and Stokes, 1976) (see also McAllister *et al.*, 1974). These different processes can add up, with correlations of 0.419 for elders with the same lifestyle as parents (Johnson and Stokes, 1976). Finally, when both parents have the same sibship size, the correlations can be stronger than those measured for all families (0.274 vs. 0.139, Murphy, 1999). In fact, Deville (1979) demonstrated the existence of this assortative mating by sibship size in a French population.

The consequences of TRS are multiple. From a demographic perspective, it allows for the maintenance of higher fertility compared to the case without transmission (Murphy and Knudsen, 2002). According to Collins and Page (2019), the United Nations predictions for global demographic change are underestimated because they do not consider TRS, which gives, over time, a more significant presence to the most fertile families. From a genetic point of view, TRS can reduce the population's genetic diversity, increasing inbreeding and the frequency of genetic diseases (Austerlitz and Heyer, 1998). We will discuss the effects of TRS in more detail in section 3 of this review.

In summary, TRS occurs in many populations with correlations that are very often positive, although sometimes relatively weak. In many populations, this tendency seems to strengthen during the modern period. This increase encourages investigation of the causes and consequences of this phenomenon. Furthermore, even when correlations are weak, the effects on population demographics and genetics can be substantial. The causes of TRS has long been debated, and we will address this issue in the next section.

## 1.2 Causes of TRS in humans

The measured intergenerational correlations in progeny size can have genetic or nongenetic causes. This question has long been debated in the literature. When the first measurements of correlations were made at the beginning of the 20$^{th}$ century, the prevailing interpretation was that of a genetic origin, a discipline that was then emerging. Later, after the Second World War, sociological and cultural interpretations were dominant. This change might stem from fear of eugenics and its harmful consequences in the post-war atmosphere (Murphy, 2013). The development of new methods in genetics, such as sequencing and association studies, subsequently gave new arguments to the proponents of the genetic causes of fertility correlations. This review will present both interpretations, with their supporting evidence. It will become clear that the answer is not clear-cut and that it is likely that both genetic and nongenetic components are at work in TRS. However, we will see that the answer may also depend on the population's characteristics (e.g., in a culturally uniform population, genetics will be primarily responsible for TRS, Pluzhnikov *et al.*, 2007).

### 1.2.1 Nongenetic causes of TRS

Three different types of nongenetic TRS have been described (Heyer *et al.*, 2012): (i) parental cultural influence on offspring (Johnson and Stokes, 1976; Anderton *et al.*, 1987; Barber, 2001; de Valk, 2013; Kolk, 2014), (ii) cooperation between siblings allowing children in large sibships to raise more children (Heyer *et al.*, 2012; Lawson and Mace, 2011; Murphy, 2013), (iii) transmission of resources that promote fertility or the desire to have children. These resources may be material (Sorokowski *et al.*, 2013), social (e.g., the transmission of social rank or polygyny, Heyer *et al.*, 2012), or cultural (such as hunting techniques, Borgerhoff Mulder *et al.*, 2009). The transmission of the propensity to leave the birthplace may have a similar effect as a nongenetic TRS as some lineages in the population will appear less fertile across time because of their tendency to emigrate (Gagnon and Heyer, 2001; Gagnon *et al.*, 2006).

Nongenetic transmission from parents to children is often less faithful than genetic transmission, for which the mutation rate in humans is very low ($1.45 \times 10^{-8}$ per base pair per generation, Narasimhan *et al.*, 2017). Moreover, cultural transmission is not only vertical (from parent to child): It can also be oblique (from one generation to the next between non-relatives) or horizontal (from one individual to

the other in the same generation) (Cavalli-Sforza and Feldman, 1981). This diversity of modes in cultural transmission reduces the influence of vertical transmission. Moreover, the notion of rebellion exists in cultural transmission: a child can purposely refuse to follow the parental culture. This lack of fidelity in the nongenetic TRS allows it to escape Fisher's paradox that we mentioned in the introduction (Heyer *et al.*, 2012). A significant amount of cultural variability is brought into each generation, preventing the"fixation" of cultural traits associated with higher fertility. Thus, variance remains stable in the population and maintains intergenerational correlations in progeny sizes over time. This conservation of variance is also true for the nongenetic TRS mediated by resource transmission, which we expect to be less faithful than genetic transmission. We will detail the three types of nongenetic TRS, gathering evidence and examples from the literature for each.

#### Cultural influence of parents on children

The cultural influence of parents on children has often been proposed to explain intergenerational progeny size correlations, a process referred to as "socialization" or "social learning" (Duncan *et al.*, 1965; Anderton *et al.*, 1987; Axinn *et al.*, 1994; Bernardi, 2003, 2013; Bernardi and Klärner, 2014). This socialization of reproductive success can be direct via the child's exposure to parental preferences or to a family environment that they will want to replicate once grown-up. It can also be indirect, with the transmission of behaviors indirectly related to fertility. For example, intergenerational transmission of divorce (Lyngstad and Jalovaara, 2010) can lead to transmission of reproductive success, as divorce decreases individual's expected number of children (Jansen *et al.*, 2009; Beaujouan, 2010; Beaujouan and Solaz, 2019). Positive correlations between ideal number of children and sibship size have been found in several studies, sometimes exceeding 0.3, revealing a parental transmission of preferences (Rodgers and Doughty, 2000; Heiland *et al.*, 2008; Régnier-Loilier and Depledge, 2006; Buhr *et al.*, 2018; de Valk, 2013). However, some authors suggest that fertility preferences are molded partly by genetic factors, which would thus be one of the sources of these correlation (Rodgers and Doughty, 2000; Rodgers *et al.*, 2001).

The opposite effect is also likely, such as a rejection of parental culture yielding a desired progeny size that differs from parental preferences (Creanza *et al.*, 2017). The population would then display negative progeny size correlations between parents and children. This trait will furthermore have oscillatory dynamics over gen-

erations: people with large progeny size would have children with small progeny size, but grandchildren with large progeny size. Cavalli-Sforza and Feldman (1981) analyze this type of cultural transmission and give the example of clothing fashion which could have such oscillatory dynamics.

Indeed, some studies measured negative correlations between the family sizes of parents and children (Wise and Condie, 1975; Levine, 1982). Cools and Kaldager Hart (2017) show from Norwegian administrative records that being raised in a large family may reduce female fertility while it increases male fertility. The interpretation relies on the distinct roles of girls and boys in the household: the girl has experienced the consequences of having many children because she helps out at home more than a boy; thus, her own fertility can be negatively affected by parental fertility (Gager *et al.*, 1999; Evertsson, 2006; Conley, 2005; Cools and Kaldager Hart, 2017). Westoff *et al.* (1961) and Hendershot (1969) suggest that the daughter's response to parental fertility depends on her childhood experience: a pleasant experience may increase the mother-daughter correlation. Parental influence on child fertility may also depend on the strength of the parent-child bond (Mönkediek *et al.*, 2017; Fasang and Raab, 2014). This influence also differs in strength across family sizes: for example, de Valk (2013) shows that children have preferences that are more distant from their parents in a large family. These last two results are consistent with a nongenetic TRS, as genetic transmission should not depend on the parent-child bond nor on progeny size.

However, it is essential to note that the negative fertility correlations cited above can sometimes be interpreted without resorting to the notion of parental culture rejection. In a population where the amount of resources correlates with fertility, individuals with more resources than average will have more children than average. By sharing resources, children will end up less fertile than average compared to single children who will not compete for resources (Easterlin, 1980). This process is similar to Falconer's experiments, who selected mice for large progeny size and found an unexpected effect: progeny size decreased instead of increasing (Falconer, 1965). This is because juveniles belonging to large sibships have to share maternal care and milk and are therefore smaller and ultimately less fertile. These mechanisms can yield cyclic patterns with alternating high and low fertility in the same lineage (Kirkpatrick and Lande, 1989), akin to the oscillatory dynamics that can occur in cultural transmission with a rejection of the parental culture. However, in human populations, the increase of a person's resources during his/her life course (e.g., enlargement of a flock) could mitigate or counteract this oscillatory effect and

maintain positive correlations.

Beyond the transmission of preferences, cultural transmission of practices that increase child survival could result in cultural TRS. For example, a transmission of breastfeeding practices, such as more prolonged breastfeeding, which increases survival, could lead to child mortality rate transmission. This would increase the mother-daughter correlation of the number of children surviving to reproductive age (Murphy, 2013; van Dijk and Mandemakers, 2018).

### Siblings cooperation

This hypothesis is based on the fact that individuals other than parents participate in human child survival, a phenomenon called allocare (Hrdy, 2009; Kokko *et al.*, 2002). Often, relatives play this role, such as aunts and uncles (Clutton-Brock, 2002; Hill and Hurtado, 2009). According to Hamilton's rule (Inclusive Fitness Theory), this cooperation of siblings has an evolutionary source, as the individual who favors the survival of his/her relatives maximizes the transmission of the alleles shared with them (Hamilton, 1964; Grafen, 1984; Sear, 2018). Because of this cooperation, the number of parental siblings correlates with the amount of support received and thus with children's survival. Siblings will be more numerous and may help each other all the more as adults and so on. Many authors consider this mechanism to be the source of the progeny size correlations measured between parents and children (Turke, 1989; Tymicki, 2004; Newson *et al.*, 2007; Lawson and Mace, 2011; Heyer *et al.*, 2012; Murphy, 2013). According to Newson *et al.* (2005, 2007), the primary cause of fertility decline in the modern period would come from lower presence and support from siblings compared to the pre-industrial period. However, in rural Gambia, Sear (2006) find no effect of maternal older sisters on a woman's fertility and the presence of maternal older brothers decreases her fertility.

This hypothesis of kinship cooperation as a source of fertility is especially emphasized in hunter-gatherer populations, where cooperation and child survival can be directly linked (Turke, 1989). This hypothesis explains the correlations of progeny size between parents and children in some hunter-gatherer populations (Hill and Hurtado, 1996; Draper and Hames, 2000; Blum *et al.*, 2006). This process is less applicable to food producers, where siblings may instead compete for resources inherited from their parents (Easterlin, 1980). Competition between siblings in inheritance is unlikely among hunter-gatherers due to their low intergenerational transmission of wealth (Borgerhoff Mulder *et al.*, 2009; Lawson and Mace, 2011). However, some

argue that this process of siblings-enhanced fertility also exists in food producers, where psychological or financial support from relatives may encourage reproductive decisions (Mathews and Sear, 2013; Rotering and Bras, 2015; Schaffnit and Sear, 2017b,a) or improve offspring health (Kana'Iaupuni *et al.*, 2005).

### Transmission of resources

The transmission of resources correlated with fertility can produce nongenetic TRS. Different types of inheritable resources could increase fertility: (1) material resources, (2) social resources, and (3) cultural resources. The strength of this type of transmission depends on two things: the fidelity of resources transmission and the correlation between resources and fitness.

**Material resources** Material resources are quite faithfully transmitted in several populations. In an analysis of 21 populations, Borgerhoff Mulder *et al.* (2009) show that among different types of resources, material resources are the best transmitted from one generation to the next (e.g., livestock transmission among the Datoga (herders) or land transmission among the Krummhörn (farmers)). This study also shows that farmers and herders have a more robust transmission of material resources than hunter-gatherer and horticultural societies. The correlation between resources and fertility is also quite common. Some studies show a correlation between material wealth and reproductive success in several traditional indigenous societies and preindustrial Western populations (Sorokowski *et al.*, 2013). In modern-day Western societies, some studies show a positive effect of both net worth and income on men reproductive success (Nettle and Pollet, 2008; Stulp *et al.*, 2016). For women, income has a negative effect on reproductive success (Nettle and Pollet, 2008; Stulp *et al.*, 2016), while net worth has a positive effect (Stulp *et al.*, 2016). Negative correlations between resources and fertility would also lead to nongenetic TRS.

However, both conditions must be met in the same population to give rise to nongenetic TRS: an accurate transmission of resources and a correlation between resources and fertility. In the Dogon of Mali, a correlation between wealth and male fertility exists (Strassmann, 1997), but no correlation in reproductive success between parents and children (Cazes, 2009). This could be explained by an imperfect transmission of resources from fathers to sons in this population. Another hypothesis is that children of the wealthiest individuals compete for parental resources and end

up with fewer resources than the average (i.e., wealth dilution). As discussed above, this phenomenon could even lead to negative correlations in progeny size between parents and children (Easterlin, 1980).

**Social resources** Several social resources can yield fertility transmission, such as social status, polygyny, and social network transmission. Many studies hypothesised or proved TRS through socioeconomic intergenerational continuity (Bengtson, 1975; Anderton *et al.*, 1987; Kahn and Anderson, 1992; Pouta *et al.*, 2005; van Poppel *et al.*, 2008; van Bavel and Kok, 2009; Jennings and Leslie, 2013). Social status positively correlates with fertility due to several factors. The higher stress experienced by individuals with a lower social rank can affect their fertility (Sapolsky, 2004; Lynch *et al.*, 2014). More generally, health correlates with social status (Bollen *et al.*, 2001; Reyes-Garcia *et al.*, 2008). This correlation remains true even in countries with a well-developed healthcare system (Marmot, 2006). Among the Maori, Murray-McIntosh *et al.* (1998) suggest that matrilineal transmission of rank could explain low mtDNA diversity, with higher-ranking offspring having a higher survival rate in this society (Heyer *et al.*, 2012). Socioeconomic status may also negatively correlate with fertility, which would also yield transmission of reproductive success, with high-status individuals transmitting their status and the associated lower fertility. However, socioeconomic status alone often cannot fully explain the correlations found. Indeed, studies controlling for socioeconomic categories nevertheless found an effect of parental influence on children's reproductive success (Murphy and Knudsen, 2002; Murphy and Wang, 2001; Kolk, 2014, 2015; Buhr *et al.*, 2018; Beaujouan and Solaz, 2019).

The transmission of polygyny from father to son may yield TRS, as polygyny may increase male fertility (Strassmann, 1997). Neel (1970) shows that polygyny is transmitted from father to son among the Yanomami and yields a decrease in Y chromosome diversity. The level of polygyny of a given individual being often correlated with his wealth (Timæus and Reynar, 1998), vertical transmission of wealth can lead to polygyny transmission and thus TRS. In some cases, polygyny is linked to the age of the man and not to his lineage, as in rural Senegal, where older men have more wives than younger men (Garenne and Van de Walle, 1989). In contrast, female fertility is often lower in the case of polygyny (Pison, 1986; Pebley and Mbugua, 1989), because of lower frequency of intercourse per wife or lower fertility of the man due to his higher age (Lardoux and van de Walle, 2003).

The transmission of a social network from parent to children may also lead

to intergenerational correlations in fertility when the social network promotes survival and fertility. Social network transmission is shown by Borgerhoff Mulder *et al.* (2009), who reveal more robust transmission for hunter-gatherers, intermediate transmission for horticulturists, and relatively weak transmission for farmers and herders. These results make sense, given the increased importance of the social network in the fickle environment of hunter-gatherers. However, studies that empirically demonstrate the impact of social relationships on fertility are few. Page *et al.* (2017), however, show in hunter-gatherers (BaYaka and Agta) that mothers who are more central in the network of social interactions produce more offspring that survive. In Agta, however, social centrality increases the risk of disease. There would then be a trade-off between cooperation and disease transmission.

**Cultural resources** Vertical transmission of cultural resources can also cause TRS when these resources increase fertility. This happens in the case of the transmission of knowledge necessary for survival, such as the vertical transmission of knowledge of edible and medicinal plants in the village of Cuyin Manzano in Patagonia (Lozada *et al.*, 2006). However, the low variability of this knowledge among village members revealed by the authors indicates low chances of TRS through this channel. Among Tsimane forager-farmers, same-sex parents contribute the most to skill transmission (Schniter *et al.*, 2022). Hewlett and Cavalli-Sforza (1986) study 50 skills among the Aka and show that 81% of these traits are vertically transmitted. They also demonstrate the presence of significant variability within the population regarding these skills, which could therefore lead to TRS. Transmission of religion (Philipov and Berghammer, 2007; Baudin, 2015) or of educational attainment (Cleland and Rodriguez, 1988; Bollen *et al.*, 2001), when correlated with fertility, are other factors yielding TRS through cultural resources transmission.

### 1.2.2 Genetic TRS

Several authors have interpreted the measured intergenerational correlations of progeny size as having a genetic cause. However, Fisher's paradox appears as an issue when considering this hypothesis: after some generations, beneficial alleles reach fixation, and no variance remains, yielding an absence of correlation. Thus, it is surprising that those intergenerational correlations can still be measured in many past and present-day populations. Studies have proposed various answers to this issue : (1) many of the traits involved in fertility are polygenic, and the total mutation rate is

thus higher than for a single locus trait, bringing a continuous flow of new variance in the trait (Houle *et al.*, 1996), (2) when the environment changes, a new variance in phenotype created by the interaction of genetics and environment can be brought in the population (Lewontin, 1974; Kirk *et al.*, 2001; Collins and Page, 2019), (3) some of the involved traits can be under balancing selection which maintains variance in the population, (4) some traits can be under selection since recent times due to the significant changes in human lifestyle in the post-industrial era (Kirk *et al.*, 2001), thus variance might not be exhausted nowadays, (5) as genes are, in fact, part of regulatory networks, some can be negatively correlated with each other, yielding a situation of trade-off where no gene can have ideal expression levels (i.e., antagonistic pleiotropy hypothesis, Williams, 1957; Barker and Thomas, 1987; Pettay *et al.*, 2005). As we can see, several hypotheses can resolve Fisher's paradox. The real issue would be to find the leading causes of the conserved variance in each population and for each trait of interest. Despite all of these answers, Fisher's paradox could be partly true, as heritability of fitness trait is smaller than other traits such as height (0.36 vs 0.8, Kirk *et al.*, 2001). This lower heritability of fitness traits could be due to their smaller variance resulting from natural selection. We will now review the various types of genetic TRS before addressing recent results from association studies.

### Types of genetic TRS

Genetic factors can impact fertility in humans through reproductive behavior (Miller *et al.*, 1999; Kohler *et al.*, 1999; Rodgers *et al.*, 2001; Kirk *et al.*, 2001; Miller *et al.*, 2010), physiological fecundity (such as age of menopause, Kirk *et al.*, 2001), and attributes that contribute to the probability of mating, mainly through sexual mating (e.g., health or appearance, Kolk, 2014). All these factors can be the origin of the measured correlations in progeny size between parents and children, and we will review each of them.

Studies supporting the behavioral genetic origin of TRS base their assumption on different results. Age at first attempt to give birth is heritable (0.35 correlation for men, 0.52 for women, Rodgers *et al.*, 2001, – Danish population). US kinship sample dataset revealed a more substantial heritability of the number of desired children compared to the realized progeny size (Rodgers and Doughty, 2000). The authors used these results to support a behavioral genetic origin of TRS. However, although those results support the transmission of behavior underlying TRS,

the genetic origin of these behaviors is not proven as it could be culture-mediated. Other studies show more directly the effects of genetics on reproductive behavior, with, for example, a correlation between carried dopamine receptor alleles and age at first intercourse (correlated often with fertility) (Miller *et al.*, 1999; Day *et al.*, 2016). Genetic variants in dopamine transporters influence the propensity for unprotected intercourse, dopamine receptors, and the monoamine oxidase gene (Daw and Guo, 2011). However, these results have been criticized because of difficulties in replicability, publication bias, and too small sample sizes (Duncan and Keller, 2011).

Several studies have also examined genetics' direct or indirect impact on physiological fertility. For example, age at menopause is inherited genetically and correlated with progeny size (broad heritability: 0.45, measured on Australian Twin Registry, Kirk *et al.*, 2001). In the same study, age at menarche has a substantial heritability (0.5) but no correlation with progeny size. However, Borgerhoff Mulder (1989) found a correlation between age at menarche and progeny size in Kipsigis. There might be a difference in this trait between different populations, with a probable distinction between pre-industrial and non-industrial populations on the one hand and post-industrial populations on the other (Kirk *et al.*, 2001). Indeed, since the age of reproduction is delayed in the latter populations, age at menarche will not affect the total number of children. In the Hutterites, authors interpreted the measured TRS as being of genetic origin due to the cultural uniformity of the population, which is subject to strict social rules, with the prohibition of contraception and uniform access to resources, preventing cultural variability in reproductive success (Pluzhnikov *et al.*, 2007). Using a pedigree-based maximum likelihood method in this population, Kosova *et al.* (2010) were able to more formally demonstrate the genetic origin of TRS in Hutterites and compute the genetic heritability of fitness components, which was higher in males than females. A similar method used on a Finnish pre-industrial population showed a heritability of 0.31 for fecundity for females and only 0.02 for males (Pettay *et al.*, 2005). Kosova *et al.* (2010) interpreted this difference as follows: Hutterites have access to a modern health care system, which reduces infant mortality and makes couple fertility less dependent on the woman. In the Finnish pre-industrial population, the woman is the key to couple fertility; thus, her fertility-associated traits are under natural selection.

Other heritable traits that correlate more indirectly with fitness could yield genetically driven TRS (physiologically or through sexual selection): height (Sear, 2010), birth weight, sickle cell anemia (Cavalli-Sforza and Bodmer, 1976), blood

type (Mengoli *et al.*, 2015), health and appearance (Kolk, 2014). The example of height is particularly complex. Height is genetically heritable (heritability of 0.8, Kirk *et al.*, 2001; Yang *et al.*, 2010) and correlates with reproductive success in some populations via increased physiological fertility or sexual selection. These effects of size on fitness depend on the population and sex considered. For example, in developing countries, female size is sometimes positively correlated with fertility (Sear *et al.*, 2004; Pollet and Nettle, 2008), sometimes negatively (Kirchengast, 2000; Devi *et al.*, 1985). A review of 42 developing countries shows a positive correlation between maternal height and child survival (Monden and Smits, 2009). In these countries, male height only weakly correlates with reproductive success (Pawlowski *et al.*, 2000; Sear, 2006) In general, the impact of height on physiological fertility is more common in women, whereas it affects male reproductive success through sexual selection (Sorokowski *et al.*, 2013). In post-industrial societies with low infant mortality, it is sexual selection that causes the impact of height on fitness in men (Stulp *et al.*, 2013). Thus, height is an example of a complex, multigenic trait correlated with fitness in some populations, either physiologically or through sexual selection.

### GWAS studies

GWAS studies are another way to address the question of the genetic origin of TRS. In Hutterites, Kosova *et al.* (2012) show 41 SNPs correlated with male fertility, consistent with studies showing robust male-mediated genetic transmission in this population (Kosova *et al.*, 2010). Barban *et al.* (2016) found 12 loci associated with the age at first reproduction or the number of children. These loci are in linkage disequilibrium with different candidate genes that could be driving the effect on reproduction, such as transcription factors activating RBM5 (the Rmb5 mutant in mice shows a lack of sperm at ejaculation) and LAMP2 (a gene on the X chromosome involved in the mechanism of sperm penetration into the egg). Some of the discovered loci have already been shown to be associated with intermediate reproductive traits such as age at menarche and age at menopause. Several studies find SNPs associated with sperm quality (Kosova *et al.*, 2012; Barban *et al.*, 2016). A more recent study finds 371 independent loci in European individuals associated with age at first sex (N=387,338) and age at first birth (N=542,901), with a similar genetic basis for both behaviors (Mills *et al.*, 2021). This study also shows that the heritability of age at first birth in women gradually changed over time: starting at 9% (95% confidence interval = 4–14%) heritability for women born in 1940, up

to 22% (95% confidence interval = 19–25%) for women born in 1965. It would be interesting to replicate this kind of study in non-European populations.

## 1.3 TRS impacts on the genome and inference

Regardless of its causes, TRS affects the genome during evolution. These effects have allowed several studies to infer the intensity of genetic (Chen and Slatkin, 2013; Kim *et al.*, 2017) or nongenetic TRS (Blum *et al.*, 2006; Heyer *et al.*, 2015) from genomic data. We will focus mainly on the effects of nongenetic TRS, since genetic TRS (natural selection) has already been treated extensively. First, we will discuss in details the effects of nongenetic TRS on genome evolution. Second, we will compare nongenetic TRS to other population genetic processes, such as natural selection, population size changes, and migration. This comparison is critical because a similar effect on the genome produced by nongenetic TRS and another process cannot be used to tell them apart. Third, we will review the studies already carried out on the inference of nongenetic TRS and propose future research directions.

### 1.3.1 Nongenetic TRS impacts on the genome

Nongenetic TRS produces different effects on demography and population genetics. The variance of progeny size increases and its distribution is altered (Sibert *et al.*, 2002). Genetic diversity is reduced (Austerlitz and Heyer, 1998), and allelic frequencies are altered compared to the neutral case (Sibert *et al.*, 2002; Guez *et al.*, 2022). The topology of coalescent trees is distorted with increased imbalance and more polytomies (Sibert *et al.*, 2002; Brandenburg *et al.*, 2012; Guez *et al.*, 2022). We will now discuss each of these effects separately.

#### Demographic effects

Nongenetic TRS produces correlations between parental and offspring progeny sizes. Studies often used these correlations to measure TRS on genealogical data (Austerlitz and Heyer, 1998; Murphy, 1999). Modeling of nongenetic TRS showed that it increases the variance of progeny size: the distribution includes more individuals without children or with large progeny size (Guez *et al.*, 2022). When additional variance is introduced into the model, nongenetic TRS will have even more effects

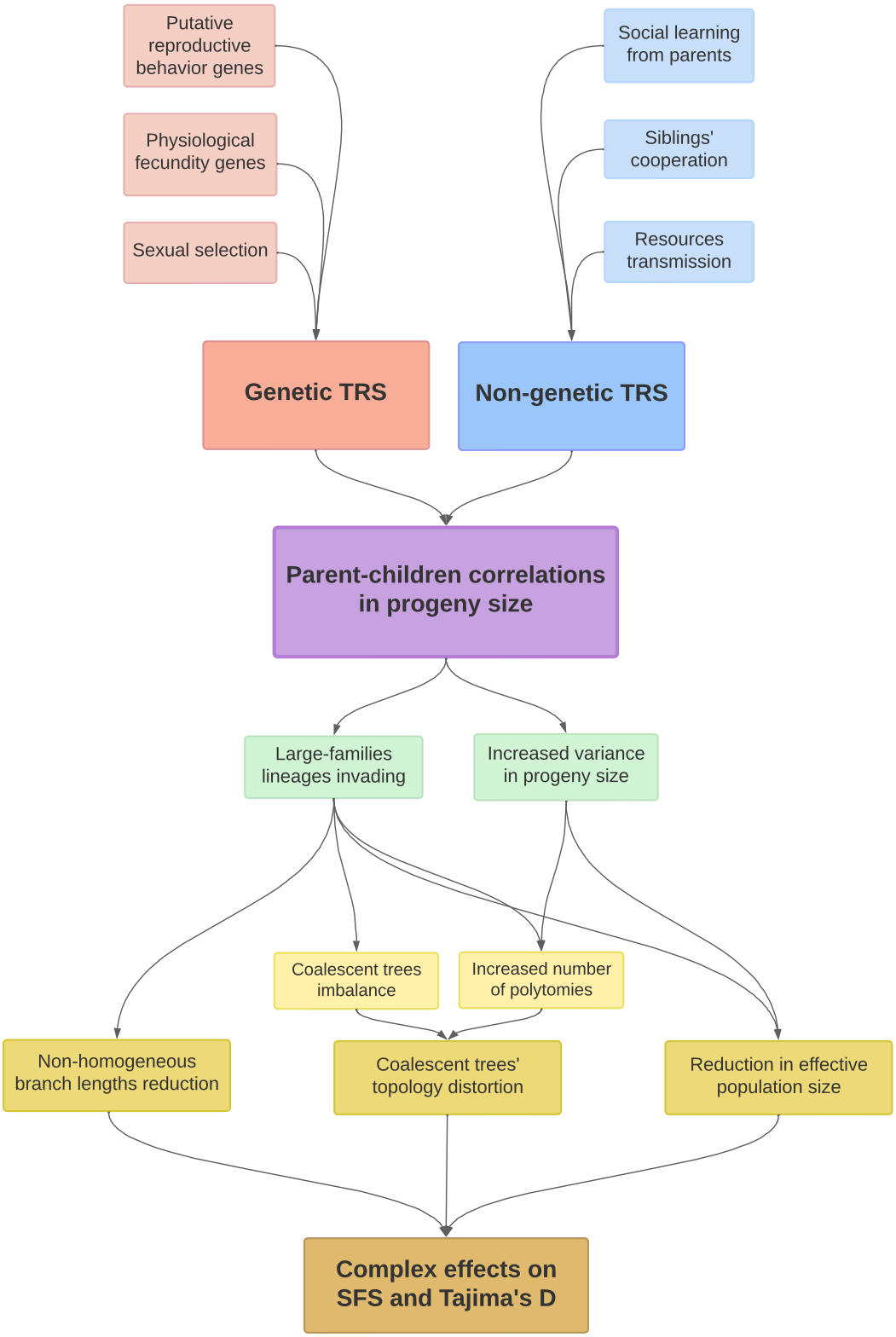


Figure 1.1: Summary of causes and consequences of TRS.

on genetic diversity (Brandenburg *et al.*, 2012). This is probably because the largest progeny sizes produced in that case are greater in their size, proportionally to the total population size, compared with the largest progeny sizes generated under the model with no additional variance. Hence, alleles of large families may invade more rapidly the population under this high-variance model. Consequently, to explain the high frequencies of genetic diseases in the Saguenay-Lac-Saint-Jean population, it was necessary to add variance in progeny size on top of nongenetic TRS (Austerlitz and Heyer, 1998). Although the effects on genetics are increased in this model of high variance, the parent-children progeny size correlations are somewhat smaller, because the added variance reduces the correlations. This result indicates that a simple measure of correlations in a population, as has been done in the literature, does not provide a complete picture of the nongenetic TRS phenomenon. Therefore, it is necessary to consider correlation and variance to characterize the intensity of the effects of nongenetic TRS in a natural population. However, these results rely on a specific model of nongenetic TRS (an extension of the Wright Fisher model, Sibert *et al.*, 2002), other modeling of the process could yield different results.

#### Effects on genetics

Genetic diversity decreases under nongenetic TRS: the effective population size is smaller than the census size, which corresponds to a reduced TMRCA. This happens for two reasons: increased variance in progeny size, and fertility transmission that accelerates allele fixation (the alleles of fertile individuals invade the population quickly because of fertility transmission). Modeling experiments show that the first component has a larger share in the diversity decrease than the second (Guez *et al.*, 2022). In natural populations, the decrease in diversity can be considerable, with a 20-fold decrease in the effective population size of Saguenay-Lac-Saint-Jean, despite exponential population growth (Mourali-Chebil and Heyer, 2006). This impact of nongenetic TRS could explain the low genetic diversity in the human species compared to other great apes despite our higher census size (Gagneux *et al.*, 1999; Kaessmann *et al.*, 2001; Blum *et al.*, 2006). The smaller effective size leads to an underestimate of the recombination rate since this rate must be higher under TRS to achieve the same number of recombination events as in a neutral case (Austerlitz and Heyer, 2000). This rationale also applies to the mutation rate, which could also be underestimated. Another consequence of this smaller effective size is the accelerated erasure of ancient processes' signals from the genome. For example, rare alleles generated by an ancient expansion disappear more rapidly under nongenetic

TRS, yielding a bias in expansion parameters inference (Guez *et al.*, 2022).

Tajima's $D$ follows a complex pattern. When TRS begins, the effective size reduction yields an increased Tajima's $D$. Conversely, when it ends, there is a decrease in Tajima's $D$ due to the increase in effective size. If the nongenetic TRS lasts for a number of generations of the order of the census size, Tajima's $D$ reaches a plateau in negative values (i.e., if no other process is at work). This negative plateau at equilibrium has two causes: (i) the distortion of the topology of coalescent trees (imbalance and number of polytomies both increasing) (Guez *et al.*, 2022), (ii) branch lengths are reduced by nongenetic TRS in a non-uniform way, with a stronger impact on branches close to the root, which increases the relative proportion of rare alleles (Sibert *et al.*, 2002). This second effect is interpreted by Sibert *et al.* (2002) as similar to a constant expansion of the population under nongenetic TRS (despite a stable effective size). Indeed, the fertile lineages in the population are constantly growing, with a regular extinction of the less fertile lineages, which impacts branch lengths similarly to an expansion. At equilibrium, allele frequencies follow a U shape: an excess of rare and common alleles. The excess of rare alleles is explained by the two reasons mentioned (distortion of coalescent tree topology and non-uniform reduction of branch sizes). In contrast, the excess of common alleles is only caused by topology distortion.

As stated above, the effect on the topology of coalescent trees is twofold: increased imbalance and increased number of polytomies. Imbalance is a property that was first studied on phylogenetic trees (Sackin, 1972; Colless, 1982; Shao and Sokal, 1990), and its application to coalescent trees is more recent (Sibert *et al.*, 2002). Several indices have been constructed to measure this topological property. They are generally classified into two types: balance indices, that increase when the tree is more balanced, and imbalance indices, whose value increases when the tree is unbalanced. These indices are affected by the nongenetic TRS, with some indices being strongly modified (such as $B_1$ (Shao and Sokal, 1990) and Colless' index (Colless, 1982)) and others less so ($B_2$, Shao and Sokal, 1990). Their power to detect nongenetic TRS is, therefore, different. Furthermore, some of these indices are affected by demographic events, such as changes in population size, while others are not (Guez *et al.*, 2022). Several indices, such as B1 and Colless, are calculated by averaging the indices for each node. Thus, they give more weight to recent events since there are more coalescences at the bottom of the tree (Agapow and Purvis, 2002; Blum *et al.*, 2006). To study particular periods, focusing on the indices of specific nodes would be interesting.

Nongenetic TRS also leads to the occurence of polytomies in coalescent trees (Guez *et al.*, 2022). Polytomies can appear for several other reasons, such as selection, skewed variance, or bottlenecks (Durrett and Schweinsberg, 2005; Eldon and Wakeley, 2006; Neher and Hallatschek, 2013; Irwin *et al.*, 2016; Menardo *et al.*, 2021). Nongenetic TRS produces polytomies for two reasons: (i) the bottleneck of effective population size, and (ii) the effect of transmission, resulting in a proliferation of individuals descended from a single ancestor. (Guez *et al.*, 2022, supplementaty material).

Theoretically, the nongenetic TRS impacts described here (e.g., on diversity, allelic frequencies, and tree topology) should allow inference of this process from genomic data. However, each of these signals may be produced by other phenomena, making disentanglement difficult. Furthermore, the different processes may interact, with simultaneous processes not summing the effects of the separate processes. The following section will discuss the relationships between nongenetic TRS and major population genetic processes (selection, population size change, and structure), comparing their effects on the genome and studying their potential interactions.

### 1.3.2 Nongenetic TRS and other processes

#### Nongenetic TRS and selection

In terms of effects, natural selection is quite similar to nongenetic TRS. Like nongenetic TRS, selection reduces genetic diversity, yields negative Tajima's $D$ (Tajima, 1989), and an excess of rare (Braverman *et al.*, 1995) and common alleles (Fay and Wu, 2000). The topology of coalescent trees is also affected, with an increase in imbalance (Fay and Wu, 2000; Li and Wiehe, 2013) and number of polytomies (Durrett and Schweinsberg, 2005; Neher and Hallatschek, 2013). However, a few differences between nongenetic and genetic TRS can be identified.

The first difference lies in the quality of these two types of transmission. Because genetic transmission is remarkably faithful, the variance of the trait under selection erodes as it approaches fixation of the beneficial allele (Fisher, 1930). For this reason, it is somewhat problematic to explain parent-child correlations in progeny size by selection because we expect the variance of fertility traits to erode, leading to the rapid disappearance of correlations (i.e., Fisher's paradox mentioned in introduction). Cultural transmission is much less accurate. One reason is that cultural traits are not only transmitted vertically (from parents to children), unlike genetic

transmission: horizontal or oblique transmissions also exist (Cavalli-Sforza and Feldman, 1981). The horizontal contagion of fertility has indeed been shown (Lois and Arránz Becker, 2014). Moreover, many other parameters can influence a child's observance of parental culture, such as level of satisfaction with childhood or position in the sibship (Johnson and Stokes, 1976). Thus, under nongenetic TRS, variance of the progeny size can remain constant, as well as parent-child correlations. Several studies modeled nongenetic CTRS in such a way variance in progeny size remains stable over time (Sibert *et al.*, 2002; Brandenburg *et al.*, 2012; Guez *et al.*, 2022). Heyer *et al.* (2012) use this assumption of cultural variance stability to efficiently resolve Fisher's paradox (as explained in the beginning of section 2). Finally, nongenetic TRS has a Lamarckian property (i.e., transmission of acquired traits): an individual acquiring during his life a preference for a large number of children, in contrast to his parents, will pass on this preference to his children.

A second difference between the two processes is the impact of recombination on hitchhiking. In the case of selection, hitchhiking occurs only for SNPs close to the locus under selection (Smith and Haigh, 1974). Correlations with SNPs further away are broken by recombination events that occur over generations between the locus under selection and the neutral sites. Thus, the signal is strongest near the locus under selection and decreases with distance from it. The length of the region carrying the signal depends on the recombination rate and the duration under selection. In the case of fixation, this duration depends on the selection coefficient: the higher the coefficient, the shorter the selection and the longer the region carrying the selection signal (Kim and Stephan, 2002; Stephan, 2019). In human population data, even very recent selection events have signals spanning only a few megabases (Tishkoff *et al.*, 2007; Tanaka and Nakayama, 2017). In contrast, under nongenetic TRS, hitchhiking affects all SNPs in the genome equally since no gene is responsible for the accrued reproductive success. Under nongenetic TRS, if there is a correlation between a neutral SNP and reproductive success (e.g., because the carriers of this SNP are part of culturally fertile families), recombination will not break it. Therefore, the nongenetic TRS signal should theoretically be similar throughout the genome, in contrast to selection, a difference that could help disentangle the two (Austerlitz and Heyer, 2000; Brandenburg *et al.*, 2012; Guez *et al.*, 2022).

However, multigenic selection can also produce effects in multiple locations in the genome, such as nongenetic TRS. In particular, background selection could affect substantial parts of the genome (Pouyet *et al.*, 2018). Nevertheless, several differences can be noted: (i) there remain parts in the genome that are considered

| | Genetic TRS | Nongenetic TRS |
|---|---|---|
| **Transmission** | Faithful | Unfaithful |
| **Fixation** | Common | Uncommon |
| **Impacted genomic region** ($\rho > 0$) | Selected locus region | Genome wide |
| **Coalescent trees along the genome** ($\rho > 0$) | Can be different | Tend to look alike |
| **In multi-pop** | Lower diversity | Higher diversity |
| **Competition** | Between loci | - |

Table 1.1: **Hypothetical differences in impacts on genetics between genetic and nongenetic TRS.** $\rho$ is the recombination rate.

neutral to selection (Pouyet *et al.*, 2018), which is not possible for nongenetic TRS, (ii) all coalescent trees in the genome will be influenced by the same nongenetic TRS history and will thus resemble, whereas the trees for each gene under selection may have a different history with a shape that depends on its selection coefficient and the temporality of selection (Barghi *et al.*, 2020; Hayward and Sella, 2022), (iii) populations that exchange migrants have a higher probability to select for the same alleles under multigenetic selection, compared to nongenetic TRS that will randomly select for different alleles in each population, (iv) when several genes are under selection and in linkage disequilibrium, they may be in competition, a phenomenon unique to multigenetic selection (Barton, 1995).

However, a population combining nongenetic TRS and selection may achieve a similar competition phenomenon between the two processes, if the families carrying the beneficial allele are not the most culturally fertile. This can lead to the conservation of deleterious alleles carried by the most culturally fertile families. Furthermore, when selection and nongenetic TRS are combined, the length of the genome carrying the selection signal is increased with larger shared haplotypes (Austerlitz and Heyer, 2000). Since the length of shared haplotypes under selection is a proxy for estimating event age, nongenetic TRS could bias this estimate. We can conclude that cultural and genetic TRS, although leading to similar effects, can be distinguished through genome-wide studies. However, the distinction seems more delicate in genetic compartments without recombination, such as Y or mitochondrial DNA. Based on the tendency of selection to reduce the variance of the favorable trait in contrast to nongenetic TRS, which retains the variance of the phenotype, a way may

exist to distinguish their signals even without recombination.

### Nongenetic TRS and population size changes

Unlike selection, changes in population size have this in common with nongenetic TRS: they affect the entire genome. Thus, Tajima's $\pi$ or Tajima's $D$ cannot be used to disentangle them, since both processes affect these statistics in the whole genome (Guez *et al.*, 2022). However, no formal comparison has yet been made regarding the distribution of these indices in the genome under nongenetic TRS or population size changes. One clear difference between these two processes is that nongenetic TRS produces a coalescent trees imbalance, which is not the case under population size changes. This is valid provided the use of a suitable imbalance index. Indeed, the index described in Brandenburg *et al.* (2012) to characterize nongenetic TRS is not affected by population size changes, whereas more traditional indices such as B1 and Sackin are (Guez *et al.*, 2022). This is because Brandenburg *et al.* (2012)'s index is independent of coalescence rates in the tree, which is not the case for all (im)balance indices.

Nongenetic TRS and changes in population size can occur in the same population, successively or at the same time (as in the Saguenay Lac Saint Jean population, where the population was under nongenetic TRS while growing exponentially, Austerlitz and Heyer, 1998). A simulation study demonstrated the impact of nongenetic TRS on demographic inference from genetic data: the magnitude of an ancient expansion may be underestimated if the population has undergone a period of nongenetic TRS (Guez *et al.*, 2022). Depending on the case, the age of the expansion will then be under or overestimated. These results warn of the consequences of not taking nongenetic TRS into account and suggest an underestimate of the extent of the Neolithic expansion (Guez *et al.*, 2022). Further study of the combination of different demographic and nongenetic TRS scenarios would provide a better understanding of their interactions. Furthermore, the development of inference tools that take into account nongenetic TRS, using for example coalescent tree imbalance, would allow correcting possible biases in the inferred human demography.

### Nongenetic TRS and structure

Few studies investigated the impact of migration on the imbalance of coalescent trees. Blum *et al.* (2006) studied the impact of three migration models on imbal-

ance: a two-island model with migration, a model of populations merging, and a model of range expansion. Only the first model seems to show a tendency towards tree imbalance, with imbalance being more pronounced when the two populations differ significantly in size (factor 100). The type of sampling in the different subpopulations also affects imbalance. These results show the importance of considering structure when inferring the nongenetic TRS. It would therefore make sense to add structure detection statistics such as $F_{st}$, in addition to imbalance, to distinguish the two processes. However, no study has investigated the impact of nongenetic TRS on genetic structure indices so far. Finally, the sampling method should be considered when analyzing the nongenetic TRS, since it seems to strengthen the effect of structure on imbalance.

### 1.3.3 Detection studies

#### Nongenetic TRS as a hypothesis for low diversity

Nongenetic TRS has been used in some studies as a hypothesis to explain low diversity rates. For example, Neel (1970) explains the reduced diversity of the Y chromosome in the Yanomami with polygyny transmission from father to son. The preponderance of a specific mtDNA haplotype in the Maori was explained by Murray-McIntosh *et al.* (1998) with rank transmission. However, in these studies, nongenetic TRS is only a hypothesis to explain the low variance in genetic data, as genetic diversity is affected by many other processes, such as bottlenecks.

#### Studies inferring nongenetic TRS from genetic data

Some studies go beyond a simple measure of diversity to hypothesize nongenetic TRS and seek to infer its intensity. Austerlitz and Heyer (1998) make such an inference based on the frequencies of genetic diseases in the Saguenay Lac Saint Jean population, using a parameterizable branching model to simulate nongenetic TRS. The inferred value corresponds to the intensity of nongenetic TRS measured on the genealogical data. Another study co-infers the growth rate of an allele and its age, based on its frequency and haplotype length. When an allele shows faster growth than the population, they assume there is TRS. This method confirms the expectations in the Saguenay Lac Saint Jean population and reveals the possibility of nongenetic TRS in Vlax Romas, although other hypotheses are possible (Austerlitz

*et al.*, 2003).

Some studies use an imbalance index to infer nongenetic TRS, such as Blum *et al.* (2006) and Heyer *et al.* (2015). Blum *et al.* (2006) focus on mitochondrial DNA to infer nongenetic TRS in the matrilines. By measuring coalescent tree imbalance in ten hunter-gatherer populations and 27 food producer populations, they show a trend toward more substantial imbalance in hunter-gatherers. The nongenetic TRS could explain the difference between these population types: hunter-gatherers rely significantly on cooperative kin networks, and individuals who receive much help from their many siblings could, in turn, have a larger than average progeny size. This also explains parent-child correlations in progeny size among the Ache of Paraguay (Hill and Hurtado, 1996) and the !Kung of Botswana (Draper and Hames, 2000).

Heyer *et al.* (2015) showed that in Central Asia, patrilineal populations are more likely to have imbalance in Y-chromosome trees compared to cognatic populations. Some of these patrilineal populations do not show mtDNA imbalance, despite Y-chromosome tree imbalance. A specific father-son correlation in progeny size could explain these results. This could happen for example in the case of a father-children wealth transmission, or the transmission of an extended social network that gives more strength in coalitions for war or for cooperative breeding. This hypothesis of cultural transmission of fertility only through the patriline is consistent with the explanations given for the high frequency of two Y-DNA haplogroups: Genghis Khan (Zerjal *et al.*, 2003) and Han (Xue *et al.*, 2005). However, Lansing *et al.* (2008) found no evidence of such transmission in Indonesian societies, probably due to differences in social structure or wealth transmission patterns (Heyer *et al.*, 2015).

Both Blum *et al.* (2006) and Heyer *et al.* (2015) use imbalance to detect nongenetic TRS. However, while it is true that nongenetic TRS strongly impacts imbalance, it can also be impacted by selection and by migration to a lesser extent, as discussed. In particular, the primary way to distinguish nongenetic TRS from selection relies on recombination that allows loci far from the site under selection to escape the sweep. This process does not occur in non-recombining genetic compartments like mtDNA or Y-DNA. Thus, it is difficult to rule out selection as an explanation for the high imbalance indices measured in these two studies (Blum *et al.*, 2006). For example, Brandenburg *et al.* (2012) consider that the differences between hunter-gatherers and food producers shown by Blum *et al.* (2006) could be due to natural selection related to feeding mode (Kivisild *et al.*, 2006). Distinguishing between the two processes will require reliance on whole nuclear genome data,

where a large number of recombination events will isolate regions under selection while providing more detection power (Guez *et al.*, 2022).

#### Inferring nongenetic TRS on the whole genome

To infer nongenetic TRS using imbalance indices, one must first reconstruct coalescent trees from the genetic data. The quality of the tree reconstruction can impact the accuracy of the inference. (Blum *et al.*, 2006) showed that the UPGMA reconstruction method added a bias, making the trees more imbalanced than neutral trees, unlike PHYML, which does not produce this bias. This type of analysis should therefore be pursued for modern tools that reconstruct trees on the whole genome, such as ARGweaver (Rasmussen *et al.*, 2014), tsinfer (Kelleher *et al.*, 2019), or relate (Speidel *et al.*, 2019) to see how well the reconstructed topology matches the actual topology. Furthermore, even if these tools reconstruct unbiased tree topology in terms of imbalance, their behavior under nongenetic TRS remains to be verified.

Nongenetic TRS impacts several imbalance indices (such as B1, B2, Colless, and Sackin, Shao and Sokal, 1990) (Guez *et al.*, 2022). Moreover, since they do not correlate perfectly, each of these indices could provide information on nongenetic TRS from coalescent trees. It should be possible to infer nongenetic TRS on whole genome data using methods such as Approximate Bayesian Computation (ABC). This method allows combining imbalance indices with other summary statistics such as SFS (for examples of combinations of statistics for ABC inference, see Sheehan and Song, 2016; Boitard *et al.*, 2016; Jay *et al.*, 2019). Alternatively, training neural networks to detect nongenetic TRS directly on simulated genetic data is possible (see Sanchez *et al.*, 2021). This would avoid the potentially biased tree reconstruction step but may require more training simulations.

## 1.4 Beyond human

### 1.4.1 Animal culture

This review address nongenetic TRS, focusing on the human species. However, animals other than humans possess culture or proto-culture transmitted between individuals (Avital and Jablonka, 2000; Galef Jr., 1998), such as chimpanzees (Whiten *et al.*, 2001; Luncz and Boesch, 2014), dolphins (Krützen *et al.*, 2005), birds (Aplin

*et al.*, 2015), fishes (Helfman and Schultz, 1984; Laland and Hoppitt, 2003), or even insects (Danchin *et al.*, 2018). For this cultural transmission to yield nongenetic TRS, three conditions must be fulfilled: (i) the trait must vary in the population, (ii) some variants of the trait must give a reproductive advantage to the individual carrying them, and (iii) the trait must be transmitted vertically (Bonduriansky and Day, 2018). For example, a study showed in bottlenose dolphins the emergence of the use of sponges to scour the seafloor, a behavioral trait culturally transmitted from mother to daughter (Krützen *et al.*, 2005). However, if this tool does not provide a reproductive advantage (condition ii), there will be no cultural TRS and, thus, none of the impacts on genetics described in the previous section. However, even without this condition, culture may have other effects on genetics, such as speciation through cultural reproductive isolation (Whitehead, 2017; Whiten, 2017).

In non-human primates, vertical transmission of social rank often leads to cultural TRS, as rank increases access to resources, protection from aggression, and fertility (Holekamp and Smale, 1990; Sapolsky, 2005). Many primates show a maternal transmission of rank: several species of macaques (Kawai, 1958; Bernstein, 1969; Estrada *et al.*, 1978; Silk *et al.*, 1981), several species of baboons (Cheney, 1977; Hausfater, 1975; Samuels *et al.*, 1987), vervets (Horrocks and Hunte, 1983) and cercopithecus (Donabedian and Cords, 2021). Maternal rank also affects gene expression (Tung *et al.*, 2012), the epigenetic profile of the placenta (Massart *et al.*, 2017), and the sex ratio at birth (Simpson and Simpson, 1982), although a meta-analysis challenged this last result (Brown and Silk, 2002). This reveals the complexity of the links between culture and genetics in non-human primates. Studies have further shown in several primates that various traditions (e.g., regarding tool use) were culturally inherited: in chimpanzees (Whiten *et al.*, 1999; Hobaiter *et al.*, 2014), orangutans (van Schaik *et al.*, 2003), gorillas (Robbins *et al.*, 2016), spider monkeys (Santorelli *et al.*, 2011) and Japanese macaques (Leca *et al.*, 2007). A study showed that one of the cultural variants might be more effective than another (Gruber *et al.*, 2009), paving the way for a potential cultural TRS in these species (Whiten, 2017).

Primates are not the only species with cultural TRS. In bottlenose dolphins, Frere *et al.* (2010) showed that female fitness depends on both genetics ($h^2 = 0.162$) and social transmission ($h^2 = 0.44$), revealing a nongenetic TRS process in this species. One of the hypotheses proposed by the authors to explain this social transmission, is that females with calves tend to associate together (Möller and Harcourt, 2008), for mutual benefits such as heightened vigilance against predators. It would be

interesting to study the loss of genetic diversity due to TRS in this species. Other cetaceans show a decrease in mtDNA diversity under cultural TRS (killer whale, sperm whale, and two pilot whale species) compared to other cetaceans with similar population sizes and latitudes (Whitehead *et al.*, 2017). These four species having matrilineality in common, the authors conclude that the reduction in diversity is due to cultural TRS, after ruling out the hypotheses of bottleneck or selection. Sometimes, however, it remains difficult to decide whether the reduction in diversity is due to selection or cultural TRS, such as in cheetahs (Kelly, 2001). Another carnivore species show cultural TRS undoubtedly. Spotted hyenas vertically inherit social rank, which correlates with fitness (Engh *et al.*, 2000; Ilany *et al.*, 2021). Other social animals could be subject to cultural TRS, such as elephants (Goldenberg *et al.*, 2016) and feral horses (Cameron *et al.*, 2009), but this requires ensuring that all three conditions are met. The simultaneous presence of the three conditions of cultural TRS is not always demonstrated and remains an interesting albeit complex field of study.

### 1.4.2 Nongenetic inheritance

Cultural inheritance is only one type of nongenetic inheritance. Other forms of nongenetic inheritance have been described, such as parental effects (often called maternal effects), ecological inheritance, structural inheritance, and epigenetic inheritance (Danchin *et al.*, 2011; Bonduriansky and Day, 2018). When TRS occurs via these inheritances, one can expect that it affects the genome, as described in section III, through a decrease in genetic diversity and an imbalance in coalescent trees. TRS will only occur if the three conditions mentioned in the previous section are met (i.e., variability of the trait in the population, correlation of the trait with fitness, and vertical transmission).

For example, ecological inheritance (Odling-Smee, 1988; Danchin *et al.*, 2011) could be a source of nongenetic TRS. Individuals born in a favorable environment will have more offspring and will transmit their birth environment and associated fitness to their children, generating a process of nongenetic TRS. This is especially true for plants whose seeds disperse little (Danchin *et al.*, 2011). Dispersal from the maternal environment corresponds in some ways to genetic mutations, or to distance from the parental culture in the case of CTRS, all three of which are random changes in the inherited trait altering the fidelity of transmission. Niche construction can be a way for parents to improve their own and their children's fitness by altering the

environment to suit them, such as the classic example of beavers (Naiman *et al.*, 1988; Danchin *et al.*, 2011).

Another example is the vertical transmission of microbiome, which exists in a large number of species (Funkhouser and Bordenstein, 2013), such as sponges (Schmitt *et al.*, 2012), insects (Greer *et al.*, 2020), and mammals (Moeller *et al.*, 2018). Since the microbiome directly affects host fitness (Suzuki, 2017), it could lead to a form of nongenetic TRS. However, the transmission of microbiome is a complex case for several reasons. First, although the maternal microbiome has the advantage of first colonization, different parameters throughout life will impact individual microbiomes (Aleman and Valenzano, 2019; de Jonge *et al.*, 2022). Second, the diversity of the microbiome can be affected by host genes, as has been shown in humans (Spor *et al.*, 2011). Thus, there would be some genetic transmission of the microbiome through these genes. Finally, the microbiome has its own metagenome, which some consider the second genome of the individual (Grice and Segre, 2012). Significant research is needed to understand the impact of vertical transmission of the microbiome on the evolution of different species (Davenport *et al.*, 2017). However, it is certain that the mechanisms involved are complex and do not solely follow classical genetic transmission.

Examples of nongenetic transmission are increasingly numerous and involve all types of species: vertebrates, insects, and plants (Bonduriansky and Day, 2018). We can therefore expect nongenetic TRS in a large number of species, which would have an impact on their genomes. Therefore, understanding the evolutionary histories of populations requires taking into account nongenetic TRS, for example, by exploring the imbalance of coalescent trees.

### 1.4.3 Cell populations and nongenetic TRS

It is possible to go even further and study the impacts of nongenetic TRS on cell populations. Several species of unicellular eukaryotes show nongenetic inheritance (Bonduriansky and Day, 2018). For example, the amoeboid protist *Difflugia corona* vertically transmits its test structure during cell division (i.e., structural inheritance). This transmission was proven by pulling out some "teeth" in the parent cell and finding the same pattern in the daughter cells (Jennings, 1937). Several other unicellulars show structural inheritance: *Paramecium aurelia* (Beisson and Sonneborn, 1965; Beisson, 2008), *Trypanosoma brucei* (Moreira-Leite *et al.*, 2001), *Cyclotella meneghiniana* (Shirokawa and Shimada, 2016). In all these cases of struc-

tural inheritance, a nongenetic TRS will appear if some variants have better fitness than others.

Furthermore, to what extent populations of cells within a multicellular organism might be subject to nongenetic inheritance is questionable. In a tumor, for example, the cells closest to the blood vessels have an advantage in access to oxygen and nutrients (Helmlinger *et al.*, 1997). Thus, without angiogenesis, a tumor cannot grow beyond a few millimeters in diameter (Pluda, 1997; Alfarouk *et al.*, 2013). Therefore, the cells closest to the vessel might have better fitness than the others. The parent cell transmits its position to the daughter cell and thus its distance to the vessel, as well as the associated fitness (i.e., a type of ecosystem inheritance): this would yield a nongenetic TRS. This effect has been compared to a riparian zone in ecology, e.g., a river crossing the desert: vegetation density is high near the river where xeric stress is low and reduces as one moves away from it (Schade *et al.*, 2002; Alfarouk *et al.*, 2013). The reality is, of course, more complex with the selection process giving the cells farthest from the blood vessel a genotype adapted to the lack of nutrients (just as plant species are adapted to their distance from the river). Nevertheless, by the time the mutations that allow cells to grow far from the vessel appear, a situation of nongenetic TRS could be at work. In addition, tumor cells will not have the same sensitivity to chemotherapy, with cells farther away from the vessel less affected by the drug it releases (Alfarouk *et al.*, 2013). This could create another fitness differential that may be independent of genetics. In general, exploring the impact of nongenetic TRS within populations of cells in multicellular organisms seems interesting.

However, in all cases of clonal reproduction, the effects of nongenetic TRS could strongly resemble those of selection. Indeed, as detailed in section 3, one of the significant differences between the effects of nongenetic TRS and selection appears in the presence of recombination. Recombination breaks the correlations between SNPs and leaves a signal only in the region of the locus under selection. On the contrary, the nongenetic TRS signal extends to the whole genome because no gene drives the selection. Therefore, distinguishing selection from nongenetic TRS in clonally replicating cell populations seems challenging. Despite this detection difficulty, the impact of nongenetic TRS can be prominent in these clonal populations, for example, by reducing genetic diversity. Moreover, an interaction between selection and nongenetic TRS would be possible, with the slowed diffusion of an advantageous mutation appearing in an environmentally disadvantaged lineage or, conversely, the rapid expansion of a deleterious mutation appearing in an environmentally advan-

taged line (similar to the high rate of genetic diseases discovered in Quebec and caused by CTRS, Austerlitz and Heyer, 1998).

### 1.4.4 Epidemiology

The same idea could be applied to epidemiology. Indeed, a faster reproduction of the pathogen is expected in a dense host population (Altizer *et al.*, 2006; Bailes *et al.*, 2020; Vanden Broecke *et al.*, 2019). In the case of a host population with geographically variable density, the "fertility" of the pathogen will also be variable across areas, with fertility transmission. Fertile lineages will give rise to fertile lineages simply by their geographic correlation. This could partly explain the polytomies frequently observed in viral populations, in addition to positive selection and bottlenecks (Irwin *et al.*, 2016).

### 1.4.5 A novel evolutionary force?

In this section, we have reviewed different mechanisms that can give rise to nongenetic TRS and presented the diversity of species involved. Furthermore, we have highlighted in section III how unique the impacts of nongenetic TRS are, and we described the possible interactions between this process and other evolutionary forces, notably natural selection. Therefore, it should be possible to consider nongenetic TRS as an evolutionary force in its own right because of its impact on the evolutionary history of species. Alternatively, it is also possible, and perhaps more parsimonious, to extend natural selection to any type of selection, whether genetically driven or not. This extension would require a mathematical development to generalize selection, which the Price equation could provide (Helanterä and Uller, 2010; Bonduriansky and Day, 2018; Helanterä and Uller, 2020).

However, giving such prominence to the nongenetic TRS in the framework of modern evolutionary theory may meet some resistance for two reasons. First, because Modern Synthesis (MS) classically views natural selection as the only source of adaptation, as stated by Charlesworth *et al.* (2017): "allele frequency change caused by natural selection is the only credible process underlying the evolution of adaptive organismal traits." Laland *et al.* (2015), in contrast, assert that "the burden of creativity in evolution (i.e., the generation of adaptation) does not rest on selection alone." Second, Modern Synthesis excludes any transmission of acquired traits (otherwise known as Larmarckism), a feature of nongenetic TRS (Bonduri-

ansky and Day, 2018). Indeed, an individual carrying a beneficial allele but giving birth by chance to a below-average number of children, will still pass on his statistically fitness-enhancing allele to his offspring. On the contrary, in the case of fertility transmitted via wealth, an individual who lost his lineage's wealth will transmit this low fertility status to his descendants. This Lamarckian property of nongenetic TRS pushes it away from Modern Synthesis framework, which exclusively relies on Darwinist foundations concerning adaptation.

These questions concerning the inclusion of nongenetic TRS in the framework of modern evolutionary theory are part of a broader debate concerning a possible extension of this theory. Indeed, a recent movement within evolutionary biology research seeks to extend the current framework by adding evolutionary mechanisms whose importance was discovered later and are now considered fundamental. Proponents of this Extended Evolutionary Synthesis (EES) consider that the predictions of Modern Synthesis are sometimes wrong because they do not take into account several processes. These processes include nongenetic inheritance, such as cultural or epigenetic inheritance (Youngson and Whitelaw, 2008; Laland *et al.*, 2015; Danchin *et al.*, 2019). Developmental aspects, related to the concept of phenotypic plasticity and the underlying systems biology, are also advanced as missing from the Modern Synthesis and included in the EES (Laland *et al.*, 2015).

EES has been the center of broad debate in the scientific community (Laland *et al.*, 2014). Recently, this debate was analyzed through the prism of the history and philosophy of science (Fábregas-Tejeda and Vergara-Silva, 2018; Lewens, 2019). Lewens distinguishes three entangled sets of arguments against the EES: (i) an empirical argument, (ii) a historical argument, and (iii) a conceptual argument. The first argument challenges the empirical importance of the processes that EES proponents want to add to the current theory. For example, Charlesworth *et al.* (2017) stated: "it remains to be determined how frequently such processes occur in nature." The second argument disputes EES proponents' historical depiction of Modern Synthesis. In fact, some detractors of EES define MS as a flexible foundation, open to subsequent development, a depiction that takes down the need for any theoretical revolution (Laland *et al.*, 2014). Finally, the third argument questions what makes a process worthy of being considered a fundamental force in evolution, while also challenging the very need to classify processes as truly fundamental versus so-called minor processes.

The nongenetic TRS could be an excellent example of a process calling for an extended synthesis, bringing valuable answers to the previously cited arguments.

Concerning the empirical argument, we have presented several evidence of cultural TRS in humans and other animal species. From a historical point of view, the progeny size correlations measured in humans have been interpreted solely as coming from genetic transmission (Fisher, 1930), illustrating the historical propensity of Modern Synthesis to conceptualize any transmission of fertility as being conveyed by genetics. Thus, there is at least a heuristic value in considering nongenetic TRS, to allow for a more comprehensive range of hypotheses, based on a broader theoretical framework (Lewens, 2019). In addition, we cited work showing that not taking nongenetic TRS into account distorted ancient processes inference from genomic data (Guez *et al.*, 2022). This could be a good criterion for categorizing truly fundamental processes in evolution: a process that alters the inference of a population's evolutionary history when not accounted for would be a so-called fundamental process. Whatever one's opinion about EES, the importance of the nongenetic TRS for understanding evolution is not in doubt, either in the framework of an extended synthesis or in the continuity of Modern Synthesis.

## Discussion

In this review, we have tried to bring together several pieces of literature that are quite distant at first sight: human demography and anthropology, which has studied the intergenerational correlations of progeny size in the human species by looking for sociological causes; quantitative genetics, which explores the genetic causes of these correlations; population genetics, which seeks to characterize the impact of these correlations on the genome; and evolutionary biology in the broad sense, which aims to define the main evolutionary mechanisms. We have tried to show that these different fields intersect concerning the question of nongenetic TRS.

We started this review by describing a widespread anthropological phenomenon: intergenerational correlations in progeny size. These correlations have been measured in a number of past and present-day human populations and are often positive, ranging between 0 and 0.2. Several trends emerge when studying these correlations, such as their increase after the demographic transition in some countries, or weaker correlations in developing countries than in developed countries. These results may be explained by higher birth control after the demographic transition in developed countries, which makes it easier for individuals to reach their ideal number of children and thus better reproduce the parental progeny size.

Then, we analyzed the two possible causes of this transmission of reproductive success, genetic or cultural, detailing how each could lead to TRS. Fisher's paradox, which expects an erosion of variance in the case of selection and thus a rapid disappearance of the phenomenon, is an argument put forward by the supporters of a cultural cause for TRS. Indeed, since culture is inherited with little fidelity, variance can be conserved for a long time, maintaining the TRS process without fixing the trait associated with the greatest fitness (the large progeny size). We gathered here the various responses to this paradox that proponents of genetically mediated TRS can offer. However, it seems likely that opposing the two causes is not the right angle of analysis. Both are probably at work at different levels depending on populations and time.

We then reported the effects of nongenetic TRS on population genetics. These effects are temporally complex, with a decrease in effective population size when the process starts, which yields a signal of demographic contraction in the population (high Tajima's D). When the process stops, a signal of population expansion appears due to the increase in effective population. When nongenetic TRS lasts long enough, the population reaches an equilibrium state of low diversity (due to the increase in variance of family sizes as well as the transmission process that accelerates allele fixation). At the same time, Tajima's $D$ remains negative, and the SFS is U-shaped due to a distortion of coalescent trees' topology (imbalance and high number of polytomies), as well as a non-uniform reduction of branch lengths. We finally reviewed studies which tried to infer TRS, and tackled the challenging question of disentangling nongenetic TRS from other processes such as demographic changes and selection.

In the last part of this review, we explored the presence of nongenetic TRS in other species. Indeed, several studies have revealed the regular presence of nongenetic inheritance in a broad spectrum of species and via different processes, such as ecology inheritance and parental effects. Nongenetic TRS has a different mechanism than natural selection, and its impacts on the genome are specific. These particularities advocate for considering it as an evolutionary force in its own right, or to extend the notion of selection to nongenetic inheritance mechanisms. We have discussed this idea, exploring it in light of existing debates about potential extensions of the theory of evolution, such as the Extended Evolutionary Synthesis that some authors promote.

Future research should explore different avenues concerning the topics addressed. First, despite the accumulated experimental evidence for the presence of TRS cul-

tures in humans, systematic studies still need to be done. Indeed, meta-analyses bring together studies carried out by different authors, according to different methodologies, in different countries and at different times. These discrepancies make comparison between studies difficult. Thanks to governmental registers, the profusion of genealogical data simplifies the computations of parent-child correlations in progeny size, throughout the World, over the last century. Such studies across space and time would help better interpret the correlations worldwide, and understand to what extent a cultural or genetic transmission causes them, leading to a better understanding of selection pressures in modern human populations.

Another critical research angle concerns the effects of nongenetic TRS on the genome. We have cited different results, all based on simulations of nongenetic TRS. As these results may depend on the model used to simulate the process, other models should be explored. For example, the model of Sibert *et al.* (2002), which has been used several times for the study of cultural TRS, computes the probability of reproduction of an individual based on his number of siblings. This model allows the simulation of two types of cultural TRS: parental cultural influence on the number of children and the transmission of resources correlated with fitness. However, for the second case, one might want an explicit model of resource transmission from parents to children, with a parameter of resource transmission fidelity, and a probability of reproduction depending on the amount of resources. Complexifying the model in this way would allow to approximate reality better. Beyond model exploration, studying the effects of TRS directly on real data is also essential. However, to do so, one must have both the genealogy of the natural populations to compute the parent-child correlations of progeny size, as well as the genome of the individuals. The Quebec population, for which such data are available (Anderson-Trocmé *et al.*, 2022), seems to be an ideal field for such a study. It will then be necessary to separate the effects of nongenetic TRS from genetic TRS and demography.

The generalization of nongenetic TRS to species other than humans is an area that has been too little explored so far. Assessing the strength of parent-child correlations of progeny size in natural populations of different species is of significant interest, while being relatively simple to achieve given the close scientific follow-up already available for some populations. In particular, the question of progeny size in animals would benefit from being studied in the broader context of animal social networks, a field that is recently receiving increasing interest (Puga-Gonzalez *et al.*, 2019; Brask *et al.*, 2021). Beyond multicellular species, studying nongenetic TRS between cells could be of major interest. This would potentially provide a better

understanding of the evolution of bacterial or cancer cell populations. Experimental evolution on yeasts would help study nongenetic TRS in a realistic yet controlled context. For example, in a medium containing a nutrient gradient, a cell inherits its parent's position together with its fertility. However, the effects of varying cell density in the medium and the emergence of favorable mutations will have to be distinguished from those of nongenetic TRS.

Finally, a fundamental line of research consists in placing nongenetic TRS in the general framework of evolutionary theory, with or without the help of new frameworks such as the Extended Evolutionary Synthesis developed by authors like Laland *et al.* (2015). Mathematical modeling would help define the different types of TRS and their dissimilarities, a work already started with the help of Price's equation. In addition, research in philosophy of science is needed to understand the extent to which such processes challenge central paradigms in evolutionary biology. We have sketched some ideas on this subject in this review. More than an evolution of scientific paradigms, it is perhaps an evolution of heuristic habits when formulating hypotheses that remains necessary. Indeed, in evolutionary biology, we continue to focus on genetic evolution alone. However, the picture remains incomplete without considering interactions between genetic and nongenetic components.

# Chapter 2

# CTRS effects on population genetics

*This chapter is an accepted paper in the journal Genetics under the title:* ***Cultural transmission of reproductive success impacts genomic diversity, coalescent tree topologies and demographic inferences.***

Jérémy Guez, Guillaume Achaz, François Bienvenu, Jean Cury, Bruno Toupance, Évelyne Heyer, Flora Jay[‡], Frédéric Austerlitz[‡]

[‡]These authors contributed equally to this work.

**Abstract**

*Cultural transmission of reproductive success (CTRS) has been observed in many human populations as well as other animals. CTRS consists of a positive correlation of nongenetic origin between the progeny size of parents and children. This correlation can result from various factors, such as the social influence of parents on their children, the increase of children's survival through allocare from uncles and aunts, or the transmission of resources. Here, we study the evolution of genomic diversity over time under CTRS. CTRS has a threefold impact on population genetics: (1) the effective population size decreases when CTRS starts, mimicking a population contraction, and increases back to its original value when CTRS stops; (2) coalescent tree topologies are distorted under CTRS, with higher imbalance and a higher number of polytomies; and (3) branch lengths are reduced nonhomogeneously, with a higher impact on older branches. Under long-lasting CTRS, the effective population size stabilizes but the distortion of tree topology and the nonhomogeneous branch length reduction remain, yielding U-shaped site frequency spectra (SFS) under a constant population size. We show that this yields a bias in SFS-based demographic inference. Considering that CTRS was detected in numerous human and animal populations worldwide, one should be cautious because inferring population past histories from genomic data can be biased by this cultural process.*

# Introduction

In recent years, numerous studies have investigated the interactions between human culture and genetics. In some cases, cultural changes yield genetic adaptations. This was the case, for example, for lactase persistence that likely evolved independently in different human populations in Eurasia and Africa, due to the emergence of pastoralism (Swallow, 2003; Bersaglieri *et al.*, 2004; Tishkoff *et al.*, 2007; Gerbault *et al.*, 2011; Segurel *et al.*, 2020). Nevertheless, cultural processes can affect human genetic evolution without involving natural selection (Heyer *et al.*, 2012): (i) polygamy (including polyandry and polygyny), (ii) descent rules (patrilineal, matrilineal, or cognatic), and (iii) cultural transmission of reproductive success (CTRS).

CTRS is a positive correlation in the number of children between parents and children resulting from nongenetic causes. In that case, individuals with many siblings tend to have more children than average. This transmission can result from multiple non-genetic causes: the social influence of parents on their children (Barber, 2001; de Valk, 2013; Kolk, 2014), the increase in child survival when uncles and aunts are present (allocare) (Heyer *et al.*, 2012; Lawson and Mace, 2011; Murphy, 2013) or the transmission of resources from parents to children. Such resources can be material resources (Sorokowski *et al.*, 2013), social resources (e.g., transmission of rank or of polygyny; Heyer *et al.*, 2012), or cultural resources (such as hunting skills; Borgerhoff Mulder *et al.*, 2009). Furthermore, transmission of migration propensity across generations can have an effect similar to CTRS, with some lineages growing less than others due to their larger tendency to leave the population (Gagnon and Heyer, 2001; Gagnon *et al.*, 2006).

CTRS yields a decrease in effective population size and genetic diversity, and may increase the frequency of severe genetic disorders (Austerlitz and Heyer, 1998). The time to the most recent common ancestor is reduced, yet in a nonhomogeneous way as the tree branches closer to the root are more strongly shortened (Sibert *et al.*, 2002). While these patterns can result from other evolutionary processes (e.g. bottlenecks, expansions), a more specific effect of CTRS is its impact on the topology of coalescent trees: CTRS yields imbalanced trees as it increases the proportion of lineages corresponding to large families (Sibert *et al.*, 2002). This specific property has been used in particular for inferring the transmission of reproductive success on Y chromosome and mitochondrial DNA (Blum *et al.*, 2006; Heyer *et al.*, 2015). Since natural selection also implies a transmission of reproductive success, it is difficult to assess whether the imbalanced trees of nonrecombining uniparental markers result

from natural selection or CTRS. Therefore, it is important to study the impact of CTRS on the nuclear genome. Recombination should indeed restrict the effects of natural selection to the genomic regions around selected loci (Li and Wiehe, 2013). Conversely, CTRS will yield an imbalance signal across the whole genome because in that case reproductive success is not linked to any locus in particular.

Studying the impact of CTRS on genomic diversity is particularly relevant, as it is a rather common phenomenon. Several demographic studies have shown a parents-children correlation in the number of children ranging generally between 0.1 and 0.25 (e.g., Murphy, 1999; Murphy and Wang, 2001; Gagnon and Heyer, 2001; Pluzhnikov *et al.*, 2007). There has been an extensive debate about whether these correlations result from cultural (Potter and Kantner, 1955; Duncan *et al.*, 1965) or genetic (Kohler *et al.*, 1999; Rodgers *et al.*, 2001; Mills and Tropf, 2015) transmission, the second case corresponding to natural selection. The correlations may, in fact, often be caused by both genetic and cultural transmission, along with interactions between genetics and the environment (Murphy, 2013), making the disentangling of those processes particularly difficult, especially as they can vary across populations and time. For instance, contemporary populations tend to have a stronger inter-generational correlation than populations that predate the demographic transition (Murphy, 1999; Murphy and Wang, 2001). Furthermore, this phenomenon is not limited to humans and has been described in various species such as hyenas (Engh *et al.*, 2000), Japanese macaques (Kawai, 1958), whales (Whitehead, 1998), dolphins (Frere *et al.*, 2010), and cheetahs (Kelly, 2001).

Another reason for studying the impact of CTRS on genomic diversity lies in its putative ability to impact summary statistics commonly used to infer other processes. For instance, Site Frequency Spectra (SFS), which might be impacted by CTRS, are widely used for demographic inferences, either alone (e.g. $\delta a \delta i$ (Gutenkunst *et al.*, 2009), Fastsimcoal (Excoffier *et al.*, 2013), Stairway Plot (Liu and Fu, 2020), ABC-DL (Mondal *et al.*, 2019)) or jointly with other summary statistics (e.g., Sheehan and Song, 2016; Boitard *et al.*, 2016; Jay *et al.*, 2019; Terhorst *et al.*, 2017). These inference tools could thus be biased when applied to populations that have been affected by CTRS during part of their history. Understanding the interactions between CTRS and demographic changes is therefore relevant not only for inferring CTRS itself but also for improving demographic inferences, which is of broad interest (Beichman *et al.*, 2018).

This article pursues three objectives. First, we aim to improve our understanding of the impact of CTRS on nuclear genomes using simulations. Brandenburg

*et al.* (2012) performed a simulation study that investigated the impact of CTRS on small sequences, ignoring intragenic recombination. Here, we study its impact on large recombining sequence data, adding numerous summary statistics not previously explored in CTRS scenarios. The summary statistics we assess are mainly of two kinds: (i) population genomic statistics, such as genetic diversity, Tajima's $D$ and SFS, and (ii) various tree topology indices, such as tree imbalance indices and number of polytomies. In addition, we investigate the interaction of demographic changes and CTRS, as we expect human populations to undergo both types of processes. In particular, we look into the effect of an expansion occurring before and during CTRS, an interaction that has not yet been explored. Second, we investigate the impact of CTRS duration and the persistence of ancient CTRS signals in the genome by measuring the evolution of the summary statistics over time (before, during, and after CTRS). In particular, this allows us to assess the impact of very short periods of CTRS on population genetics. Although long-lasting CTRS is not theoretically excluded, available anthropological evidence only indicates the presence of CTRS over short periods. For example, pedigrees from the Saguenay-Lac-Saint-Jean population show CTRS for 12 generations (Austerlitz and Heyer, 1998). For CTRS induced by variance in fertility among lineages within a population, the persistence of CTRS requires that individuals can trace back their lineage affiliation for several generations (in central Asia, Chaix *et al.* (2004) estimated this number of generations to be 7-10 depending on the population). Finally, we assess whether CTRS impacts demographic inference. For various CTRS scenarios, we compare the true and estimated instantaneous growth factor and timing of expansion.

## 2.1 Methods

### 2.1.1 Model

We implemented the CTRS model designed by Sibert *et al.* (2002) and Brandenburg *et al.* (2012) using the forward-in-time simulation framework SLiM (Haller and Messer, 2019). Individuals are diploid and monogamous, generations are nonoverlapping, and the population has a fixed number of individuals $N$ with a 1:1 sex-ratio. At each generation, couples are formed uniformly at random before reproduction and never separated. One parental couple is randomly drawn from the population for each newborn child. This process is repeated until $N$ offspring are produced.

The probability $p_i$ for a given couple $i$ of being drawn for reproduction is given by:

$$p_i = \frac{\gamma_i(b) \times s_i^{\alpha}}{\sum_{j=1}^{N_c} \gamma_j(b) \times s_j^{\alpha}},$$

where $s_i$ is the average sibship size of the two members of couple $i$, $\alpha$ is the parameter controlling the intensity of CTRS and b is the parameter controlling the variance in reproductive success. We denote $N_c$ as the number of couples ($N_c = N/2$). The higher $\alpha$ is, the stronger the CTRS ($\alpha = 0$ means no CTRS, $\alpha = 2$ means a very strong CTRS). $\gamma_i(b)$ is a random gamma distributed variable drawn independently for each couple $i$, with shape parameter $b$ and mean 1. Here, we considered only two cases: $b \to \infty$ (low variance in reproductive success, resulting in a Poisson-like distribution for the progeny size in the absence of CTRS, as $\lim_{b\to\infty} \gamma(b) = 1$) or $b = 1$ (high variance, resulting in a geometric-like distribution, as $\gamma(1)$ is an exponential of mean 1 distribution). Some results are shown for both values of $b$, but we focused mainly on the $b = 1$ case, as Austerlitz and Heyer (1998) found that the geometric-like model was more consistent with demographic data than the Poisson-like model and better explained the occurrence of genetic diseases in Saguenay-Lac-Saint-Jean.

For the demographic parameters, we compared two scenarios of constant population sizes (200 and 5000 individuals) and explored a scenario of sudden demographic expansion by a fivefold factor (200 to 1000 individuals). This expansion occurred 300 generations before the present.

### 2.1.2 Simulations

Unless specified otherwise, the simulations correspond to 200 replicates per scenario, a population size of 1000 individuals and a sample size of 30 individuals. Genomes were made of one chromosome of $10^7$ bp in length, with a recombination rate and mutation rate of $10^{-8}$ per bp, which are commonly used parameters in human population modeling. We used the geometric-like model ($b = 1$) since Austerlitz and Heyer (1998) showed it was more realistic than the Poisson-like model ($b = \infty$) in the population of Saguenay-Lac-Saint-Jean where CTRS is documented from pedigree datasets. Coalescent trees are built in two steps: (1) forward-in-time simulations using our model implemented in SLiM (Haller and Messer, 2019) starting before the beginning of CTRS, resulting in trees that did not fully coalesce when the CTRS period is short, (2) a backward neutral coalescent process in order to complete the

trees from the first step (i.e., to reach the most recent common ancestors throughout the genome). This step uses the *tskit* package functionality called *recapitation* (Kelleher *et al.*, 2016, 2019).

To assess the impact of CTRS on reproduction, we measured three demographic parameters : (1) the correlation between progeny sizes of all individuals and their parents' progeny sizes as a function of $\alpha$, the strength of CTRS; (2) the variance of progeny size, and (3) the distribution of progeny sizes in the population for $\alpha = 0$, 1 and 2.

To investigate the effect of CTRS across time, we measured the genomic summary statistics on batches of individuals sampled through time for the following scenario: 2000 generations of CTRS, followed by 2000 generations with no CTRS. Every 50 generations, individuals were sampled for analysis. Following any cultural change (starting or stopping CTRS), we sampled more frequently to capture rapid fluctuations of summary statistics (at generations 2, 5, 10, 15, and 20 postchange).

### 2.1.3 Summary statistics

To assess the effects of CTRS on the genome, we explored the following diversity summary statistics as a function of time using the *tskit* package (Kelleher *et al.*, 2016, 2019): (1) the number of trees per chromosome, which is the number of recombination breakpoints plus 1, (2) the number of pairwise differences among the sampled chromosomes, (3) the average number of pairwise differences per tree, and (4) the number of SNPs in the chromosomes, (5) the average number of SNPs per tree, (6) Tajima's $D$, (7) the unfolded site frequency spectrum (SFS). For the SFS, we computed a transformed version (Lapierre *et al.*, 2017) that consists of multiplying singletons by 1, doubletons by 2, and $n$-tons by $n$. We then divided all bins by $\theta$, which is estimated by taking the average of all bins so that the expected transformed SFS for the neutral case is a flat line with a value of 1.

We computed the theoretical effective size $N_{\text{exp}}$ according to the equation $N_{\text{exp}} = 4N/(2 + s^2)$, where $s^2$ is the variance in progeny size (Wright, 1938; Wang *et al.*, 2016). This formula computes the effective size as a function of the census population size $N$ and the variance in progeny size only. We compared $N_{\text{exp}}$ to the observed effective size $N_{\text{obs}}$ which was computed as follows: $N_{\text{obs}} = \theta/(4\mu L)$, with the average number of pairwise differences, $\hat{\theta}_\pi$, as an estimator of $\theta$, $L$ the genome length and $\mu$ the mutation rate per base pair.

We also computed various topology indices, to assess the effect of CTRS on the topology of coalescent trees, with the help of the *tskit* package (Kelleher *et al.*, 2016, 2019). Balance and imbalance indices: (1) $I_b$, the Brandenburg imbalance index (Brandenburg *et al.*, 2012; Blum *et al.*, 2006); (2) $I_s^*$, a normalized Sackin imbalance index (Sackin, 1972; Shao and Sokal, 1990); (3) $I_{ce}^*$ and $I_{ca}^*$, two modified versions of the Colless imbalance index (Colless, 1982), ; (4) the $B_1$ balance index (Shao and Sokal, 1990); (5) the $B_2$ balance index (Shao and Sokal, 1990; Bienvenu *et al.*, 2021). Other topology indices: (1) the number of polytomies (nodes that have more than two direct children); (2) the number of interior nodes (all nodes excluding leaves and root). To compare different indices, we also used their standardized versions using their mean and standard deviation at generations preceding CTRS.

$I_b$, $I_s^*$, $I_{ca}^*$ and $I_{ce}^*$ measure the imbalance of trees, meaning that those indices take higher values for more imbalanced trees. $I_b$ was computed using the script provided by Brandenburg *et al.* (2012). For one tree, $I_b$ is the average of $I_{b,node}$ computed for each node in the tree according to the formula:

$$I_{b,node} = \frac{B - m_{s,l}}{D - m_{s,l}}, \text{ with } m_{s,l} = 2B_{s,l,coal} - D,$$

where $s$ is the number of direct subnodes under the considered node and $l$ the number of leaves descending from it. For each direct subnode under the considered node, leaves are counted and the maximum value is denoted $B$. $D$ is the maximum value that $B$ can possibly take (i.e., in the most imbalanced configuration) and is equal to $l - s + 1$. Thus, $\frac{B}{D}$ is the level of imbalance at this specific node. The correction factor $m_{s,l}$ enforces the expectation of $I_b$ to be 0.5 for a standard population without CTRS. This parameter is evaluated based on simulations: $B_{s,l,coal}$ is the average $B$ value of 1000 simulated random Kingman's (1982) incomplete coalescent trees with $l$ leaves that were stopped when $s$ parent nodes remained.

The Sackin imbalance index $I_s$ is computed by counting for each leaf the number of nodes to reach the root and summing up all values. The Colless imbalance index $I_c$ is computed by counting for each node (except for the root in our case) the difference in the number of leaves between its two children and summing up all values. However, this can be done only for binary trees. To handle polytomies, we designed two modified versions of the Colless imbalance index, $I_{ce}$ and $I_{ca}$. For $I_{ce}$, the two children chosen for calculating the difference are those with the highest and lowest number of leaves ($e$, as for extreme number of leaves). $I_{ca}$ is computed by taking the average of differences for all pairs of children among all children of

a given node ($a$, as for average). Since the Sackin and Colless indices minimum and maximum values depend on the number of nodes (Shao and Sokal, 1990) which varies across trees when permitting polytomies, we computed a corrected version of the Sackin ($I_s^*$) and Colless ($I_{ce}^*$ and $I_{ca}^*$) indices which divides the index of each tree by the number of its interior nodes.

$B_1$ and $B_2$ are balance indices; we thus expect their value to be lower when trees are imbalanced. The $B_1$ balance index is computed by counting for each node the maximum path length to its leaves and taking the inverse of this value before summing up all of the values (one value per interior node). The $B_2$ balance index is based on $p_k$ the probabilities to reach the leaf $k$ assuming a random walk starting from the root and choosing a random direction at each node. $B_2$ is equal to the Shannon entropy of the $p_k$; a uniform distribution (an entropy of 1) corresponds to a balanced tree (Shao and Sokal, 1990; Bienvenu *et al.*, 2021).

Because of recombination, one chromosome corresponds to a sequence of coalescent trees. Summary statistics can be computed for each of the trees, with close trees having similar values. To consider the various histories represented by each of those trees, we explored not only the average summary statistics but also the shape of their distributions across the genome. The summary statistics were computed separately on each tree along the genome using the *tskit* package.

We also assessed the effect of sample size (number of individuals sampled) and of number of genomic regions on the power of detecting CTRS, using a Wilcoxon test with the significance threshold set to 0.01. For this assessment, we simulated 3000 independent genomic regions of 1 Mb for two populations of 1000 individuals: one that went through a CTRS process of strength $\alpha = 1$ during 20 generations before present, and one with $\alpha = 0$ (no CTRS). We then sampled 5, 10, 30, 60, 90 and 120 diploid individuals from each of the two sets of 3000 simulated regions and the four summary statistics ($I_b$, number of polytomies, $B_1$, and Tajima's $D$) on all of them (2 scenarios $\times$ 3000 regions $\times$ 6 sample sizes $\times$ 4 summary statistics computations). For each sample size, we sampled $3, 4, 5, \ldots, 100$ regions from the two sets of 3000 simulated regions, before using a Wilcoxon test to compare the four summary statistics values between the two populations ($\alpha = 0$ and $\alpha = 1$). For each combination of sample size and number of sampled replicates ($6 \times 98$ combinations), the sampling among replicates and the Wilcoxon test were repeated 1000 times, with the proportion of $p$ values lower than or equal to 0.01 equaling the power of the test.

### 2.1.4 Assessing demography inference bias

To assess the bias in SFS-based demography inference, we used the software $\delta a \delta i$ with a one-event model (Gutenkunst *et al.*, 2009). Two scenarios were studied: (1) a sudden fivefold expansion in population size that occurred 280 generations before a short period of CTRS (20 generations); and (2) a sudden fivefold expansion in population size that occurred during CTRS, after the first 1200 generations of a 1500-generations period of CTRS (Figure 2.1). We chose a fivefold sudden expansion as a simple illustration of a demographic event, which has the advantage of mimicking the past Neolithic expansion in human population history. From 30 diploid individuals sampled 300 generations after the demographic event, we inferred two parameters: the growth factor (expected value of 5) of the population and the number of generations since the event (expected value of 300 generations). The strength of CTRS was set to $\alpha = 1$. We compared the quality of inference in both scenarios to equivalent demographic scenarios without CTRS ($\alpha = 0$).

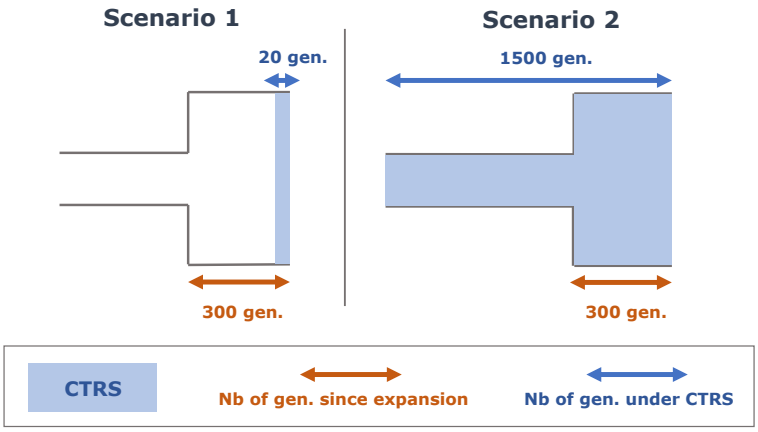


Figure 2.1: The two studied scenarios for SFS computation and $\delta a \delta i$ inference.
In both scenarios, the expansion event occurs 300 generations before SFS computation and $\delta a \delta i$ inference. Scenario 1: 20 generations of CTRS before the present. Scenario 2: 1500 generations of CTRS before present.

We inferred the parameters of 200 replicates for each of the four scenarios (scenarios 1 and 2 with $\alpha = 0$ or 1). Because the $\delta a \delta i$ optimization algorithm depends on the initialization of the model parameters, we repeated the inference three times for each replicate with different initialization values. We set the boundaries for the inferred growth factor at [0.01; 100] and for the inferred growth time at [0; 5] (time is expressed in $2N$ generations in $\delta a \delta i$, where $N$ is the population size before the event). When the results were too close to the boundaries ($> 99$ or $< 1/99$ for the growth factor, $> 4.9$ or $< 0.1$ for the time since the event), the results were discarded. For each replicate, the remaining results among the three trials were kept, and their

median was considered as the inferred parameter for this replicate. To convert time into generations, we multiplied the inferred time value of each replicate $r$ by $2\hat{N}_r$; where $\hat{N}_r$ denotes the ancestral population size estimated for replicate $r$, using a $\hat{\theta}_r$ estimate computed by $\delta a \delta i$.

We removed outliers among replicates (i.e., values that were higher than $Q3 + 1.5 \times IQR$ and lower than $Q1 - 1.5 \times IQR$, with $Q3$ being the third quartile, $Q1$ being the first quartile and $IQR$ being the interquartile range). We then computed the mean squared relative error (MSRE) and relative bias.

## 2.2 Results and discussion

### 2.2.1 Impact of CTRS on reproductive patterns

To assess the impact of CTRS on reproductive patterns, we simulated various strengths of CTRS (defined by $\alpha$) for two models of variance in reproductive success (low variance with $b = \infty$ and high variance with $b = 1$). We computed the Pearson correlation coefficient between parents and children $\mathrm{Cor}_{P,C}$ and the variance and distribution of progeny size. As expected, $\mathrm{Cor}_{P,C}$ increases with $\alpha$. However, this effect is weaker for smaller population sizes. This is due to an increased effect of stochastic processes in small populations, counteracting the impact of parents on children's progeny size (Figure 2.2A). The slope of the relationship between $\mathrm{Cor}_{P,C}$ and $\alpha$ is also lower for the $b = 1$ model than for the $b = \infty$ model (Figure 2.2A). Indeed, the higher variance in progeny size in the $b = 1$ model decreases the correlations, compared to the $b = \infty$ model.

Higher values of $\alpha$ yield more extreme progeny sizes (Figure 2.2B-C, purple compared to orange and green) and a higher variance (Supp. Fig. S1). This variance reaches a plateau after a few generations (Supp. Fig. S1). At this plateau, the exact progeny size distribution differs depending on the model: compared to the $b = \infty$ model, the $b = 1$ model yields a higher proportion of couples with no offspring and a lower proportion of couples with medium-sized families (1 to 3 children) (Figure 2.2B versus 2.2C).

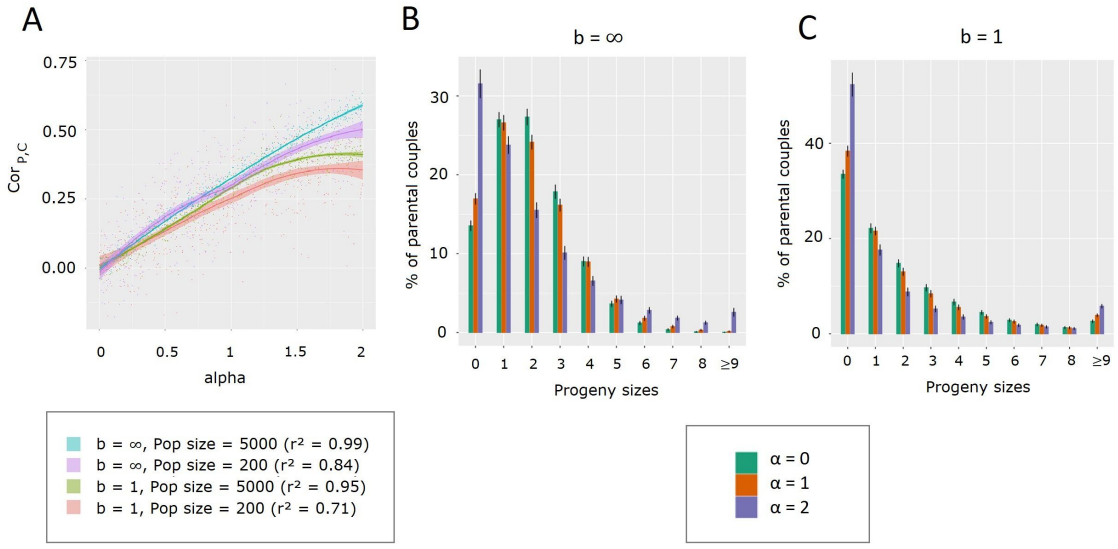


Figure 2.2: Impact of CTRS on two population reproduction variables.
A. Correlation between parents and children progeny size as a function of $\alpha$, for four scenarios. In brackets: correlation between $\text{Cor}_{P,C}$ and $\alpha$ for each scenario. Lines are drawn using locally weighted regression with the 95% confidence interval using the function loess of the R package ggplot2.
B. Distribution of progeny sizes for $\alpha = 0$ (green), 1 (orange) and 2 (purple), population size = 1000. The $b = \infty$ model is used (low variance of reproductive success).
C. Distribution of progeny sizes for $\alpha = 0$ (green), 1 (orange) and 2 (purple), population size = 1000. The $b = 1$ model is used (low variance of reproductive success).

### 2.2.2 Impact of CTRS on the genome

#### Effective population size

We then assessed the impact of CTRS on population genomic parameters. When CTRS begins, genomic diversity, measured either as the number of SNPs (Supp. Fig. S2A) or as the number of pairwise differences (Fig. 2.3A), declines and eventually reaches a plateau, showing a decrease in effective population size of 40 % for the $b = \infty$ model and of 75 % for the for the $b = 1$ model (for $\alpha = 1$, at the plateau), demonstrating a stronger effect of CTRS under the second model (Fig. 2.3B).

Because of this decrease in effective population size, the number of coalescent trees across the genome is lower due to fewer recombination events, and the TMRCA is smaller (Supp. Fig. S2B-C). For all these parameters, the plateau is lower for $\alpha = 2$, since it yields lower effective population sizes than $\alpha = 1$. Moreover, the higher $\alpha$ is, the faster the plateau is reached. This happens because genetic drift, which is stronger when $\alpha$ is high, swiftly erases past diversity. As soon as CTRS stops, diversity starts to increase slowly (Figure 2.3A), taking more time to recover than

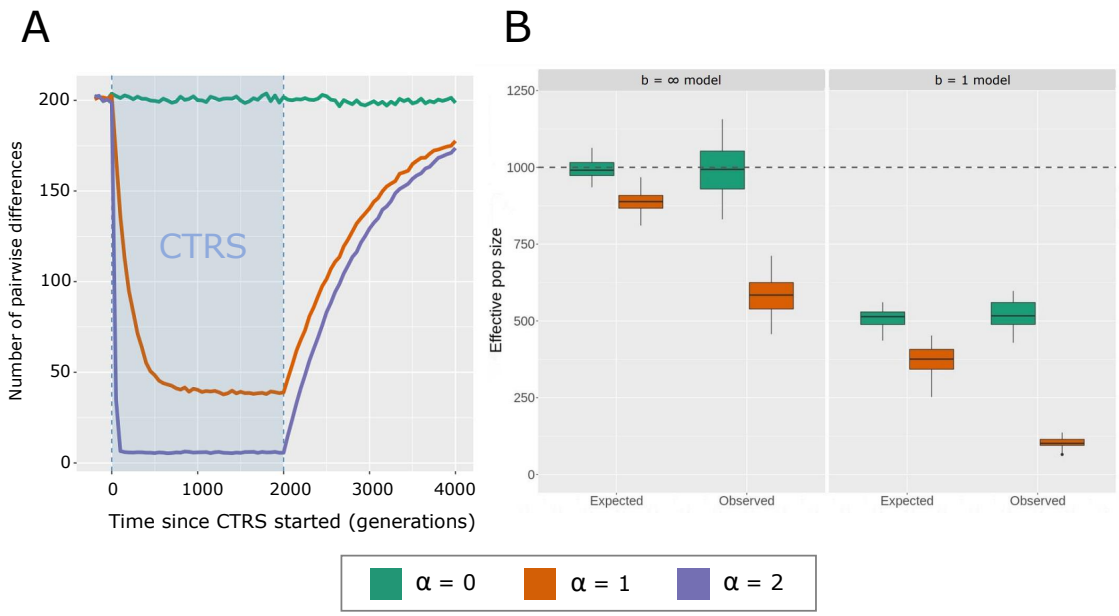


Figure 2.3: Factors of effective population size decrease under CTRS.
A: Average number of pairwise differences across time for three levels of CTRS: $\alpha = 0$, $\alpha = 1$ and $\alpha = 2$. In all cases, the $b = 1$ model of variance in progeny size is used. The blue rectangle corresponds to the period when populations are under CTRS. Generations are counted from the beginning of CTRS.
B: Expected effective population size given the observed offspring variance ($N_{\text{exp}}$) and observed effective population size measured using the number of pairwise differences at the plateau in Panel A as an estimator of $\theta$ ($N_{\text{obs}}$), for $\alpha = 0$ and $\alpha = 1$ and both models of variance in progeny size ($b = \infty$ and $b = 1$). The dotted line represents the census N value, which is 1000 individuals.

it took to decrease. Indeed, as the effective population size becomes larger, drift becomes weaker and the impact of past events lasts longer (i.e., diversity is close to equilibrium after $10N_e$ generations).

This decrease in effective population size results both from the increase in the variance of progeny size due to CTRS and the transmission of progeny size itself, which amplifies allele fixations by helping alleles carried by large lineages to spread faster in the population. To assess the respective impact of these two factors on effective population size, we compared $N_{\text{exp}}$ (the expected effective population size when taking into account the variance in progeny size only), to $N_{\text{obs}}$ which is impacted by both components (Fig. 2.3B). We show that while a substantial decrease in effective population size is caused by the increased variance in progeny size, most of this decrease is due to the transmission component (around 70 % of the decrease in the $b = \infty$ model and 65 % of the decrease in the $b = 1$ model, for $\alpha = 1$).

### Tajima's D

Tajima's $D$ follows a more complex pattern than does genetic diversity. This pattern can be decomposed into four steps (Figure 2.4A): (1) as soon as CTRS begins, it increases rapidly towards a peak in positive values then (2) it decreases toward a plateau in negative values, (3) when CTRS stops, it rapidly decreases again toward more negative values, and (4) it slowly recovers to pre-CTRS levels. The first peak (1) results from a sudden decrease in effective population size when CTRS starts, as explained above, yielding a demographic contraction-like signal with positive values of $D$. Once this contraction signal is erased (i.e., the effective population size is still lower but there is no "memory" of the ancient effective population size due to an MRCA born after the change), $D$ reaches a negative plateau at equilibrium; (2): the population is composed of many related individuals coming from large family lineages and few individuals from small family lineages, the latter yielding an excess of rare alleles. The nonhomogeneous reduction of coalescent times, stronger for the branches closer to the root (Sibert *et al.*, 2002), also contributes to this excess of rare alleles. When CTRS stops, the decrease toward more negative values (3) is due to the increase in effective population size (expansion-like event). This negative peak is followed by a slow recovery (4) until the expansion signal is completely erased. These steps are not followed at the same pace along the genome: some coalescent trees will enter the equilibrium stage, while others retain a strong signal of the effective population size contraction, transiently yielding a bimodal distribution of $D$ across the genome (Supp. Fig. S3B and C for $\alpha = 2$, Figure S3D for $\alpha = 1$).

Thus, understanding the effect of CTRS on Tajima's $D$ requires accounting for three processes: changes in effective population size, an increased variance in relatedness among individuals as compared to a neutral population and a non homogeneous reduction in branch lengths. Timing is then an important factor: the relationship between $\alpha$ and Tajima's $D$ changes over time after the beginning of CTRS, and the impact of CTRS on genetic diversity and $D$ persists long after CTRS has stopped.

The interaction between demographic events and CTRS is also important, since both can happen in the same period of human history. When a fivefold expansion occurs during the equilibrium stage, Tajima's $D$ decreases as expected, but the extent of this decrease depends on $\alpha$: the stronger $\alpha$ is, the weaker the decrease will be, showing the nonadditivity of the two processes regarding $D$ (Figure 2.4B, generation 1200). The recovery from the effect of this fivefold expansion also depends on $\alpha$: when $\alpha = 1$, Tajima's $D$ recovers faster than with no CTRS ($\alpha = 0$) (Figure 2.4B,

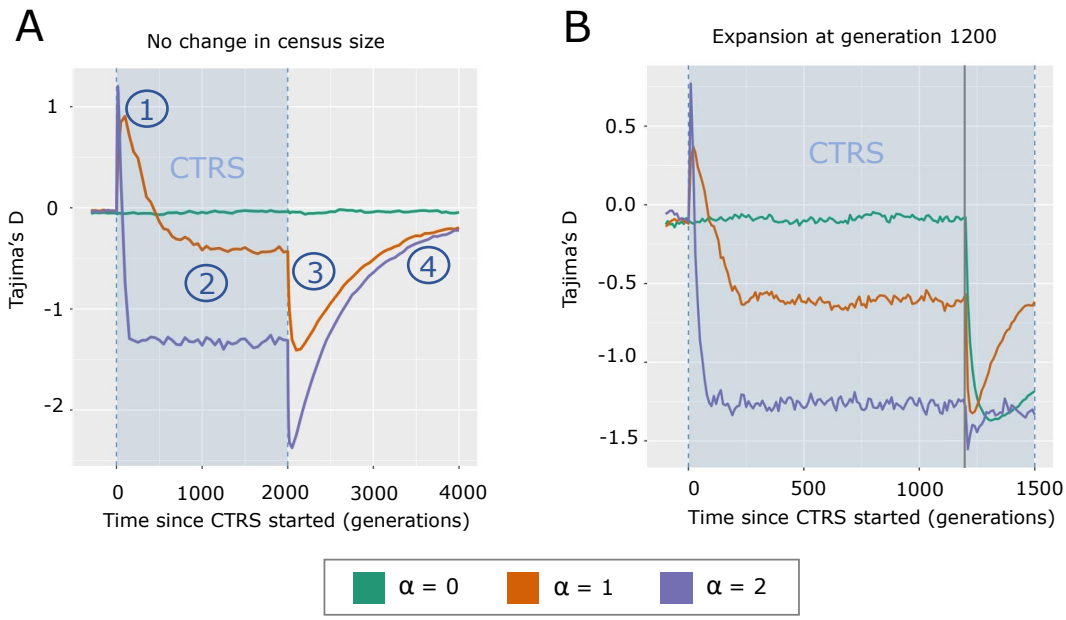


Figure 2.4: Tajima's $D$ through time under various CTRS and demographic conditions.
A-B. The blue rectangle corresponds to the period when populations are under CTRS. Generations are counted from the beginning of CTRS. In all cases, the $b = 1$ model of variance in progeny size is used.
A. Tajima's $D$ across generations for three values of $\alpha$ (0, 1 and 2), with a constant population size of 1000 individuals.
B. Tajima's $D$ across generations for three values of $\alpha$ (0, 1 and 2). A fivefold expansion event occurs at generation 1200 (200 individuals to 1000 individuals - gray vertical line).

generations 1200 to 1500). This is due to the smaller population effective size when $\alpha = 1$, which quickly erases past signals. Thus, we expect populations under CTRS to lose the genetic signals of past demographic events faster.

### Coalescent tree topology

It is likely that neither diversity indices nor Tajima's $D$ would be sufficient alone to infer CTRS in population genetics data, since demographic events also impact these statistics. In contrast, the shape of coalescent trees has been shown to display a CTRS-specific signal, with trees being more imbalanced only when CTRS is present, irrespective of the variation in total population size. Brandenburg *et al.*'s (2012) imbalance index $I_b$ (Figure 2.5A) grows rapidly when CTRS starts and decreases as soon as it stops, recovering in a few dozens of generations, unlike Tajima's $D$ (Figure 2.4A), which did not fully recover after $2N = 2000$ generations. The number of polytomies follows a pattern similar across time as $I_b$ (Supp. Fig. S4). However, this increased number of polytomies can stem from the contraction in effective size

yielded by CTRS (4-fold decrease when $\alpha = 1$ and $b = 1$), as coalescent rates are higher for smaller population sizes, increasing the probabilities of polytomies. To assess this hypothesis, we compared the number of polytomies after 500 generations of CTRS ($\alpha = 1$ and $b = 1$) to the number of polytomies after a 4-fold contraction 500 generations before the present, without CTRS. The results show that the 4-fold contraction indeed yields a higher number of polytomies than the neutral case, but a lower number of polytomies compared to the scenario of CTRS (Supp. Fig. S5A). Thus, the increased number of polytomies under CTRS is caused not only by the contraction of the effective size, but also by the transmission property of CTRS. The same comparison for $I_b$ shows that none of the imbalance under CTRS is due to the contraction of effective size, as the mean imbalance after contraction is equal to the mean imbalance of the neutral case, with a higher variance due to the smaller population size (Supp. Fig. S5B).

The distribution of $I_b$ across the genome was bell-shaped and unimodal for all tested strengths of CTRS ($\alpha = 0$, 1 and 2), with a shift toward high values when $\alpha$ increased (Supp. Fig. S6). This is because CTRS is not conveyed by any locus in particular, unlike natural selection, for which we could expect in some cases a multimodal distribution due to imbalanced trees in the region under selection and balanced trees elsewhere in the genome. Unlike the distribution of Tajima's $D$ (Supp. Fig. S3), the distribution of $I_b$ does not evolve during the process of CTRS, as shown when comparing the distributions after 20 and 500 generations of CTRS (Supp. Fig. S6). In fact, $I_b$ is only impacted by the imbalance property of coalescent trees and thus only displays its effects, which are constant through time after the first few generations, contrary to Tajima's $D$, which is affected by imbalance and by changes in effective size as well, with the latter's effects depending strongly on time.

### Short-lasting CTRS

We have thus far simulated cases of long-lasting CTRS, in order to investigate the values of the different statistics at the equilibrium state under CTRS (Figure 2.4). However, as the CTRS duration could be much shorter in reality, we also investigated cases where CTRS lasted for only a few generations. This situation was simulated for both low ($b = \infty$) and high variance in progeny-size ($b = 1$). We show that two or three generations of CTRS are sufficient to have an impact on genetic statistics (Supp. Fig. S7). Tajima's $D$ displays an effect under medium ($\alpha = 1$) and high

levels of CTRS ($\alpha = 2$), for both models of variance in progeny-size ($b = \infty$ and $b = 1$). Conversely, $I_b$ seems affected under medium levels of CTRS only in the case of high variance in progeny size. Note that these realistic short periods of CTRS lead to an increase in Tajima's $D$ toward positive values due to the effective size contraction, as explained above. Finally, we show that after such a short period of CTRS, a few generations without CTRS are not sufficient to erase the effects on the genome (Supp. Fig. S7).

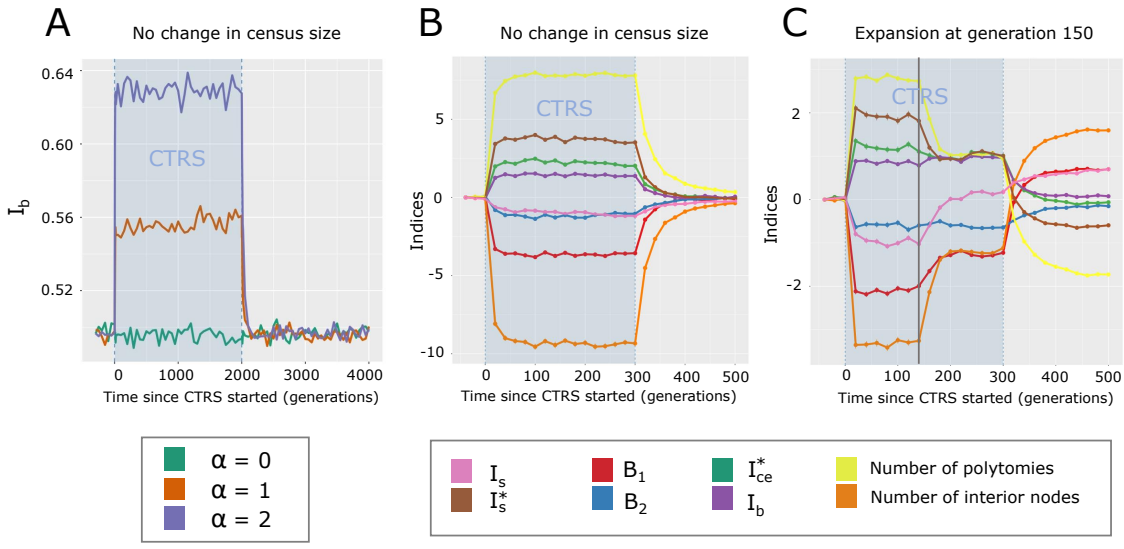


Figure 2.5: Imbalance indices over time.
A-C. The blue rectangle corresponds to the period when populations are under CTRS. Generations are counted from the beginning of CTRS. In all cases, the $b = 1$ model of variance in progeny size is used.
A. $I_b$ across generations for three values of $\alpha$ (0, 1 and 2).
B. Various indices across generations for $\alpha = 1$. For each point, bars show the standard error of the mean.
C. Various indices across generations for $\alpha = 1$. An expansion event occurs at generation 150 (vertical gray line). For each point, bars show the standard error of the mean

### CTRS detection

Some indices seem to be more effective for CTRS detection than others (Figure 2.5B). When $\alpha = 1$, of all tree (im)balance indices, $B_1$ and $I_s^*$ are the most affected, with a shift of 3 to 4 standard deviations, while this shift is only between 1 and 2 standard deviations for other (im)balance indices such as $I_b$, $I_s$, $B_2$. $I_{ca}^*$ and $I_{ce}^*$, the two Colless indices handling polytomies, display a similar pattern with a shift of 2 standard deviations (Supp. Fig. S8). However, $I_{ce}^*$ seems slightly more affected by

CTRS, due probably to its algorithm focusing on children with an extreme number of leaves (see Methods). The number of interior nodes and the number of polytomies are affected by CTRS more than all other measured indices, with a shift of 8 to 9 standard deviations (Figure 2.5B). Interestingly, each of these indices seems to contain specific information about tree topology, as the correlations between their absolute values range between 0.99 and -0.17, although they all are correlated to $\alpha$ (Supp. Fig. S9). Thus, a method combining various indices (e.g., using approximate Bayesian computation) might be able to detect CTRS from population genomic data more accurately than a method using a single index. Furthermore, not all indices are robust to demographic events, as shown in Figure 2.5C: only $I_b$ and $B_2$ seem unchanged when an expansion occurs during CTRS (vertical gray line at generation 150), with a small change for $I^*_{ce}$ and wider changes for other indices. The remaining indices are all affected by the demographic event, although they still show tree imbalance of samples collected after the event (except for $I_s$, which reaches 0 soon after the event).

As with many evolutionary processes, the ability to detect CTRS also depends on the number of sampled individuals and loci. We assessed the effect of these two parameters on our ability to discriminate two scenarios using a Wilcoxon rank test: one of 20 generations of CTRS (strength $\alpha = 1$) before present and one without CTRS ($\alpha = 0$). We show that for all four studied summary statistics (i.e., $I_b$, $B_2$, Number of polytomies and Tajima's D), power increases with both the number of sampled individuals and the number of sampled loci (Supp. Fig. 3.5). The number of polytomies and Tajima's $D$ are the most effective indices, with the first index reaching a power above 0.95 (at Type I error = 0.01) for 60 genomic regions of 1 Mb and 10 sampled individuals, and the second reaching this power for 100 genomic regions of 1 Mb and 10 sampled individuals. However, as shown previously, both indices are also impacted by changes in census population size and cannot thus be used alone for CTRS inference. Conversely, $I_b$ and $B_2$ are independent from changes in population size, but display a much lower power of detection compared to the two previous indices. $I_b$ needs 30 individuals and 100 genomic regions of 1 Mb in order to reach a power of 0.95, while $B_2$ needs 90 individuals and 100 genomic regions of 1 Mb to reach this power of detection. For CTRS detection, the number of individuals seems to have a stronger impact on power of detection than the number of genomic regions, with a power above 0.9 reached with $I_b$ for 100 individuals and 10 independent regions of 1 Mb, compared to a power of 0.15 with 10 individuals and 100 independent regions of 1 Mb, possibly due to the need to have a minimum number of sampled individuals in order to assess topological properties

of the population coalescent trees. As stated above, we expect a combination of multiple indices using methods such as ABC to be even more effective for CTRS estimation from genomic data, compared to single indices. Additionally, using the distribution of indices along the genome might provide more information about past CTRS compared to the use of mere averages.

In conclusion, the evolution of Tajima's $D$ and imbalance measures over time highlights the complexity and the timing of CTRS impacts on population genetics. When CTRS starts or stops, sudden changes in effective population size occur. During the process, CTRS affects coalescent tree topology (imbalance and number of polytomies) and branch lengths with a nonhomogeneous reduction (young branches less impacted than old branches). Imbalance is due to the transmission process, which yields asymmetrical genealogies. The higher number of polytomies stems from the higher coalescence rate. The nonhomogeneous branch length reduction is similar to what occurs during an expansion. Although the effective population size remains stable during CTRS, a pseudoexpansion occurs, due to the expansion of large family lineages, which is compensated by the extinction of small family lineages (Sibert *et al.*, 2002). All of these mechanisms affect the genomic signal commonly used for population genetic inferences, and the next section will illustrate, based on simulations of an instantaneous expansion, how demographic inference is impacted both before and after CTRS equilibrium.

### 2.2.3 Impact of CTRS on demographic inference

In this section, we investigate the impact of CTRS on demographic inference before and after CTRS equilibrium. In the first case, the genomic signal of expansion is affected by the distortion in tree topology (i.e., imbalance and higher number of polytomies) and by the recent change in effective population size, while in the second case only changes in tree topology remain. We explored the "Before CTRS equilibrium" scenario by inferring demography 20 generations after the beginning of CTRS, and the "At equilibrium" scenario by inferring demography 1500 generations after the beginning of CTRS. The fivefold expansion event to be inferred occurs in both scenarios 300 generations before the inference (more details in Methods).

Before CTRS equilibrium, we measured a strong bias in the demography inferred by $\delta a \delta i$. When $\alpha = 1$, the inferred growth factor has a median of 3 instead of 5 (relative bias = -0.37, MSRE = 0.18, compared to 0 and 0.04, respectively, for $\alpha = 0$) (Figure 2.6C). $\delta a \delta i$ inferences are based solely on the SFS. After 20 generations of

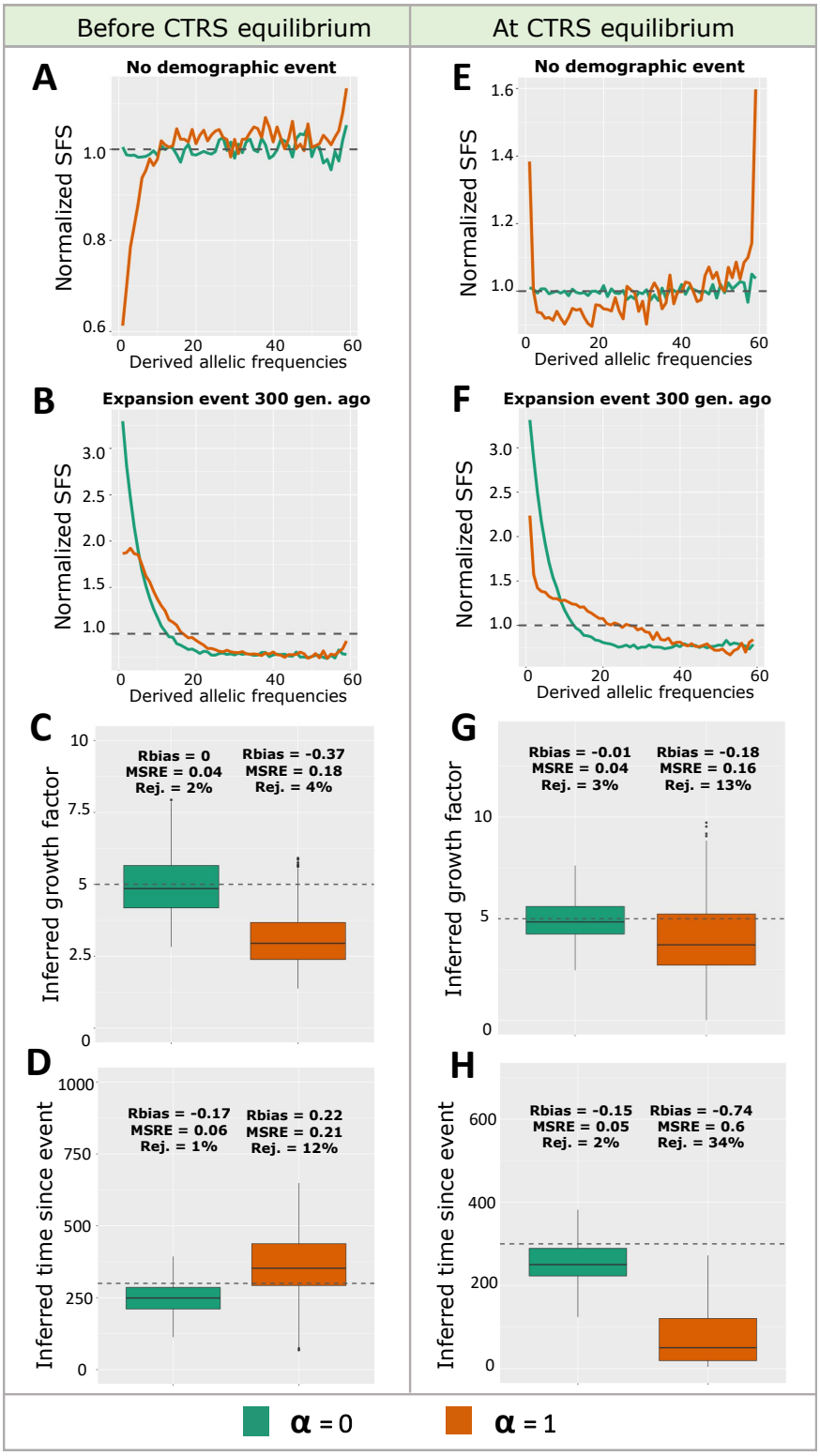


Figure 2.6: SFS and $\delta a \delta i$ inference of expansion parameters at two stages of CTRS.
A and E: SFS for $\alpha = 0$ and 1 with no demographic event.
B and F: SFS for $\alpha = 0$ and 1 after a 5-fold expansion 300 generations ago.
C and G: inferred growth factor for $\alpha = 0$ and 1, after a 5-fold expansion 300 generations ago.
D and H: inferred number of generations since expansion for $\alpha = 0$ and 1, after a 5-fold expansion 300 generations ago.
A-D: Scenario "Before CTRS equilibrium" (20 generations of CTRS before present).
E-F: Scenario "At CTRS equilibrium" (1500 generations of CTRS before present).
MSRE, relative bias and percentage of rejected replicates displayed above each boxplot. In all cases, the $b = 1$ model of variance in progeny size is used.

CTRS and without any change in census population size, SFS shows a marked deficit of rare alleles due to the contraction of effective population size caused by the initiation of CTRS, and an excess of common alleles due to this contraction combined with the presence of many related individuals coming from large family lineages (Figure 2.6A). Conversely, in a scenario of 20 generations of CTRS following an event of expansion, the SFS for $\alpha = 1$ is expectedly a mix between the expansion-only pattern ($\alpha = 0$) and the CTRS pattern for $\alpha = 1$ (Figure 2.6B). In this case, the SFS displays a smaller excess of rare alleles compared to the expansion-only pattern. Since the excess of rare alleles is the main signal of expansions, a smaller expansion is inferred. The contraction of the effective population size due to the initiation of CTRS reduces the excess of rare alleles caused by the expansion event, yielding an inference of a smaller growth factor. Time since the demographic event is also inferred less accurately after a period of 20 generations of CTRS (for $\alpha = 0$: relative bias = -0.17, MSRE = 0.06; for $\alpha = 1$: relative bias = 0.22, MSRE = 0.21).

At CTRS equilibrium, for $\alpha = 1$, a median growth factor of 3.8 is inferred instead of 5 (relative bias = -0.18, MSRE = 0.16, compared to -0.01 and 0.04, respectively, for $\alpha = 0$) (Figure 2.6G). The SFS at CTRS equilibrium with no demographic event is U-shaped (Figure 2.6E). Tree imbalance and the higher number yield the excess of rare and common alleles, while nonhomogeneous reduction of branch lengths contributes to the excess of rare alleles. When a demographic expansion occurs at CTRS equilibrium, the SFS displays a tilted U-shape, with less excess of rare alleles in comparison to the expansion-only scenario (Figure 2.6F). This is due to the smaller effective population size during the generations where CTRS occurs, which induces an accelerated loss of part of the rare alleles created by the fivefold expansion event. Since rare alleles are the main traces of this past expansion event, a smaller expansion is inferred. The inferred time since the demographic event when the population experienced 1500 generations of CTRS was strongly biased, with a median inference of 50 generations since the demographic event instead of 300 ($\alpha = 0$: relative bias = -0.15, MSRE = 0.05; $\alpha = 1$: relative bias = -0.74, MSRE = 0.6) (Figure 2.6H).

We thus showed that after a period of CTRS, whether short (20 generations) or long (1500 generations), past growth factors of expansion events are underestimated with an SFS-based inference method, due to a lack of rare alleles compared to the neutral case scenario. The time since the expansion event can be largely underestimated if it happened after a long period of CTRS and slightly overestimated after a short period of CTRS.

## 2.3 Conclusions

Many studies evaluating CTRS strength in human populations rely on the computation of correlations between parents and children progeny size from pedigree datasets (Murphy, 1999). However, we show here that this measure cannot by itself account for the magnitude of CTRS effects on population genetics. Indeed, under the high variance in progeny size model ($b = 1$), correlations are lower than under the low variance model ($b = \infty$), while the impacts on population genetics are increased. Thus, a more precise evaluation of CTRS from pedigree data would require considering the distributions of parents and child progeny sizes in addition to the correlation values. Furthermore, the higher correlations under the low variance model ($b = \infty$) could explain the higher correlations observed in populations that exhibited a demographic transition (Murphy, 1999; Jennings *et al.*, 2012; Jennings and Leslie, 2013). Indeed, a main characteristic of this transition is a decrease in progeny size variance. Finally, we observe that CTRS has a stronger impact on effective size than the variance introduced in the model. This result is supported by measurements in the Saguenay-Lac-Saint-Jean population for similar levels of progeny size correlation (Heyer *et al.*, 2012).

CTRS impacts genomic diversity in two ways: (i) when CTRS begins or ends, populations undergo a decrease (resp. increase) in effective size that impacts several population genetic statistics such as Tajima's $D$ and SFS. This lower effective size stems from the increased variance in progeny size under CTRS and from the transmission component itself. We could show that the latter accounts for most part of the decrease in effective population size under CTRS. (ii) During the CTRS process and shortly after the process stops, coalescent tree topologies (i.e., tree shape properties that are not related to branch length) are distorted, which also impacts Tajima's $D$ and SFS. When CTRS lasts long enough, the effect of the change in effective size disappears while tree topology distortion persists, inducing lower genetic diversity and a U-shaped SFS. These two processes start together but have different dynamics, yielding a complex effect on population genetics over time.

We showed that the distortion in coalescent tree topology affects two topological properties: (1) trees are more imbalanced, which can be shown with balance and imbalance indices, and (2) the number of polytomies increases. In theory, both of these effects could happen independently, as binary trees can be imbalanced and polytomies do not necessarily induce imbalance. However, under CTRS, we show that trees undergo a complex change in their topology, with an interplay between

these two properties of imbalance and polytomies. These two effects increase the proportions of rare and common alleles, while a nonhomogeneous reduction in branch lengths (Sibert *et al.*, 2002) increases only the proportion of rare alleles, yielding a U-shaped SFS. Further studies could evaluate the relative impacts and possible interactions between these processes.

The impact of CTRS on SFS explains why the SFS-based demographic inference performed by $\delta a \delta i$ was biased for populations undergoing CTRS. After a few generations of CTRS, the growth factors of past expansion events are underestimated. This result implies that past expansions, such as the Neolithic ones, might be underestimated in populations experiencing CTRS, at least when inferred based on SFS. After many generations under CTRS, the timing of expansion is strongly underestimated as well. Furthermore, due to the decrease in effective population size induced by CTRS, past expansion signals were lost more rapidly, as compared to scenarios without CTRS. Similarly, the signal of other past events, such as bottlenecks, selection or migration, is expected to be erased more rapidly in the presence of CTRS. We established that CTRS impacts an SFS-based inference method and expect other approaches to be affected given that CTRS distorts coalescent trees, which are directly or indirectly at the core of any inference method. CTRS is thus one more process among others that can affect demographic inference (e.g., purifying and background selection (Johri *et al.*, 2021; Pouyet *et al.*, 2018), biased gene conversion (Pouyet *et al.*, 2018), population structure (Mazet *et al.*, 2016), selection, gene conversion, and biased sampling in microbial populations (Lapierre *et al.*, 2016)).

To disentangle the effects of demographic events from CTRS, imbalance indices that are unaffected by variations in the census population size can be used. We showed that the power of detection of CTRS from genomic data is less impacted by the number of independent regions than by the number of sequenced individuals that should be high enough, a condition easily achieved with modern datasets. However, these indices are computed from coalescent trees which first need to be reconstructed from genomic data (e.g., using tools such as ARGweaver (Rasmussen *et al.*, 2014), tsinfer (Kelleher *et al.*, 2019), or relate (Speidel *et al.*, 2019)). This tree reconstruction step might not be able to infer a perfectly accurate topology, yielding potential biases in the estimated (im)balance indices. Moreover, in addition to the expected imprecision of the reconstruction of neutral trees, the behavior of these tools under CTRS remains to be checked. Another possibility would be to build and train deep learning networks directly on raw genomic data without

reconstructing coalescent trees, as in Sanchez *et al.* (2021), which would prevent the introduction of biases due to tree reconstruction, but might require a larger amount of simulated data for training. To generate this large dataset, it would be useful to develop a backward coalescent model of CTRS, as forward-in-time simulations are particularly time-consuming.

To conclude, one should note that the impacts of CTRS on the genome studied here should happen in the case of selection as well: effective population size and coalescent trees topology should be affected, yielding qualitatively similar patterns in Tajima's $D$, SFS and other statistical indices throughout time. However, due to the process of recombination, all these effects would be restricted to the region linked to the locus under selection. Conversely, CTRS impacts the whole genome because it is not caused by any genetic locus in particular. CTRS would thus qualitatively resemble an extreme case of multiloci selection, where all loci in the genome would be under selection pressure. Because of this impact on the whole genome, the bias produced by CTRS in demographic inference are non-trivial to escape from, whereas bias caused by selection on a few locus can be avoided by inferring demography from neutral regions. Furthermore, CTRS and multiloci selection might be particularly prone to blur each other due to their similarity, and we expect the distinction between the two processes in real genomic data to be a challenging issue.

Finally, we should address the question of the similarity between CTRS and natural selection: in both cases, some individuals have more offspring than others and transmit this higher fertility to their descendants. However, in the case of CTRS, fertility is culturally transmitted, whereas for selection, it is genetically transmitted. The question is to what extent these processes affect the genome differently. Without recombination, one might expect qualitatively similar effects of the two processes on the genome: lower diversity and similar patterns for Tajima's D over time. Moreover, tree topology is also expected to be distorted with an increase in imbalance (Fay and Wu, 2000; Li, 2011; Li and Wiehe, 2013) and number of polytomies (Durrett and Schweinsberg, 2005; Neher and Hallatschek, 2013) under selection. The resemblance of the two processes is confirmed by a similar U-shaped signature in SFS: selection also yields an excess of rare (Braverman *et al.*, 1995) and common alleles (Fay and Wu, 2000).

However, a fairly clear difference exists between the CTRS model (based on the $\alpha$ parameter) used here and the commonly used model of positive selection (based on the selection coefficient $s$, Wright, 1932). Under this model of selection, the beneficial allele can go to fixation, and selection stops at that point. However, in

the case of CTRS, the model is constructed in such a way that the transmission of reproductive success may continue indefinitely. The CTRS model would more closely resemble a positive selection model with a high mutation rate, preventing fixation. This difference between the two models makes sense relative to reality: cultural transmission can be expected to be quite inaccurate in real life compared to genetic transmission. This argument of "high mutation rate" in cultural transmission has been used to resolve the so-called Fisher's paradox (Pettay *et al.*, 2005): how can correlations between parents' and children's progeny size remain positive over time given the expected erosion of variance in the fertility phenotype? The answer would be that these correlations stem from a CTRS and not a genetic TRS. Thus, the unfaithful cultural transmission of fertility would explain why variance is maintained, with the "high mutation rate" preventing the "fixation" of high-fertility cultural traits (Heyer *et al.*, 2012). This difference in fixation between the two models might yield distinctive dynamics in population genetics statistics. To further compare CTRS and selection models, an analytical reconciliation that would link $\alpha$ to the selection coefficient would be pertinent.

A second difference between CTRS and selection appears when recombination is considered. In this case, the selection signal is restricted over time to the locus under selection, as recombination events accumulate, with a remaining local effect on nearby loci due to hitchhiking (Smith and Haigh, 1974). The length of the region impacted by hitchhiking depends on the recombination rate, as well as on the time under which selection has been acting. When fixation occurrs, this time is equivalent to the time to fixation, which is inversely proportional to the selection coefficient $s$ (Kim and Stephan, 2002; Stephan, 2019). In human populations, even selection events that started rather recently have been shown to give rise to a signal restricted to only a few megabases. For example, in the case of the selection for lactase persistence in Africa (event dated to ∼7000 years ago), the selection signal decreases very rapidly over the 3 Mb sequenced (Tishkoff *et al.*, 2007). An even more recent selection event, such as the one on the 3p12.1 chromosomal region in Mongolians, associated with energy metabolism and reproductive traits, dated to approximately 50 generations ago (∼1500 years), is almost undetectable outside the 4 Mb region around the locus under selection (Nakayama *et al.*, 2017). Conversely, in the case of CTRS, the effects are uniform over the whole genome since the transmission of fertility is not conveyed by genetics: we showed in this paper the shift of the whole distribution of tree imbalances in the genome toward higher values. We expect the distribution of indices across the genome to be quite different in the case of selection, which would help distinguish between the two processes.

We can go farther and compare polygenic selection to CTRS, because of their propensity to affect simultaneously distant loci in the genome. In particular, background selection, which has this ability to affect large parts of the genome (Pouyet *et al.*, 2018), could strongly resemble CTRS in its effects. Because of their potential similarity, distinguishing highly polygenic selection from CTRS might be troublesome. However, it seems unlikely that even highly polygenic selection would have an effect identical to CTRS for several reasons. First, the neutral parts of the genome are under the effect of CTRS but not under that of polygenic selection (e.g., Pouyet *et al.* (2018) identified a set of SNPs that are mostly unaffected by background selection). Second, in a polygenic selection, selective pressure may have different parameters depending on the gene: the temporality may differ (selective pressure does not start at the same time on each gene) as well as intensity (different selection coefficients for each gene), yielding different coalescent trees across the genome (each gene tree telling its own history). In fact, theoretical analyses showed different temporal dynamics in polygenic adaptation, with large effect alleles contributing first, followed by small/intermediate-effect alleles (Barghi *et al.*, 2020; Hayward and Sella, 2022). This process has been shown to be responsible for maize domestication, with a central transcription factor (*teosinte branched 1*) driving adaptation (Studer *et al.*, 2011), although most of the network controlled by this gene displays a selection signal as well (Wang *et al.*, 1999; Studer *et al.*, 2017; Barghi *et al.*, 2020). Conversely, CTRS will tend to create trees that look similar across the genome, since they are all affected uniformly by the same cultural history (a single $\alpha$ parameter for the whole genome). Third, populations exchanging migrants will tend to have the same alleles selected by multigenetic selection, whereas nongenetic TRS will select for different alleles in each population (alleles randomly carried by large family lineages). Fourth, under polygenic selection, genes can undergo a complex effect, combining not only the effects of their selection pressure, but also the effects of nearby genes due to hitchhiking (Barton, 1995). This competing effect would not happen under CTRS only, adding another difference between the effects of CTRS and of highly polygenic selection. Ultimately, these three listed differences might help distinguish the two processes in real data.

Furthermore, one may ask what happens when CTRS and selection are combined, which might be the case in a number of populations. Competition between selection and CTRS might arise in the case of a culturally fertile lineage carrying a disadvantageous allele. In fact, Austerlitz and Heyer (1998) have shown that CTRS can increase the propensity of a population to maintain genetic diseases. This increase in genetics disease can also stem from the reduction in diversity created by

CTRS, under which conditions, selection is less effective. Studying coalescent tree shapes under the combined effects of selection and CTRS is also interesting: will trees be even more imbalanced compared to CTRS alone, or is imbalance already saturated by CTRS? It is also possible that the sum of the two processes will result in more balanced trees due to the aforementioned competition between them. The study of the combination of these two processes is crucial to be able to distinguish them in real populations, where both are likely to happen, in order to find their respective impact on genetic diversity and tree topologies.

Finally, the analysis of CTRS provided here might be valid for any transmission of reproductive success (TRS) that is not genetic. For example, ecological inheritance (Odling-Smee, 1988; Danchin *et al.*, 2011), where an individual passes on its environment to its offspring, could yield a similar process provided that: (1) the population is settled in diverse environments, (2) the fitness varies with the environment, and (3) there is a vertical transmission of the environment (Bonduriansky and Day, 2018). These conditions might be achieved in plants whose seeds disperse little (Danchin *et al.*, 2011). Therefore, although the literature has focused on *cultural TRS* until now (Blum *et al.*, 2006; Heyer *et al.*, 2012, 2015), one could generalize this evolutionary process and call it *nongenetic TRS*.

## 2.4 Data availability

The SLiM code used to generate the simulated data and the Python code for summary statistics computing and $\delta a \delta i$ inference can be found at `https://github.com/jeremyguez/CTRS`.

## 2.5 Acknowledgments

We thank the editor and three anonymous reviewers for their helpful comments and suggestions. We thank Matteo Fumagalli, Olivier François, Aurélien Tellier, Fanny Pouyet, Jean-Tristan Brandenburg, Théophile Sanchez, Romain Laurent, Ferdinand Petit and Arnaud Quelin for the insightful interactions.

## 2.6 Funding

JG was supported by a French National Center for Scientific Research (CNRS) fellowship: 80Prime (TransIA). FB was supported by Dr. Max Rössler, the Walter Haefner Foundation and the ETH Zürich Foundation. JC was supported by the Human Frontier Science Project (number RGY0075/2019). We also thank ANR-20-CE45-0010-01 RoDAPoG.

## 2.7 Conflicts of interest

The authors declare no conflicts of interest.

## 2.8 Supplementary material

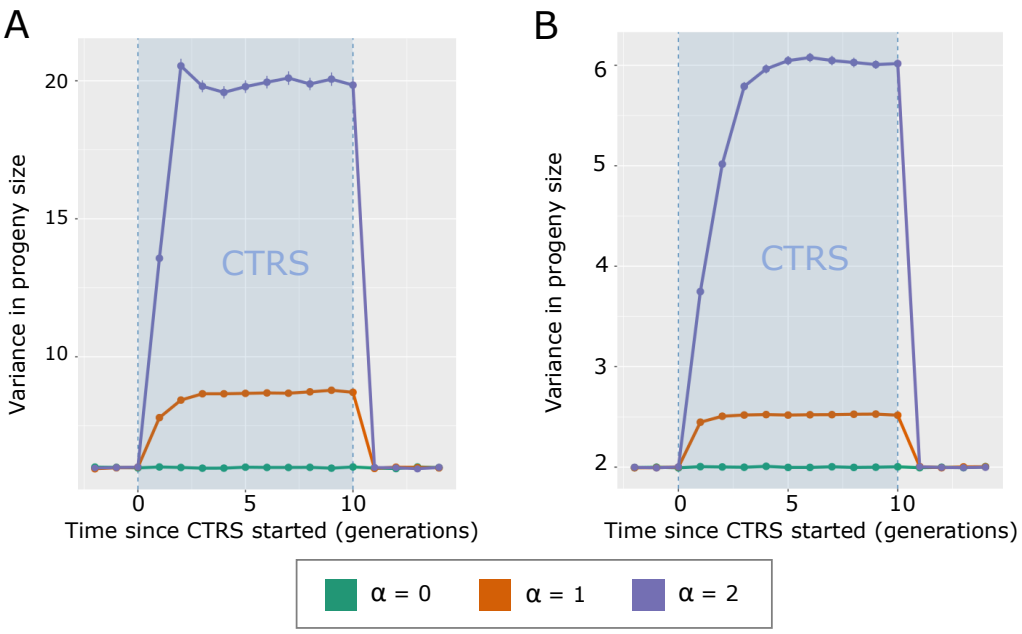


Figure S1: Variance of progeny size as a function of time for $\alpha = 0$, 1, and 2. The blue rectangle corresponds to the period when populations are under CTRS. Generations are counted from the beginning of CTRS.
A. $b = \infty$ model (low variance of progeny size).
B. $b = 1$ model (high variance of progeny size).

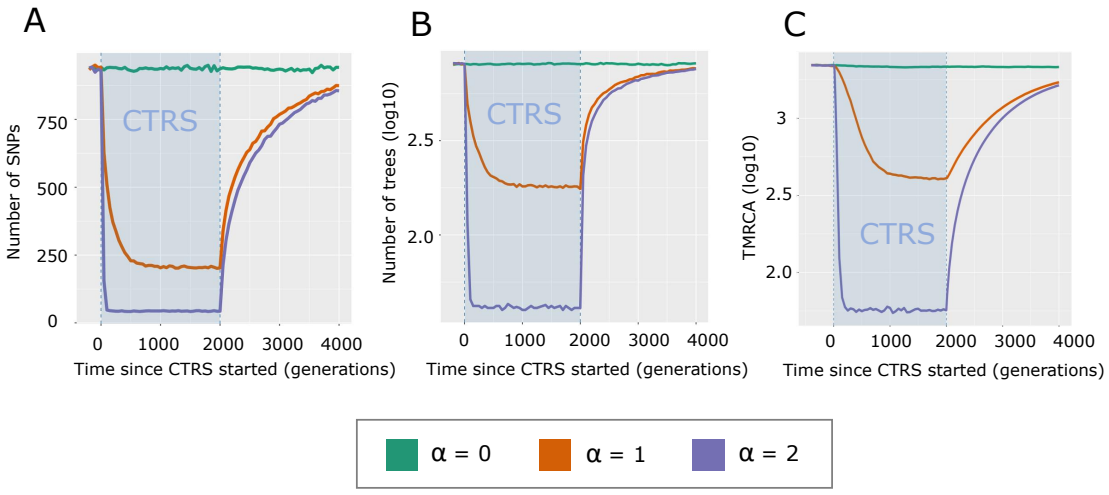


Figure S2: Number of SNPs (A), number of trees (log 10 scale) (B), and TMRCA (log 10 scale) (C) across generations. In all cases, the $b = 1$ model of variance in progeny size is used.

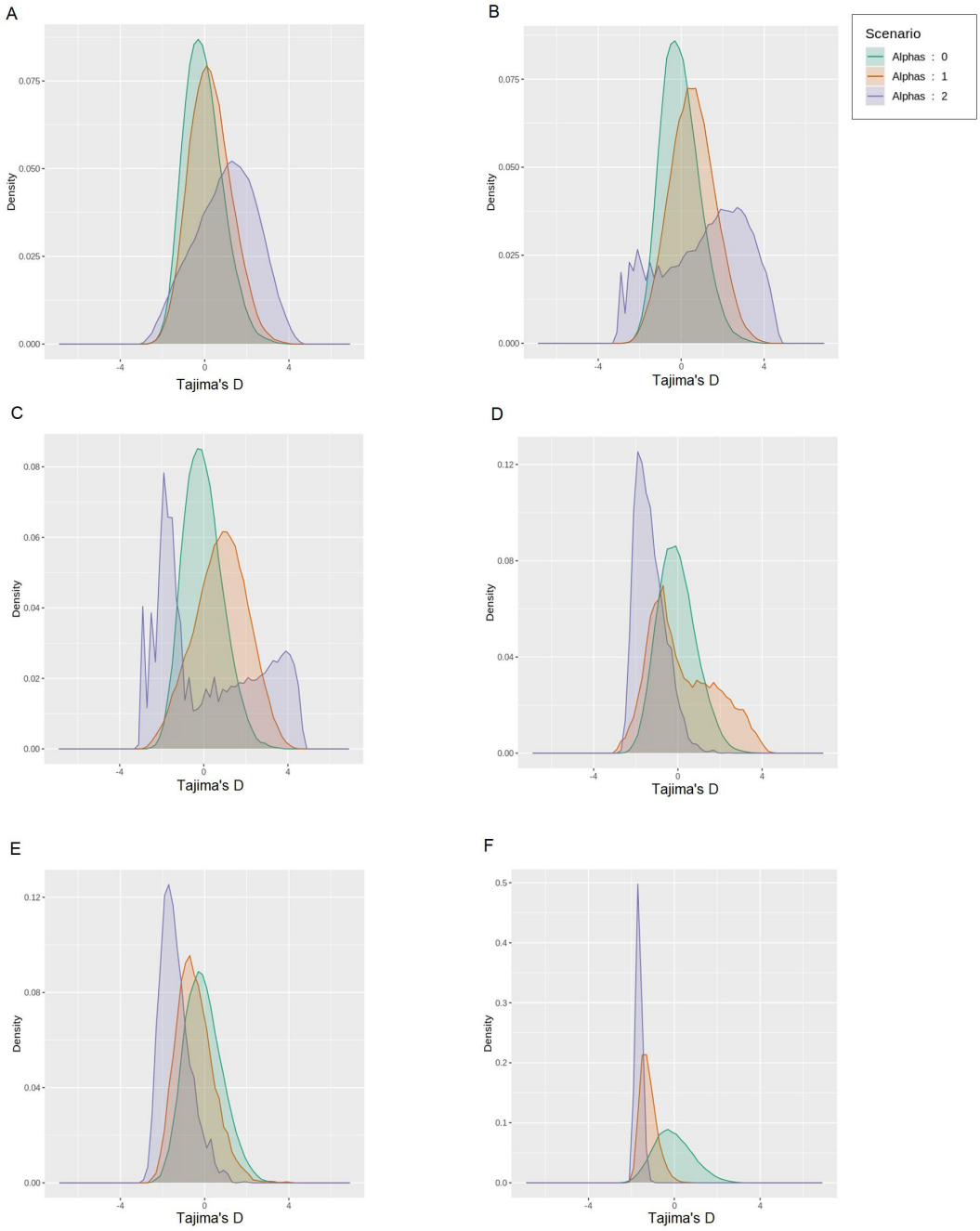


Figure S3: Distribution of Tajima's $D$ across the genome (from A to E: 10, 20, 50, 500, 1500 generations since the starting of CTRS. F: 500 generations without CTRS, after a period of 2000 generations of CTRS. The $b = 1$ model of variance in progeny size is used.)

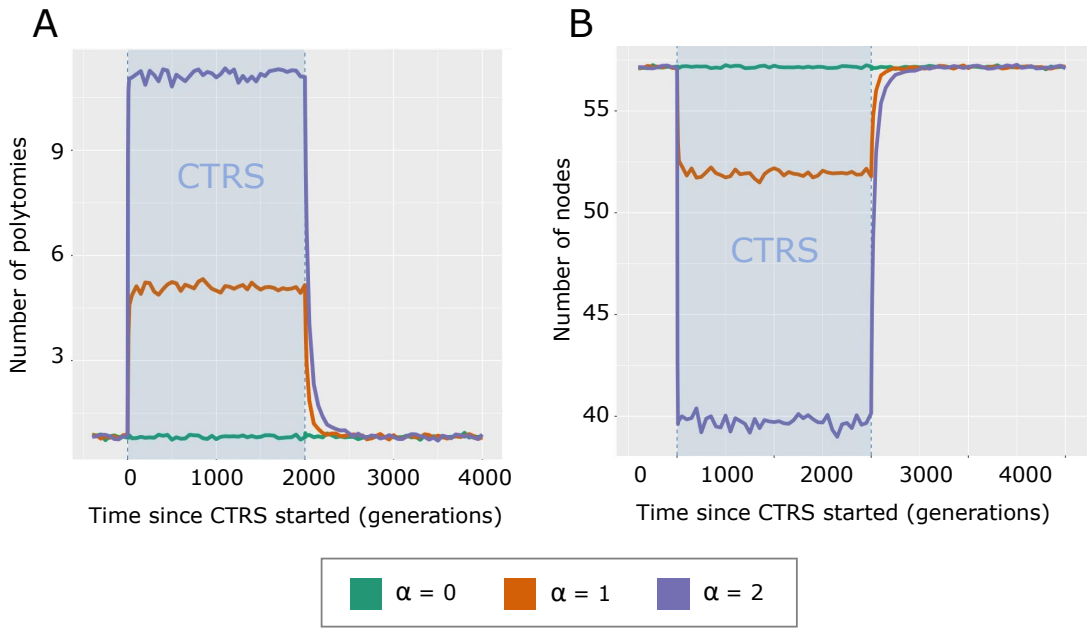


Figure S4: Number of polytomies (A) and number of nodes (B) throughout generations. The $b = 1$ model of variance in progeny size is used.

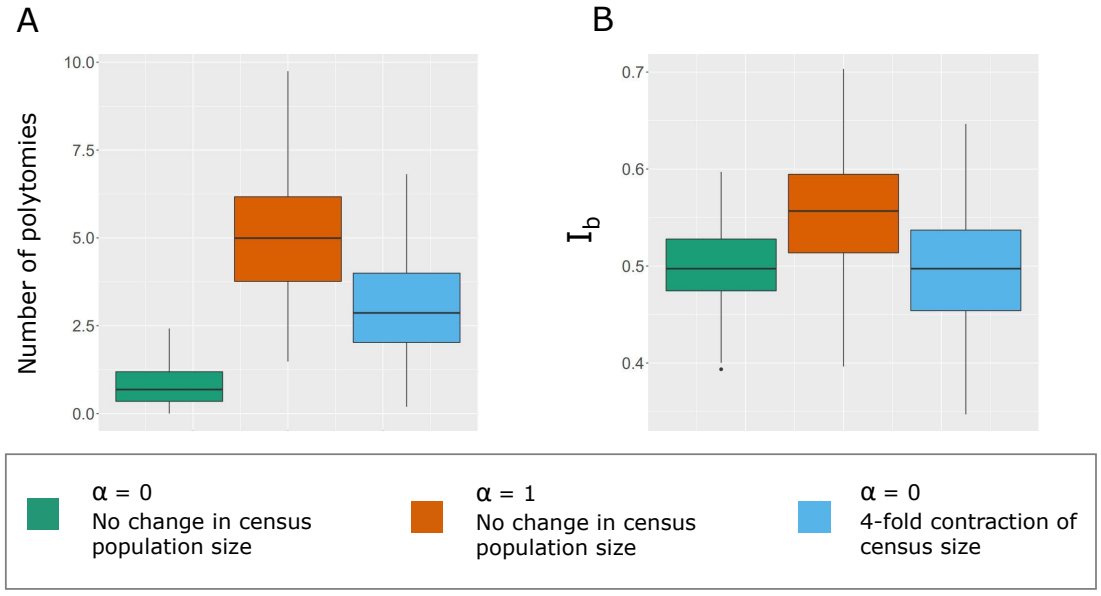


Figure S5: $I_b$ and average number of polytomies for three scenarios. The CTRS in the $\alpha = 1$ scenario lasted for 500 generations before present. The 4-fold contraction happened 500 generations before present. In all cases, the $b = 1$ model of variance in progeny size is used.

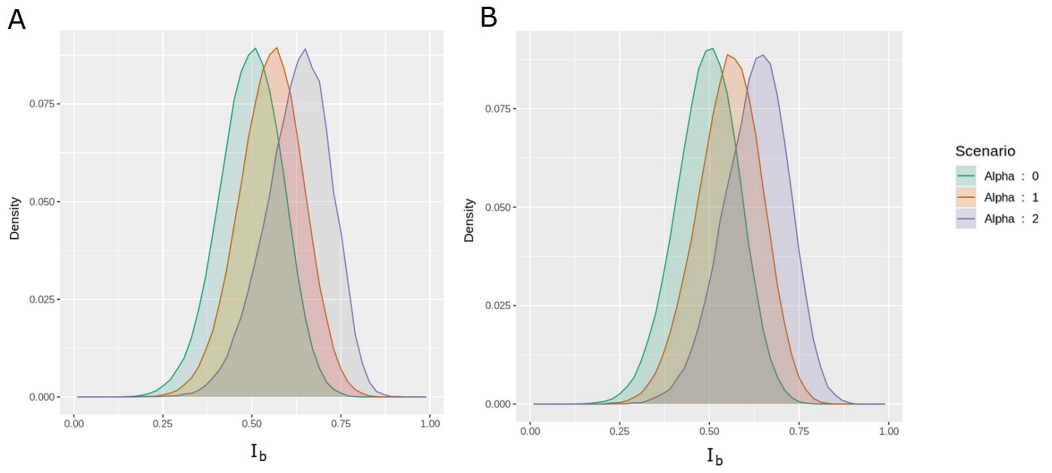


Figure S6: $I_b$ distributions across the genome for $\alpha = 0$, 1 and 2, after 20 (A) and 500 (B) generations of CTRS. The $b = 1$ model of variance in progeny size is used.

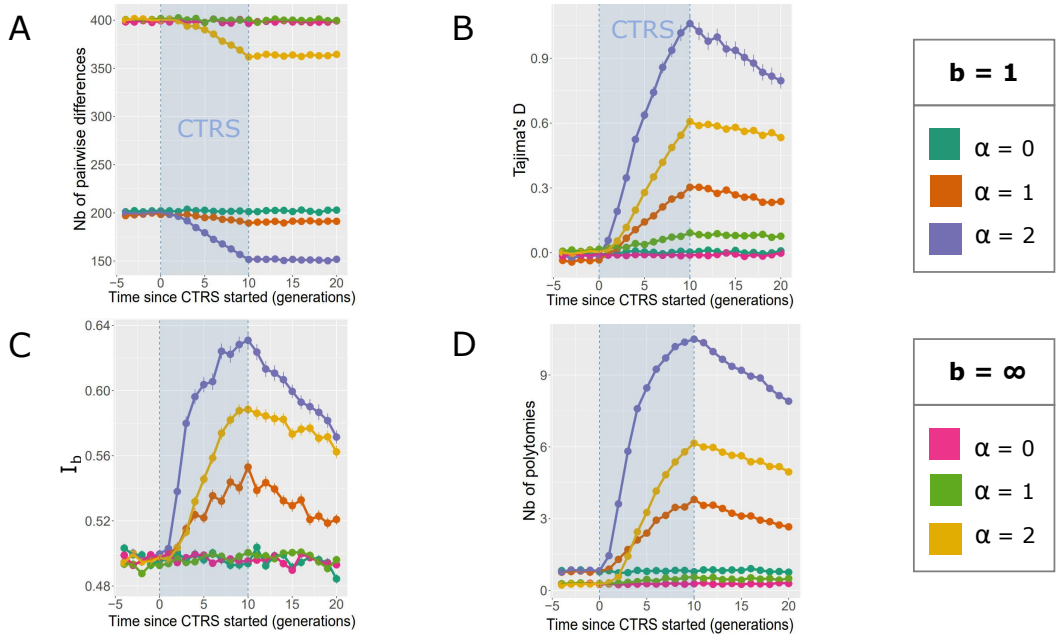


Figure S7: Number of pairwises differences, Tajima's D, number of polytomies and $I_b$ under 10 generations of CTRS followed by 10 generations without CTRS. Both $b = 1$ and $b = \infty$ models of variance in progeny size are used.

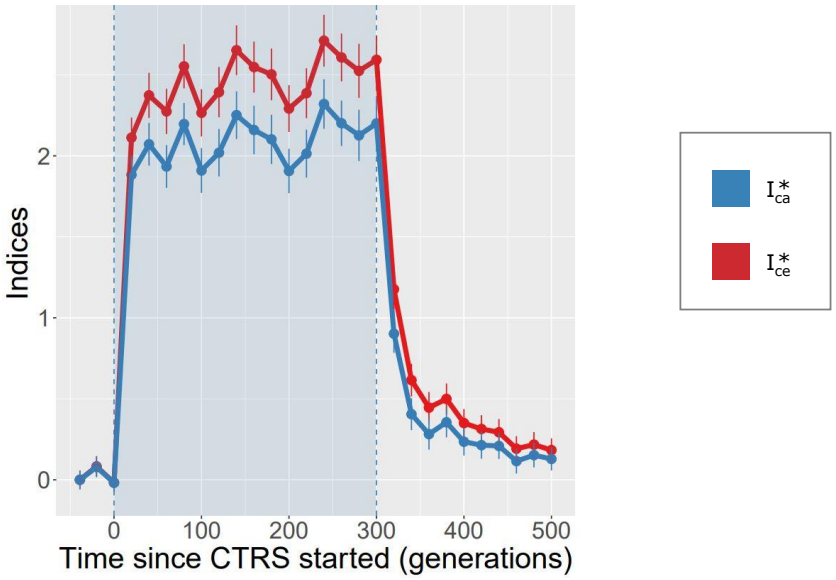


Figure S8: Two Colless index modifications to handle polytomies: $I^*_{ca}$ and $I^*_{ce}$. See Methods for details on algorithms.

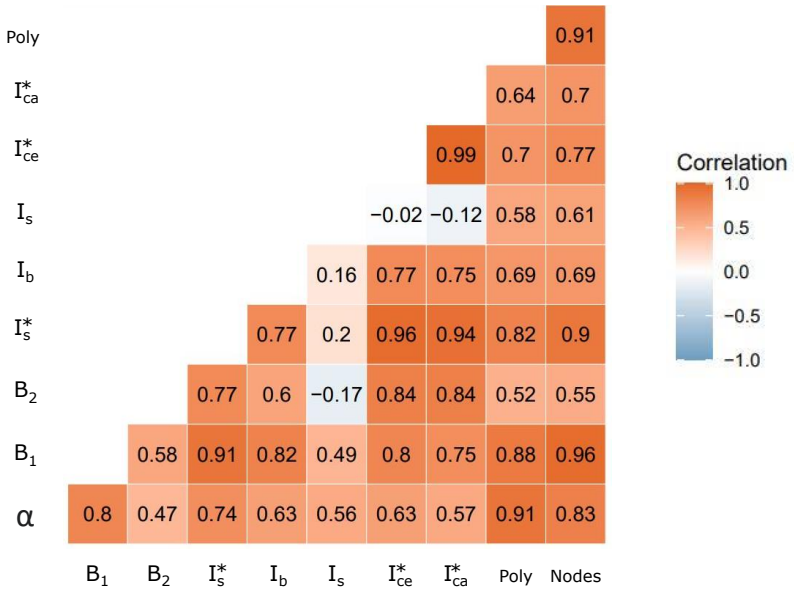


Figure S9: Correlations between indices after 50 generations of CTRS.

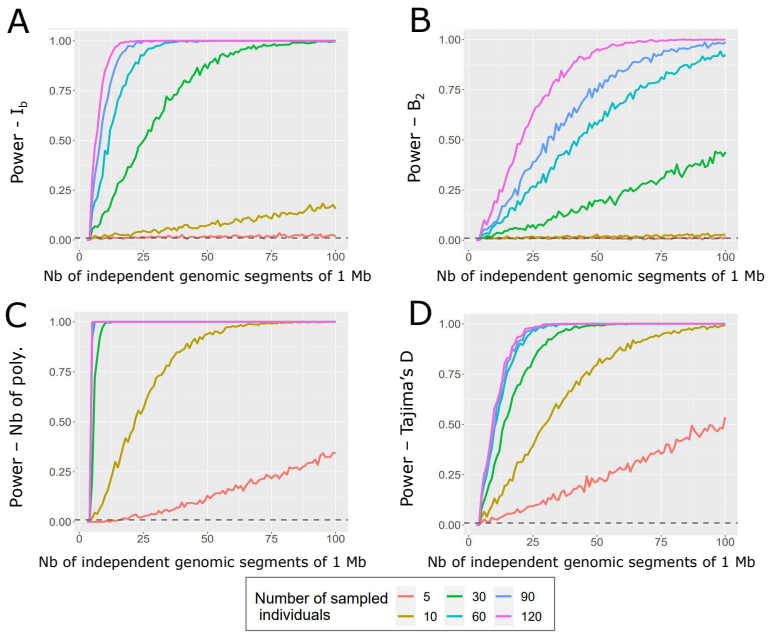


Figure S10: Power of distinguishing $\alpha = 1$ from $\alpha = 0$ scenarios (using a Wilcoxon test with the significance threshold set to 0.01), for 4 indices: $I_b$ (A), $B_2$ (B), number of polytomies (C), Tajima's $D$ (D).

# Chapter 3

# Joint inference of TRS and demography

*Some of the analyses presented here are the result of a collaboration with Ferdinand Petit and Arnaud Quelin during their masters internship.*

## Introduction

A variety of processes can impact the genetic diversity of a population. For example, after a bottleneck (i.e., a reduction in population size followed by an expansion), one would expect to find lower genetic diversity in the population than before this event. This process has for example led to the current low genetic diversity in human populations outside of Africa compared to African populations (Yu *et al.*, 2002). Past evolutionary events can thus be retrieved from population genomes by analyzing specific patterns. Recently, the increasing availability of high-quality genomic data allows to infer past histories at higher resolution. It becomes possible to reconstruct different types of past events from current population genetic data, such as changes in population sizes (Gattepaille *et al.*, 2013), migrations (Peña-Malavera *et al.*, 2014), or natural selection on specific genomic regions (Bank *et al.*, 2014). Statistics computed on the genomes of a sample of individuals, often called summary statistics, allow the reconstruction of these past events with various degrees of certainty. Some statistics are well-known and commonly used, such as the mean number of pairwise differences ($\pi$), Tajima's $D$, the site frequency spectrum (SFS),

the fixation index ($F_{st}$), linkage disequilibrium (LD), and shared identity by state (IBS) tracts.

However, many processes affect the same statistics simultaneously, making their disentanglement difficult. For example, a decrease in genetic diversity can stem from a bottleneck, but also from natural selection. Another example is Tajima's $D$, initially invented to detect selection: a negative $D$ can result from positive selection (Tajima, 1989), but also from a population expansion. Therefore, distinguishing selection from expansion can be complex, and the former can impact the latter's inference (Schrider *et al.*, 2016). Various recent studies seek to disentangle processes with similar effects on genetics (Williamson *et al.*, 2005; Sackman *et al.*, 2019; DeWitt *et al.*, 2021).

Our objective in this study is to distinguish between two such interacting processes. The first, changes in population size over time, is a commonly studied and inferred process (Beichman *et al.*, 2018). It includes expansions, contractions, and any temporal succession of these two types of events. The second process, the nongenetic transmission of reproductive success (nongenetic TRS), is less widely studied. This process occurs when individuals' progeny size correlates with their number of siblings for nongenetic reasons (Austerlitz and Heyer, 1998; Sibert *et al.*, 2002). In humans, there may be cultural reasons for this process, such as parental influence on the progeny size of their own children. In this case, we will call this process cultural transmission of reproductive success (CTRS). This process affects many human populations, with an increasing tendency in modern times (Murphy, 1999), due to birth control that allows for better reproduction of parental preferences (Bongaarts, 2001; Murphy, 2013; Beaujouan and Solaz, 2019). Several animal species also experience nongenetic TRS, such as monkeys (Santorelli *et al.*, 2011; Hobaiter *et al.*, 2014; Robbins *et al.*, 2016), cetaceans (Frere *et al.*, 2010; Whitehead *et al.*, 2017), and hyenas (Engh *et al.*, 2000; Ilany *et al.*, 2021). Furthermore, it is possible that this process affects species of all types, even outside the animal kingdom (Bonduriansky and Day, 2018) (Chapter 1).

These two processes, population size changes and nongenetic TRS, have in common that they affect the population genetic diversity, Tajima's $D$, and allelic frequencies (Sibert *et al.*, 2002; Guez *et al.*, 2022). Moreover, both processes impact the whole genome, unlike selection whose effects are restricted to the region of the locus under selection due to recombination (Smith and Haigh, 1974; Austerlitz and Heyer, 2000; Guez *et al.*, 2022). Therefore, it will be challenging to distinghuish between demographic and nongenetic TRS when they affect the same population. This is

the case in the Saguenay-Lac-Saint-Jean region of Quebec, whose population has undergone simultaneously a recent strong expansion and a cultural transmission of reproductive success (Austerlitz and Heyer, 1998). In particular, dadi (Gutenkunst *et al.*, 2009), a software tool that relies on allelic frequencies to infer demography, is biased by the presence of nongenetic TRS (Guez *et al.*, 2022). The fact that inference of demographic processes is affected by the presence of nongenetic TRS is problematic, given the large number of studies that focus on demographic inference without considering nongenetic TRS. The decrease in genetic diversity generated by nongenetic TRS might also erase the imprints of other phenomena. Our main objective here is to explore different methods to correctly infer the demographic history of a population that underwent nongenetic TRS, while allowing the inference of the intensity of the nongenetic TRS itself.

The first approach belongs to a family of methods that combine multiple summary statistics for inference and are often used to disentangle two processes in population genetics. This family includes approximate Bayesian computation (ABC) approaches (Beaumont *et al.*, 2002; Csilléry *et al.*, 2010; Blum and François, 2010; Csilléry *et al.*, 2012; Pudlo *et al.*, 2016; Raynal *et al.*, 2019), or neural networks (McCulloch and Pitts, 1943; Lecun *et al.*, 1998). These methods will process different summary statistics obtained from a simulated training dataset, and learn their association to the targeted parameters (such as population sizes at different timesteps). Various recent studies used this type of method in population genetics. Sheehan and Song (2016) used deep neural networks with a large combination of summary statistics including SFS, LD and IBS to tell apart demography from selection. Jay *et al.* (2019) used ABC (including adjustments provided by shallow neural networks) on a large number of summary statistics to infer complex demographic scenarios while jointly estimating the genotyping error rate. Mondal *et al.* (2019) applied ABC to statistics automatically computed by a deep neural network processing joint SFS to infer the history of Eurasian populations and introgressions from archaic populations.

For this approach, on top of the classical summary statistics we described, information on coalescent tree imbalance can be helpful for efficiently distinguishing demography and nongenetic TRS (Shao and Sokal, 1990; Sibert *et al.*, 2002; Blum *et al.*, 2006; Brandenburg *et al.*, 2012; Guez *et al.*, 2022). Indeed, this measure focuses on tree topology and does not consider branch length, which is affected by demography. Therefore, some imbalance indices are unaffected or minimally affected by demographic processes and can detect nongenetic TRS (Blum *et al.*, 2006; Guez

*et al.*, 2022). However, in order to use these measures, it is necessary to have access to the coalescent trees of the population of interest. This requires inferring the trees from the genetic data, a process that can add biases. Moreover, because of recombination, the human genome is a sequence of many coalescent trees, each tracing the history of a small genome region. Therefore, inferring trees on the whole genome can be very computationally intensive. We will use here two recent software packages that allow for fast, efficient, and parallelizable inference of coalescent tree sequences along the human genome: relate (Speidel *et al.*, 2019) and tsinfer (Kelleher *et al.*, 2016).

Deep learning on raw genomic data is an alternative method for inferring past processes. It consists in building a neural network that takes as input the genomes of the different sampled individuals. The network can be trained so that it outputs the targeted evolutionary parameters. This method is also based on simulations to build training, validation, and test datasets. However, unlike ABC, there is no choice of summary statistics: all computations are done automatically within the neural network. This has the advantage of requiring little knowledge of the system studied, but has the disadvantage of the so-called *black box*: even when the learning process works, the internal algorithm of the network is not easy to analyze. Recent developments in deep learning allow us to use complex and innovative architectures, often developed for other engineering domains, and apply them for population genetic inference. An excellent example is the convolutional neural network (CNN), a type of network that detects shift-invariant patterns in data, initially invented in the field of image recognition (Lecun *et al.*, 1998). However, applying CNNs to genetic data requires resolving several issues, such as ordering the input individuals, as CNNs are sensitive to spatial information. Some recent studies built and applied deep learning methods for inferring population genetics parameters from raw genomic data (Flagel *et al.*, 2019; Chan *et al.*, 2018; Torada *et al.*, 2019; Sanchez *et al.*, 2021).

In this paper, we will use two of the methods presented above: (1) ABC random forest using summary statistics including classical diversity measures as well as tree imbalance measures, and (2) deep learning on raw genomic data based on a permutation-invariant CNN. We will infer the intensity of the nongenetic TRS and the demographic history. Comparing these two methods will allow us to investigate to what extent the summary statistics used for ABC contain all the information necessary for the inference. Indeed, when deep learning gives a better inference than ABC, it reveals that other summary statistics could be added for improving ABC

inference. Additionally, by comparing various ABC methods with different combinations of summary statistics, we will be able to understand which of them are critical to separate the two studied processes. This should allow a better understanding of the impacts of these processes on population genetics.

The objective of this article is threefold. First, we aim at building a tool that infers demography accurately, even in the case of nongenetic TRS. Our previous research has shown that an SFS-based inference tool such as dadi gives biased demographic inferences when the population also underwent nongenetic TRS (Guez *et al.*, 2022). Thus, we will use dadi's inference as a reference point. The second axis, carried out in conjunction with the first, aims to infer the intensity of nongenetic TRS, without being biased by population size fluctuations. Previous studies have taken a discriminative approach, distinguishing between populations with and without TRS, rather than estimating the intensity coefficient. Moreover, these studies have focused on mtDNA (Blum *et al.*, 2006) or Y chromosome (Heyer *et al.*, 2015) which can be particularly affected by natural selection in comparison with autosomes where recombination prevent hitchhiking on the whole chromosome. Thus, our goal here is to develop a whole genome method that would allow a more precise inference of the intensity of past nongenetic TRS by focusing on neutral regions of the genome. The third objective will be the study of the respective importance of the different summary statistics for ABC inference. This analysis will yield a better understanding of the intersecting impacts of demographic changes and nongenetic TRS on population genetics.

## 3.1 Methods

### 3.1.1 Simulations

We simulated 2000 scenarios of 20 replicates each. These scenarios simulate the history of a population of $N$ diploid individuals, with a chromosome length of $2 \times 10^6$ bp, a mutation rate of $1.45 \times 10^{-8}$ per bp per generation (Narasimhan *et al.*, 2017), and a recombination rate of $10^{-8}$ per bp. For each scenario, we randomly drew four parameters: three demographic parameters and one parameter controlling the intensity of nongenetic TRS. The scenarios only differed from each other for these four parameters. The 20 replicates of a scenario have the same parameters but are simulated independently. They can be considered as independent genomic regions

from the same population (Sanchez *et al.*, 2021). The three demographic parameters are the population sizes at three fixed timesteps during the history of the population. The population size changes suddenly at the end of each timestep. $N_1$ is the ancestral population size up to 700 generations before present. $N_2$ is the population size between 700 and 300 generations before present. $N_3$ is the modern population size between 300 generations before present and the present. These three population size parameters were randomly drawn in a uniform distribution $[2000, 12000]$. The nongenetic TRS occurred only over the last 20 generations before present. We used a modification of the Wright-Fisher model to simulate this process (Sibert *et al.*, 2002; Brandenburg *et al.*, 2012; Guez *et al.*, 2022). For each of these last 20 generations, we created $N_3$ individuals by choosing for each one a parent couple at random in the previous generation. Each couple had a probability $p_i$ of being drawn such as $p_i = \frac{\gamma_i \times s_i^\alpha}{\sum_{j=1}^{N_c} \gamma_j \times s_j^\alpha}$, with $N_c = N/2$ (the number of couples), $\alpha$ controlling the intensity of nongenetic TRS, and $\gamma$ a random gamma-distributed variable drawn independently for each couple $i$, with shape parameter 1 and mean 1. This $\gamma$ will increase the variance in progeny-size compared to a Wright-Fisher model, and yield a geometric-like distribution of progeny size. It has been shown in one human population undergoing nongenetic TRS that this model with $\gamma$ is more realistic than the Wright-Fisher model (Austerlitz and Heyer, 1998). For each scenario, $\alpha$ was drawn randomly in a uniform distribution $[0, 2]$.

As in Guez *et al.* (2022), simulations were performed forward-in-time with SLiM (Haller and Messer, 2019) for the 20 generations of nongenetic TRS (the last 20 generations before the present). Each replicate corresponded to a sequence of coalescent trees, generally without root (i.e., common ancestor). We then completed these coalescent tree sequences backward using the *msprime* python package (Kelleher *et al.*, 2016; Baumdicker *et al.*, 2021) for the period without nongenetic TRS (from 20 generations before present until a common ancestor is reached). A number $n$ of diploid individuals were sampled in this population, yielding a tree with $2n$ leaves. Mutations were then randomly applied to these coalescent trees and saved into VCFs containing the SNPs of the 2n genomes.

### 3.1.2 Tree reconstruction

In order to compute topology indices on the coalescence trees, we could not use the exact simulated trees. Indeed, we do not have access to these trees in real populations and they need to be inferred from observed genomic data instead. We

thus decided to apply the same tree inference process to simulated data in order to integrate potential reconstruction uncertainty and biases into the calculation of topology indices. We applied and compared two independent coalescent tree reconstruction tools: tsinfer (Kelleher *et al.*, 2019) (version 0.2.3) and relate (Speidel *et al.*, 2019) (version 1.1.9). These programs take genomic data as input (e.g., in VCF format) and provide coalescent tree sequences as output. We will use these inferred tree sequences for the computation of topology indices. For both tools, default parameters were used.

### 3.1.3 Summary statistics

We computed several summary statistics for the ABC analysis. They can be divided into two main categories: genetic diversity indices and coalescent tree (im)balance indices. The first category contains indices that can be computed directly on the genome: number of pairwise differences ($\pi$), Tajima's $D$, and the unfolded SFS. We used the tskit package (Kelleher *et al.*, 2016) for computing the indices. The second category contains several (im)balance indices: the Fusco index (Fusco and Cronk, 1995), the $B_1$ index (Shao and Sokal, 1990), and the $B_2$ index (Shao and Sokal, 1990). The Fusco index is an imbalance index (i.e., the higher its value, the more imbalanced the tree). It is the average of all $f_i$ values, with $f_i$ calculated for each node $i$ of the tree having more than four leaves as follows: $(M_n - m)/(M_t - m)$. $M_n$ is the largest number of observed leaves under the subnodes of $i$. $M_t$ is the maximum possible number of leaves that $M_n$ can reach (i.e., $t_i + s_i - 1$, with $t_i$ the number of leaves under node $i$, and $s_i$ the number of subnodes of $i$). $m$ is the ratio between the number of leaves under node $i$ and the number of subnodes of $i$. $B_1$ and $B_2$ are balance indices (i.e., the higher their value, the more balanced is the tree). $B_1$ index is computed by summing all the $b_i$ values in the tree (one value per interior node). The $b_i$ are computed for each node $i$ by counting the maximum path length to its leaves and taking the inverse of this value. $B_2$ index is equal to the Shannon entropy of the values $p_k$, with $p_k$ computed for each leave. $p_k$ is equal to the probability of reaching the leaf $k$ when following a random walk starting from the root and choosing a random sub-node at each node. A uniform distribution of the $p_k$ values (an entropy of 1) corresponds to a balanced tree (Shao and Sokal, 1990; Bienvenu *et al.*, 2021).

### 3.1.4 ABC random forest

ABC allows performing a Bayesian inference without knowing the likelihood function by relying on simulations reduced into summary statistics (see section 0.1.3). Here we consider 40,000 total simulations, consisting in 2000 scenarios of 20 replicates. The 20 replicates are considered as 20 independent 2 Mb regions in the genome of the same population, since all replicates have the same values for the four randomly drawn parameters (three demographic parameters and the parameter controlling the nongenetic TRS intensity, $\alpha$). Each scenario represents a population. Instead of associating each scenario to a vector of $s \times 20$ values ($s$ being the number of summary statistics), we computed the first four moments of the distribution (i.e., mean, variance, skewness and kurtosis) of each summary statistic among the 20 replicates and associated each scenario to $s \times 4$ values. Using the moments instead of the 20 values may ease the generalization to data with a larger number of genomic regions available.

We used a particular ABC algorithm: ABC random forest for parameter inference (Raynal *et al.*, 2019). This method was developed based on the random forest method (Breiman, 2001). A random forest is composed of $B$ decision trees (we used $B = 500$). A decision tree is binary and built from the root to the leaves in an iterative way until the stopping rule is satisfied. At each node, the observations of the training dataset are divided into two sets, following a rule applied to summary statistic $S$. Observations for which $S > s$ are put in a sub-node and those for which $S <= s$ are placed in the other sub-node. $s$ is chosen specifically to minimize a $L^2$-loss criterion. Building a tree can be done in practise with several summary statistics (we used the third of all summary statistics), sampled randomly for each node. Nodes are split using this process until only five observations are left in the subnode, turning it into a leaf (i.e., a terminal node). Once the tree is built, it is possible to infer the value of the parameter of a new observation by taking the average of the parameters of the leaf in which it falls. The random forest aggregates several decision trees built from a random subset of the data (here, we rather used all the data points in the training set since their number was not too high). The prediction for a given observation is equal to the average of the predictions made by all trees. The ABC random forest has the advantage of being little impacted by strongly correlated summary statistics, nor by irrelevant summary statistics (Raynal *et al.*, 2019). However it requires building one forest per parameter, hence yielding independent posteriors rather than a joint distribution.

We performed ABC random forest training and inference using the *abcrf* package (Raynal *et al.*, 2019), with default hyperparameters. We also used the information provided on variable importance by this package.

### 3.1.5 Deep learning

The second inference method used is deep learning on raw genomic data (see section 0.2.2). For each replicate, we build the corresponding SNP matrix. This matrix contains $n$ rows corresponding to $n$ haplotypes and $k$ columns corresponding to $k$ SNPs. Each SNP equals 0 or 1 depending on the presence or absence of the mutation at this position for this haplotype. To this matrix is added a vector which contains the position of each SNP. These matrices will be the input data of the neural network. The chosen architecture requires the input data to be of the same dimension, hence only the first 400 SNPs in the 2 Mb are kept to create the matrix. When a replicate has less than 400 SNPs, the scenario containing this replicate is discarded. The matrices are thus of dimension $n \times 400$. The output vector of the network contains four values, which are the network inference for this SNP matrix.

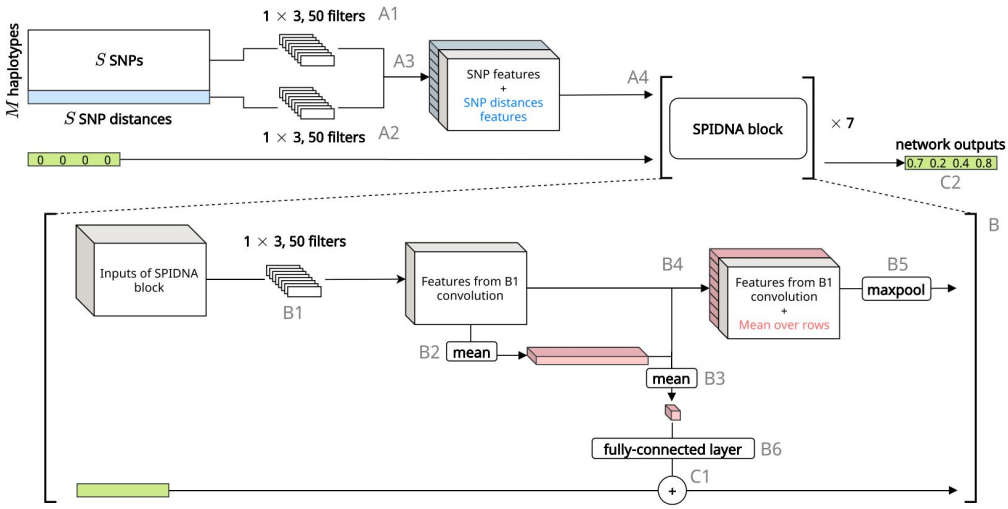


Figure 3.1: **SPIDNA architecture** (from Sanchez *et al.*, 2021)

The neural network used is based on SPIDNA (Sanchez *et al.*, 2021) (Fig. 3.1), that we modified to predict $\alpha$ and $N_{1-3}$ instead of 21 population sizes through time. It consists of a first convolution applied to the SNPs as well as a convolution applied to the positions. The results of these two convolutions are concatenated. They are then passed through a series of seven so-called *SPIDNA blocks*. These blocks are identical and consist of: B1, a convolution layer; B2, a row average of the

B1 results; B3, a column average of the B2 results. The results of B1 and B2 are concatenated (B4), then maxpooled (B5). A fully connected layer is applied to B3 (B6). The prediction vector is updated at each block by summing the value at the previous block and B6 (C1). The last of the blocks gives C2, which is the predicted parameter vector. The row average performed in each SPIDNA block (B2) allows reaching an invariance in the order of the haplotypes, although the fully connected or convolution layers are not invariant.

### 3.1.6 Comparing inference methods

We compared several inference methods, which can be divided into three categories: (i) different ABC random forests which differ by the summary statistics used, (ii) deep learning on raw genomic data with SPIDNA, (iii) an ABC random forest using as input summary statistics and inferences made by SPIDNA (as in Sanchez *et al.*, 2021). In the following paragraphs, we detail these three categories.

For the ABC random forest, we used different combinations of summary statistics. For diversity statistics, the following combinations were tested: (1) the mean number of pairwise differences ($\pi$), (2) Tajima's $D$, (3) the full unfolded Site Frequency Spectrum (SFS), (4) the combination of 1, 2 and 3. For imbalance statistics, we tested: (5) the Fusco imbalance index ($I_F$) on trees reconstructed with tsinfer, (6) the Fusco imbalance index on trees reconstructed with relate, (7) the combination of 5 and 6, (8) $B_2$ index on tsinfer and $B_2$ index on relate trees, (9) $B_1$ index on tsinfer and $B_1$ index on relate trees, (10) the combination of 7, 8 and 9. We also combined the diversity and imbalance statistics (4 and 10). For all these statistics, we calculated the first four moments on the values of the 20 replicates. By default, these four moments are used as separate statistics for the ABC random forest. Furthermore, we could compare the quality of inference using the first moment only (as in Sanchez *et al.*, 2021), to the one based on the first four moments.

For deep learning, we performed one inference per replicate. We compared two methods to integrate the 20 predictions per scenario. The first method is to take the average of the 20 predictions and consider it the inference for the scenario, corresponding to averaging the results of 20 independent genomic regions of 2 Mb in one population genomic data. The second method uses an ABC random forest trained to combine the 20 values optimally (using default hyperparameters). For the four parameters, the first four moments of the distribution of the 20 inference values are computed, and this vector of length $4 \times 4$ is used as the summary statistics vector

for the ABC. This method stems from Jiang *et al.* (2017)'s work concerning the automatic learning of optimal summary statistic for ABC using deep neural networks, which have already been applied to population genetics inference by Sanchez *et al.* (2021).

Finally, a third group of methods combines the summary statistics with SPIDNA's predicted values using ABC random forest. We used as summary statistic vector the concatenation of the 4 parameters $\times$ 4 moments of SPIDNA inference and the 4 moments of chosen summary statistics. We explored three combinations. The first one combines the diversity statistics ($\pi$, Tajima's $D$ and SFS) with SPIDNA's inference. The second combines the imbalance indices with SPIDNA's inference. The third combination ($ABC_{all+DL}$) uses all the summary statistics mentioned ("all") with the SPIDNA inference results ("DL").

For all methods, the training dataset is the same, as well as the test dataset. We simulated 2000 scenarios, 1400 attributed to training and 600 to validation and test (the same dataset was used for both, since no hyperparameter optimization was performed). Some scenarios were removed because they contained at least one replicate with less than 400 SNPs. After this, the training dataset consisted of 1366 scenarios of 20 replicates, and the test dataset of 585 scenarios of 20 replicates. We computed three measures on the test dataset to evaluate a method: the correlation between the true and inferred parameters, the Mean Squared Error (MSE), and the bias. These evaluations are performed for all methods. We also explored the impact of the number of sampled haplotypes for different methods: we sampled 5, 10, 20, 40, or 80 (default case) diploid individuals to compute the summary statistics for ABC, and to build the SNP matrices for deep learning. For each of these sample sizes, we used 5, 10, 15, or 20 (default case) replicates. This allows for an evaluation of the importance of the sample size and the number of genomic regions for the different inference methods.

### 3.1.7 Dadi inference

We used the dadi software (Gutenkunst *et al.*, 2009) to have a benchmark for inferring demographic parameters. Dadi takes the SFS as input and infers from it the demographic history using the diffusion approximation model. Dadi requires a model as input in order to infer the parameters. We used the three epoch model, which allows inferring the population sizes at three timesteps and the duration of the two most recent timesteps (the first one going back to the common ancestor).

We fed the true time parameters values to the model, so it only has to infer the population size parameters. This method allowed the comparison with the previously mentioned methods, which only infer the three population sizes, with the timesteps fixed. We evaluated the correlation between the true and inferred parameters, the MSE, and the bias.

## 3.2 Results

### 3.2.1 Diversity summary statistics

We first applied ABC random forest (ABCrf) using as a summary statistic only the average mean number of pairwise differences ($\pi$) across the 20 replicates. In that case, only the inference of the oldest population size ($N_1$) was possible (cor = 0.91, MSE = 0.18) (Fig. 3.2B, Supp. Fig. S1B). The other two inferred population sizes ($N_2$ and $N_3$) and $\alpha$ (i.e., the intensity of the nongenetic TRS) have null or close to null correlations with their true values (Fig. 3.2A, 3.2C-D). This is because $N_1$ is the parameter with the highest impact on genetic diversity, since it is the population size that has been maintained for the longest time. On the other hand, when we used the first four moments of $\pi$, the inference of $\alpha$ became possible (cor = 0.72, MSE = 0.57), with an improved inference of $N_1$ (cor = 0.98, MSE = 0.05) (Supp. Fig. S2B, S3B). Therefore, the distribution of $\pi$ in the genome seems influenced by $\alpha$ independently from population size changes.

When ABCrf uses the average Tajima's $D$ as the only summary statistic, $\alpha$ had a higher correlation (cor = 0.63, MSE = 0.74) than $N_{1-3}$. These results can be improved by using the first 4 moments of Tajima's $D$ distribution (e.g., for $\alpha$: cor = 0.86, MSE = 0.28) (Supp. Fig. S2). A more accurate inference of all 4 parameters was observed when using the full unfolded SFS, each bin considered as a summary statistic (with the first moment: $\alpha$: cor = 0.9, MSE = 0.2; $N_1$: cor = 0.78, MSE = 0.44; $N_2$: cor = 0.58, MSE = 0.83; $N_3$: cor = 0.71, MSE = 0.59) (Fig. 3.2, with better results with all four moments in Supp. Fig. S2). These results are much better than dadi's, which also relies on the first moment of the SFS ($N_1$: cor = 0.69, MSE = 0.62; $N_2$: cor = 0.16, MSE = 1.68; $N_3$: cor = 0.31, MSE = 1.38) (Fig. 3.2). Moreover, dadi showed a strong bias for the three timesteps, which does not appear with ABCrf using the SFS (Supp. Fig. S4, S5).

Combining all diversity summary statistics ($\pi$, Tajima's $D$ and SFS), we ob-

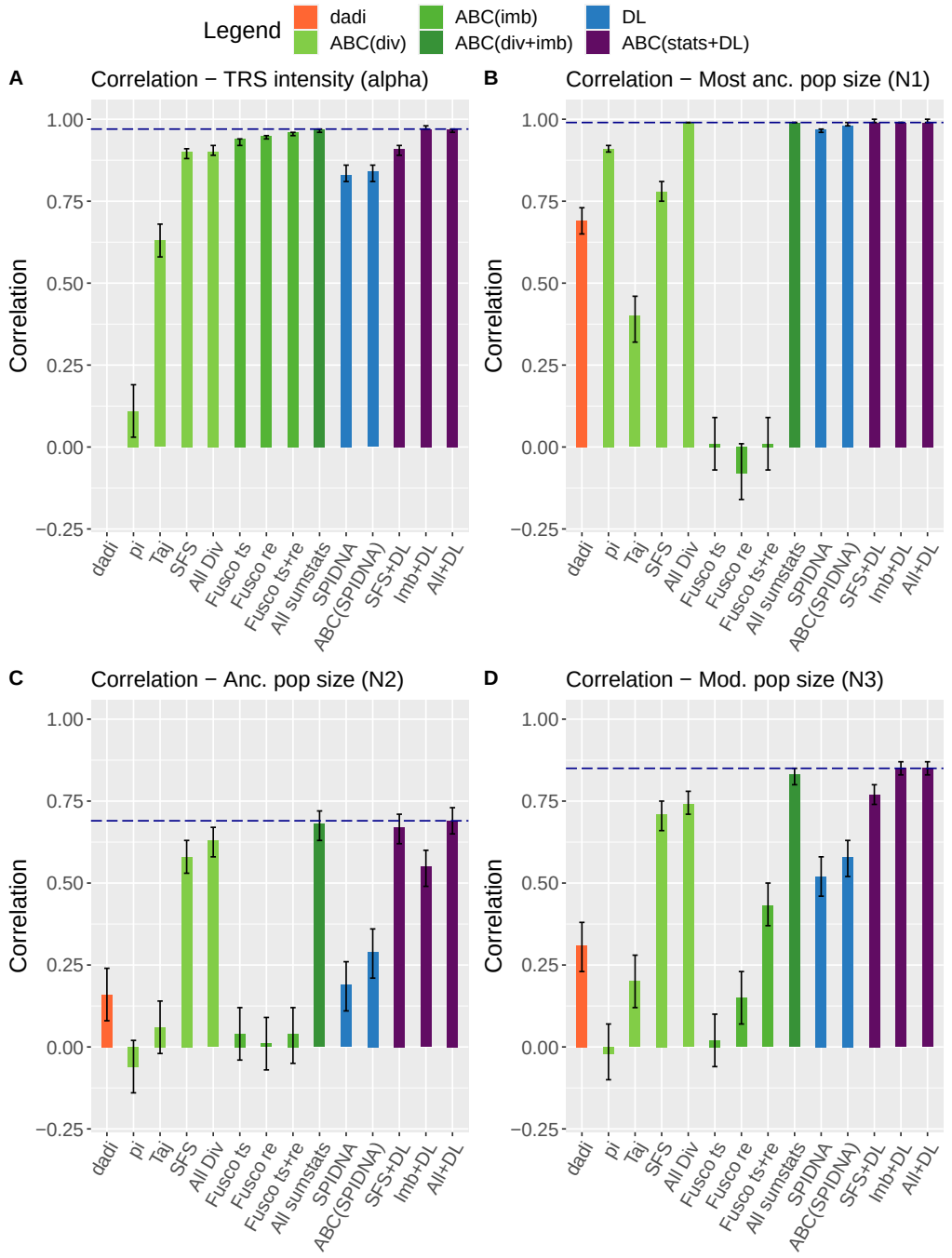


Figure 3.2: **Comparison of inference methods accuracy using correlations.**
The correlations were computed between inferred and true values on the test set. Only the first moment (mean) of the 20 replicates was used for training and inference. The sample size was of 80 diploid individuals. Error bars correspond to the 95% confidence interval of the correlations, computed with the *test.cor* R function in the *stats* package. The dashed line corresponds to the highest correlation reached for each parameter.
In orange: dadi inference. In light green: ABCrf using various diversity statistics. In green: ABCrf using various imbalance statistics. In dark green: ABCrf combining all diversity and imbalance indices. In blue: deep learning using SPIDNA. In purple: ABCrf combining summary statistics and SPIDNA results.

tained a better inference than with each statistic independently (with the first four moments: $\alpha$: cor = 0.92, MSE = 0.15; $N_1$: cor = 0.99, MSE = 0.02; $N_2$: cor = 0.69, MSE = 0.62; $N_3$: cor = 0.77, MSE = 0.47) (Supp. Fig. S2). The SFS provides information on $\alpha$, $N_1$ and $N_2$, while $\pi$ is crucial for the inference of $N_3$ (Supp. Fig. S2, Fig. 3.2).

### 3.2.2 (Im)balance summary statistics

Using the average of the Fusco index ($I_F$) on the trees inferred by tsinfer or relate, we have information only on $\alpha$, with a slightly but significantly higher correlation for relate compared to tsinfer (Fig. 3.2, cor $I_F$ tsinfer = 0.9438, cor $I_F$ relate = 0.9516, one-sided Hittner's test p-value $< 0.001$). Using the four moments, we also obtained information on $N_3$ (Supp. Fig. S2D). Thus, the modern population size affects the imbalance distribution in the genome, without affecting its average. This probably stems from the increase of imbalance variance in smaller populations due to stronger drift (Guez *et al.*, 2022). By combining the indices computed on the tsinfer and relate trees, the inference of $\alpha$ is further improved (cor $I_F$ tsinfer and relate = 0.9589, one-sided Hittner's test p-value with $I_F$ relate $< 0.001$). Therefore, each tree inference software provides complementary relevant information about the topology. By using other topology indices, such as $B_1$ and $B_2$, we reached a higher correlation on $N_1$ (Supp. Fig. S6B, Supp. Fig. S7B). For $B_1$, this might be because it is impacted by demography (Guez et al. 2022). Combining all the imbalance statistics helped achieve a better inference for the four parameters than the imbalance statistics taken independently (Supp. Fig. S6, Supp. Fig. S7). Moreover, by combining all the diversity and imbalance statistics, we attained an overall better inference than any other statistics combination (with the first four moments: $\alpha$: cor = 0.97, MSE = 0.06; $N_1$: cor = 0.99, MSE = 0.02; $N_2$: cor = 0.69, MSE = 0.61; $N_3$: cor = 0.84, MSE = 0.33) (Supp. Fig. S2).

### 3.2.3 Deep learning

Our deep learning on raw genomic data approach performed worse than ABCrf. In particular, $N_2$ (cor = 0.19, MSE = 1.62) is not well inferred (Fig. 3.2C). Results can be improved by applying an ABCrf on the average of the 20 deep learning predictions, and even further improved by applying an ABCrf on the first four moments of the deep learning predictions ($N_2$: cor = 0.32, MSE = 1.35) (Supp.

Fig. S2C). These results are still well below those from the ABCrf using the four first moments of all summary statistics. However, using an ABCrf that combined the four first moments of the summary statistics with the four first moments of the predictions made by deep learning ($ABC_{all+DL}$), we obtained slightly improved results compared to ABCrf on summary statistics only ($\alpha$: cor = 0.97, MSE = 0.06; $N_1$: cor = 0.99, MSE = 0.01; $N_2$: cor = 0.71, MSE = 0.58; $N_3$: cor = 0.85, MSE = 0.3; p-value $<$ 0.001 for all parameters) (Supp. Fig. S2). This improvement shows that despite performing worse than ABCrf on summary statistics, SPIDNA still recovered from the raw genomic data some information that was not contained in any of the summary statistics.

### 3.2.4 Important variables

We analyzed the variables that are the most important for inference based on the best-performing ABCrf (i.e., ABCrf using all summary statistics and the deep learning features obtained with SPIDNA, denoted $ABC_{all+DL}$) (Fig. 3.3). The scores show that the most important variables for inferring $\alpha$ are the imbalance indices, with the average of $I_F$ on tsinfer and the average of $I_F$ on relate in first and second place respectively. This suggests that $I_F$ is less influenced by population size changes than the other summary statistics used. This confirms previous results which showed that an index derived from $I_F$ (index from Brandenburg *et al.*, 2012) was not influenced by demography (Guez *et al.*, 2022). Interestingly, the number of singletons (SFS1) and the number of the alleles at highest frequency (SFS159) can also be used for inference, consistent with simulation results showing a U-shaped SFS under nongenetic TRS (Guez et al. 2022). This type of SFS is indeed impossible to reach theoretically with population size changes only (under the Kingman coalescent, Freund *et al.*, 2022). Therefore, this U-shape is helpful in distinguishing nongenetic TRS from population size changes. We note that the inference performed by deep learning for $\alpha$ is not used among the important variables, confirming that SPIDNA must have difficulties constructing topological features.

To infer the ancient population size ($N_1$), the most important statistic is the inference performed by deep learning (Fig. 3.3). In second and third place come the mean and variance of $\pi$. For inferring the intermediate population size ($N_2$), the most important summary statistics are the means of the number of rare alleles (SFS6, SFS7, SFS8 and SFS9). Interestingly, the $\alpha$ predicted by deep learning, now considered as an input feature for ABC, can help to infer $N_2$. For inferring the most

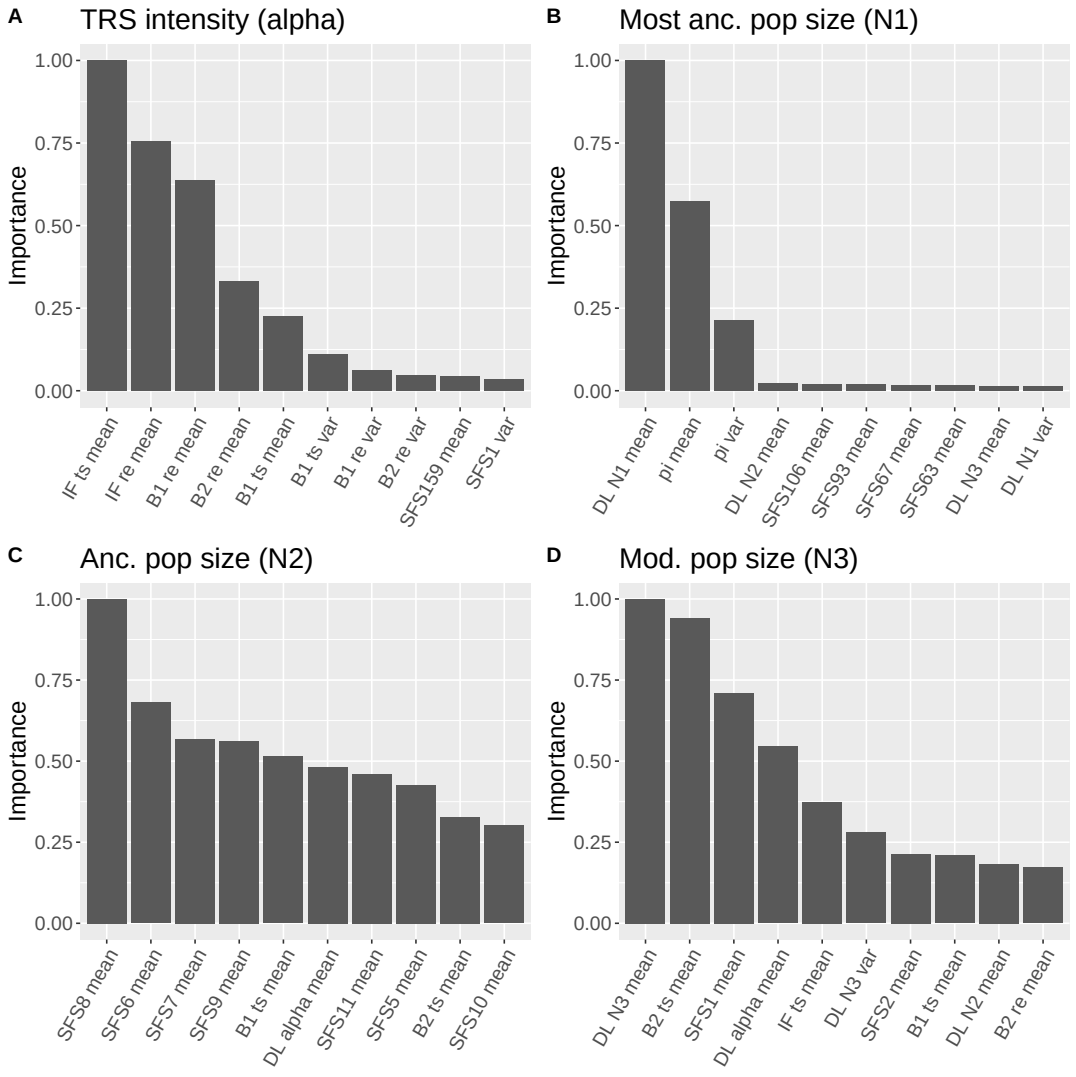


Figure 3.3: **Variable importance for best-performing ABCrf inference ($ABC_{all+DL}$).** Only the ten most important variables are shown.

recent population size ($N_3$), the most important statistic is the inference made by deep learning. This is followed by the mean of $B_2$, the mean number of singletons, and the inference of $\alpha$ by deep learning. The importance of this last statistic in inferring $N_2$ and $N_3$, suggests that ABCrf can distinguish the impacts of recent population sizes from those of $\alpha$ by observing the deep learning prediction of $\alpha$.

### 3.2.5 Application example

We then focused on the inference of a specific scenario: a bottleneck with an old population size of 10,000, an intermediate population size of 3,000, and a modern size of 10,000. We set the nongenetic TRS over the last 20 generations to $\alpha = 1$,

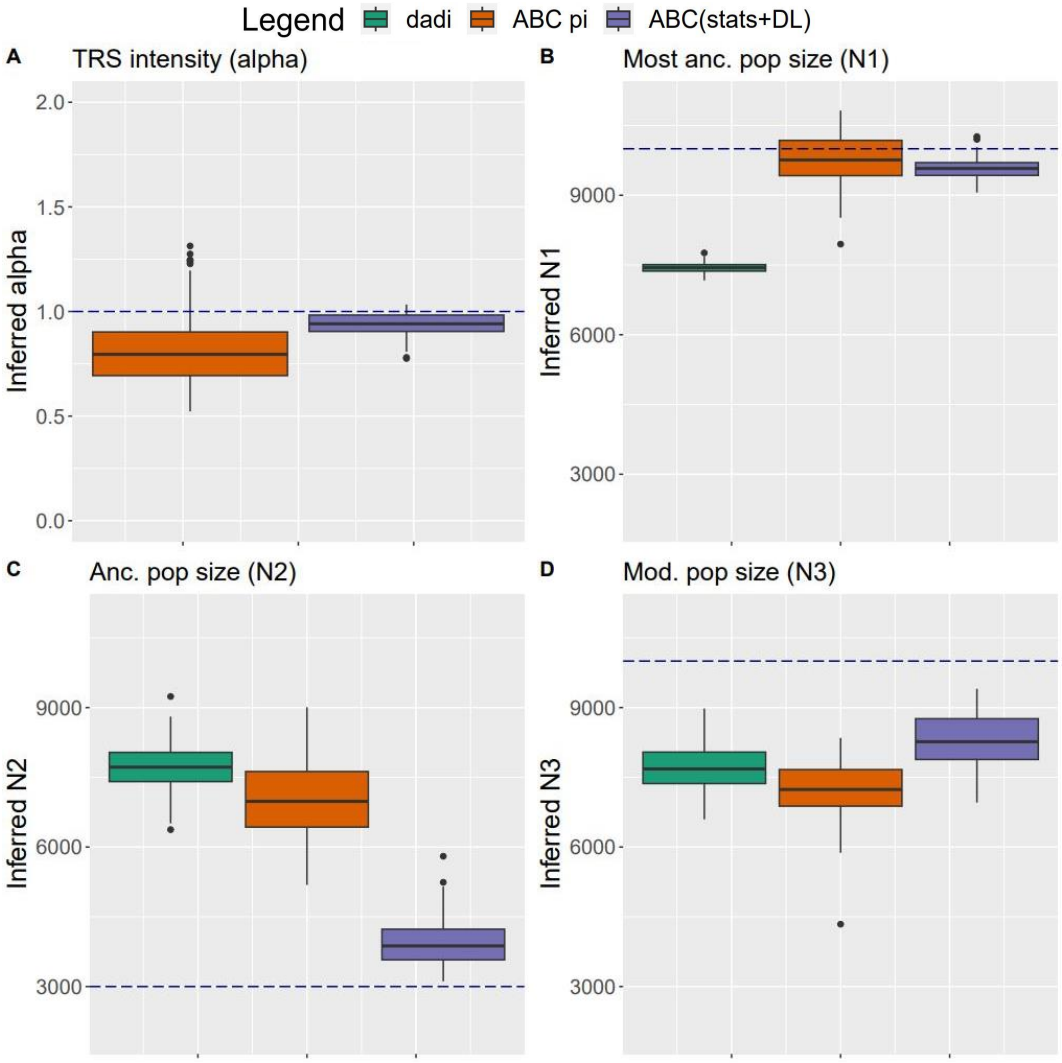


Figure 3.4: **Inference on a simulated bottleneck example with TRS intensity of $\alpha = 1$.** Parameters inferred by dadi (green), $ABC_{\pi}$ (orange), and $ABC_{all+DL}$ (purple). Sample size = 80 diploid individuals. 50 independent identical scenarios were simulated, each consisting in 20 replicates of 2 Mb. Inference was performed on each scenario, each yielding one data point for the boxplots computing. The dashed line is the true value to be inferred.

corresponding to a strong but previously observed level of progeny size correlation between parents and children (correlation approximately equal to 0.25, close to levels found in Pearson *et al.*, 1899; Bresard, 1950; Wise and Condie, 1975; Murphy, 1999; Murphy and Wang, 2001; Pluzhnikov *et al.*, 2007). Three inference models are compared: dadi, $ABC_{\pi}$ (using the four moments of $\pi$), $ABC_{all+DL}$ (using the four moments of all summary statistics and the four moments of deep learning predictions). The previous sections showed the latter model to perform best on average across all scenarios.

The results show that $\alpha$ is fairly well recovered by $ABC_{all+DL}$, while $ABC_{\pi}$ shows a negative bias (Fig. 3.4A). For the demographic inference, dadi finds a median population size close to 8,300 for the three timesteps ($N_1$, $N_2$ and $N_3$) (Fig. 3.4B-D). Dadi seems strongly influenced by the most ancient population size and does not detect the recent bottleneck. $ABC_{\pi}$ estimates correctly that $N_1$ is around 10,000, but that both $N_2$ and $N_3$ are around 7,000 (medians): it thus detects the contraction but not the most recent expansion (Fig. 3.4B-D). Finally, $ABC_{all+DL}$ detects the bottleneck, estimating $N_1$ to be close to 10,000, $N_2$ close to 4,000, and $N_3$ close to 7,000 (medians) (Fig. 3.4B-D). $N_3$ remains the most poorly inferred parameter, probably because the nongenetic TRS occurs on this last timestep, or because the very recent demographic events are generally difficult to infer.

### 3.2.6 Effects of sample size and number of genomic regions

We then studied the impact of the number of genomic regions and sample size on inference accuracy using $ABC_{all+DL}$. For each sample size (5, 10, 20, 40, and 80 individuals), the first four moments of the summary statistics are computed on 5, 10, 15, or 20 genomic regions of 2 Mb. When using 20 genomic regions, the sample size improves the inference of $\alpha$, with correlations increasing from 0.89 (sample size = 5) to 0.97 (sample size = 80) (Fig. 3.5A). The number of genomic regions has almost no effect on the inference of $\alpha$ (0.96 vs. 0.97 when using 5 or 20 regions for 80 samples) (Fig. 3.5A). The correlation for $N_3$ is around 0.99, whatever the sample size or the number of genomic regions (Fig. 3.5B). For $N_2$, the effect of sample size is less clear, with the best inferences for a sample between 20 and 80. The number of genomic regions has a positive effect, but correlations reached a plateau at 15 regions (Fig. 3.5C). For $N_3$, the sample size has a very strong impact: with 20 genomic regions, correlations rise from 0.51 (sample size = 5) to 0.86 (sample size = 80). However, the difference between the sample size of 40 and 80 is small, indicating a plateau in improvement. Thus, sampling more than 80 individuals should not improve the inference by a large margin (Fig. 3.5D). The number of regions impacts the inference of $N_3$ (0.76 for 5 genomic regions vs. 0.86 for 20 genomic regions, when sample size = 80), however a plateau seems to be quickly reached (at 10 regions) for sample sizes higher that 20 (Fig. 3.5D).

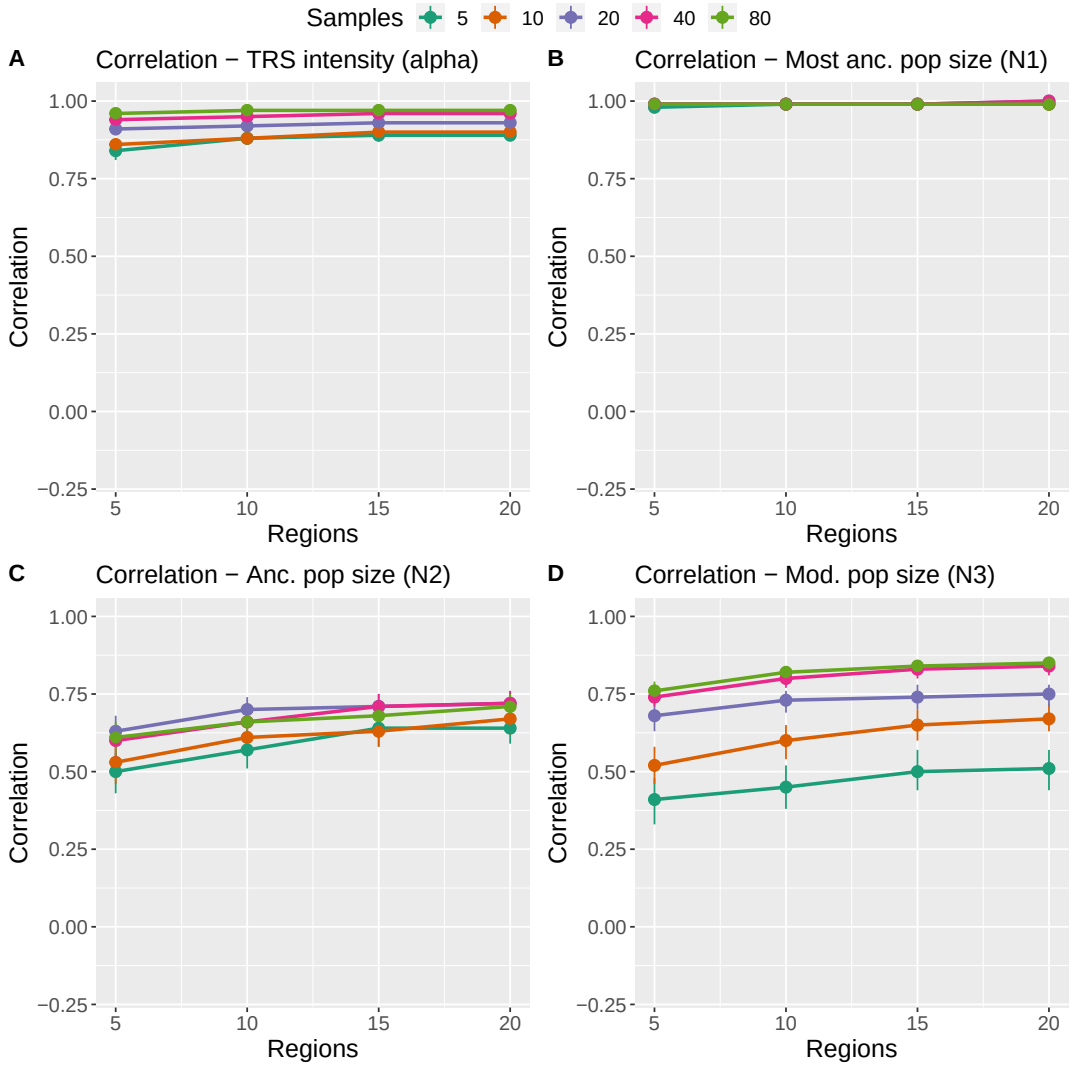


Figure 3.5: **Impacts of sample size and number of genomic regions on inference correlations for the four parameters.** The best-performing ABC was used here (i.e., $ABC_{all+DL}$).

## 3.3 Discussion

This paper explored different methods to jointly infer nongenetic TRS intensity and demographic parameters. The main result is the design of an efficient tool for this inference. We have seen that a bottleneck was indeed well inferred by the best-performing ABCrf, unlike dadi which inferred a constant size. We compared in detail different inference models. The results show that ABCrf based on handcrafted summary statistics gives better results than the SPIDNA deep neural network applied to raw genomic data. However, an ABCrf combining summary statistics and automatically-learned deep learning features led to slightly better results than ABCrf using summary statistics only, and was the best-performing model. By performing

several ABCrf with different combinations of summary statistics, we were able to reveal the importance of each summary statistic for the inference of each parameter. This analysis was completed by examining the importance of the variables that were used by the best-performing ABCrf model. Finally, we explored the impact of the sample size and the number of regions used on inference accuracy. We have shown that the sample size strongly impacts the inference, while the number of regions has a weaker impact. However, the importance of having a large sample size varies depending on the inferred parameter. In this section, we will discuss some of the results.

Results showed that the mean of $\pi$ is sufficient to correctly infer the oldest size ($N_1$). Using the four first moments of $\pi$, one can additionally infer the intensity of nongenetic TRS ($\alpha$). This indicates that the distribution of $\pi$ in the genome is impacted by TRS independently of demographic changes, enough to tell them apart. Often, using the distribution of a summary statistic over the different replicates (as in Jay *et al.*, 2019) added information compared to the simple average (as in Sanchez *et al.*, 2021). Another interesting result is that the unfolded SFS contains less information than $\pi$ for inferring $N_1$, although many diversity summary statistics can be derived from an SFS. Some ABC studies have used only SFS as summary statistics (e.g., Mondal *et al.*, 2019), but our results show that $\pi$ can ease information extraction and increase inference accuracy. In general, it seems useful to perform several ABCrf with different combinations of summary statistics to understand how the simulation parameters impact these different indices.

By applying this method to the imbalance indices, we understood their respective importance. First, any single imbalance index gives a better inference of $\alpha$ than all the diversity indices combined. Moreover, the diversity indices ($\pi$, Tajima's $D$, and SFS) were insufficient to achieve the best possible inference: the addition of imbalance indices substantially improved the inference for three out of four parameters. This indicates that the imbalance indices improve demographic inference, although not impacted by population size changes, because they help disentangle nongenetic TRS from demography. Furthermore, these results show that tsinfer and relate are able to extract from genomic data information absent in the diversity indices used.

By comparing the inferences made with $I_F$ computed on tsinfer only and $I_F$ computed on relate only, we could show that the latter gives a better inference of $\alpha$ than the former. This could be evidence that relate is better at retrieving the imbalance property than tsinfer. We also observed that combining these two $I_F$ gives a better inference than each index taken alone. This shows that the informa-

tion retrieved by the two software does not overlap completely, and that each finds information that the other does not. This result can be generalized to other types of inferences requiring a reconstruction of the tree topology, such as selection which can be inferred from tree imbalance (Li and Wiehe, 2013; Yang *et al.*, 2018; Dilber and Terhorst, 2022). Combining multiple tree reconstruction software to extract maximum information from genomic data would be helpful in that case.

We showed that ABCrf using diversity indices only ($\pi$, Tajima's $D$, and SFS) gave better results than deep learning with SPIDNA. This can stem from several reasons. First, the amount of training data needed to train SPIDNA is probably much more extensive than what is needed for ABC. Indeed, ABC methods take as an input already computed summary statistics, while deep neural networks are heavily parameterized models and are known to require large training sets (Goodfellow *et al.*, 2016). Second, this SPIDNA architecture only uses the first 400 SNPs of each 2 Mb replicate. Therefore, when the 2 Mb contains more than 400 SNPs, deep learning will have less information than ABC since the latter has access to the entire 2 Mb. Third, the SPIDNA architecture has horizontal $1 \times 3$ convolution filters (i.e., matching the SNP matrix rows, which is the SNPs dimension). Thus, it might recognize more easily patterns in the SNPs dimension than in the individuals' dimension (i.e., the SNP matrix columns), a specialization that corresponds to the population size inference task it was developed for by Sanchez *et al.* (2021). Such an architecture might struggle to reconstruct imbalance indices efficiently since they require a comparison between individuals. We could use square convolution filters (e.g., $3 \times 3$) to correct this issue, but we would loose SPIDNA's permutation-invariant property. Another possibility would be to use the mixed attention version of SPIDNA, which uses an attention mechanism rather than a simple average in the dimension of the individuals. This architecture is more efficient than SPIDNA on a demographic inference task (Sanchez, 2022). This version of SPIDNA might be particularly efficient for topology information extraction, due to its hubs-based architecture allowing it to compute features on subgroups of individuals from the sample.

On the other hand, results show that SPIDNA retrieved information not present in the summary statistics, as the ABC is improved when SPIDNA predictions are given in addition to the summary statistics. Therefore, the information present in other summary statistics, such as LD and IBS, should be explored (Jay *et al.*, 2019; Sanchez *et al.*, 2021). It seems that comparison with the ABC is a helpful way to investigate the interpretability of neural networks, an issue of central interest in the

field of deep learning (Murdoch *et al.*, 2019). With the multiple comparisons made, we slowly begin to open the black box of our network and understand the type of information it extracts from raw genomic data.

We have investigated only the co-inference of two processes, nongenetic TRS and changes in population size. Applying the inference tool developed here to real genomic data may require including other processes in the model. For example, selection impacts the summary statistics of diversity (Braverman *et al.*, 1995; Fay and Wu, 2000) and imbalance (Li, 2011; Li and Wiehe, 2013) used in this study. A solution would be to apply our inference tool only to neutral genome regions (Gazave *et al.*, 2014). However, background selection and biased gene conversion affect more than 95% of the genome and can impact inference (Pouyet *et al.*, 2018). Therefore, with a conservative filter, only around 150 Mb would remain to co-infer nongenetic TRS and demographic history. Our results showed that it is possible to focus on this part of the genome since ten independent regions of 2 Mb already give a good inference. Using only neutral regions would avoid including positive and background selection, or gene conversion in our model.

Finally, migration processes and sampling effects affect the whole genome and impact diversity and imbalance summary statistics (Wakeley and Aliacar, 2001; Przeworski, 2002; Blum *et al.*, 2006). Therefore, their impacts on inference should be tested, and they might have to be included in the method before its application to real data. Another possibility would be to first analyze the sample structure and retain only individuals of relatively homogeneous ancestry (as done by Gazave *et al.*, 2014). However, it is possible that the structure analysis itself is biased by the presence of nongenetic TRS. A third way to disentangle structure from nongenetic TRS would be to first study populations for which genealogical records, which contain the TRS information, are available on top of genomic data. Such extensive genealogical records and genomic data exist for the Quebec population (Anderson-Trocmé *et al.*, 2022), where nongenetic TRS has been occurring in the last twelve generations (Austerlitz and Heyer, 1998).

In summary, we showed here that we can theoretically disentangle nongenetic TRS from population size changes, using machine learning in genomic data. Subsequent developments would further improve the inference methods, better understand the key summary statistics needed for this task, and add other processes that could be confused with nongenetic TRS, such as selection and migration.

## 3.4 Supplementary material

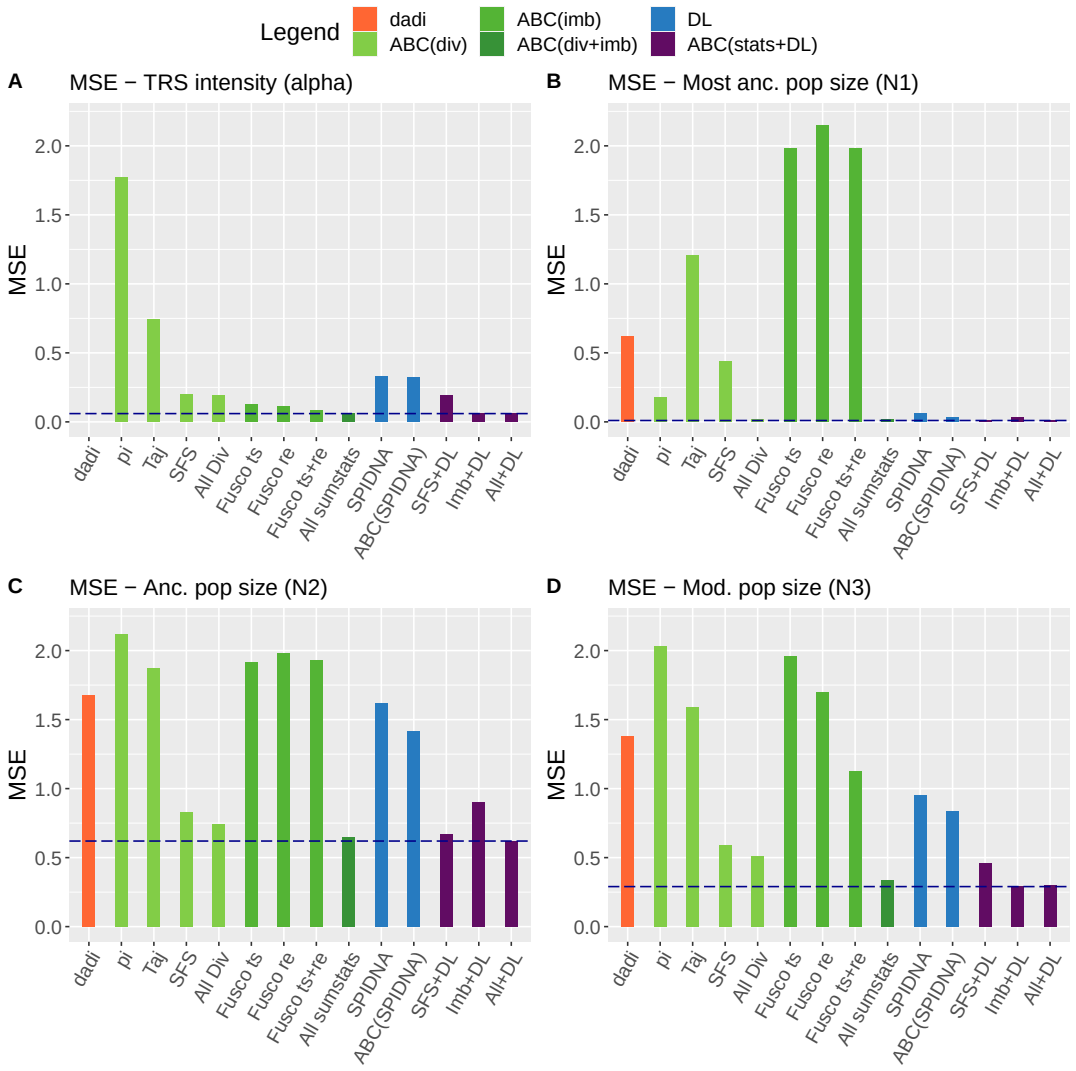


Figure S1: **Comparison of inference methods accuracy using MSE.**
MSE were computed between inferred and true values on the test set. Only the first moment (mean) of the 20 replicates was used for training and inference. The sample size was of 80 diploid individuals. The dashed line corresponds to the lowest MSE reached for each parameter.
In orange: dadi inference. In light green: ABCrf using various diversity statistics. In green: ABCrf using various imbalance statistics. In dark green: ABCrf combining all diversity and imbalance indices. In blue: deep learning using SPIDNA. In purple: ABCrf combining summary statistics and SPIDNA results.

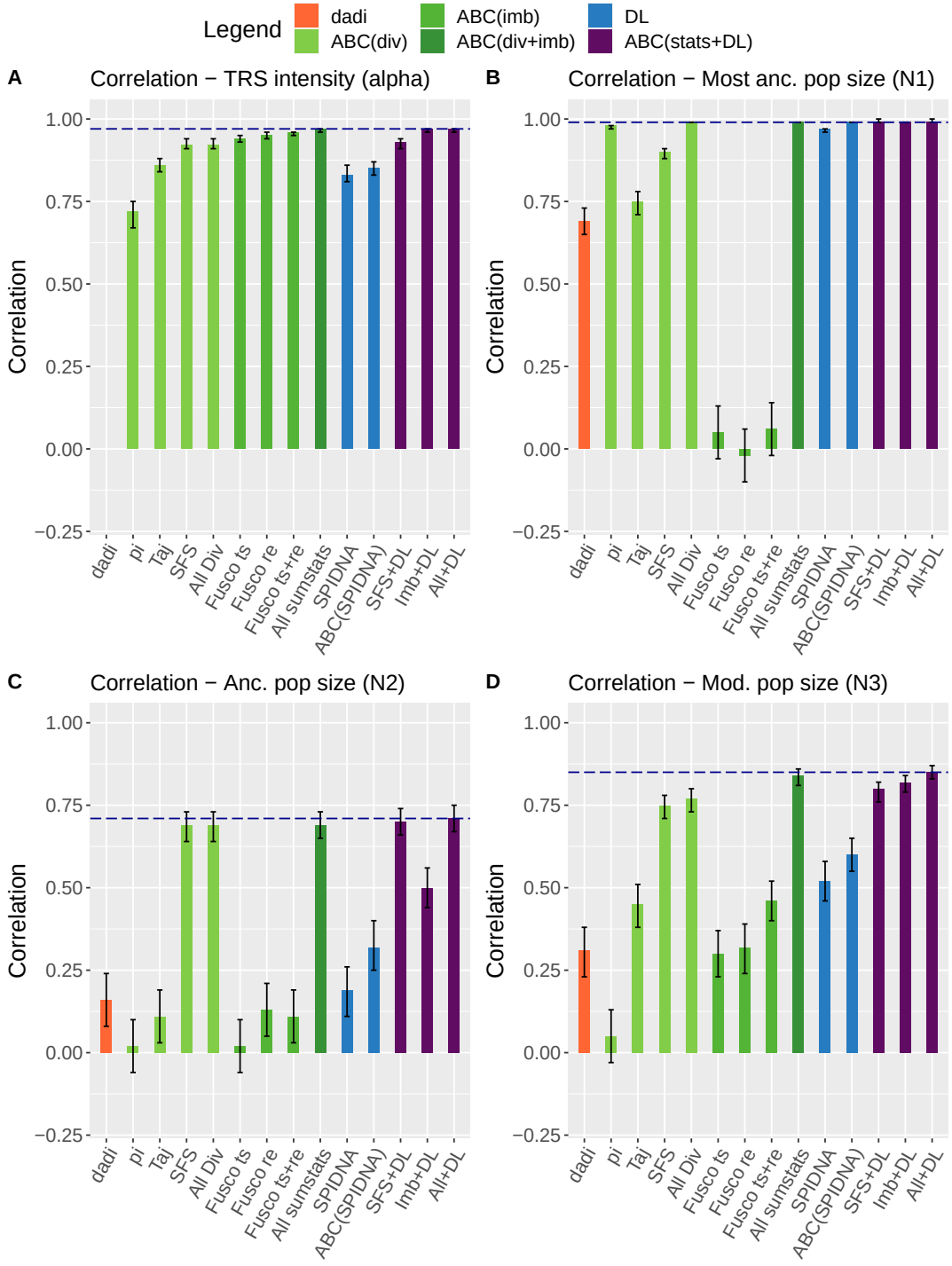


Figure S2: **Comparison of inference methods accuracy using correlations.**
The correlations were computed between inferred and true values on the test set. The first four moments (mean, variance, skewness, kurtosis) of the 20 replicates were used for training and inference. The sample size was of 80 diploid individuals. Error bars correspond to the 95% confidence interval of the correlations, computed with the *test.cor* R function in the *stats* package. The dashed line corresponds to the highest correlation reached for each parameter.
In orange: dadi inference. In light green: ABCrf using various diversity statistics. In green: ABCrf using various imbalance statistics. In dark green: ABCrf combining all diversity and imbalance indices. In blue: deep learning using SPIDNA. In purple: ABCrf combining summary statistics and SPIDNA results.

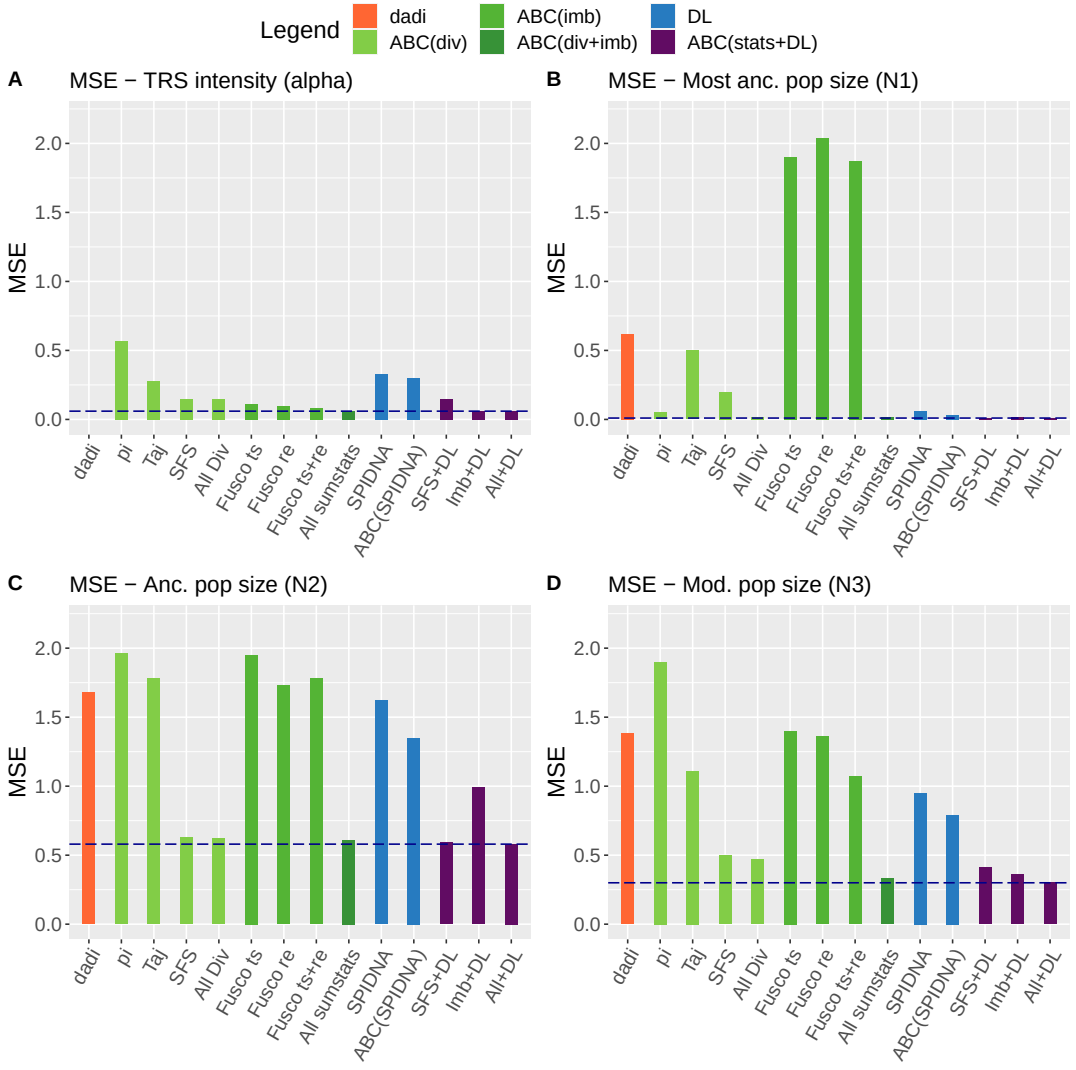


Figure S3: **Comparison of inference methods accuracy using MSE.**
MSE were computed between inferred and true values on the test set. The first four moments (mean, variance, skewness, kurtosis) of the 20 replicates were used for training and inference. The sample size was of 80 diploid individuals. The dashed line corresponds to the lowest MSE reached for each parameter.
In orange: dadi inference. In light green: ABCrf using various diversity statistics. In green: ABCrf using various imbalance statistics. In dark green: ABCrf combining all diversity and imbalance indices. In blue: deep learning using SPIDNA. In purple: ABCrf combining summary statistics and SPIDNA results.

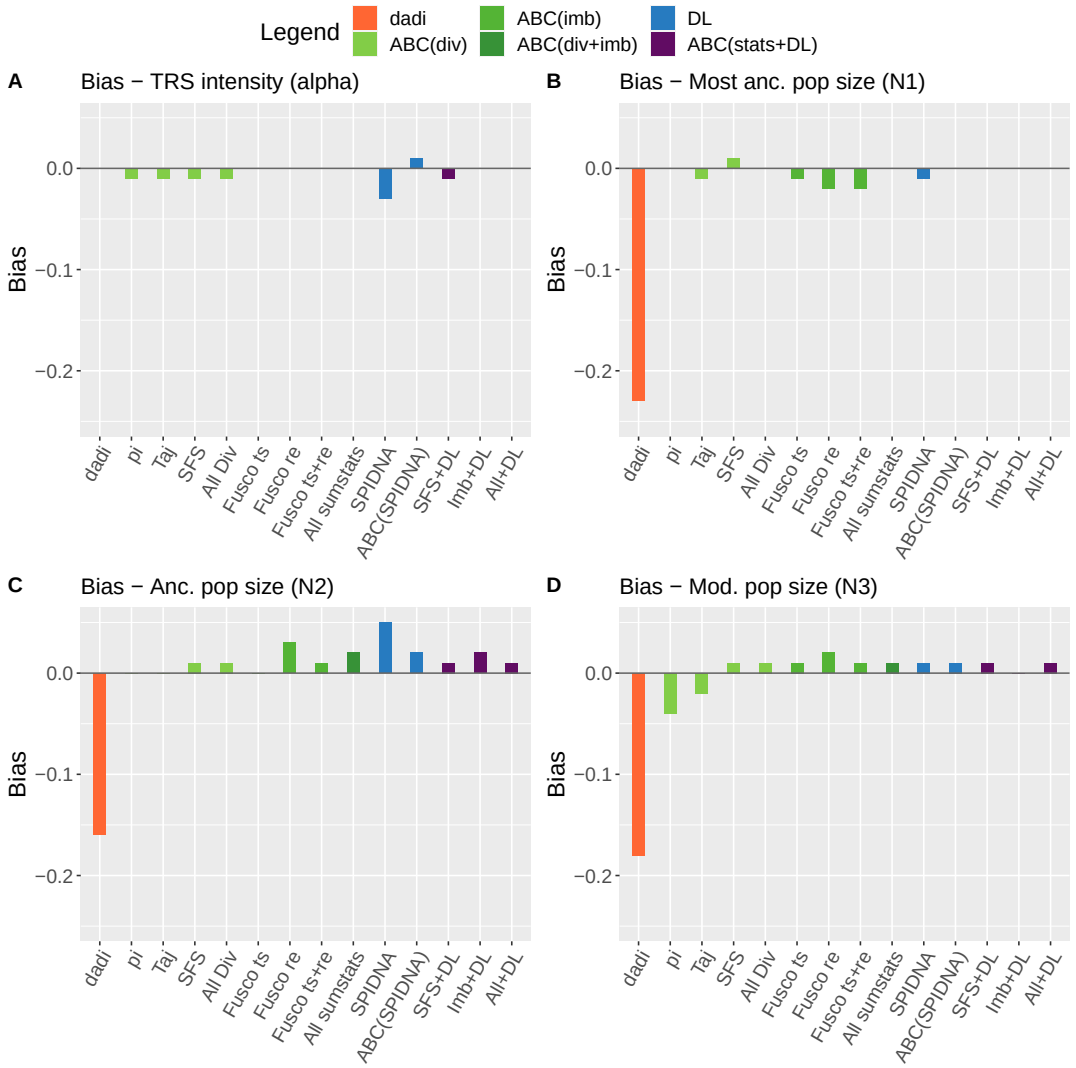


Figure S4: **Comparison of inference methods accuracy using bias computation.**
Biases were computed between inferred and true values on the test set. Only the first moment (mean) of the 20 replicates was used for training and inference. The sample size was of 80 diploid individuals.
In orange: dadi inference. In light green: ABCrf using various diversity statistics. In green: ABCrf using various imbalance statistics. In dark green: ABCrf combining all diversity and imbalance indices. In blue: deep learning using SPIDNA. In purple: ABCrf combining summary statistics and SPIDNA results.

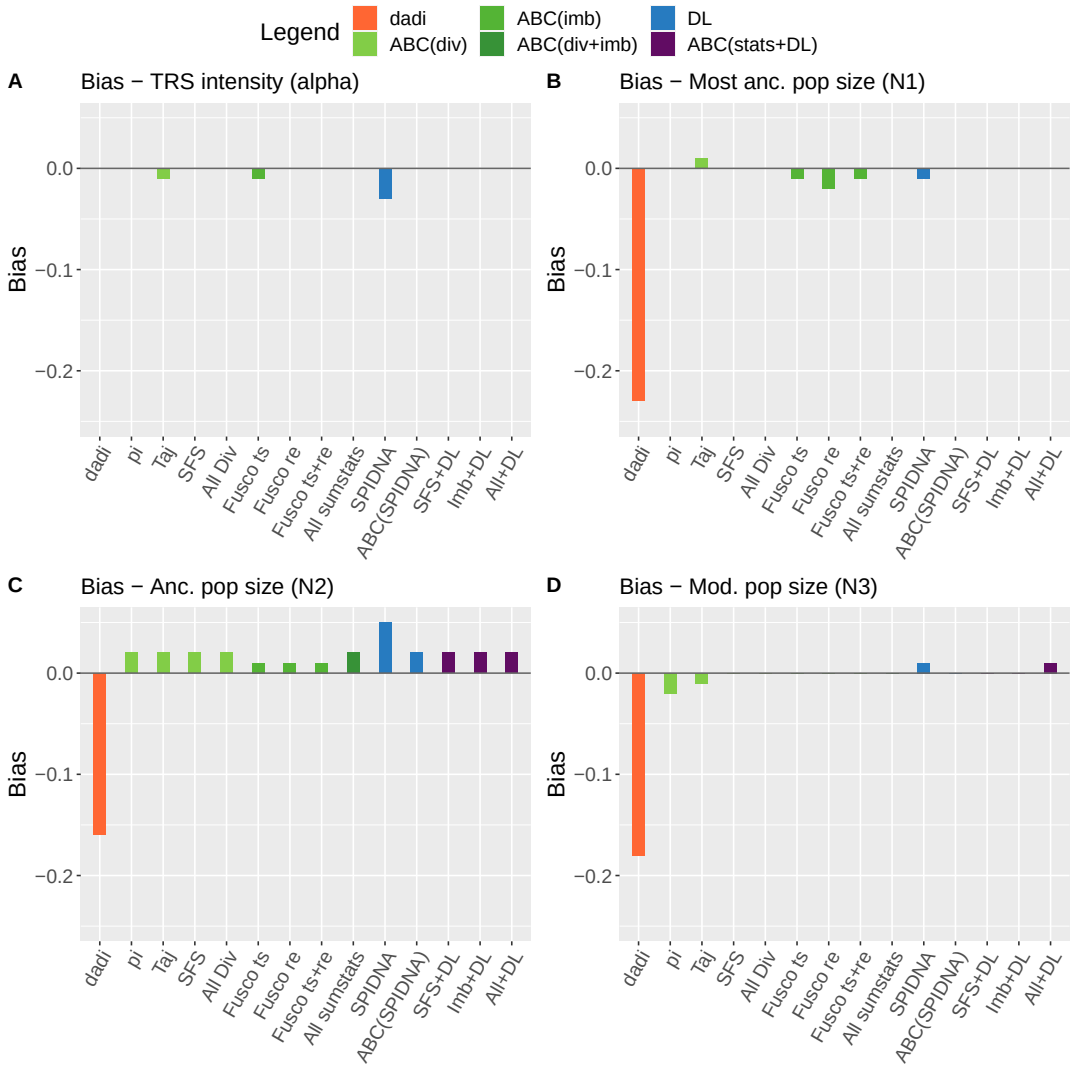


Figure S5: **Comparison of inference methods accuracy using bias computation.** Biases were computed between inferred and true values on the test set. The first four moments (mean, variance, skewness, kurtosis) of the 20 replicates were used for training and inference. The sample size was of 80 diploid individuals.
In orange: dadi inference. In light green: ABCrf using various diversity statistics. In green: ABCrf using various imbalance statistics. In dark green: ABCrf combining all diversity and imbalance indices. In blue: deep learning using SPIDNA. In purple: ABCrf combining summary statistics and SPIDNA results.

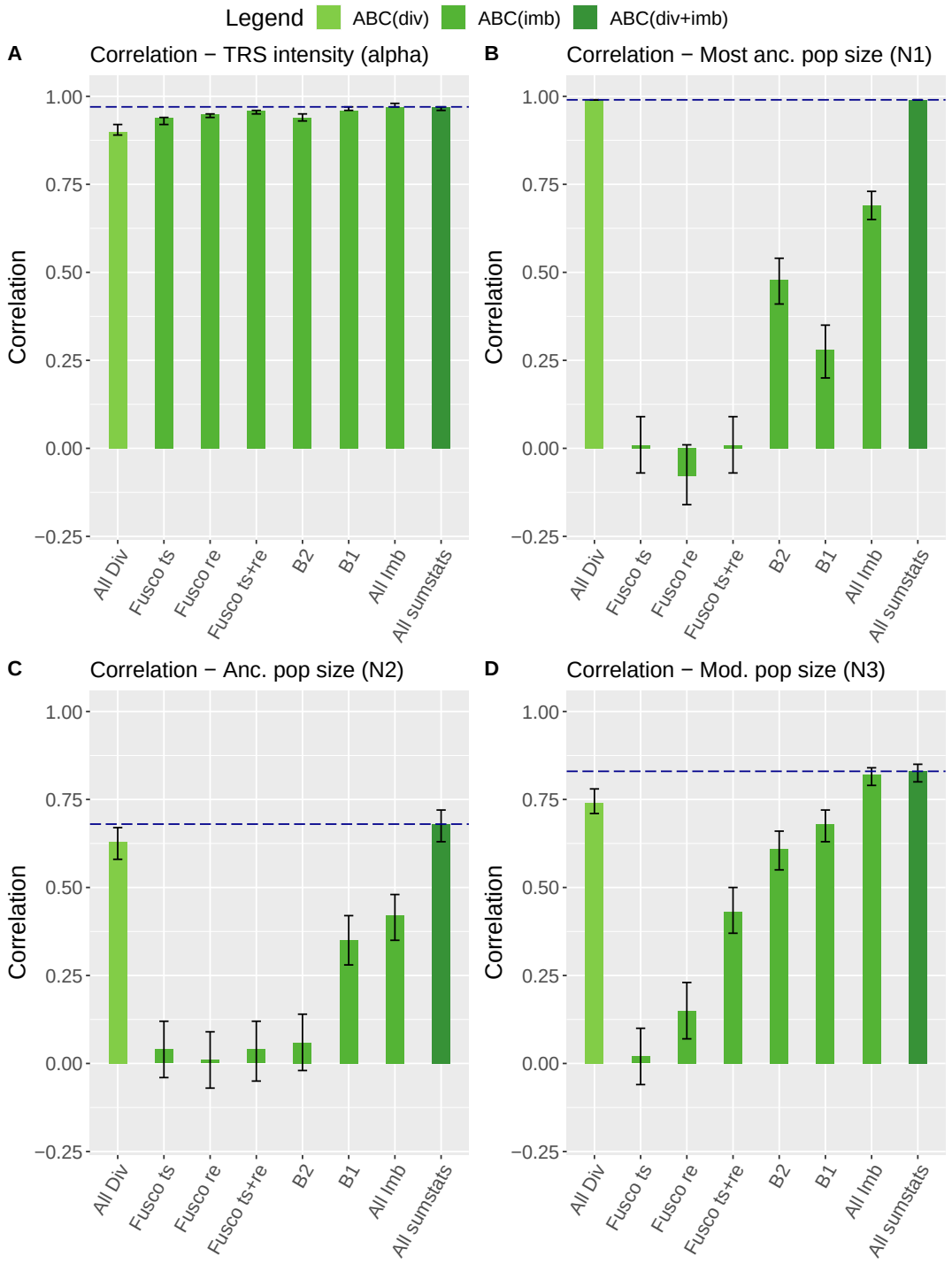


Figure S6: **Comparison of inference methods accuracy using correlations.**
Correlations were computed between inferred and true values on the test set. Only the first moment (mean) of the 20 replicates was used for training and inference. The sample size was of 80 diploid individuals. Error bars correspond to the 95% confidence interval of the correlations, computed with the *test.cor* R function in the *stats* package. The dashed line corresponds to the highest correlation reached for each parameter.
In light green: ABCrf using various diversity statistics. In green: ABCrf using various imbalance statistics. In dark green: ABCrf combining all diversity and imbalance indices.

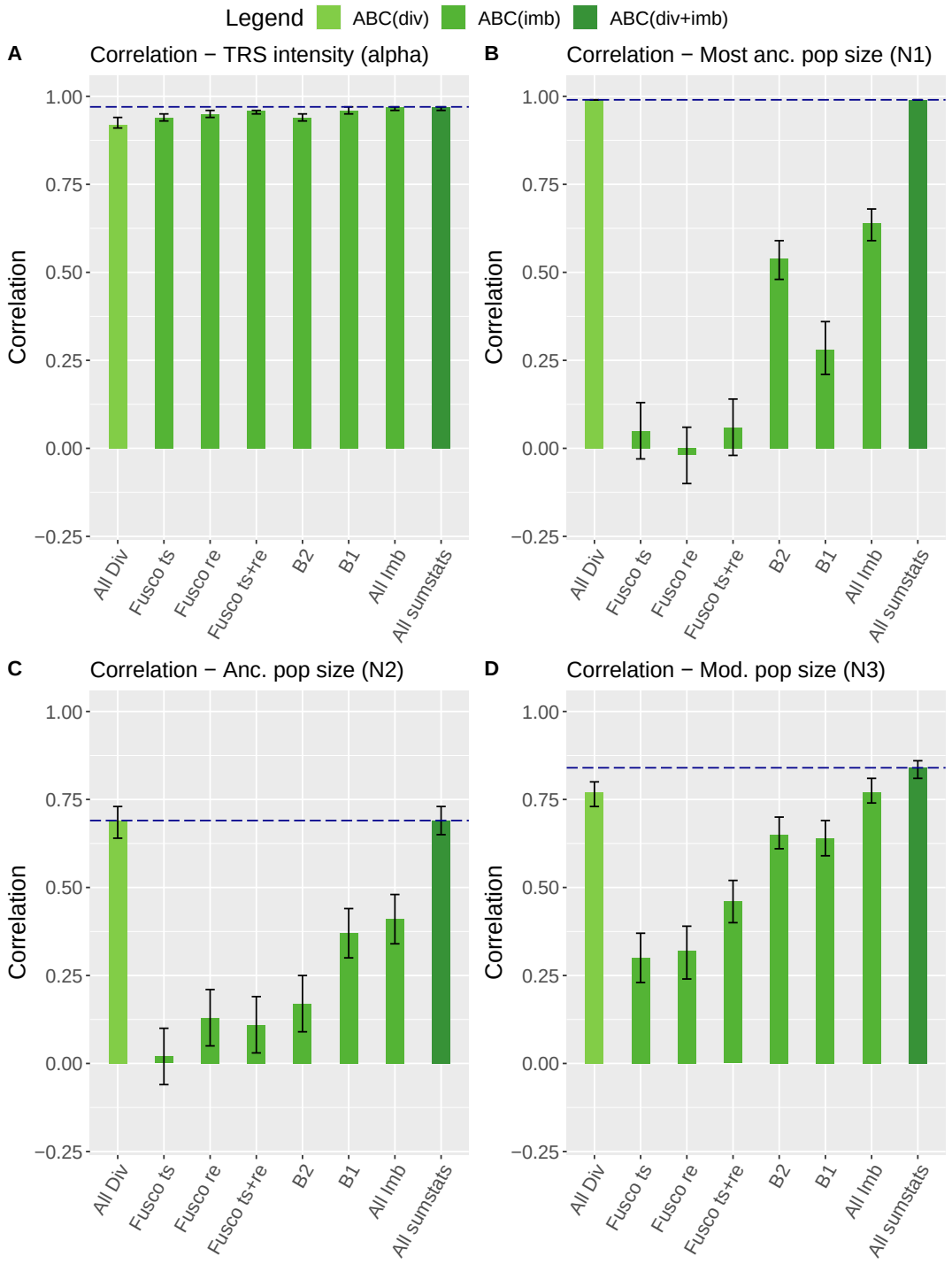


Figure S7: **Comparison of inference methods accuracy using correlations.**
Correlations were computed between inferred and true values on the test set. The first four moments (mean, variance, skewness, kurtosis) of the 20 replicates were used for training and inference. The sample size was of 80 diploid individuals. Error bars correspond to the 95% confidence interval of the correlations, computed with the *test.cor* R function in the *stats* package. The dashed line corresponds to the highest correlation reached for each parameter.
In light green: ABCrf using various diversity statistics. In green: ABCrf using various imbalance statistics. In dark green: ABCrf combining all diversity and imbalance indices.

# Chapter 4

# Nongenetic TRS and other processes

*Some of the preliminary analyses presented here are the result of a collaboration with Arnaud Quelin during his masters internship.*

## 4.1 Nongenetic TRS and natural selection

One of the major remaining issues in the study of nongenetic TRS is its comparison with natural selection (i.e., genetic TRS). At first glance, one might want to compare them and assume that this difference in the transmission mechanism is only anecdotal. However, in Chapters 1 and 2, we listed four potentially essential differences between these two processes, based on the literature. To demonstrate these differences, however, it would be appropriate to explore each of them through simulations, which we have done for two of these differences.

The first difference between genetic and nongenetic TRS concerns the fidelity of transmission. Genetic transmission being very faithful, only a limited amount of variance is introduced by mutation at each generation. Consequently, the favorable alleles will, in general, reach fixation rapidly. In contrast, in nongenetic TRS, and in particular cultural TRS, transmission is rather unfaithful. As a result, there will be no rapid fixation of the cultural trait that promotes a high reproductive rate, since the offspring can quickly move away from the parental trait (e.g., rebellion towards parental culture). This difference is described accurately in the models representing

these two processes. Indeed, the Sibert *et al.* (2002) model of nongenetic TRS, that we used in this thesis, is constructed in a way that removes the possibility of fixation: an individual's probability of reproduction is above average if his/her number of siblings is also above average. In contrast, in the classical selection model with alleles associated with different selection coefficients (Wright, 1932), the allele with the highest coefficient is likely to invade the population.

Therefore, the dynamics of summary statistics over time are expected to differ between the two models. In the selection model, the proportion of alleles evolves during the process; hence, the type of selection changes from selection of a rare allele to selection of a common allele. In the case of nongenetic TRS, the distribution of progeny sizes remains indefinitely unchanged once the equilibrium distribution is reached (i.e., after a few generations, see Chapter 2). Thus, we can expect coalescent tree shapes to differ: in selection, the tree is affected by a process that changes over time, while in nongenetic TRS, the tree is affected by a stable process (provided that nongenetic TRS occurs for a sufficiently long period of time).

We thus compared the dynamics of several summary statistics over time ($B_2$, $I_F$, number of polytomies, and $\pi$) by simulating these two models without recombination (Fig. 4.1). We observed an effect on all summary statistics under both models (nongenetic TRS alone versus selection alone), as well as under their combination (nongenetic TRS and selection simultaneously). These effects follow the same general trends: $B_2$ and $\pi$ decrease, while $I_F$ and number of polytomies increase. These results demonstrate that selection also impacts the topology indices ($I_F$ and $B_2$ imbalance indices and the number of polytomies), confirming previous studies that used imbalance-related indices for selection inference (Li, 2011; Li and Wiehe, 2013; Yang *et al.*, 2018).

Although both phenomena impact all summary statistics in the same direction, the dynamics are different. The effects last during all the time nongenetic TRS is occurring, because fixation is impossible in this case as said above, which maintains the process. Conversely, the effects are transient in case of selection, due to the fixation of the favorable allele, and all summary statistics return to neutral levels, but with different dynamics. $B_2$ and $I_F$ return to neutral levels around 20 generations after the most extreme value was reached. The number of polytomies has almost decreased to neutral levels after 250 generations since the peak. $\pi$ is slowly increasing back (the slope is weakly positive after the lowest point reached), but is still far from neutral levels after 300 generations.

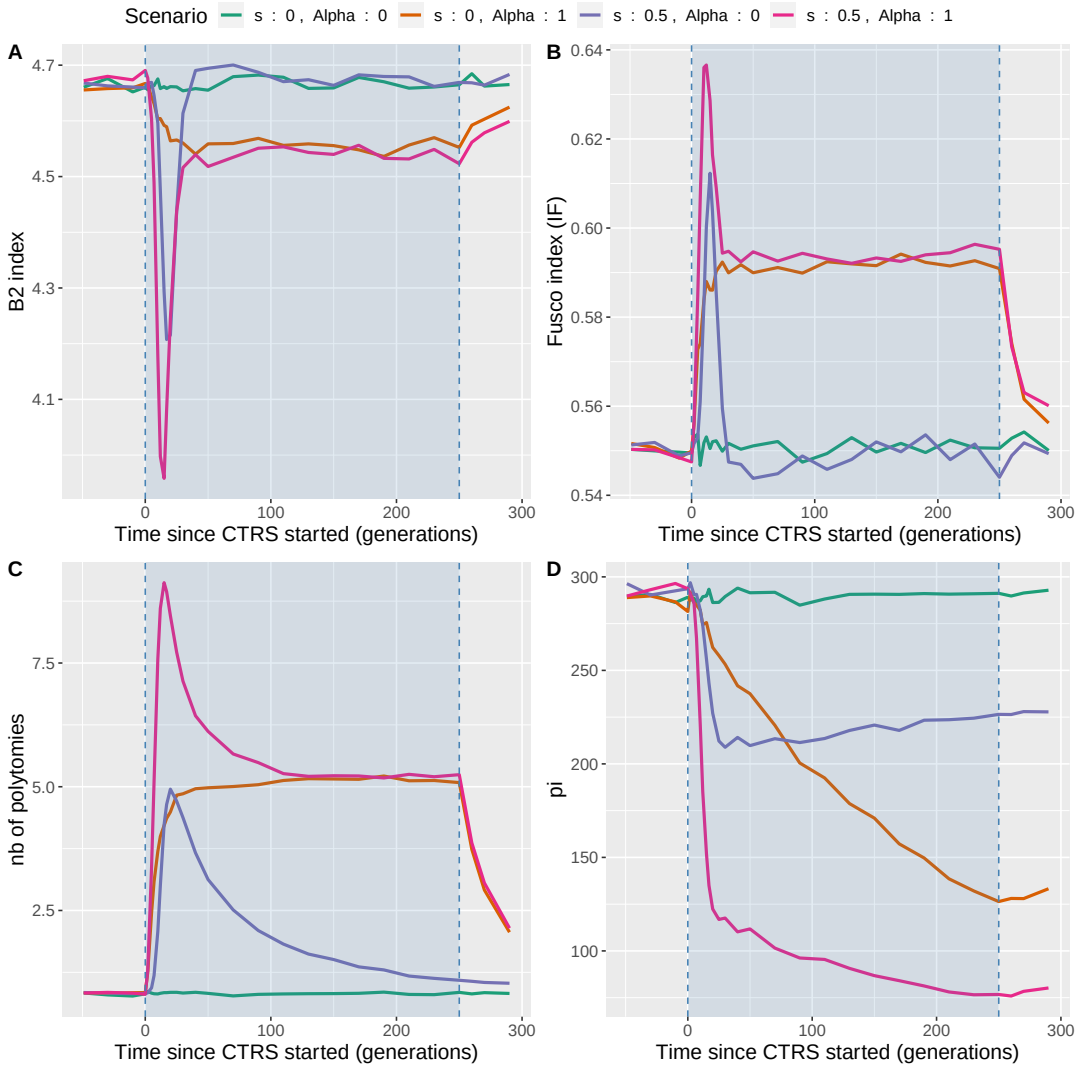


Figure 4.1: **Summary statistics across time in four scenarios without recombination.** Green: nongenetic TRS is absent ($\alpha = 0$) and selection is absent ($s = 0$). Orange: nongenetic TRS is present ($\alpha = 1$) and selection is absent ($s = 0$). Purple: nongenetic TRS is absent ($\alpha = 0$) and selection is present ($s = 0.5$). Magenta: nongenetic TRS is present ($\alpha = 1$) and selection is present ($s = 0.5$). Selection and nongenetic TRS start at generation 0. Nongenetic TRS stops at generation 250. $\pi$ is used for measuring diversity (panel D).

Those differences in dynamics between the summary statistics can be explained as follows. Imbalance indices are known to be mostly impacted by the recent events (Blum *et al.*, 2006), so they show a signal during and shortly after the selection process. Once fixation is reached, imbalance indices return rapidly to their original levels. $\pi$, on the other hand, is impacted by the tree imbalance, but also by its height (i.e., the TMRCA). This is why, although the tree is not imbalanced anymore, its TMRCA remains at a low value for a long time (i.e., due to the contraction of

effective size generated by selection). Finally, the number of polytomies increases under selection for two reasons: the contraction of effective size, and the imbalance of the tree which concentrates many coalescence events on one side of the tree, yielding polytomies. When trees are not imbalanced anymore the latter mechanism is eliminated, but the first still remains, as it is linked to the height of the tree (like $\pi$). This is the reason why the number of polytomies returns to its original levels faster than $\pi$, but slower than imbalance indices.

It is interesting to notice also that, besides the differences in dynamics between the two processes, they affect the imbalance indices differently in terms of values at the most extreme point. Indeed, the impact of the nongenetic TRS is relatively weak on $B_2$ (4% decrease compared to the neutral case) compared to $I_F$ (7% increase), while both indices change similarly under the selection model ($B_2$ : 11% decrease, $I_F$ : 11% increase). This result shows a qualitative difference in tree topology under the two models, which may stem from the evolution of the selection process across time (due to changes in the beneficial allele frequencies), whereas nongenetic TRS is a constant process because it does not allow fixation.

Nevertheless, this difference between the two processes on the propensity to reach fixation may not be so systematic. Here we have assumed, based on reality, that nongenetic TRS differs from genetic TRS in the level of fidelity of transmission. However, with a very high rate of genetic mutation, fixation will not happen, even in the case of genetic TRS, especially in cases of highly polygenic selection. On the other hand, in the case of a very faithful transmission of membership to given social group with different fertility levels, we would have a phenomenon of invasion of the most fertile group (i.e., if the population size is fixed). Therefore, this difference between the two processes is not fundamental but related to an extrinsic, although realistic, difference in the mutation rate.

The second difference between the two processes goes beyond the simple mutation rate. However, it only exists in the presence of recombination, unlike the previous difference. Indeed, recombination will break the link between the locus under selection and the rest of the genome. The effects will therefore be restricted to the region of the locus under selection. In the case of nongenetic TRS, the whole genome will be impacted in the same way, since it does not depend on any particular locus.

We therefore briefly explored different summary statistics along a chromosome in a case of selection on a single locus in the center of a chromosome, without

nongenetic TRS occurring (Fig. 4.2). For the four summary statistics explored ($\pi$, $B_2$, number of polytomies, and $I_b$), the strongest effects are restricted to the center of the chromosome, with a progressive decrease of the effects as one moves away from the locus under selection (the V-shaped pattern at generation 30). At generation 90, the number of polytomies and $\pi$ are evolving towards the values before selection, while preserving the V-shaped pattern. At this generation, the imbalance indices show a surprising pattern (W-shaped for $B_2$ in Fig. 4.2A, inverted W-shape for $I_b$ in Fig. 4.2B). This pattern reveals a faster return to the neutral situation for the regions farthest and closest to the locus under selection, and slower for the regions at medium distance. This probably stems from an increased reduction of local effective population size near the locus, causing imprints of past selection to be very quickly erased (i.e., the TMRCA is shorter or roughly equal to the time since the selection event). Taking into account this W-shaped pattern on the imbalance indices could therefore allow to better locate and date the selection events. However, further analysis is necessary to understand why this W-shape does not appear for the number of polytomies. This could stem from a difference its the dynamics compared to imbalance indices, corresponding to their slower decrease seen in Fig. 4.1C. According to this explanation, we can expect this W-shape to appear later on in the number of polytomies across the genome, which should easily be verified.

We also analyzed the summary statistics across a chromosome, in a simulated population simultaneously under selection (a locus at the center of the chromosome) and nongenetic TRS (Supp. Fig. S1). We find the V-shape at generation 30 for $B_2$, $\pi$, and the number of polytomies, as in Fig. 4.2. However, this shape does not appear for $I_b$, which has rather uniform values along the genome. This is probably because $B_2$ is less impacted than $I_b$ by nongenetic TRS, as seen above (Fig. 4.2), maintaining selection imprints in $B_2$ across the chromosome. Hence, $B_2$ appears to be better than $I_b$ in distinguishing loci under selection in a population under strong nongenetic TRS. At generation 90, we find the W-shape for $B_2$ and $I_b$, but less marked than for the population without nongenetic TRS (Fig. 4.2). In conclusion, under nongenetic TRS, the locus under selection remain detectable using the imbalance statistics across the genome, but are attenuated compared to the case without nongenetic TRS.

With the results from Fig. 4.2 and Supp. Fig. S1, we could confirm that imbalance indices are unequally impacted in a genome under monogenic selection, unlike nongenetic TRS which affects all loci identically. Hence, in the case of recombination, one should be able to distinguish between the two processes through

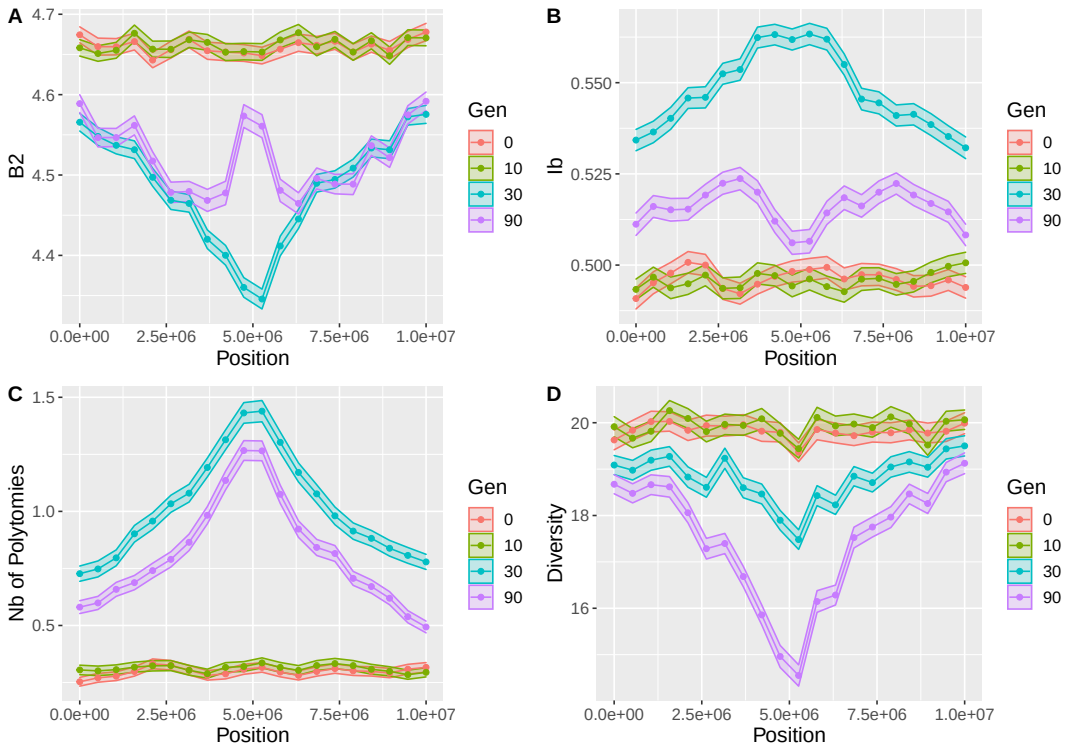


Figure 4.2: **Summary statistics across time along the genome with one locus under selection in the center.** Nongenetic TRS is absent ($\alpha = 0$), selection coefficient $s = 0.2$, population size $N = 1000$, and recombination rate $\rho = 10^{-8}$. Selection starts at generation 10. $\pi$ is used for measuring diversity (panel D).

imbalance statistics patterns along the genome. However, it would be necessary to explore the case of multigenic selection as well, which could be harder to disentangle from nongenetic TRS. Measuring various indices across the genome in real population genomic data would be another step towards understanding both processes impacts. We performed preliminary analyses (Fig. 4.3) on a small data set (chromosome 22 from Sardinians and Yakut, data from HGDP, Bergström *et al.*, 2020). They show that relate-inferred $I_b$ may vary a lot across the genome and that strong differences between the two studied populations appear. These results are compatible with the joint impact of various processes. Disentangling selection from nongenetic TRS effects in these real genomes patterns remains to be tackled.

## 4.2 Nongenetic TRS and structure

Population structure is another process that can be confused with nongenetic TRS. Indeed, it has been shown that it produces U-shaped SFS (Wakeley and Aliacar,

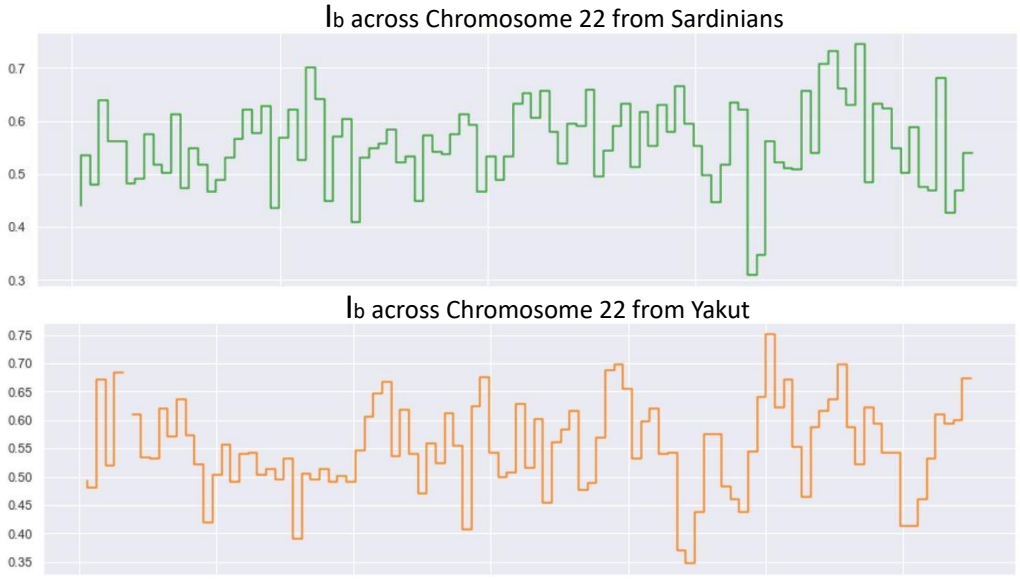


Figure 4.3: **Imbalance index $I_b$ computed on relate-inferred trees across whole chromosome 22 in Sardinians and Yakut.** Data from HGDP (Bergström *et al.*, 2020). Coalescent trees were inferred using relate (Speidel *et al.*, 2019) and $I_b$ index (Brandenburg *et al.*, 2012) was computed on all trees. Trees were grouped in one hundred bins of equal length (in base pairs), and $I_b$ weighted averages were computed for each bin. The weights corresponded to the number of base pairs each tree spans.

2001) as well as an imbalance of coalescence trees (Blum *et al.*, 2006), two valuable pieces of information to infer nongenetic TRS. A first approach to disentangle the impact of population structure from that of nongenetic TRS would be to perform a test on the absence of structure before inferring nongenetic TRS from the genomic data. However, the impacts of nongenetic TRS on structure tests have yet to be analyzed. Another approach would consist in including migration parameters in the model used for generating the simulated training dataset of the machine learning algorithms. More generally, it is necessary to explore in depth the behavior of the different imbalance indices under structured population models with migration, in order to distinguish them from the patterns created by nongenetic TRS or multigenic selection.

In addition to the impact of selection and structure on imbalance indices, their impacts on the reconstruction of coalescent trees by tsinfer and relate has not been explored and could further add biases to the imbalance indices estimations. We observed the tree imbalance in a multipopulation model with three populations exchanging migrants, under population size changes and nongenetic TRS. We used the demographic parameters (i.e., population sizes and migration rates across time)

that were previously inferred by Gravel *et al.* (2011) from real genomic data, with each population corresponding to a continent (Africa, Asia, and Europe). We found that the tsinfer-inferred trees have different $I_b$ levels depending on the continent, regardless of the strength of nongenetic TRS (Supp. Fig. S2). Since population size changes do not impact $I_b$ (Guez *et al.*, 2022), this could stem from the structure itself, which differs among the continents, or from the interaction between population structure and tsinfer tree reconstruction. The impacts of structure may also explain part of the differences observed in $I_b$ across the genome in Yakut versus Sardinians (Fig. 4.3). Beyond topology indices, the impacts of the interactions of population size changes, structure, selection, and nongenetic TRS on allelic frequencies and other classical summary statistics deserve further investigation.

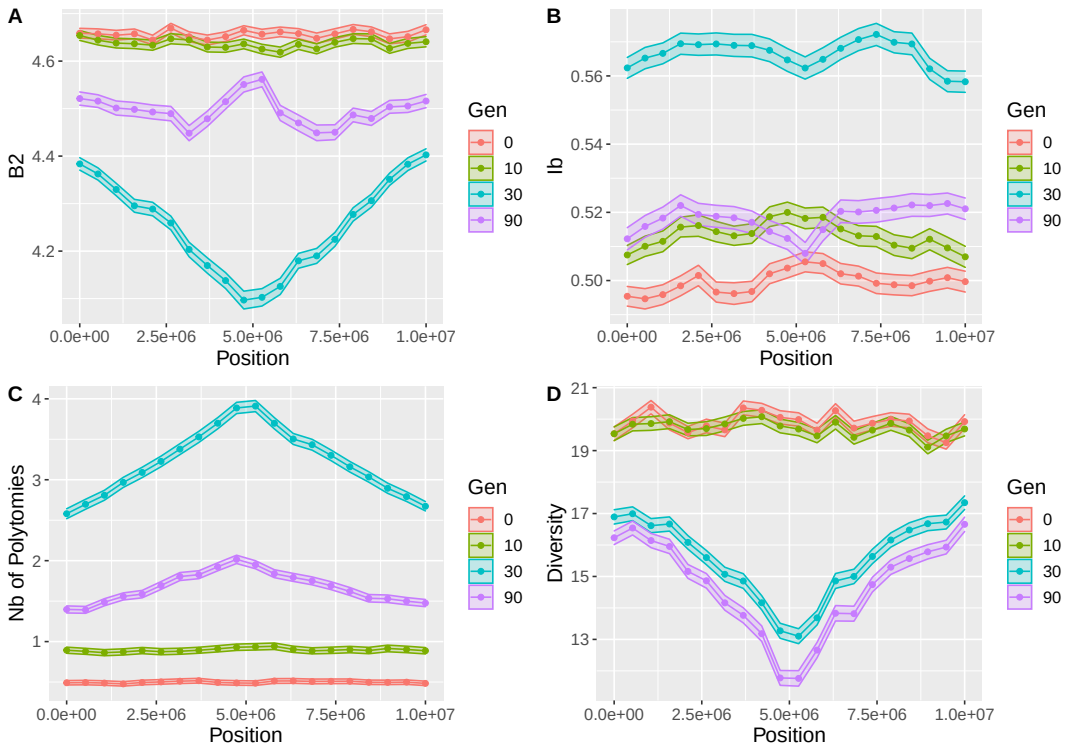


Figure S1: **Summary statistics across time along the genome with one locus under selection in the center.** Nongenetic TRS is present ($\alpha = 1$), selection coefficient $s = 0.2$, population size $N = 1000$, and recombination rate $\rho = 10^{-8}$. Selection starts at generation 10 and nongenetic TRS starts at generation 0. $\pi$ is used for measuring diversity (panel D).

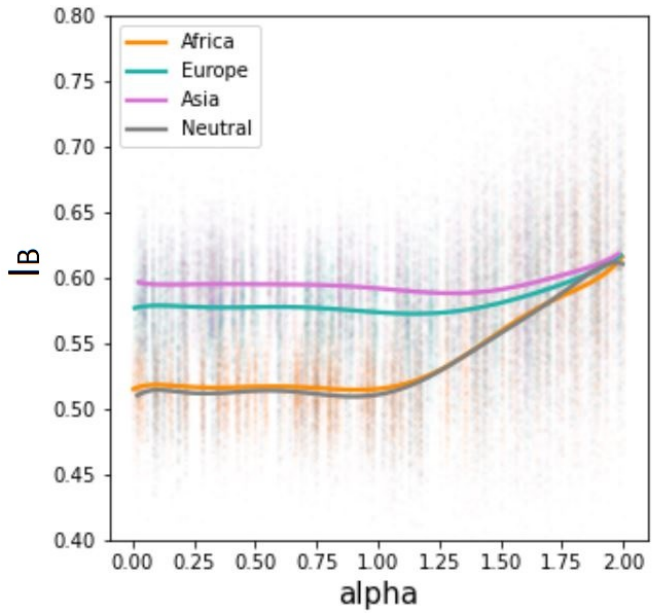


Figure S2: $I_b$ **measured on three demographic models with varying** $\alpha$**.** The models were designed according to Gravel *et al.* (2011) for each continent. The neutral model (in gray) does not contain any population size changes nor migration.

# Conclusion and perspectives

We have shown in this thesis that nongenetic TRS is a widespread phenomenon with diverse origins (Chapter 1), that it has an impact on population genetics and demographic inference (Chapter 2), that it can be inferred from genomic data using machine learning (Chapter 3), and that it can be disentangled from natural selection (Chapter 4). Here we will summarize these main findings. Then, we will discuss various perspectives.

## Main findings

In the first chapter, we showed from the literature that TRS is widespread in human populations. Its causal mechanisms can be complex and might integrate genetic and cultural components. Cultural TRS is also present in animals, especially in species with a strong social structure (Ilany *et al.*, 2021; Donabedian and Cords, 2021). This evidence in animals opens perspectives in ethology (Krützen *et al.*, 2005; Sapolsky, 2005; Hobaiter *et al.*, 2014), genetics (Whitehead *et al.*, 2017), and conservation biology (Kelly, 2001). Finally, we have generalized cultural TRS to any TRS of nongenetic origin, which makes it theoretically applicable to species outside the animal kingdom. Even at the cellular level, a nongenetic transmission of cell survival and mitosis rate could give rise to such a process (e.g., the transmission of the distance to a blood vessel from tumor cells to their daughters, a distance that impacts nutrient levels (Alfarouk *et al.*, 2013), and hence, can be correlated with cell survival and mitosis rate). This generalization of the nongenetic TRS process and its diverse impacts on the genome led us to discuss the addition of this evolutionary force to the general framework of evolutionary theory.

In the second chapter, we explored in detail the impacts of nongenetic TRS on genomic diversity over time. We showed that this process produces several stages

during evolution. These stages are due to three effects of nongenetic TRS: reduction of effective size, non-homogeneous reduction of branch lengths, and changes in the topology of coalescent trees (imbalance and higher number of polytomies). We also showed that nongenetic TRS produces a U-shaped SFS, as observed also for some cases of selection (Braverman *et al.*, 1995; Fay and Wu, 2000) and migration (Wakeley and Aliacar, 2001). Because of these effects, nongenetic TRS induces a bias in demographic inference from genomic data, which we showed using the inference software dadi (Gutenkunst *et al.*, 2009). This study of CTRS reveal the importance of studying this process for its own effects, as well as for disentangling it from other evolutionary processes.

In the third chapter, we studied the possibility of inferring nongenetic TRS from genomic data. We showed that machine learning models could be trained to jointly infer the intensity of nongenetic TRS as well as the demographic history of the population. This joint inference avoids obtaining a biased demographic inference, as it is the case for inference tools not considering nongenetic TRS, such as dadi (Gutenkunst *et al.*, 2009). We have also compared several machine learning methods: ABC random forest using summary statistics (*abcrf* R package from Raynal *et al.*, 2019), neural networks trained directly on raw genomic data (using SPIDNA from Sanchez *et al.*, 2021), or a combination of both. Combining the two methods being the most efficient, we concluded that some summary statistics not present in our ABC approach contain helpful information to co-infer the two processes.

In the fourth chapter, we compared the effects of two processes (natural selection and migration) to those of nongenetic TRS. We described simulation results exploring the two main differences between selection and nongenetic TRS. The first difference lies in the possibility of fixation in the case of natural selection, which is not possible for the nongenetic TRS model that we studied in this thesis (from Sibert *et al.*, 2002). This yields disparities in the dynamics of the summary statistics across time, as well as in the most extreme values reached by the imbalance indices. The second difference stems from the fact that natural selection effects are linked to the locus under selection, contrary to nongenetic TRS effects. We thus explored summary statistics along the genome under selection, showing V-shaped and W-shaped patterns that confirmed this specificity of natural selection. We also explored the impacts of migrations on the detection of nongenetic TRS, using a multipopulation model (from Gravel *et al.*, 2011). We showed that in Europe and Asia the detection of nongenetic TRS using imbalance indices might indeed be challenging due population structure, and we discussed potential solutions.

# Perspectives

One of the contributions of this thesis was to apprehend the importance of nongenetic TRS through two main aspects. First, through a bibliographical review, we showed its commonness and the diversity of its occurrence modes in humans and other species (Chapter 1). Second, we demonstrated the magnitude and variety of its impacts on genetics (Chapter 2). Combining these two aspects led us to consider nongenetic TRS as a full-fledged evolutionary force. However, research in different areas is still needed to develop this generalization. Mainly, we will focus here on (i) nongenetic TRS modeling developments, and (ii) applications to real data.

## i. Modeling nongenetic TRS

Our results of the impacts of nongenetic TRS on genetics (Chapter 2) are all based on an extension of the Wright-Fisher model (Sibert *et al.*, 2002). This can be considered a serious limitation. Indeed, some impacts on genetics may depend on the use of this particular model, and may need to be more generalized. This problem related to population genetics modeling also concerns other processes such as drift or selection. Nevertheless, it specifically affects nongenetic TRS due to the absence of a competing model. Indeed, for modeling neutral evolution with random genetic drift, for example, one can compare the Wright-Fisher model (Wright, 1931) with the Moran model (Moran, 1958) to evaluate the impact of model assumptions (as well as their generalization in the Cannings model, Cannings 1974, 1975). In natural selection, a large number of models can also be compared (for example selection in gene-networks models, such as in Wagner 1994, 1996; Siegal and Bergman 2002, selection on polygenic traits, such as in Lande 1980; Latta 1998; Le Corre and Kremer 2003, and selection with epistasis such as in Hansen and Wagner 2001; Jiang and Reif 2015). Therefore, developing new models would be a step forward in understanding nongenetic TRS.

For example, in the model we used in Chapter 2, an individual's probability of reproducing is directly proportional to his/her number of siblings (Sibert *et al.*, 2002). This model is supposed to fit any case of nongenetic TRS. However, one might want to model some subtypes of nongenetic TRS more realistically, such as TRS mediated by the vertical transmission of a resource correlated with reproductive success. This model would assign a resource value $\xi$ to each individual, which is correlated to the resource value of his/her parents. The probability of reproduction $p_i$ of an

individual $i$, would then be proportional to his/her resource quantity, according to: $p_i = \frac{\xi_i^\tau}{\sum_{j=1}^{N} \xi_j^\tau}$. This model would have two parameters to control the TRS, contrary to Sibert *et al.*'s model which only uses $\alpha$. The first parameter, $\tau$, would control the impact of resources on fertility (similar to $\alpha$ controlling the impact of sibship size on fertility in Sibert *et al.*'s model). The second parameter, an error parameter $\beta$, would control the transmission of resources from parents to children, which can be more or less faithful (i.e., resembling a mutation rate: high $\beta$ yielding lower correlations between parents and children resources). It remains to be studied to what extent this new model would bring different results compared to Sibert *et al.*'s model. One difference would be related to fixation, as this model would allow it contrary to Sibert *et al.*'s model, provided that $\beta$ is low. However, unlike a selection model, the effects would span the entire genome and not be linked to any locus in particular. Furthermore, in a variation of this new model, the parental resource value $\xi$ could be shared among siblings instead of being transmitted entirely, in order to model material resources transmission.

Another important point regarding the modeling of nongenetic TRS concerns its possible unification with a genetic TRS model. A model that allows to treat all types of TRS jointly would be more parsimonious and has already been investigated. One avenue that has been particularly explored to unify the different forms of TRS is the Price equation (Price, 1970). This equation defines the change in a trait average from one generation to the next in a population, as a function of the covariance of that trait with fitness and the fitness-weighted fidelity of transmission. Several studies have used this equation as a basis for nongenetic inheritance (Gardner, 2020; Baravalle and Luque, 2021), or to unify genetic and nongenetic inheritance (Otto *et al.*, 1995; Bonduriansky and Day, 2009; Day and Bonduriansky, 2011; Aguilar and Akçay, 2018). However, this has not yet been applied to the nongenetic transmission of reproductive success, which would be an exciting topic of research.

## ii. Using real data

Beyond these theoretical modeling issues, studying real data is an important pathway for understanding and generalizing nongenetic TRS. We have seen in Chapter 1 that many human and animal populations show the presence of nongenetic TRS, for example based on estimations of parent-child correlations in progeny size. When genealogical and genomic data are concurrently available, it becomes possible to distinguish the different evolutionary processes more efficiently. For example, by

knowing the intensity of nongenetic TRS in a population thanks to demographic data, it is possible to explore the genome in its different types of regions (coding and non-coding regions, neutral or under selection regions), in order to understand the effects of nongenetic TRS and its interactions with selection. This is feasible with data from Quebec where cultural TRS has occurred over 12 generations (Austerlitz and Heyer, 1998), and from where a large amount of genomic and genealogical data are publicly available (Anderson-Trocmé *et al.*, 2022).

It should be possible to have, as for Quebec, anonymized demographic data for other regions of the world. For example, in France, the law requires to declare births since 1803. Social security systems, for example, oblige citizens to declare the birth of their children in many countries, and statistical institutes already gather and use family-related data (such as in Beaujouan and Solaz, 2019). These demographic data would allow for a more precise analysis of progeny size correlations with a finer geographic granularity, as well as an estimation of the evolution of correlations over time. However, these data are only available for some countries where birth registrations are systematic. In some countries, such as China or Indonesia, despite laws requiring this practice, the rate of birth registrations is low and can vary greatly from one region to another (Li *et al.*, 2010; Prasetyo and Hamudy, 2016; Duff *et al.*, 2016).

In wild animal populations, pedigree data would also provide a better understanding of nongenetic TRS. Pedigree data are relatively easier to obtain for some species, such as small birds or large mammals, compared to other groups (Pemberton, 2008). However, next-generation sequencing techniques make constructing or correcting these databases easier, and will help expand their use to other species (Petty *et al.*, 2021). Using pedigree and genetic data jointly in wild populations will allow dissecting the evolutionary processes involved. For example, using genetic and pedigree data, Chen *et al.* (2019) could reveal the different evolutionary processes occurring in a Florida Scrub-Jays population. Regarding TRS in particular, analysis of pedigree data is of great value. For example, Kelly (2001) analyzed 63 cheetah matrilines, and demonstrated that five of these matrilines yielded 45% of the cheetah population, leading to an effective population size of 15% of the census population. In another example, Thompson *et al.* (2017) revealed increased aggression between related individuals in a wild mongoose population based on pedigree data. This harmful discrimination against kin could lead to negative correlations in progeny size between parents and offspring. Indeed, offspring with many siblings would then receive more aggression, which could reduce their reproductive success (similar to

the negative correlations due to sharing maternal resources among offspring, see Chapter 1). Hence, pedigree data need to be collected from many different species to better understand the links between genetics, evolution, and social behavior.

Regarding the generalization of nongenetic TRS to unicellulars, it is possible to leverage experimental evolution (Kawecki *et al.*, 2012; Barrick and Lenski, 2013). Experimental evolution has already led to a better understanding of many evolutionary processes, such as selection, mutation rate, and their interactions (Raynes and Sniegowski, 2014; Tenaillon *et al.*, 2016). Thus, implementing nongenetic TRS experiments may lead to a better understanding of the process. For example, it is possible to reproduce nongenetic TRS by letting yeast grow on a nutrient gradient, yielding a reproduction differential in the population. Particular attention should be paid to the methodology of the experiment. For example, in order to reproduce the nongenetic TRS correctly, the transmission of the advantage from parents to children must be unfaithful, so that it is maintained over time without reaching fixation (see Chapters 2 and 4). In this case, fixation of the favorable trait would result in yeast development only in the nutritive part of the medium. It is therefore necessary to create an imperfect transmission of the position, for example with a semi-liquid medium that allows a movement of the cells. To follow the genealogy of the cells, it would be possible to use barcoding methods specifically developed for yeast (Nguyen Ba *et al.*, 2022). It will then be possible to have access to real coalescent trees on which the different summary statistics studied in this thesis can be computed (Chapter 2). The real trees can also be compared to the inferred trees to identify the possible biases in tree reconstruction. Finally, this type of experiments would be an effective field for testing the inference tools we have developed in Chapter 3.

In summary, research avenues encompass both theoretical and practical aspects. On one hand, mathematical models of TRS can be developed to reinforce and expand the findings of Chapter 2. On the other hand, these models can be applied to real data to advance the inference methods outlined in Chapter 3.

# Bibliography


Adeyemo AA, Shriner D, Bentley AR, Gbadegesin RA, Rotimi CN. 2021. Evolutionary genetics and acclimatization in nephrology. Nature Reviews Nephrology. 17:827–839. Number: 12 Publisher: Nature Publishing Group.

Agapow PM, Purvis A. 2002. Power of eight tree shape statistics to detect nonrandom diversification: a comparison by simulation of two models of cladogenesis. Systematic Biology. 51:866–872.

Aguilar EG, Akçay E. 2018. Gene-Culture Coinheritance of a Behavioral Trait. The American Naturalist. 192:311–320.

Aleman FDD, Valenzano DR. 2019. Microbiome evolution during host aging. PLoS Pathogens. 15:e1007727.

Alfarouk KO, Ibrahim ME, Gatenby RA, Brown JS. 2013. Riparian ecosystems in human cancers. Evolutionary Applications. 6:46–53.

Altizer S, Dobson A, Hosseini P, Hudson P, Pascual M, Rohani P. 2006. Seasonality and the dynamics of infectious diseases. Ecology Letters. 9:467–484.

Anderson-Trocmé L, Nelson D, Zabad S, Diaz-Papkovich A, Baya N, Touvier M, Jeffery B, Dina C, Vézina H, Kelleher J *et al*. 2022. On the Genes, Genealogies, and Geographies of Quebec.

Anderton DL, Tsuya NO, Bean LL, Mineau GP. 1987. Intergenerational Transmission of Relative Fertility and Life Course Patterns. Demography. 24:467–480.

Aplin LM, Farine DR, Morand-Ferron J, Cockburn A, Thornton A, Sheldon BC. 2015. Experimentally induced innovations lead to persistent culture via conformity in wild birds. Nature. 518:538–541.

Austerlitz F, Heyer E. 1998. Social transmission of reproductive behavior increases frequency of inherited disorders in a young-expanding population. Proceedings of the National Academy of Sciences. 95:15140–15144.

Austerlitz F, Heyer E. 2000. Allelic association is increased by correlation of effective family size. European journal of human genetics: EJHG. 8:980–985.

Austerlitz F, Kalaydjieva L, Heyer E. 2003. Detecting population growth, selection and inherited fertility from haplotypic data in humans. Genetics. 165:1579–1586.

Avital E, Jablonka E. 2000. *Animal Traditions: Behavioural Inheritance in Evolution*. Cambridge University Press.

Axinn WG, Clarkberg ME, Thornton A. 1994. Family Influences on Family Size Preferences. Demography. 31:65–79.

Bailes EJ, Bagi J, Coltman J, Fountain MT, Wilfert L, Brown MJF. 2020. Host density drives viral, but not trypanosome, transmission in a key pollinator. Proceedings of the Royal Society B: Biological Sciences. 287:20191969.

Bank C, Ewing GB, Ferrer-Admettla A, Foll M, Jensen JD. 2014. Thinking too positive? Revisiting current methods of population genetic selection inference. Trends in Genetics. 30:540–546.

Baravalle L, Luque VJ. 2021. Towards a Pricean foundation for cultural evolutionary theory. THEORIA. An International Journal for Theory, History and Foundations of Science. Accepted: 2021-08-30T15:19:30Z.

Barban N, Jansen R, de Vlaming R, Vaez A, Mandemakers JJ, Tropf FC, Shen X, Wilson JF, Chasman DI, Nolte IM *et al*. 2016. Genome-wide analysis identifies 12 loci influencing human reproductive behavior. Nature Genetics. 48:1462–1472.

Barber JS. 2001. The Intergenerational Transmission of Age at First Birth among Married and Unmarried Men and Women. Social Science Research. 30:219–247.

Barghi N, Hermisson J, Schlötterer C. 2020. Polygenic adaptation: a unifying framework to understand positive selection. Nature Reviews Genetics. 21:769–781.

Barker JSF, Thomas RH. 1987. A Quantitative Genetic Perspective on Adaptive Evolution. In: Loeschcke V, editor, *Genetic Constraints on Adaptive Evolution*. pp. 3–23. Berlin, Heidelberg. Springer.

Barrick JE, Lenski RE. 2013. Genome dynamics during experimental evolution. Nature Reviews Genetics. 14:827–839. Number: 12 Publisher: Nature Publishing Group.

Barton NH. 1995. Linkage and the limits to natural selection. Genetics. 140:821–841.

Baudin T. 2015. Religion and fertility: The French connection. Demographic Research. 32:397–420.

Bauer G, Kneip T. 2013. Fertility From a Couple Perspective: A Test of Competing Decision Rules on Proceptive Behaviour. European Sociological Review. 29:535–548.

Baumdicker F, Bisschop G, Goldstein D, Gower G, Ragsdale AP, Tsambos G, Zhu S, Eldon B, Ellerman EC, Galloway JG *et al*. 2021. Efficient ancestry and mutation simulation with msprime 1.0. Genetics. 220:iyab229.

Beaujouan E. 2010. How is fertility affected by separation and repartnering?. .

Beaujouan E, Solaz A. 2019. Is the Family Size of Parents and Children Still Related? Revisiting the Cross-Generational Relationship Over the Last Century. Demography. 56:595–619.

Beaumont MA, Zhang W, Balding DJ. 2002. Approximate Bayesian Computation in Population Genetics. Genetics. 162:2025–2035.

Beichman AC, Huerta-Sanchez E, Lohmueller KE. 2018. Using Genomic Data to Infer Historic Population Dynamics of Nonmodel Organisms. Annual Review of Ecology, Evolution, and Systematics. 49:433–456.

Beisson J. 2008. Preformed cell structure and cell heredity. Prion. 2:1–8.

Beisson J, Sonneborn TM. 1965. CYTOPLASMIC INHERITANCE OF THE ORGANIZATION OF THE CELL CORTEX IN PARAMECIUM AURELIA*. Proceedings of the National Academy of Sciences of the United States of America. 53:275–282.

Ben-Porath Y. 1975. First-generation effects on second-generation fertility. Demography. 12:397–405.

Bengtson VL. 1975. Generation and family effects in value socialization. American Sociological Review. 40:358–371.

Berent J. 1953. Relationship between family sizes of two successive generations. The Milbank Memorial Fund Quarterly. 31:39–50.

Bergström A, McCarthy SA, Hui R, Almarri MA, Ayub Q, Danecek P, Chen Y, Felkel S, Hallast P, Kamm J *et al*. 2020. Insights into human genetic variation and population history from 929 diverse genomes. Science. 367:eaay5012.

Bernardi L. 2003. Channels of Social Influence on Reproduction. Population Research and Policy Review. 22:527–555.

Bernardi L. 2013. From mothers to daughters: Intergenerational transmission of fertility norms, In: Ellingsaeter AL, Jensen AM, Lie M, editors, *The social meaning of children and fertility change in Europe*, Routledge. New York. pp. 153–169.

Bernardi L. 2016. The Intergenerational Transmission of Fertility, In: , John Wiley & Sons, Ltd. pp. 1–16. _eprint: https://onlinelibrary.wiley.com/doi/pdf/10.1002/9781118900772.etrds0413.

Bernardi L, Klärner A. 2014. Social networks and fertility. Demographic Research. S16:641–670.

Bernstein IS. 1969. Stability of the status hierarchy in a pigtail monkey group (Macaca nemestrina). Animal Behaviour. 17:452–458.

Bersaglieri T, Sabeti PC, Patterson N, Vanderploeg T, Schaffner SF, Drake JA, Rhodes M, Reich DE, Hirschhorn JN. 2004. Genetic Signatures of Strong Recent Positive Selection at the Lactase Gene. The American Journal of Human Genetics. 74:1111–1120.

Bienvenu F, Lambert A, Steel M. 2021. Combinatorial and stochastic properties of ranked tree-child networks. arXiv:2007.09701 [math, q-bio]. .

Blum MGB, François O. 2010. Non-linear regression models for Approximate Bayesian Computation. Statistics and Computing. 20:63–73.

Blum MGB, Heyer E, François O, Austerlitz F. 2006. Matrilineal Fertility Inheritance Detected in Hunter–Gatherer Populations Using the Imbalance of Gene Genealogies. PLoS Genetics. 2:e122.

Bocquet-Appel JP, Jakobi L. 1993. A test of a path model of biocultural transmission of fertility. Annals of Human Biology. 20:335–347.

Boehnke K, Hadjar A, Baier D. 2007. Parent-Child Value Similarity: The Role of Zeitgeist. Journal of Marriage and Family. 69:778–792.

Boitard S, Rodríguez W, Jay F, Mona S, Austerlitz F. 2016. Inferring Population Size History from Large Samples of Genome-Wide Molecular Data - An Approximate Bayesian Computation Approach. PLOS Genetics. 12:1–36.

Bollen KA, Glanville JL, Stecklov G. 2001. Socioeconomic Status and Class in Studies of Fertility and Health in Developing Countries. Annual Review of Sociology. 27:153–185.

Bonduriansky R, Day T. 2009. Nongenetic Inheritance and Its Evolutionary Implications. Annual Review of Ecology, Evolution, and Systematics. 40:103–125. _eprint: https://doi.org/10.1146/annurev.ecolsys.39.110707.173441.

Bonduriansky R, Day T. 2018. *Extended Heredity: A New Understanding of Inheritance and Evolution*. Princeton University Press.

Bongaarts J. 2001. Fertility and Reproductive Preferences in Post-Transitional Societies. Population and Development Review. 27:260–281.

Booker TR, Jackson BC, Keightley PD. 2017. Detecting positive selection in the genome. BMC Biology. 15:98.

Booth AL, Kee HJ. 2009. Birth Order Matters: The Effect of Family Size and Birth Order on Educational Attainment. Journal of Population Economics. 22:367–397.

Borgerhoff Mulder M. 1989. Menarche, menopause and reproduction in the Kipsigis of Kenya. Journal of Biosocial Science. 21:179–192.

Borgerhoff Mulder M, Bowles S, Hertz T, Bell A, Beise J, Clark G, Fazzio I, Gurven M, Hill K, Hooper PL *et al*. 2009. Intergenerational Wealth Transmission and the Dynamics of Inequality in Small-Scale Societies. Science. 326:682–688.

Brandenburg JT, Austerlitz F, Toupance B. 2012. Impact of fertility transmission and other sociodemographic factors on reproductive success and coalescent trees. Genetics Research. 94:121–131.

Bras H, Van Bavel J, Mandemakers K. 2013. Unraveling the intergenerational transmission of fertility: genetic and shared-environment effects during the demographic transition in the Netherlands, 1810–1910. The History of the Family. 18:116–134.

Brask JB, Ellis S, Croft DP. 2021. Animal social networks: an introduction for complex systems scientists. Journal of Complex Networks. 9:cnab001.

Braverman JM, Hudson RR, Kaplan NL, Langley CH, Stephan W. 1995. The hitchhiking effect on the site frequency spectrum of DNA polymorphisms. Genetics. 140:783–796.

Breen R. 2010. Educational Expansion and Social Mobility in the 20th Century. Social Forces. 89:365–388.

Breiman L. 2001. Random Forests. Machine Learning. 45:5–32.

Bresard M. 1950. Mobilité sociale et dimension de la famille. Population. 5:533–566.

Breton D, Prioux F. 2009. The one-child family: France in the European context. Demographic Research. 20:657–692.

Breton D, Prioux F, Dutreuilh C. 2005. Two Children or Three?: Influence of Family Policy and Sociodemographic Factors. Population (English Edition, 2002-). 60:415–445.

Brown GR, Silk JB. 2002. Reconsidering the null hypothesis: Is maternal rank associated with birth sex ratios in primate groups? Proceedings of the National Academy of Sciences. 99:11252–11255.

Buhr P, Lutz K, Peter T. 2018. The influence of the number of siblings on expected family size in a cohort of young adults in Germany. Demographic Research. 39:315–336.

Cameron EZ, Setsaas TH, Linklater WL. 2009. Social bonds between unrelated females increase reproductive success in feral horses. PNAS Proceedings of the National Academy of Sciences of the United States of America. 106:13850–13853.

Cannings C. 1974. The Latent Roots of Certain Markov Chains Arising in Genetics: A New Approach, I. Haploid Models. Advances in Applied Probability. 6:260–290. Publisher: Applied Probability Trust.

Cannings C. 1975. The Latent Roots of Certain Markov Chains Arising in Genetics: A New Approach, II. Further Haploid Models. Advances in Applied Probability. 7:264–282. Publisher: Applied Probability Trust.

Cavalli-Sforza LL, Feldman MW. 1981. *Cultural Transmission and Evolution: A Quantitative Approach*. Princeton University Press.

Cavalli-Sforza LLLL, Bodmer WFWF. 1976. *Genetics, Evolution and Man*. Freeman & Company.

Cazes MH. 2009. Mesure de la reproduction et du renouvellement des populations : quelques paramètres importants pour le généticien, In: . Dijon, France.. pp. 49–57.

Chaix R, Austerlitz F, Khegay T, Jacquesson S, Hammer MF, Heyer E, Quintana-Murci L. 2004. The Genetic or Mythical Ancestry of Descent Groups: Lessons from the Y Chromosome. American Journal of Human Genetics. 75:1113–1116.

Chan J, Perrone V, Spence JP, Jenkins PA, Mathieson S, Song YS. 2018. A Likelihood-Free Inference Framework for Population Genetic Data using Exchangeable Neural Networks. Advances in Neural Information Processing Systems. 31:8594–8605.

Charlesworth D, Barton NH, Charlesworth B. 2017. The sources of adaptive variation. Proceedings. Biological Sciences. 284:20162864.

Chen H, Slatkin M. 2013. Inferring selection intensity and allele age from multilocus haplotype structure. G3 (Bethesda, Md.). 3:1429–1442.

Chen N, Juric I, Cosgrove EJ, Bowman R, Fitzpatrick JW, Schoech SJ, Clark AG, Coop G. 2019. Allele frequency dynamics in a pedigreed natural population. Proceedings of the National Academy of Sciences. 116:2158–2164. Publisher: Proceedings of the National Academy of Sciences.

Cheney DL. 1977. The Acquisition of Rank and the Development of Reciprocal Alliances among Free-Ranging Immature Baboons. Behavioral Ecology and Sociobiology. 2:303–318.

Cleland J, Rodriguez G. 1988. The Effect of Parental Education on Marital Fertility in Developing Countries. Population Studies. 42:419–442.

Clutton-Brock T. 2002. Breeding together: kin selection and mutualism in cooperative vertebrates. Science (New York, N.Y.). 296:69–72.

Colless DH. 1982. Review of Phylogenetics: The Theory and Practice of Phylogenetic Systematics. Systematic Zoology. 31:100–104.

Collins J, Page L. 2019. The heritability of fertility makes world population stabilization unlikely in the foreseeable future. Evolution and Human Behavior. 40:105–111.

Conley D. 2005. *The Pecking Order: A Bold New Look at how Family and Society Determine who We Become*. Vintage Books.

Cools S, Kaldager Hart R. 2017. The Effect of Childhood Family Size on Fertility in Adulthood: New Evidence From IV Estimation. Demography. 54:23–44.

Creanza N, Kolodny O, Feldman MW. 2017. Cultural evolutionary theory: How culture evolves and why it matters. Proceedings of the National Academy of Sciences. 114:7782–7789.

Csilléry K, Blum MGB, Gaggiotti OE, François O. 2010. Approximate Bayesian Computation (ABC) in practice. Trends in Ecology & Evolution. 25:410–418.

Csilléry K, François O, Blum MGB. 2012. abc: an R package for approximate Bayesian computation (ABC). Methods in Ecology and Evolution. 3:475–479. _eprint: https://onlinelibrary.wiley.com/doi/pdf/10.1111/j.2041-210X.2011.00179.x.

Dahlberg J. 2013. Family influence in fertility: A longitudinal analysis of sibling correlations in first birth risk and completed fertility among Swedish men and women. Demographic Research. 29:233–246.

Danchin E, Nöbel S, Pocheville A, Dagaeff AC, Demay L, Alphand M, Ranty-Roby S, van Renssen L, Monier M, Gazagne E *et al*. 2018. Cultural flies: Conformist social learning in fruitflies predicts long-lasting mate-choice traditions. Science. 362:1025–1030.

Danchin E, Pocheville A, Rey O, Pujol B, Blanchet S. 2019. Epigenetically facilitated mutational assimilation: epigenetics as a hub within the inclusive evolutionary synthesis. Biological Reviews. 94:259–282.

Danchin Charmantier A, Champagne FA, Mesoudi A, Pujol B, Blanchet S. 2011. Beyond DNA: integrating inclusive inheritance into an extended theory of evolution. Nature Reviews Genetics. 12:475–486.

Danziger L, Neuman S. 1989. Intergenerational effects on fertility: theory and evidence from Israel. Journal of Population Economics. 2:25–37.

Darlu P. 2019. La transmission de la fécondité dans le contexte béarnais, du XVIIIe au XXe siècle. Annales de démographie historique. 138:119–141.

Davenport ER, Sanders JG, Song SJ, Amato KR, Clark AG, Knight R. 2017. The human microbiome in evolution. BMC Biology. 15:127.

Daw J, Guo G. 2011. The influence of three genes on whether adolescents use contraception, USA 1994–2002. Population Studies. 65:253–271.

Day FR, Helgason H, Chasman DI, Rose LM, Loh PR, Scott RA, Helgason A, Kong A, Masson G, Magnusson OT *et al*. 2016. Physical and neurobehavioral determinants of reproductive onset and success. Nature Genetics. 48:617–623.

Day T, Bonduriansky R. 2011. A unified approach to the evolutionary consequences of genetic and nongenetic inheritance. The American Naturalist. 178:E18–36.

de Jonge N, Carlsen B, Christensen MH, Pertoldi C, Nielsen JL. 2022. The Gut Microbiome of 54 Mammalian Species. Frontiers in Microbiology. 13:886252.

de Valk HA. 2013. Intergenerational discrepancies in fertility preferences among immigrant and Dutch families. The History of the Family. 18:209–225.

Desjardins B, Bideau A, Heyer E, Brunet G. 1991. Intervals between marriage and first birth in mothers and daughters. Journal of Biosocial Science. 23:49–54.

Desplanques G. 1985. Fécondité et milieu social. Economie et Statistique. 175:21–38.

Devi MR, Kumari JR, Srikumari C. 1985. Fertility and mortality differences in relation to maternal body size. Annals of Human Biology. 12:479–484.

Deville JC. 1979. La fécondité serait-elle héréditaire ? Economie et Statistique. 116:3–11.

DeWitt WS, Harris KD, Ragsdale AP, Harris K. 2021. Nonparametric coalescent inference of mutation spectrum history and demography. Proceedings of the National Academy of Sciences of the United States of America. 118:e2013798118.

Dilber E, Terhorst J. 2022. Robust detection of natural selection using a probabilistic model of tree imbalance. Genetics. 220:iyac009.

Donabedian R, Cords M. 2021. Maternal rank acquisition in a primate with low aggression and coalition rates. Behavioral Ecology and Sociobiology. 75:90.

Draper P, Hames R. 2000. Birth order, sibling investment, and fertility among Ju/'Hoansi (!Kung). Human Nature (Hawthorne, N.Y.). 11:117–156.

Duff P, Kusumaningrum S, Stark L. 2016. Barriers to birth registration in Indonesia. The Lancet Global Health. 4:e234–e235. Publisher: Elsevier.

Duncan LE, Keller MC. 2011. A critical review of the first 10 years of candidate gene-by-environment interaction research in psychiatry. The American Journal of Psychiatry. 168:1041–1049.

Duncan OD, Freedman R, Coble JM, Slesinger DP. 1965. Marital Fertility and Size of Family of Orientation. Demography. 2:508–515.

Durrett R, Schweinsberg J. 2005. A coalescent model for the effect of advantageous mutations on the genealogy of a population. Stochastic Processes and their Applications. 115:1628–1657.

Easterlin RA. 1980. Fertility and development. Population Bulletin of the United Nations Economic Commission for Western Asia. 18:5–40.

Eldon B, Wakeley J. 2006. Coalescent processes when the distribution of offspring number among individuals is highly skewed. Genetics. 172:2621–2633.

Engh AL, Esch K, Smale L, Holekamp KE. 2000. Mechanisms of maternal rank 'inheritance' in the spotted hyaena, Crocuta crocuta. Animal Behaviour. 60:323–332.

Estrada A, Sandoval JM, Manzolillo D. 1978. Further data on predation by free-ranging Stumptail macaques (Macaca arctoides). Primates. 19:401–407.

Evertsson M. 2006. The reproduction of gender: Housework and attitudes towards gender equality in the home among Swedish boys and girls. The British journal of sociology. 57:415–36.

Excoffier L, Dupanloup I, Huerta-Sánchez E, Sousa VC, Foll M. 2013. Robust Demographic Inference from Genomic and SNP Data. PLoS Genetics. 9:e1003905.

Falconer DS. 1965. Maternal effects and selection response, In: Geerts SJ, editor, *Genetics Today, Proceedings of the XI International Congress on Genetics*, Pergamon. Oxford. volume 3. pp. 763–774.

Fasang A, Raab M. 2014. Beyond Transmission: Intergenerational Patterns of Family Formation Among Middle-Class American Families. Demography. 51:1703–1728.

Fay JC, Wu CI. 2000. Hitchhiking under positive Darwinian selection. Genetics. 155:1405–1413.

Fisher RA. 1930. *The genetical theory of natural selection*. The genetical theory of natural selection. Clarendon Press. Oxford, England.

Flagel L, Brandvain Y, Schrider DR. 2019. The Unreasonable Effectiveness of Convolutional Neural Networks in Population Genetic Inference. Molecular Biology and Evolution. 36:220–238.

Frere CH, Krutzen M, Mann J, Connor RC, Bejder L, Sherwin WB. 2010. Social and genetic interactions drive fitness variation in a free-living dolphin population. Proceedings of the National Academy of Sciences. 107:19949–19954.

Freund F, Kerdoncuff E, Matuszewski S, Lapierre M, Hildebrandt M, Jensen JD, Ferretti L, Lambert A, Sackton TB, Achaz G. 2022. Interpreting the pervasive observation of U-shaped Site Frequency Spectra. Pages: 2022.04.12.488084 Section: New Results.

Funkhouser LJ, Bordenstein SR. 2013. Mom Knows Best: The Universality of Maternal Microbial Transmission. PLOS Biology. 11:e1001631.

Fusco G, Cronk QCB. 1995. A new method for evaluating the shape of large phylogenies. Journal of Theoretical Biology. 175:235–243.

Fábregas-Tejeda A, Vergara-Silva F. 2018. The emerging structure of the Extended Evolutionary Synthesis: where does Evo-Devo fit in? Theory in Biosciences = Theorie in Den Biowissenschaften. 137:169–184.

Gager CT, Cooney TM, Call KT. 1999. The Effects of Family Characteristics and Time Use on Teenagers' Household Labor. Journal of Marriage and Family. 61:982–994.

Gagneux P, Wills C, Gerloff U, Tautz D, Morin PA, Boesch C, Fruth B, Hohmann G, Ryder OA, Woodruff DS. 1999. Mitochondrial sequences show diverse evolutionary histories of African hominoids. Proceedings of the National Academy of Sciences of the United States of America. 96:5077–5082.

Gagnon A, Heyer E. 2001. Intergenerational correlation of effective family size in early Québec (Canada): Correlation of Effective Family Size. American Journal of Human Biology. 13:645–659.

Gagnon A, Toupance B, Tremblay M, Beise J, Heyer E. 2006. Transmission of migration propensity increases genetic divergence between populations. American Journal of Physical Anthropology. 129:630–636.

Galef Jr. BG. 1998. Recent progress in studies of imitation and social learning in animals, In: , Psychology Press/Erlbaum (UK) Taylor & Francis. Hove, England. pp. 275–299.

Gardner A. 2020. Price's equation made clear. Philosophical Transactions of the Royal Society B: Biological Sciences. 375:20190361. Publisher: Royal Society.

Garenne M, Van de Walle E. 1989. Polygyny and Fertility among the Sereer of Senegal. Population Studies. 43:267–283.

Gattepaille LM, Jakobsson M, Blum MGB. 2013. Inferring population size changes with sequence and SNP data: lessons from human bottlenecks. Heredity. 110:409–419.

Gazave E, Ma L, Chang D, Coventry A, Gao F, Muzny D, Boerwinkle E, Gibbs RA, Sing CF, Clark AG *et al*. 2014. Neutral genomic regions refine models of recent rapid human population growth. Proceedings of the National Academy of Sciences. 111:757–762. Publisher: Proceedings of the National Academy of Sciences.

Gerbault P, Liebert A, Itan Y, Powell A, Currat M, Burger J, Swallow DM, Thomas MG. 2011. Evolution of lactase persistence: an example of human niche construction. Philosophical Transactions of the Royal Society B: Biological Sciences. 366:863–877.

Glass J, Bengtson VL, Dunham CC. 1986. Attitude Similarity in Three-Generation Families: Socialization, Status Inheritance, or Reciprocal Influence? American Sociological Review. 51:685–698.

Goldenberg SZ, Douglas-Hamilton I, Wittemyer G. 2016. Vertical Transmission of Social Roles Drives Resilience to Poaching in Elephant Networks. Current Biology. 26:75–79.

Goldscheider F, Bernhardt E, Lappegård T. 2015. The Gender Revolution: A Framework for Understanding Changing Family and Demographic Behavior. Population and Development Review. 41:207–239.

Goodfellow IJ, Bengio Y, Courville A. 2016. *Deep Learning*. MIT Press.

Goody J. 1973. Strategies of Heirship. Comparative Studies in Society and History. 15:3–20.

Grafen A. 1984. Natural selection, kin selection and group selection [Polistes fuscatus, wasps]. Behavioural ecology : an evolutionary approach / edited by J.R. Krebs and N.B. Davies. .

Gravel S, Henn BM, Gutenkunst RN, Indap AR, Marth GT, Clark AG, Yu F, Gibbs RA, 1000 Genomes Project, Bustamante CD. 2011. Demographic history and rare allele sharing among human populations. Proceedings of the National Academy of Sciences of the United States of America. 108:11983–11988.

Greer JA, Swei A, Vredenburg VT, Zink AG. 2020. Parental Care Alters the Egg Microbiome of Maritime Earwigs. Microbial Ecology. 80:920–934.

Grice EA, Segre JA. 2012. The Human Microbiome: Our Second Genome. Annual review of genomics and human genetics. 13:151–170.

Gruber T, Muller MN, Strimling P, Wrangham R, Zuberbühler K. 2009. Wild Chimpanzees Rely on Cultural Knowledge to Solve an Experimental Honey Acquisition Task. Current Biology. 19:1806–1810.

Grünwald NJ, Goss EM. 2011. Evolution and Population Genetics of Exotic and Re-Emerging Pathogens: Novel Tools and Approaches. Annual Review of Phytopathology. 49:249–267. _eprint: https://doi.org/10.1146/annurev-phyto-072910-095246.

Guez J, Achaz G, Bienvenu F, Cury J, Toupance B, Heyer E, Jay F, Austerlitz F. 2022. Cultural transmission of reproductive success impacts genomic diversity, coalescent tree topologies and demographic inferences.

Gutenkunst RN, Hernandez RD, Williamson SH, Bustamante CD. 2009. Inferring the Joint Demographic History of Multiple Populations from Multidimensional SNP Frequency Data. PLoS Genetics. 5:e1000695.

Haller BC, Messer PW. 2019. SLiM 3: Forward Genetic Simulations Beyond the Wright–Fisher Model. Molecular Biology and Evolution. 36:632–637.

Hamilton WD. 1964. The genetical evolution of social behaviour. I. Journal of Theoretical Biology. 7:1–16.

Hansen TF, Wagner GP. 2001. Modeling genetic architecture: a multilinear theory of gene interaction. Theoretical Population Biology. 59:61–86.

Hausfater G. 1975. *Dominance and Reproduction in Baboons (Papio cynocephalus)*. Karger Book.

Hayward LK, Sella G. 2022. Polygenic adaptation after a sudden change in environment. eLife. 11:e66697.

Heiland F, Prskawetz A, Sanderson WC. 2008. Are Individuals' Desired Family Sizes Stable? Evidence from West German Panel Data / La taille de famille désirée est-elle stable? Analyse de données de panel en Allemagne de I'Ouest. European Journal of Population / Revue Européenne de Démographie. 24:129–156.

Helanterä H, Uller T. 2010. The Price Equation and Extended Inheritance. Philosophy & Theory in Biology. 2.

Helanterä H, Uller T. 2020. Different perspectives on non-genetic inheritance illustrate the versatile utility of the Price equation in evolutionary biology. Philosophical Transactions of the Royal Society B: Biological Sciences. 375:20190366.

Helfman GS, Schultz ET. 1984. Social transmission of behavioural traditions in a coral reef fish. Animal Behaviour. 32:379–384.

Helmlinger G, Netti PA, Lichtenbeld HC, Melder RJ, Jain RK. 1997. Solid stress inhibits the growth of multicellular tumor spheroids. Nature Biotechnology. 15:778–783.

Hendershot GE. 1969. Familial Satisfaction, Birth Order, and Fertility Values. Journal of Marriage and Family. 31:27–33.

Hewlett BS, Cavalli-Sforza LL. 1986. Cultural Transmission Among Aka Pygmies. American Anthropologist. 88:922–934.

Heyer E, Brandenburg JT, Leonardi M, Toupance B, Balaresque P, Hegay T, Aldashev A, Austerlitz F. 2015. Patrilineal populations show more male transmission of reproductive success than cognatic populations in Central Asia, which reduces their genetic diversity: Cultural Transmission of Fitness. American Journal of Physical Anthropology. 157:537–543.

Heyer E, Chaix R, Pavard S, Austerlitz F. 2012. Sex-specific demographic behaviours that shape human genomic variation. Molecular Ecology. 21:597–612.

Hill K, Hurtado AM. 1996. *Ache Life History: The Ecology and Demography of a Foraging People*. Routledge. New York.

Hill K, Hurtado AM. 2009. Cooperative breeding in South American hunter–gatherers. Proceedings of the Royal Society B: Biological Sciences. 276:3863–3870.

Hobaiter C, Poisot T, Zuberbühler K, Hoppitt W, Gruber T. 2014. Social Network Analysis Shows Direct Evidence for Social Transmission of Tool Use in Wild Chimpanzees. PLOS Biology. 12:e1001960.

Holekamp KE, Smale L. 1990. Provisioning and food sharing by lactating spotted hyenas, Crocuta crocuta (Mammalia: Hyaenidae). Ethology. 86:191–202.

Horrocks J, Hunte W. 1983. Maternal rank and offspring rank in vervet monkeys: An appraisal of the mechanisms of rank acquisition. Animal Behaviour. 31:772–782.

Houle D, Morikawa B, Lynch M. 1996. Comparing mutational variabilities. Genetics. 143:1467–1483.

Hrdy SB. 2009. *Mothers and others: The evolutionary origins of mutual understanding*. Mothers and others: The evolutionary origins of mutual understanding. Harvard University Press. Cambridge, MA, US.

Hudson RR, Kaplan NL. 1995. Deleterious background selection with recombination. Genetics. 141:1605–1617.

Hughes KA, Burleson MH. 2000. Evolutionary Causes of Genetic Variation in Fertility and other Fitness Components, In: Rodgers JL, Rowe DC, Miller WB, editors, *Genetic Influences on Human Fertility and Sexuality: Theoretical and Empirical Contributions from the Biological and Behavioral Sciences*, Springer US. Boston, MA. pp. 7–33.

Huxley J. 1942. *Evolution The Modern Synthesis*.

Ilany A, Holekamp K, Akçay E. 2021. Rank-dependent social inheritance determines social network structure in spotted hyenas. Science. 373:348–352.

Irwin KK, Laurent S, Matuszewski S, Vuilleumier S, Ormond L, Shim H, Bank C, Jensen JD. 2016. On the importance of skewed offspring distributions and background selection in virus population genetics. Heredity. 117:393–399.

Jansen M, Wijckmans B, Bavel J. 2009. Divorce and the cumulated fertility of men and women across Europe. .

Jay F, Boitard S, Austerlitz F. 2019. An ABC Method for Whole-Genome Sequence Data: Inferring Paleolithic and Neolithic Human Expansions. Molecular Biology and Evolution. 36:1565–1579.

Jennings HS. 1937. Formation, inheritance and variation of the teeth in Difflugia corona. A study of the morphogenic activities of rhizopod protoplasm. Journal of Experimental Zoology. 77:287–336.

Jennings J, Leslie P. 2013. Differences in intergenerational fertility associations by sex and race in Saba, Dutch Caribbean, 1876–2004. Anthropology Faculty Scholarship. .

Jennings J, Sullivan A, Hacker J. 2012. Intergenerational Transmission of Reproductive Behavior during the Demographic Transition. The Journal of interdisciplinary history. 42:543–69.

Jiang B, Wu TY, Zheng C, Wong WH. 2017. Learning Summary Statistic for Approximate Bayesian Computation Via Deep Neural Network. Statistica Sinica. 27:1595–1618. Publisher: Institute of Statistical Science, Academia Sinica.

Jiang Y, Reif JC. 2015. Modeling Epistasis in Genomic Selection. Genetics. 201:759–768.

Johnson NE, Stokes CS. 1976. Family size in successive generations: the effects of birth order, intergenerational change in lifestyle, and familial satisfaction. Demography. 13:175–187.

Johri P, Riall K, Becher H, Excoffier L, Charlesworth B, Jensen JD. 2021. The Impact of Purifying and Background Selection on the Inference of Population History: Problems and Prospects. Molecular Biology and Evolution. 38:2986–3003.

Kaessmann H, Wiebe V, Weiss G, Pääbo S. 2001. Great ape DNA sequences reveal a reduced diversity and an expansion in humans. Nature Genetics. 27:155–156.

Kahn JR, Anderson KE. 1992. Intergenerational patterns of teenage fertility. Demography. 29:39–57.

Kana'Iaupuni SM, Donato KM, Thompson-Colón T, Stainback M. 2005. Counting on Kin: Social Networks, Social Support, and Child Health Status. Social Forces. 83:1137–1164.

Kaplan NL, Darden T, Hudson RR. 1988. The Coalescent Process in Models with Selection. Genetics. 120:819–829.

Kaplan NL, Hudson RR, Langley CH. 1989. The "hitchhiking effect" revisited. Genetics. 123:887–899.

Kawai M. 1958. On the rank system in a natural group of Japanese monkey (I): —the Basic and Dependent Rank—. Primates. 1:111–130.

Kawecki TJ, Lenski RE, Ebert D, Hollis B, Olivieri I, Whitlock MC. 2012. Experimental evolution. Trends in Ecology & Evolution. 27:547–560.

Kelleher J, Etheridge AM, McVean G. 2016. Efficient Coalescent Simulation and Genealogical Analysis for Large Sample Sizes. PLOS Computational Biology. 12:e1004842.

Kelleher J, Wong Y, Wohns AW, Fadil C, Albers PK, McVean G. 2019. Inferring whole-genome histories in large population datasets. Nature Genetics. 51:1330–1338.

Kelly MJ. 2001. Lineage Loss in Serengeti Cheetahs: Consequences of High Reproductive Variance and Heritability of Fitness on Effective Population Size. Conservation Biology. 15:11.

Kim BY, Huber CD, Lohmueller KE. 2017. Inference of the Distribution of Selection Coefficients for New Nonsynonymous Mutations Using Large Samples. Genetics. 206:345–361.

Kim Y, Stephan W. 2002. Detecting a Local Signature of Genetic Hitchhiking Along a Recombining Chromosome. Genetics. 160:765–777.

Kimura M. 1968. Evolutionary rate at the molecular level. Nature. 217:624–626.

Kingman JFC. 1982. The coalescent. Stochastic Processes and their Applications. 13:235–248.

Kirchengast S. 2000. Differential reproductive success and body size in !Kung San people from northern Namibia. Collegium Antropologicum. 24:121–132.

Kirk KM, Blomberg SP, Duffy DL, Heath AC, Owens IP, Martin NG. 2001. Natural selection and quantitative genetics of life-history traits in Western women: a twin study. Evolution; International Journal of Organic Evolution. 55:423–435.

Kirkpatrick M, Lande R. 1989. The Evolution of Maternal Characters. Evolution. 43:485–503.

Kivisild T, Shen P, Wall DP, Do B, Sung R, Davis K, Passarino G, Underhill PA, Scharfe C, Torroni A *et al*. 2006. The Role of Selection in the Evolution of Human Mitochondrial Genomes. Genetics. 172:373–387.

Kohler HP, Rodgers JL, Christensen K. 1999. Is Fertility Behavior in Our Genes? Findings from a Danish Twin Study. Population and Development Review. 25:253–288.

Kokko H, Brooks R, McNamara JM, Houston AI. 2002. The sexual selection continuum. Proceedings. Biological Sciences. 269:1331–1340.

Kolk M. 2014. Multigenerational transmission of family size in contemporary Sweden. Population Studies. 68:111–129.

Kolk M. 2015. The causal effect of an additional sibling on completed fertility: An estimation of intergenerational fertility correlations by looking at siblings of twins. Demographic Research. 32:1409–1420.

Kosova G, Abney M, Ober C. 2010. Heritability of reproductive fitness traits in a human population. Proceedings of the National Academy of Sciences. 107:1772–1778.

Kosova G, Scott NM, Niederberger C, Prins GS, Ober C. 2012. Genome-wide Association Study Identifies Candidate Genes for Male Fertility Traits in Humans. The American Journal of Human Genetics. 90:950–961.

Krützen M, Mann J, Heithaus MR, Connor RC, Bejder L, Sherwin WB. 2005. Cultural transmission of tool use in bottlenose dolphins. Proceedings of the National Academy of Sciences of the United States of America. 102:8939–8943.

Laland K, Uller T, Feldman M, Sterelny K, Müller GB, Moczek A, Jablonka E, Odling-Smee J, Wray GA, Hoekstra HE *et al*. 2014. Does evolutionary theory need a rethink? Nature. 514:161–164.

Laland KN, Hoppitt W. 2003. Do animals have culture? Evolutionary Anthropology: Issues, News, and Reviews. 12:150–159.

Laland KN, Uller T, Feldman MW, Sterelny K, Müller GB, Moczek A, Jablonka E, Odling-Smee J. 2015. The extended evolutionary synthesis: its structure, assumptions and predictions. Proceedings of the Royal Society B: Biological Sciences. 282:20151019.

Lande R. 1980. The Genetic Covariance between Characters Maintained by Pleiotropic Mutations. Genetics. 94:203–215.

Langford CM, Wilson C. 1985. Is there a connection between a woman's fecundity and that of her mother? Journal of Biosocial Science. 17:437–443.

Lansing JS, Watkins JC, Hallmark B, Cox MP, Karafet TM, Sudoyo H, Hammer MF. 2008. Male dominance rarely skews the frequency distribution of Y chromosome haplotypes in human populations. Proceedings of the National Academy of

Sciences. 105:11645–11650. Publisher: Proceedings of the National Academy of Sciences.

Lapierre M, Blin C, Lambert A, Achaz G, Rocha EPC. 2016. The Impact of Selection, Gene Conversion, and Biased Sampling on the Assessment of Microbial Demography. Molecular Biology and Evolution. 33:1711–1725.

Lapierre M, Lambert A, Achaz G. 2017. Accuracy of Demographic Inferences from the Site Frequency Spectrum: The Case of the Yoruba Population. Genetics. 206:439–449. Publisher: Genetics _eprint: https://www.genetics.org/content/206/1/439.full.pdf.

Lardoux S, van de Walle E. 2003. Polygyny and Fertility in Rural Senegal. Population. 58:717–743.

Latta RG. 1998. Differentiation of allelic frequencies at quantitative trait loci affecting locally adaptive traits. The American Naturalist. 151:283–292.

Lawson DW, Mace R. 2011. Parental investment and the optimization of human family size. Philosophical Transactions of the Royal Society B: Biological Sciences. 366:333–343.

Le Corre V, Kremer A. 2003. Genetic variability at neutral markers, quantitative trait land trait in a subdivided population under selection. Genetics. 164:1205–1219.

Leca JB, Gunst N, Watanabe K, Huffman MA. 2007. A new case of fish-eating in Japanese macaques: implications for social constraints on the diffusion of feeding innovation. American Journal of Primatology. 69:821–828. _eprint: https://onlinelibrary.wiley.com/doi/pdf/10.1002/ajp.20401.

Lecun Y, Bottou L, Bengio Y, Haffner P. 1998. Gradient-based learning applied to document recognition. Proceedings of the IEEE. 86:2278–2324.

Lehrer EL, Chiswick CU. 1993. Religion as a Determinant of Marital Stability. Demography. 30:385–404.

Levine D. 1982. "For Their Own Reasons": Individual Marriage Decisions and Family Life. Journal of Family History. 7:255–264.

Lewens T. 2019. The Extended Evolutionary Synthesis: what is the debate about, and what might success for the extenders look like? Biological Journal of the Linnean Society. 127:707–721.

Lewontin RC. 1974. *The Genetic Basis of Evolutionary Change*. Columbia University Press.

Li H. 2011. A new test for detecting recent positive selection that is free from the confounding impacts of demography. Molecular Biology and Evolution. 28:365–375.

Li H, Wiehe T. 2013. Coalescent Tree Imbalance and a Simple Test for Selective Sweeps Based on Microsatellite Variation. PLOS Computational Biology. 9:e1003060.

Li S, Zhang Y, Feldman MW. 2010. Birth Registration in China: Practices, Problems and Policies. Population Research and Policy Review. 29:297–317.

Liu X, Fu YX. 2020. Stairway Plot 2: demographic history inference with folded SNP frequency spectra. Genome Biology. 21:280.

Lois D, Arránz Becker O. 2014. Is fertility contagious? Using panel data to disentangle mechanisms of social network influences on fertility decisions. Advances in Life Course Research. 21:123–134.

Lozada M, Ladio A, Weigandt M. 2006. Cultural Transmission of Ethnobotanical Knowledge in a Rural Community of Northwestern Patagonia, Argentina. Economic Botany. 60:374–385.

Lucas T, Tallec C, Verbeek J, Ollivier Y. 2018. Mixed batches and symmetric discriminators for GAN training. volume 80. p. 2844.

Luncz LV, Boesch C. 2014. Tradition over trend: Neighboring chimpanzee communities maintain differences in cultural behavior despite frequent immigration of adult females. American Journal of Primatology. 76:649–657.

Lynch CD, Sundaram R, Maisog JM, Sweeney AM, Buck Louis GM. 2014. Preconception stress increases the risk of infertility: results from a couple-based prospective cohort study–the LIFE study. Human Reproduction (Oxford, England). 29:1067–1075.

Lyngstad T, Jalovaara M. 2010. A review of the antecedents of union dissolution. Demographic Research. 23:257–292.

Manlove J. 1997. Early Motherhood in an Intergenerational Perspective: The Experiences of a British Cohort. Journal of Marriage and Family. 59:263–279.

Marmot M. 2006. Health in an unequal world: social circumstances, biology and disease. Clinical Medicine. 6:559–572.

Massart R, Suderman MJ, Nemoda Z, Sutti S, Ruggiero AM, Dettmer AM, Suomi SJ, Szyf M. 2017. The Signature of Maternal Social Rank in Placenta Deoxyribonucleic Acid Methylation Profiles in Rhesus Monkeys. Child Development. 88:900–918.

Mathews P, Sear R. 2013. Family and fertility: kin influence on the progression to a second birth in the British Household Panel Study. PloS One. 8:e56941.

Mazet O, Rodríguez W, Grusea S, Boitard S, Chikhi L. 2016. On the importance of being structured: instantaneous coalescence rates and human evolution—lessons for ancestral population size inference? Heredity. 116:362–371.

McAllister P, Stokes CS, Knapp M. 1974. Size of Family of Orientation, Birth Order, and Fertility Values: A Reexamination. Journal of Marriage and Family. 36:337–342.

McCulloch WS, Pitts W. 1943. A logical calculus of the ideas immanent in nervous activity. The bulletin of mathematical biophysics. 5:115–133.

Menardo F, Gagneux S, Freund F. 2021. Multiple Merger Genealogies in Outbreaks of Mycobacterium tuberculosis. Molecular Biology and Evolution. 38:290–306.

Mengoli C, Bonfanti C, Rossi C, Franchini M. 2015. ABO blood group and fertility: a single-centre study. Blood Transfusion. 13:521–523.

Miller WB, Bard DE, Pasta DJ, Rodgers JL. 2010. Biodemographic modeling of the links between fertility motivation and fertility outcomes in the NLSY79. Demography. 47:393–414.

Miller WB, Pasta DJ, MacMurray J, Chiu C, Wu H, Comings DE. 1999. Dopamine receptor genes are associated with age at first sexual intercourse. Journal of Biosocial Science. 31:43–54.

Mills MC, Tropf FC. 2015. The Biodemography of Fertility: A Review and Future Research Frontiers. KZfSS Kölner Zeitschrift für Soziologie und Sozialpsychologie. 67:397–424.

Mills MC, Tropf FC, Brazel DM, van Zuydam N, Vaez A, Pers TH, Snieder H, Perry JRB, Ong KK, den Hoed M *et al*. 2021. Identification of 371 genetic variants

for age at first sex and birth linked to externalising behaviour. Nature Human Behaviour. 5:1717–1730.

Minsky M, Papert S. 1969. *Perceptrons*. Perceptrons. M.I.T. Press. Oxford, England.

Moeller AH, Suzuki TA, Phifer-Rixey M, Nachman MW. 2018. Transmission modes of the mammalian gut microbiota. Science. 362:453–457.

Mondal M, Bertranpetit J, Lao O. 2019. Approximate Bayesian computation with deep learning supports a third archaic introgression in Asia and Oceania. Nature Communications. 10:246.

Monden C, Smits j. 2009. Maternal Height and Child Mortality in 42 Developing Countries. American journal of human biology : the official journal of the Human Biology Council. 21:305–11.

Moran PaP. 1958. Random processes in genetics. Mathematical Proceedings of the Cambridge Philosophical Society. 54:60–71. Publisher: Cambridge University Press.

Moreira-Leite FF, Sherwin T, Kohl L, Gull K. 2001. A Trypanosome Structure Involved in Transmitting Cytoplasmic Information During Cell Division. Science. 294:610–612. Publisher: American Association for the Advancement of Science.

Mourali-Chebil S, Heyer E. 2006. Evolution of Inbreeding Coefficients and Effective Size in the Population of Saguenay Lac-St.-Jean (Que´bec). Human Biology. 78.

Murdoch WJ, Singh C, Kumbier K, Abbasi-Asl R, Yu B. 2019. Definitions, methods, and applications in interpretable machine learning. Proceedings of the National Academy of Sciences. 116:22071–22080. Publisher: Proceedings of the National Academy of Sciences.

Murphy M. 1999. Is the relationship between fertility of parents and children really weak? Biodemography and Social Biology. 46:122–145.

Murphy M. 2012. Intergenerational fertility correlations in contemporary developing counties. American Journal of Human Biology. 24:696–704.

Murphy M. 2013. The intergenerational transmission of reproductive behaviour: comparative perspectives. The History of the Family. 18:107–115.

Murphy M, Knudsen LB. 2002. The Intergenerational Transmission of Fertility in Contemporary Denmark: The Effects of Number of Siblings (Full and Half), Birth Order, and Whether Male or Female. Population Studies. 56:235–248.

Murphy M, Wang D. 2001. Family-Level Continuities in Childbearing in Low-Fertility Societies. European Journal of Population / Revue Européenne de Démographie. 17:75–96.

Murray-McIntosh RP, Scrimshaw BJ, Hatfield PJ, Penny D. 1998. Testing migration patterns and estimating founding population size in Polynesia by using human mtDNA sequences. Proceedings of the National Academy of Sciences. 95:9047–9052.

Möller LM, Harcourt RG. 2008. Shared Reproductive State Enhances Female Associations in Dolphins. International Journal of Ecology. 2008:e498390. Publisher: Hindawi.

Mönkediek B, Rotering P, Bras H. 2017. Regional Differences in the Intergenerational Transmission of Family Size in Europe. Population, Space and Place. 23:e2003.

Naiman RJ, Johnston CA, Kelley JC. 1988. Alteration of North American Streams by Beaver. BioScience. 38:753–762. Publisher: [American Institute of Biological Sciences, Oxford University Press].

Nakayama K, Ohashi J, Watanabe K, Munkhtulga L, Iwamoto S. 2017. Evidence for Very Recent Positive Selection in Mongolians. Molecular Biology and Evolution. 34:1936–1946.

Narasimhan VM, Rahbari R, Scally A, Wuster A, Mason D, Xue Y, Wright J, Trembath RC, Maher ER, van Heel DA *et al*. 2017. Estimating the human mutation rate from autozygous segments reveals population differences in human mutational processes. Nature Communications. 8:303.

Neel JV. 1970. Lessons from a "Primitive" People. Science. 170:815–822.

Neher RA, Hallatschek O. 2013. Genealogies of rapidly adapting populations. Proceedings of the National Academy of Sciences of the United States of America. 110:437–442.

Nei M, Murata M. 1966. Effective population size when fertility is inherited. Genetical Research. 8:257–260.

Nettle D, Pollet TV. 2008. Natural selection on male wealth in humans. The American Naturalist. 172:658–666.

Newson L, Postmes T, Lea SEG, Webley P. 2005. Why are modern families small? Toward an evolutionary and cultural explanation for the demographic transition.

Personality and Social Psychology Review: An Official Journal of the Society for Personality and Social Psychology, Inc. 9:360–375.

Newson L, Postmes T, Lea SEG, Webley P, Richerson PJ, Mcelreath R. 2007. Influences on communication about reproduction: the cultural evolution of low fertility. Evolution and Human Behavior. 28:199–210.

Nguyen Ba AN, Lawrence KR, Rego-Costa A, Gopalakrishnan S, Temko D, Michor F, Desai MM. 2022. Barcoded bulk QTL mapping reveals highly polygenic and epistatic architecture of complex traits in yeast. eLife. 11:e73983. Publisher: eLife Sciences Publications, Ltd.

Nordborg M. 1997. Structured Coalescent Processes on Different Time Scales. Genetics. 146:1501–1514.

Nordborg M, Charlesworth B, Charlesworth D. 1996. The effect of recombination on background selection. Genetical Research. 67:159–174.

Odling-Smee FJ. 1988. Niche-constructing phenotypes, In: , The MIT Press. Cambridge, MA, US. pp. 73–132.

Otto S, Christiansen F, Feldman M. 1995. Genetic and Cultural Inheritance of Continuous Traits. .

Page AE, Chaudhary N, Viguier S, Dyble M, Thompson J, Smith D, Salali GD, Mace R, Migliano AB. 2017. Hunter-Gatherer Social Networks and Reproductive Success. Scientific Reports. 7:1153.

Palamara PF, Pe'er I. 2013. Inference of historical migration rates via haplotype sharing. Bioinformatics. 29:i180–i188.

Pawlowski B, Dunbar RIM, Lipowicz A. 2000. Tall men have more reproductive success. Nature. 403:156–156.

Pearson K, Lee A, Bramley-Moore L. 1899. Mathematical Contributions to the Theory of Evolution. VI. Genetic (Reproductive) Selection: Inheritance of Fertility in Man, and of Fecundity in Thoroughbred Racehorses. Philosophical Transactions of the Royal Society of London. Series A, Containing Papers of a Mathematical or Physical Character. 192:257–330.

Pebley AR, Mbugua W. 1989. Polygyny and Fertility in Sub-Saharan Africa. pp. 338–364.

Pemberton J. 2008. Wild pedigrees: the way forward. Proceedings of the Royal Society B: Biological Sciences. 275:613–621. Publisher: Royal Society.

Pettay JE, Kruuk LEB, Jokela J, Lummaa V. 2005. Heritability and genetic constraints of life-history trait evolution in preindustrial humans. Proceedings of the National Academy of Sciences. 102:2838–2843.

Petty LE, Phillippi-Falkenstein K, Kubisch HM, Raveendran M, Harris RA, Vallender EJ, Huff CD, Bohm RP, Rogers J, Below JE. 2021. Pedigree reconstruction and distant pairwise relatedness estimation from genome sequence data: A demonstration in a population of rhesus macaques (Macaca mulatta). Molecular Ecology Resources. 21:1333–1346. _eprint: https://onlinelibrary.wiley.com/doi/pdf/10.1111/1755-0998.13317.

Peña-Malavera A, Bruno C, Fernandez E, Balzarini M. 2014. Comparison of algorithms to infer genetic population structure from unlinked molecular markers. Statistical Applications in Genetics and Molecular Biology. 13:391–402. Publisher: De Gruyter.

Philipov D, Berghammer C. 2007. Religion and fertility ideals, intentions and behaviour: a comparative study of European countries. Vienna Yearbook of Population Research. 5:271–305.

Pison G. 1986. La démographie de la polygamie. Population. 41:93–122.

Pluda JM. 1997. Tumor-associated angiogenesis: mechanisms, clinical implications, and therapeutic strategies. Seminars in Oncology. 24:203–218.

Pluzhnikov A, Nolan DK, Tan Z, McPeek MS, Ober C. 2007. Correlation of Intergenerational Family Sizes Suggests a Genetic Component of Reproductive Fitness. The American Journal of Human Genetics. 81:165–169.

Pollet T, Nettle D. 2008. Taller women do better in a stressed environment: Height and reproductive success in rural Guatemalan women. American journal of human biology : the official journal of the Human Biology Council. 20:264–9.

Potter RG, Kantner JF. 1955. Social and Psychological Factors Affecting Fertility. XXVIII. The Influence of Siblings and Friends on Fertility. The Milbank Memorial Fund Quarterly. 33:246.

Pouta A, Järvelin MR, Hemminki E, Sovio U, Hartikainen AL. 2005. Mothers and daughters: intergenerational patterns of reproduction. European Journal of Public Health. 15:195–199.

Pouyet F, Aeschbacher S, Thiéry A, Excoffier L. 2018. Background selection and biased gene conversion affect more than 95% of the human genome and bias demographic inferences. eLife. 7:e36317.

Prasetyo H, Hamudy MIA. 2016. Increasing the Scope of Birth and Death Registration: Issues and Challenges. Jurnal Bina Praja: Journal of Home Affairs Governance. 8:13–26. Number: 1.

Price GR. 1970. Selection and Covariance. Nature. 227:520–521. Number: 5257 Publisher: Nature Publishing Group.

Przeworski M. 2002. The signature of positive selection at randomly chosen loci. Genetics. 160:1179–1189.

Pudlo P, Marin JM, Estoup A, Cornuet JM, Gautier M, Robert CP. 2016. Reliable ABC model choice via random forests. Bioinformatics. 32:859–866.

Puga-Gonzalez I, Sosa S, Sueur C. 2019. Editorial: Social networks analyses in primates, a multilevel perspective. Primates. 60:163–165.

Rasmussen MD, Hubisz MJ, Gronau I, Siepel A. 2014. Genome-Wide Inference of Ancestral Recombination Graphs. PLOS Genetics. 10:e1004342.

Raynal L, Marin JM, Pudlo P, Ribatet M, Robert CP, Estoup A. 2019. ABC random forests for Bayesian parameter inference. Bioinformatics. 35:1720–1728.

Raynes Y, Sniegowski PD. 2014. Experimental evolution and the dynamics of genomic mutation rate modifiers. Heredity. 113:375–380. Number: 5 Publisher: Nature Publishing Group.

Reher D, Ortega J, Sanz-Gimeno A. 2008. Intergenerational Transmission of Reproductive Traits in Spain during the Demographic Transition. Human Nature. 19:23–43.

Reyes-Garcia V, Molina JL, Broesch J, Calvet L, Huanca T, Saus J, Tanner S, Leonard WR, McDade TW. 2008. Do the aged and knowledgeable men enjoy more prestige? A test of predictions from the prestige-bias model of cultural transmission. Evolution and Human Behavior. 29:275–281.

Robbins MM, Ando C, Fawcett KA, Grueter CC, Hedwig D, Iwata Y, Lodwick JL, Masi S, Salmi R, Stoinski TS *et al*. 2016. Behavioral Variation in Gorillas: Evidence of Potential Cultural Traits. PLOS ONE. 11:e0160483.

Rodgers JL, Doughty D. 2000. Genetic and Environmental Influences on Fertility Expectations and Outcomes Using NLSY Kinship Data, In: Rodgers JL, Rowe DC, Miller WB, editors, *Genetic Influences on Human Fertility and Sexuality: Theoretical and Empirical Contributions from the Biological and Behavioral Sciences*, Springer US. Boston, MA. pp. 85–105.

Rodgers JL, Kohler HP, Kyvik KO, Christensen K. 2001. Behavior genetic modeling of human fertility: findings from a contemporary danish twin study. 38:14.

Rotering P. 2017. Intergenerational Transmission of Reproductive Behavior in Sweden, 1850-1889. Historical Life Course Studies. 4:181–202.

Rotering PPP, Bras H. 2015. With the help of kin? Household composition and reproduction in the Netherlands, 1842-1920. Human Nature (Hawthorne, N.Y.). 26:102–121.

Rumelhart DE, Hinton GE, Williams RJ. 1986. Learning representations by back-propagating errors. Nature. 323:533–536. Number: 6088 Publisher: Nature Publishing Group.

Régnier-Loilier A, Depledge R. 2006. Influence of Own Sibship Size on the Number of Children Desired at Various Times of Life. Population. 61:165–194.

Sackin MJ. 1972. "Good" and "Bad" Phenograms. Systematic Biology. 21:225–226.

Sackman AM, Harris RB, Jensen JD. 2019. Inferring Demography and Selection in Organisms Characterized by Skewed Offspring Distributions. Genetics. 211:1019–1028.

Samuels A, Silk JB, Altmann J. 1987. Continuity and change in dominance relations among female baboons. Animal Behaviour. 35:785–793.

Sanchez T. 2022. *Reconstructing our past  deep learning for population genetics*. These de doctorat. université Paris-Saclay.

Sanchez T, Cury J, Charpiat G, Jay F. 2021. Deep learning for population size history inference: Design, comparison and combination with approximate Bayesian computation. Molecular Ecology Resources. 21:2645–2660.

Santorelli CJ, Schaffner CM, Aureli F. 2011. Universal Behaviors as Candidate Traditions in Wild Spider Monkeys. PLOS ONE. 6:e24400.

Sapolsky RM. 2004. Social Status and Health in Humans and Other Animals. Annual Review of Anthropology. 33:393–418.

Sapolsky RM. 2005. The influence of social hierarchy on primate health. Science (New York, N.Y.). 308:648–652.

Schade JD, Marti E, Welter JR, Fisher SG, Grimm NB. 2002. Sources of Nitrogen to the Riparian Zone of a Desert Stream: Implications for Riparian Vegetation and Nitrogen Retention. Ecosystems. 5:68–79.

Schaffnit S, Sear R. 2017a. Supportive families versus support from families: The decision to have a child in the Netherlands. Demographic Research. 37:414–454.

Schaffnit SB, Sear R. 2017b. Support for new mothers and fertility in the United Kingdom: Not all support is equal in the decision to have a second child. Population Studies. 71:345–361.

Schmitt S, Tsai P, Bell J, Fromont J, Ilan M, Lindquist N, Perez T, Rodrigo A, Schupp PJ, Vacelet J *et al*. 2012. Assessing the complex sponge microbiota: core, variable and species-specific bacterial communities in marine sponges. The ISME Journal. 6:564–576.

Schniter E, Kaplan HS, Gurven M. 2022. Cultural transmission vectors of essential knowledge and skills among Tsimane forager-farmers. Evolution and Human Behavior. .

Schrider DR, Shanku AG, Kern AD. 2016. Effects of Linked Selective Sweeps on Demographic Inference and Model Selection. Genetics. 204:1207–1223.

Sear R. 2006. Size, body condition and adult mortality in rural Gambia: a life history perspective. Biodemography and Social Biology. 53:172–188.

Sear R. 2010. Height and reproductive success : is bigger always better ? Book chapter: In Homo Novus: A Human Without Illusions. Edited by Ulrich Frey, Charlotte Stoermer & Kai Willfuehr. Pp127-143. .

Sear R. 2018. Family and fertility: does kin help influence women's fertility, and how does this vary worldwide? Population Horizons. 14.

Sear R, Allal N, Mace R. 2004. Height, marriage and reproductive success in Gambian women. Research in Economic Anthropology. 23.

Segurel L, Guarino-Vignon P, Marchi N, Lafosse S, Laurent R, Bon C, Fabre A, Hegay T, Heyer E. 2020. Why and when was lactase persistence selected for? Insights from Central Asian herders and ancient DNA. PLoS biology. 18:e3000742.

Shao KT, Sokal RR. 1990. Tree Balance. Systematic Zoology. 39:266–276.

Sheehan S, Song YS. 2016. Deep Learning for Population Genetic Inference. PLOS Computational Biology. 12:1–28.

Shirokawa Y, Shimada M. 2016. Cytoplasmic inheritance of parent–offspring cell structure in the clonal diatom Cyclotella meneghiniana. Proceedings of the Royal Society B: Biological Sciences. 283:20161632.

Sibert A, Austerlitz F, Heyer
. 2002. Wright–Fisher Revisited: The Case of Fertility Correlation. Theoretical Population Biology. 62:181–197.

Siegal ML, Bergman A. 2002. Waddington's canalization revisited: Developmental stability and evolution. Proceedings of the National Academy of Sciences of the United States of America. 99:10528–10532.

Silk JB, Samuels A, Rodman PS. 1981. The Influence of Kinship, Rank, and Sex On Affiliation and Aggression Between Adult Female and Immature Bonnet Macaques (Macaca Radiata). Behaviour. 78:111–137.

Simpson MJA, Simpson AE. 1982. Birth sex ratios and social rank in rhesus monkey mothers. Nature. 300:440–441.

Smith JM, Haigh J. 1974. The hitch-hiking effect of a favourable gene. Genetics Research. 23:23–35.

Sorokowski P, Sorokowska A, Danel DP. 2013. Why pigs are important in Papua? Wealth, height and reproductive success among the Yali tribe of West Papua. Economics & Human Biology. 11:382–390.

Speidel L, Forest M, Shi S, Myers SR. 2019. A method for genome-wide genealogy estimation for thousands of samples. Nature Genetics. 51:1321–1329.

Spor A, Koren O, Ley R. 2011. Unravelling the effects of the environment and host genotype on the gut microbiome. Nature Reviews Microbiology. 9:279–290.

Stanfors M, Scott K. 2013. Intergenerational transmission of young motherhood. Evidence from Sweden, 1986–2009. The History of the Family. 18:187–208.

Steenhof L, Liefbroer AC. 2008. Intergenerational transmission of age at first birth in the Netherlands for birth cohorts born between 1935 and 1984: Evidence from municipal registers. Population Studies. 62:69–84.

Stephan W. 2019. Selective Sweeps. Genetics. 211:5–13.

Strassmann BI. 1997. Polygyny as a Risk Factor for Child Mortality among the Dogon. Current Anthropology. 38:688–695.

Studer A, Zhao Q, Ross-Ibarra J, Doebley J. 2011. Identification of a functional transposon insertion in the maize domestication gene tb1. Nature Genetics. 43:1160–1163.

Studer AJ, Wang H, Doebley JF. 2017. Selection During Maize Domestication Targeted a Gene Network Controlling Plant and Inflorescence Architecture. Genetics. 207:755–765.

Stulp G, Buunk AP, Pollet TV, Nettle D, Verhulst S. 2013. Are Human Mating Preferences with Respect to Height Reflected in Actual Pairings? PLOS ONE. 8:e54186.

Stulp G, Sear R, Schaffnit SB, Mills MC, Barrett L. 2016. The Reproductive Ecology of Industrial Societies, Part II. Human Nature (Hawthorne, N.y.). 27:445–470.

Sunnåker M, Busetto AG, Numminen E, Corander J, Foll M, Dessimoz C. 2013. Approximate Bayesian Computation. PLOS Computational Biology. 9:e1002803. Publisher: Public Library of Science.

Suzuki TA. 2017. Links between Natural Variation in the Microbiome and Host Fitness in Wild Mammals. Integrative and Comparative Biology. 57:756–769.

Swallow DM. 2003. Genetics of Lactase Persistence and Lactose Intolerance. Annual Review of Genetics. 37:197–219.

Tajima F. 1983. Evolutionary relationship of DNA sequences in finite populations. Genetics. 105:437–460.

Tajima F. 1989. Statistical method for testing the neutral mutation hypothesis by DNA polymorphism. Genetics. 123:585–595.

Tanaka M, Nakayama J. 2017. Development of the gut microbiota in infancy and its impact on health in later life. Allergology International: Official Journal of the Japanese Society of Allergology. 66:515–522.

Tenaillon O, Barrick JE, Ribeck N, Deatherage DE, Blanchard JL, Dasgupta A, Wu GC, Wielgoss S, Cruveiller S, Médigue C *et al*. 2016. Tempo and mode of genome evolution in a 50,000-generation experiment. Nature. 536:165–170.

Terhorst J, Kamm JA, Song YS. 2017. Robust and scalable inference of population history from hundreds of unphased whole-genomes. Nature genetics. 49:303–309.

Thompson FJ, Cant MA, Marshall HH, Vitikainen EIK, Sanderson JL, Nichols HJ, Gilchrist JS, Bell MBV, Young AJ, Hodge SJ *et al*. 2017. Explaining negative kin discrimination in a cooperative mammal society. Proceedings of the National Academy of Sciences. 114:5207–5212. Publisher: Proceedings of the National Academy of Sciences.

Timæus IM, Reynar A. 1998. Polygynists and Their Wives in Sub-Saharan Africa: An Analysis of Five Demographic and Health Surveys. Population Studies. 52:145–162.

Tishkoff SA, Reed FA, Ranciaro A, Voight BF, Babbitt CC, Silverman JS, Powell K, Mortensen HM, Hirbo JB, Osman M *et al*. 2007. Convergent adaptation of human lactase persistence in Africa and Europe. Nature Genetics. 39:31–40.

Torada L, Lorenzon L, Beddis A, Isildak U, Pattini L, Mathieson S, Fumagalli M. 2019. ImaGene: a convolutional neural network to quantify natural selection from genomic data. BMC Bioinformatics. 20:337.

Tung J, Barreiro LB, Johnson ZP, Hansen KD, Michopoulos V, Toufexis D, Michelini K, Wilson ME, Gilad Y. 2012. Social environment is associated with gene regulatory variation in the rhesus macaque immune system. Proceedings of the National Academy of Sciences. 109:6490–6495.

Turke PW. 1989. Evolution and the Demand for Children. Population and Development Review. 15:61–90.

Tymicki K. 2004. Kin influence on female reproductive behavior: The evidence from reconstitution of the Bejsce parish registers, 18th to 20th centuries, Poland. American Journal of Human Biology. 16:508–522.

van Bavel J, Kok J. 2009. Social Control and the Intergenerational Transmission of Age at Marriage in Rural Holland, 1850-1940. Population. 64:341–360.

van Dijk IK, Mandemakers K. 2018. Like mother, like daughter. Intergenerational transmission of infant mortality clustering in Zeeland, the Netherlands, 1833-1912. Historical Life Course Studies. 7:28–46.

van Poppel F, Monden C, Mandemakers K. 2008. Marriage Timing over the Generations. Human Nature (Hawthorne, N.Y.). 19:7–22.

van Schaik CP, Ancrenaz M, Borgen G, Galdikas B, Knott CD, Singleton I, Suzuki A, Utami SS, Merrill M. 2003. Orangutan Cultures and the Evolution of Material Culture. Science. 299:102–105.

Vanden Broecke B, Mariën J, Sabuni CA, Mnyone L, Massawe AW, Matthysen E, Leirs H. 2019. Relationship between population density and viral infection: A role for personality? Ecology and Evolution. 9:10213–10224.

Wagner A. 1994. Evolution of gene networks by gene duplications: a mathematical model and its implications on genome organization. Proceedings of the National Academy of Sciences of the United States of America. 91:4387–4391.

Wagner A. 1996. Does Evolutionary Plasticity Evolve? Evolution. 50:1008–1023. Publisher: [Society for the Study of Evolution, Wiley].

Wakeley J, Aliacar N. 2001. Gene genealogies in a metapopulation. Genetics. 159:893–905.

Wang J, Santiago E, Caballero A. 2016. Prediction and estimation of effective population size. Heredity. 117:193–206. Number: 4 Publisher: Nature Publishing Group.

Wang RL, Stec A, Hey J, Lukens L, Doebley J. 1999. The limits of selection during maize domestication. Nature. 398:236–239.

Watterson GA. 1975. On the number of segregating sites in genetical models without recombination. Theoretical Population Biology. 7:256–276.

Westoff CF, Potter RG, Sagi PC, Mishler EG. 1961. *Family Growth in Metropolitan America*. Princeton University Press.

Whitehead H. 1998. Cultural Selection and Genetic Diversity in Matrilineal Whales. Science. 282:1708–1711.

Whitehead H. 2017. Gene–culture coevolution in whales and dolphins. Proceedings of the National Academy of Sciences. 114:7814–7821.

Whitehead H, Vachon F, Frasier TR. 2017. Cultural Hitchhiking in the Matrilineal Whales. Behavior Genetics. 47:324–334.

Whiten A. 2017. A second inheritance system: the extension of biology through culture. Interface Focus. 7:20160142. Publisher: Royal Society.

Whiten A, Goodall J, McGrew WC, Nishida T, Reynolds V, Sugiyama Y, Tutin CEG, Wrangham RW, Boesch C. 1999. Cultures in chimpanzees. Nature. 399:682–685.

Whiten A, Goodall J, McGrew WC, Nishida T, Reynolds V, Sugiyama Y, Tutin CEG, Wrangham RW, Boesch C. 2001. Charting Cultural Variation in Chimpanzees. Behaviour. 138:1481–1516.

Williams GC. 1957. Pleiotropy, Natural Selection, and the Evolution of Senescence. Evolution. 11:398–411.

Williamson SH, Hernandez R, Fledel-Alon A, Zhu L, Nielsen R, Bustamante CD. 2005. Simultaneous inference of selection and population growth from patterns of variation in the human genome. Proceedings of the National Academy of Sciences. 102:7882–7887.

Wise JM, Condie SJ. 1975. Intergenerational fertility throughout four generations. Social Biology. 22:144–150.

Wright S. 1931. Evolution in Mendelian Populations. Genetics. 16:97–159.

Wright S. 1932. The Roles of Mutation, Inbreeding, crossbreeding and Selection in Evolution. Proceedings of the XI International Congress of Genetics. .

Wright S. 1938. Size of population and breeding structure in relation to evolution. Science. 87:430–431.

Xue Y, Zerjal T, Bao W, Zhu S, Lim SK, Shu Q, Xu J, Du R, Fu S, Li P *et al*. 2005. Recent Spread of a Y-Chromosomal Lineage in Northern China and Mongolia. American Journal of Human Genetics. 77:1112–1116.

Yang J, Benyamin B, McEvoy BP, Gordon S, Henders AK, Nyholt DR, Madden PA, Heath AC, Martin NG, Montgomery GW *et al*. 2010. Common SNPs explain a large proportion of the heritability for human height. Nature Genetics. 42:565–569.

Yang Z, Li J, Wiehe T, Li H. 2018. Detecting Recent Positive Selection with a Single Locus Test Bipartitioning the Coalescent Tree. Genetics. 208:791–805.

Youngson NA, Whitelaw E. 2008. Transgenerational epigenetic effects. Annual Review of Genomics and Human Genetics. 9:233–257.

Yu N, Chen FC, Ota S, Jorde LB, Pamilo P, Patthy L, Ramsay M, Jenkins T, Shyue SK, Li WH. 2002. Larger Genetic Differences Within Africans Than Between Africans and Eurasians. Genetics. 161:269–274.

Zaheer M, Kottur S, Ravanbakhsh S, Poczos B, Salakhutdinov RR, Smola AJ. 2017. Deep Sets. In: . volume 30. Curran Associates, Inc.

Zerjal T, Xue Y, Bertorelle G, Wells RS, Bao W, Zhu S, Qamar R, Ayub Q, Mohyuddin A, Fu S *et al*. 2003. The Genetic Legacy of the Mongols. American Journal of Human Genetics. 72:717–721.